

http://researchcommons.waikato.ac.nz/

Research Commons at the University of Waikato

Copyright Statement:

The digital copy of this thesis is protected by the Copyright Act 1994 (New Zealand).

The thesis may be consulted by you, provided you comply with the provisions of the Act and the following conditions of use:

- Any use you make of these documents or images must be for research or private study purposes only, and you may not make them available to any other person.
- Authors control the copyright of their thesis. You will recognise the author's right to be identified as the author of the thesis, and due acknowledgement will be made to the author where appropriate.
- You will obtain the author's permission before publishing any material from the thesis.

QUATERNARY STRATIGRAPHY

OF THE TAURANGA BASIN

A thesis

submitted in partial fulfilment

of the requirements for the Degree

of

Master of Science in Earth Sciences

at the

University of Waikato

by

GARTH RICHARD HARMSWORTH

University of Waikato

1983

ABSTRACT

A 1:25000 scale geological map of the southern part of the Tauranga Basin is presented together with numerous stratigraphic columns to illustrate the late Cenozoic stratigraphic development and depositional patterns of the Basin.

The Tauranga Basin lies 40 km north of the Taupo Volcanic Zone and immediately east of the Kaimai Range where Beesons Island Volcanics, aged 16 - 7 m.y. B.P., outcrop as an effective basement to the west and south of the Basin. The Basin originated by the northeast tilting of a large fault block, the western upturned edge now comprises the Kaimai Range and the Quaternary sequence infills the downtilted eastern margin. The tilting and hence age of the Basin mainly post-dates emplacement of the Waiteariki Ignimbrite, aged 0.84 m.y. B.P., which now immediately underlies both the Whakamarama Plateau of the southeastern Kaimai Range and the Quaternary succession in the Basin. At a few localities within the Basin Waiteariki Ignimbrite surrounds and laps onto Minden Rhyolite (4.34 m.y. B.P.) and Aongatete Ignimbrite (∿1.26 - 0.86 m.y. B.P.); these older rocks are sometimes overlain by Pleistocene deposits.

The Matua Subgroup is formally erected to classify the Quaternary sequence within the Tauranga Basin. It comprises up to 240 m of terrestrial and estuarine sediments with interdigitating pyroclastic deposits both of an air-fall and flow origin (ignimbrites). The ignimbrites are classified and mapped as formations where they are subaerially exposed, and in stratigraphic order are: Wairoa Ignimbrite (∿0.6 m.y. B.P.), Te Puna Ignimbrite (∿0.4 m.y. B.P.), Te Ranga (∿0.3 m.y. B.P.) and the Waimakariri Ignimbrite (∿0.18 m.y. B.P.). The ignimbrites are unwelded and have suffered substantial post-depositional erosion thus providing the major source of the interstratified sediments of the Matua Subgroup. In many cases individual sedimentary units throughout the stratigraphic succession can be related by petrofacies studies to source ignimbrites. This enables the discrete tongues and lenses of sediments to be mapped as post-ignimbrite units. However these sedimentary units have not been formally defined as formations. A sequence of white to grey rhyolitic tephras up to 20 m thick and named the Pahoia tephras, are invariably part of the upper 40 m of the Subgroup and are intercalated with or overlie fluvial and pyroclastic flow deposits. Brown Hamilton Ash beds inturn overlie the Pahoia tephras and/or Matua Subgroup. The 42,000 yr B.P. Rotoehu Ash and younger Late Pleistocene-Holocene tephras mantle the present topography, and may overlie any of the stratigraphically older units.

The pyroclastic flow deposits of the Matua Subgroup each show distinct but different textural and morphologic characteristics. These deposits are distinguished from air-fall units by their poorly sorted nature, coarser grain-sizes, and valley ponded distribution. The air-fall units are invariably thinner, shower bedded and mantle the paleo-topography. The fluvial sediments are dominated by planar stratification (Lenticular, Horizontal parallel, Horizontal discontinuous, Graded), and cross-stratification (Rho, Nu, and Alpha), and are interpreted as mainly braided river facies.

The Taupo Volcanic Zone is considered the source of the Waiteariki Ignimbrite and younger pyroclastic flow deposits of the Matua Subgroup. A more northern, Coromandel Range, source is suggested for the older Aongatete Ignimbrite (∿1.26 - 0.86 m.y. B.P.).

Abstract continued

The Quaternary geological history of the region has been informally considered as three main periods: early Ignimbrite period (0.84 - 0.50 m.y. B.P.), a late Ignimbrite period (0.50 - 0.14 m.y. B.P.), and an upper Matua Subgroup period (~0.16 m.y. B.P. - Present). The principal influences on the stratigraphic development and depositional patterns of the Basin are attributed to block faulting and tilting of the basement and adjacent Kaimai Range, volcanic activity in the Taupo Volcanic Zone, and to a lesser extent, climatic and glacio-eustatic sea-level changes.

ACKNOWLEDGEMENTS

I would like to acknowledge the assistance of the following people in the preparation of this thesis:

Dr C.S. Nelson for his excellent advice throughout the project and constructive criticism of the manuscript. Dr R.M. Briggs and Mr P.J.J. Kamp for invaluable assistance in the field, for comment on the manuscript and for helpful discussion. Dr B.F. Houghton for suggesting this research topic, for his diligent guidance in the field and for fruitful discussion in the course of this research. I would also like to acknowledge Mr P.J.B. Fransen for his assistance in the field and for helpful discussion during the project, and Mr Laurie Gaylor for his help.

I thank Elaine Norton for producing an excellent typescript and Frank Bailey for his highly skilful draughtsmanship. I extend my thanks to the Althuizen family of Tauranga for their five-star accommodation, and a special thanks to the Price family of Hamilton for their gracious hospitality. Finally, to Christine for moral and family support during the compilation of the project.

TABLE OF CONTENTS

		Page
ABSTRACT		ii
ACKNOWLEDGEMENTS		iv
TABLE OF CONTENTS		v
LIST OF TABLES AND FIGURES		x
CHAPTER ONE:	INTRODUCTION	
1.1	Study area	1
1.2	Objectives	1
1.3	Physiography	1
1.3.1	Terraces	8
1.4	Geological setting	13
1.5	Soils	16
1.6	Previous work	16
CHAPTER TWO:	METHODS	
2.1	Field methods	24
2.1.1	Introduction	24
2.1.2	Mapping method	24
2.2	Laboratory methods	27
2.2.1	Introduction	27
2.2.2	Textural analysis	27
2.2.3	Compositional analysis	30
2.2.4	Microfossil analysis	35
CHAPTER THREE:	STRATIGRAPHY OF THE TAURANGA BASIN	
3.1	Introduction	37
3.2	Stratigraphic usage	37
3.3	Stratigraphy	38
3.4	Lithologic descriptions	40

		Page
3.4.1	Beesons Island Volcanics	40
3.4.2	Minden Rhyolite	43
3.4.3	Waitawheta Dacite	44
3.4.4	Aongatete Ignimbrite	44
3.4.5	Waitearíki Ignimbrite	45
3.4.6	Papamoa Ignimbrite	48
3.4.7	Wairoa Ignimbrite	51
3.4.8	Te Puna Ignimbrite	52
3.4.9	Te Ranga Ignimbrite	54
3.4.10	Waimakariri Ignimbrite	56
3.4.11	Mamaku Ignimbrite	59
3.4.12	Tauranga Group	59
3.4.13	Matua Subgroup	60
3.5	Air-fall tephra sequences	66
3.5.1	Older (pre-Rotoehu Ash tephras)	69
3.5.2	Younger (Rotoehu Ash and post-Rotoehu Ash) tephras	76
3.5.3	Stratigraphic relationships of tephra sequences	77

CHAPTER FOUR: STRUCTURE

4.1	Introduction	83
4.2	Structural relationships and subsidence	83
4.2.1	Intrabasinal faulting	96
4.3	Hauraki Depression: Comparison with the Tauranga Basin	96
4.4	Tectonic setting of the Tauranga Basin	101

		Page
CHAPTER FIVE:	TEXTURAL PROPERTIES OF THE MATUA SUBGROUP DEPOSITS	
5.1	Introduction	104
5.2	Textural characteristics of fluvial deposits	104
5.2.1	Textural plots	104
5.2.2	Grain-size distribution curves	108
5.2.3	Statistical parameters	111
5.3	Textural characteristics of pyroclastic flow deposits	119
5.3.1	Textural plots	119
5.3.2	Grain-size distribution curves	119
5.3.3	Statistical parameters	124
5.4	Textural characteristics of pyroclastic fall deposits	131
5.4.1	Textural plots	131
5.4.2	Grain-size distribution curves	131
5.4.3	Statistical parameters	135
CHAPTER SIX:	COMPOSITION OF MATUA SUBGROUP DEPOSITS	
6.1	Introduction	144
6.2	Discussion of bulk mineralogy	144
6.3	Component composition	144
6.3.1	Light mineralogy	146
6.3.2	Heavy mineralogy	147
6.3.3	Rock fragments	149
6.3.4	Clay minerals	152
6.4	Fluvial deposits	152
6.4.1	Results	152

		Page
6.5	Pyroclastic flow deposits	159
	6.5.1 Results	159
6.6	Pyroclastic fall deposits	164
	6.6.1 Results	164
6.7	Mineralogical Groups	170
6.8	Petrofacies distribution and Interpretation; with emphasis on fluvial deposits	175
6.9	Provenance	178
CHAPTER SEVEN:	SEDIMENTARY STRUCTURES, HYDRODYNAMICS AND PALEOENVIRONMENTS OF FLUVIAL DEPOSITS OF THE MATUA SUBGROUP	
7.1	Introduction	182
7.2	Sedimentary structures of fluvial deposits	182
	7.2.1 Planar stratification	184
	7.2.2 Cross-stratification	195
	7.2.3 Deformation structures	208
7.3	Broad depositional environment	211
7.4	Lithofacies	211
7.5	Facies assemblages	217
	7.5.1 Sequences	222
7.6	Lithofacies of the upper Matua Subgroup: physiographic model	228
7.7	Interpreation of Lithofacies in terms of depositional environment: (post-Te Ranga Ignimbrite emplacement).	231
7.8	Discussion of upper Matua Subgroup model	233

		Page
CHAPTER EIGHT:	STRUCTURES AND EMPLACEMENT MECHANISMS OF PYROCLASTIC DEPOSITS OF THE MATUA SUBGROUP	
8.1	Terminology for pyroclastic deposits and fragments	236
8.2	Pyroclastic flow deposits	239
8.2.1	Introduction	239
8.2.2	Types of pyroclastic flow deposits in the Tauranga Basin	244
8.3	Pyroclastic air-fall deposits	268
8.3.1	Pyroclastic air-fall deposits in the Tauranga Basin	268
8.4	Conclusions	273
CHAPTER NINE:	ENVIRONMENTAL SYNTHESIS AND GEOLOGIC HISTORY	
9.1	Introduction	275
9.2	Early Ignimbrite Period	278
9.3	Late Ignimbrite Period	282
9.4	Upper Matua Subgroup Period	288
CHAPTER TEN:	CONCLUSIONS	297
APPENDIX 1:	Stratigraphic sections of the Tauranga Basin	301
APPENDIX 2:	Textural and Mineralogical data	321
2.1	Sample reference	322
2.2	Textural data	323
2.3	Mineralogic analysis results	326
MAP FOLIO:	Terraces (Fig. 1.8), cross-sections of the Tauranga Basin (Fig. 4.3) and geologic map of the Tauranga Basin.	

LIST OF TABLES

		Page
Table 1.1	Summary table of geological events in the Tauranga Basin since the Mesozoic	15
1.2	General soil types within the map area and areas adjacent to the Tauranga Basin	18
1.3	Soil types within the Tauranga Region	19
2.1	Grain-size scale	29
3.1	Stratigraphy of the Tauranga Region	41
3.2	Major distinguishing features of principal ignimbrites subaerially exposed within the Tauranga Basin	42
3.3	Tephrostratigraphy of the Tauranga Basin	68
3.4	Description of Pahoia tephras at Omokoroa	73
3.5	Description of Hamilton Ash beds at Omokoroa	75
4.1	Recorded depths at which volcanic deposits were sampled in boreholes	94
4.2	Sedimentation rates in the Tauranga Basin	95
4.3	Structural history of the Tauranga Basin	98
5.1	Conclusions showing the major textural differences, between fluvial, pyroclastic flow and pyroclastic fall deposits	143
6.1	Locations of fluvial samples used for rock fragment analysis	150
6.2	Rock fragment types in fluvial deposits	151
6.3	Locations of fluvial samples used for heavy mineral analysis	153
6.4	Heavy mineral content(%) of fine sand fractions in fluvial deposits	154
6.5	Heavy mineral content(%) of pumice blocks in fluvial deposits	155
6.6	Location of pyroclastic flow deposit samples used for heavy mineral analysis	163
6.7	Heavy mineral content(%) of fine sand fractions in pyroclastic flow deposits	163
6.8	Location of pyroclastic fall deposit samples used for heavy mineral analysis	165

		Page
Table 6.9	Heavy mineral content(%) of fine sand fractions in pyroclastic air-fall deposits	166
6.10	Clay mineralogy	168
6.11	Main ignimbrite source rock contributing sediment to different broad areas within the Tauranga Basin	181
7.1	Fluvial structures in the Tauranga Basin	183
7.2	Criteria for recognition of planar stratification types in the Tauranga Basin	187
7.3	Planar stratification types	188
7.4	Criteria for recognition of Rho Cross-Stratification types	204
7.5	Criteria used to define Rho- and Nu-cross-stratification types	205
7.6	Two main types of Nu-cross-stratification	206
7.7	Lithofacies codes as based on interpretation by Miall (1978)	214
7.8	Vertical sequences observed in some fluvial deposits	224
7.9	Observed facies relationship code	225
7.10	Sedimentological characteristics and environmental interpretation of lithofacies for fluvial sediments in the Tauranga Basin	229
8.1	Granulometric classification of pyroclasts and of unimodal, well-sorted pyroclastic deposits	238
8.2	Terms for mixed pyroclastic-epiclastic rocks	238
8.3	Chapter contents showing various types of pyroclastic deposit in the Tauranga Basin	240
8.4	Genetic classification of pyroclastic flow types based on fluidization behaviour	240
8.5	Structural characteristics of pyroclastic flow deposits	241
8.6	Criteria for distinguishing between pyroclastic flow and fall deposits in the Tauranga Basin	242
8.7	Lithofacies definition for pyroclastic deposits in the Tauranga Basin	243

		Page
Table 8.8	Chalazoidite/Accretionary lapilli four phase development	272
9.1	Summary table of events in the Tauranga Basin during the Quaternary	277
9.2	Andesitic gravels in the stratigraphic record	283

LIST OF FIGURES

		Page
Figure 1.1	Locality map of the Tauranga Basin	2
1.2	Sketchmap of the Tauranga Basin	3
1.3	Study area	4
1.4	Physiography of the Tauranga area	6
1.5	Drainage characteristics of the Tauranga Basin	7
1.6	Terraces at Waihi	9
1.7	Three dimensional models of the Tauranga Basin	10
1.8	Map showing terraces in the study area	(map folio)
1.9	Volcanic constructional surface	12
1.10	Fluvial degradation surfaces	12
1.11	Geology of the Tauranga area	14
1.12	Soils of the Tauranga Basin	17
2.1	Location of cores and stratigraphic section	25
2.2	Laboratory techniques used in sample analysis	28
2.3	Statistical Parameters	31
2.4	XRD intensity-concentration plots for quartz, plagioclase and clay minerals	33
2.5	XRD intensity-concentration curves for quartz and plagioclase feldspar from the Tauranga Basin deposits	34
3.1	Stratigraphic column for the Tauranga Basin	39
3.2	Waitearíki Ignimbrite	49
3.3	Wairoa Ignimbrite (new name)	49
3.4	Te Puna Ignimbrite (new name)	55
3.5	Te Ranga Ignimbrite (new name)	55
3.6	Columnar jointed Waimakariri Ignimbrite	58
3.7	Stratigraphic column for the Otumoetai area	61

		Page
Figure 3.8	Sketch of the Matua stratigraphic section	62
3.9	Sketch of the Te Puna stratigraphic section	62
3.10	Sketch of the Omokoroa stratigraphic section	62
3.11	Lignite at Omokoroa	64
3.12	Age and distribution of tephra marker beds in the Tauranga Basin	67
3.13	The Pahoia tephras exposed at Omokoroa	71
3.14	Distribution map of the soil forming ash showers in the Tauranga area, showing the extensive Waihi Ashes.	71
3.15	Stratigraphic columns for air-fall cover deposits in the Tauranga Basin.	78
3.16	The Pahoia tephras overlying a chalazoidite bed at Omokoroa East.	79
4.1	Subsurface stratigraphy of the Tauranga Basin	84
4.2	Structural relationships between the Tauranga Basin, the Hauraki Lowlands and the Mamaku Plateau.	85
4.3	Cross-sections through the Tauranga Basin	(map folio)
4.4	Cross-sections through the Coromandel Range	86
4.5	Sketched cross-sections W-E across the Tauranga Basin since the mid-Pleistocene	87
4.6	Sketch showing ignimbrite distribution relationships	90
4.7	Schematic sketches of the Tauranga Basin since the mid-Pleistocene	91
4.8	Structural events in the Tauranga area since the Pliocene	97
4.9	Small scale normal faults exposed in coastal cliffs on Motuhoa Island	99
4.10	Simplified geological cross-section across the Hauraki Depression	99
4.11	General geology of the Hauraki Depression and position of faults	100
4.12	Location of Mayor Island and its relationship to the Ngatoro Basin in the Bay of Plenty	103

		Page
Figure 5.1	Textural terminology	105
5.2	Textural plot of representative fluvial sediment samples	106
5.3	Major textural lithotypes of fluvial sediments	107
5.4	Relation of sediment transport dynamics to populations and truncation points in a grain-size distribution	109
5.5	Cumulative grain-size frequency curves for fluvial sediments	109
5.6	Histograms of grain-size statistical parameters for fluvial sediments	112
5.7	Relationships between grain-size statistical parameters for fluvial sediments	113
5.8	Basic C-M patterns after Passega	117
5.9	CM pattern for representative fluvial sediment samples from the Tauranga Basin	118
5.10	CM pattern for sediments of the Hinuera Formation from both the southern Hauraki Lowlands and the Hamilton Basin	118
5.11	Textural plot of representative pyroclastic flow deposits	120
5.12	Major textural lithotypes of pyroclastic flow deposits	121
5.13	Cumulative grain-size frequency curves for pyroclastic flow deposits	121
5.14	Histograms of grain-size statistical parameters for pyroclastic flow deposits	125
5.15	Relationships between grain-size statistical parameters for pyroclastic flow deposits.	126
5.16	CM plot for representative pyroclastic flow deposits	130
5.17	CM diagrams for pyroclastic fall and pyroclastic flow deposits;from Sheridan	130
5.18	Textural plot for representative pyroclastic fall deposits	132
5.19	Major textural lithotypes of pyroclastic fall deposits	133
5.20	Cumulative grain-size frequency curves for pyroclastic fall deposits	133

		Page
Figure 5.21	Histograms of grain-size statistical parameters for pyroclastic fall deposits	136
5.22	Relationships between grain-size statistical parameters for pyroclastic fall deposits	137
5.23	Contoured plots for pyroclastic fall and pyroclastic flow deposits comparing those of Walker (1971) to those from the Tauranga Basin	141
5.24	CM plot for representative pyroclastic fall deposits	142
6.1	Bulk mineralogy of representative fluvial, pyroclastic flow and pyroclastic fall samples	145
6.2	Bulk mineralogy of representative samples showing heavy mineral percentage comparison between fluvial, pyroclastic flow and pyroclastic fall samples	145
6.3	Content(%) and possible source areas of rock fragments in fluvial deposits	156
6.4	Content(%) and possible source areas of heavy minerals in fluvial deposits	156
6.5	Average heavy mineral content(%) of the fine sand fraction in representative fluvial sediment samples	157
6.6	Average heavy mineral content(%) of the fine sand fraction from selected pyroclastic flow deposits	161
6.7	Possible analogous pyroclastic flow deposits exposed at the coast to those exposed further inland, as based on petrofabric and mineralogic studies	162
6.8	Average heavy mineral content(%) of the fine sand fraction from selected representative pyroclastic fall deposits	167
6.9	Map showing petrofacies distribution	172
6.10	Petrofacies columns showing distribution and corresponding types of deposits	173
6.11	Map of petrofabric-mineralogic cross-section sites	176
6.12	Schematic cross-sections showing the present compositiional (mineralogic) variation in deposits in the Tauranga Basin	176

		Page
Figure 6.13	Schemiatic W-E cross-sections through the Tauranga Basin showing compositional variations with time	179
7.1	Summary of paleoenvironmental synthesis	185
7.2	Planar stratification types	186
7.3	Lenticular stratification	189
7.4	Horizontal parallel stratification	189
7.5	Horizontal discontinuous stratification	192
7.6	Graded stratification	192
7.7	Low angle cross-stratification	196
7.8	Avalanche front cross-stratification	196
7.9	Sketch of avalanche cross-stratification formed by migrating sand-waves	199
7.10	Infill of a trough by aggradation to a profile of equilibrium under uniform conditions of flow and transport	199
7.11	Origin of coarse and fine foreset laminae by continuous avalanching	199
7.12	Rho-cross-stratification	202
7.13	Large scale trough cross-beds	202
7.14	Block diagrams of Planar and Rho-cross-stratification types	203
7.15	Chalazoidite bed on Motuhoa Island intruded by sand	209
7.16	Compactional faulting in Rho-cross-stratified slightly gravelly sands	209
7.17	Paleocurrent data	212
7.18	Stratigraphic section of fluvial sediments	218
7.19	Fluvial sediment assemblages	220
7.20	Principal bar types	221
7.21	Sequences as interpreted in an assemblage	221
7.22	Group assemblages in fluvial sequences showing vertical stacking relationships and interpretation	223
7.23	Observed facies relationships and number of reported observations	226

		Page
Figure 7.24	Simplified facies relationship model	227
7.25	Physiographic model of fluvial sequences	235
8.1	Schematic section through the products of an ignimbrite eruption showing one flow unit	241
8.2	Sketches showing the structure of the Type F1 and the Type F2 deposits	245
8.3	The Type F1 deposit	246
8.4	The Type F2 deposit	246
8.5	Cross-stratification at the base of the Type F2 deposit	251
8.6	A post-depositionally modified Type F2 deposit showing a series of weathering bands	251
8.7	The Type F3 deposit	253
8.8	Sketches showing the structure of the Type F3 and Type F4 deposit	254
8.9	Inverse grading in the Type F5 deposit	257
8.10	The Type F5 deposit at Omokoroa	257
8.11	Debris flow/slump deposit exposed on Motuhoa Island	261
8.12	Sketches showing the structure of the Type F5 and F6	262
8.13	The Type F6 deposit at Matua	265
8.14	Chalazoidite bed underlying the Waimakariri Ignimbrite at Ruahihi	265
8.15	Lithofacies diagram showing the relationships between pyroclastic and fluvial deposits at various localities in the southeastern part of the Tauranga Basin	274
9.1	Location of the Taupo Volcanic Zone	276
9.2	Relationship of volcanism to the structural development in the North Island during the Late Cenozoic	276
9.3	Taupo Volcanic Zone and Volcanic Centres within this Zone	279
9.4	A sketch showing distribution relationships between various ignimbrites in the Tauranga Basin	287

Page

Figure 9.5 General timetable of events and effects in the Tauranga Basin 290

9.6 Summary sketches of events in the Tauranga Basin since the Middle Pleistocene 296

CHAPTER ONE

INTRODUCTION

1.1 STUDY AREA

The Tauranga Basin (Figs. 1.1 and 1.2) covering an area 38 km by 15 km (570 km^2), is occupied by a large (200 km^2 estuarine lagoon (Tauranga Harbour) on the western Bay of Plenty coastline. Tauranga city (pop. 37,500) is situated in this Basin. Research was confined to an area covering some 180 km^2, in the southern parts of the Basin (map series: NZMS 260 U14 Tauranga, 1 : 50,000 scale map), extending from Welcome Bay (U14/907819) to Omokoroa (U14/798928). Field work was also carried out in an area between Pyes Pa Road (U14/852760) and the Wairoa River (U14/790760) (Fig. 1.3).

1.2 OBJECTIVES

The aims of this study were two-fold: firstly to determine the subaerial (and shallow subsurface) stratigraphy of the Tauranga Basin and to compile a geological map; and secondly, to study in some detail the subaerially exposed sediments in the Basin and to determine their origin, both in terms of source and environment of deposition. From this work, the main objectives were to establish a general history of sedimentary and volcanic events and create a paleoenvironmental depositional model for the subaerially exposed deposits.

1.3 PHYSIOGRAPHY

The Tauranga Basin covers about 570 km^2 and is bounded by the Kaimai Range and Whakamarama Plateau in the west, the Papamoa Hills in the southeast, and the Mamaku Plateau in the south. The Basin shows little surface evidence of faulting and is a northeasterly dipping tilted block inundated to the east and northeast by the sea. Former stream valleys have been drowned by the most recent post-glacial marine transgression and the Basin is now dominated by the tidal estuarine

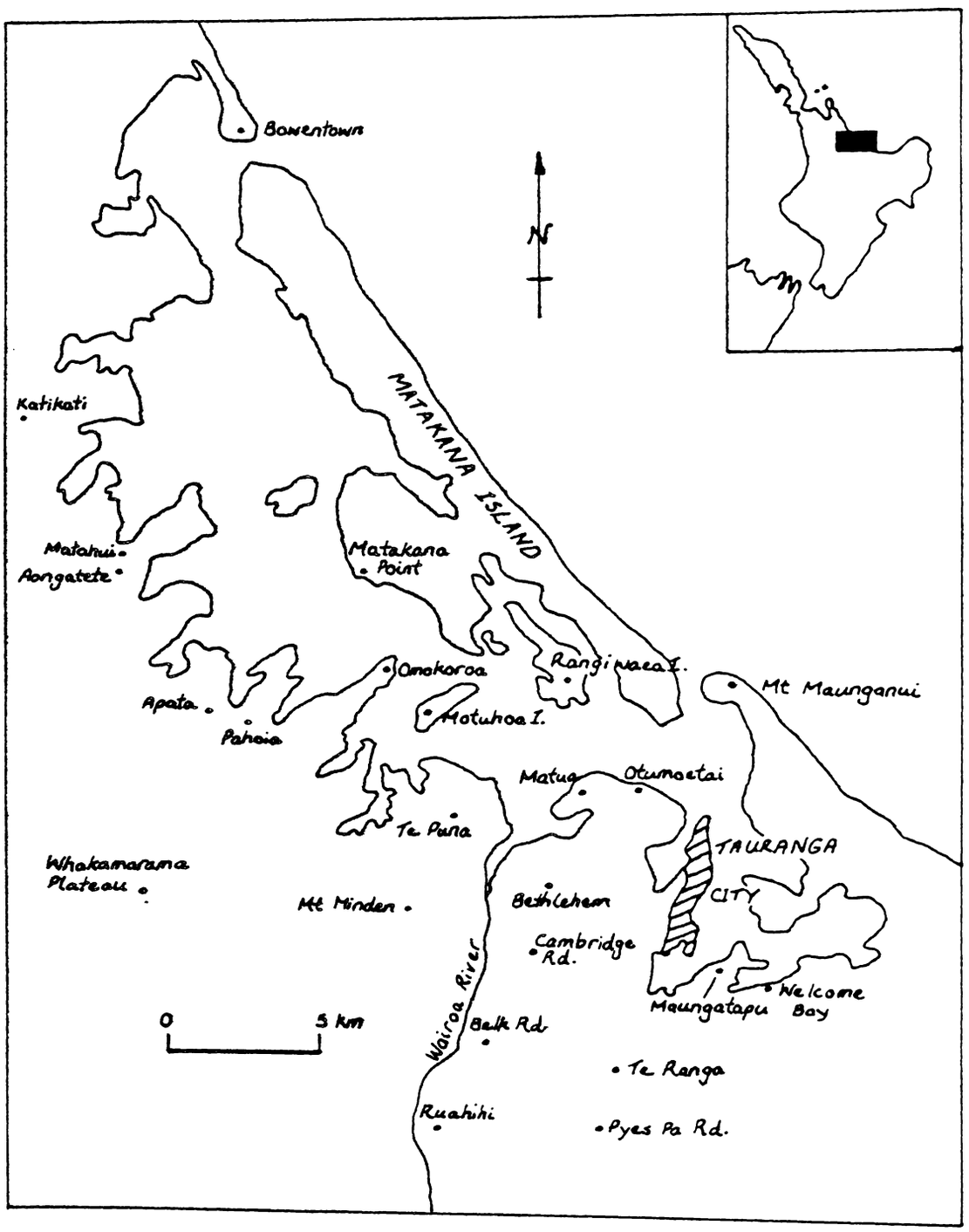


Fig. 1.1 Locality map of the Tauranga Basin.

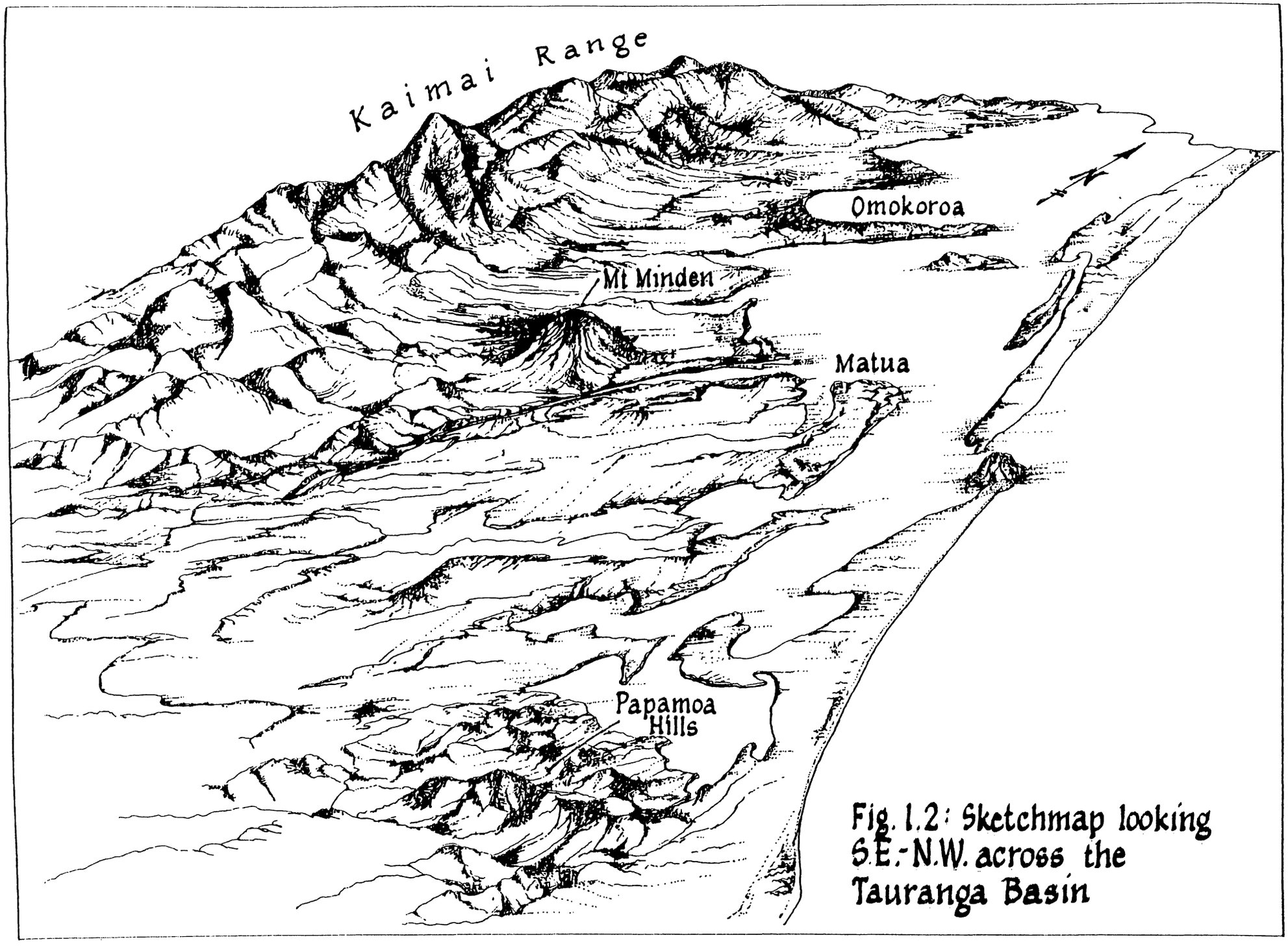


Fig. 1.2: Sketchmap looking S.E.-N.W. across the Tauranga Basin

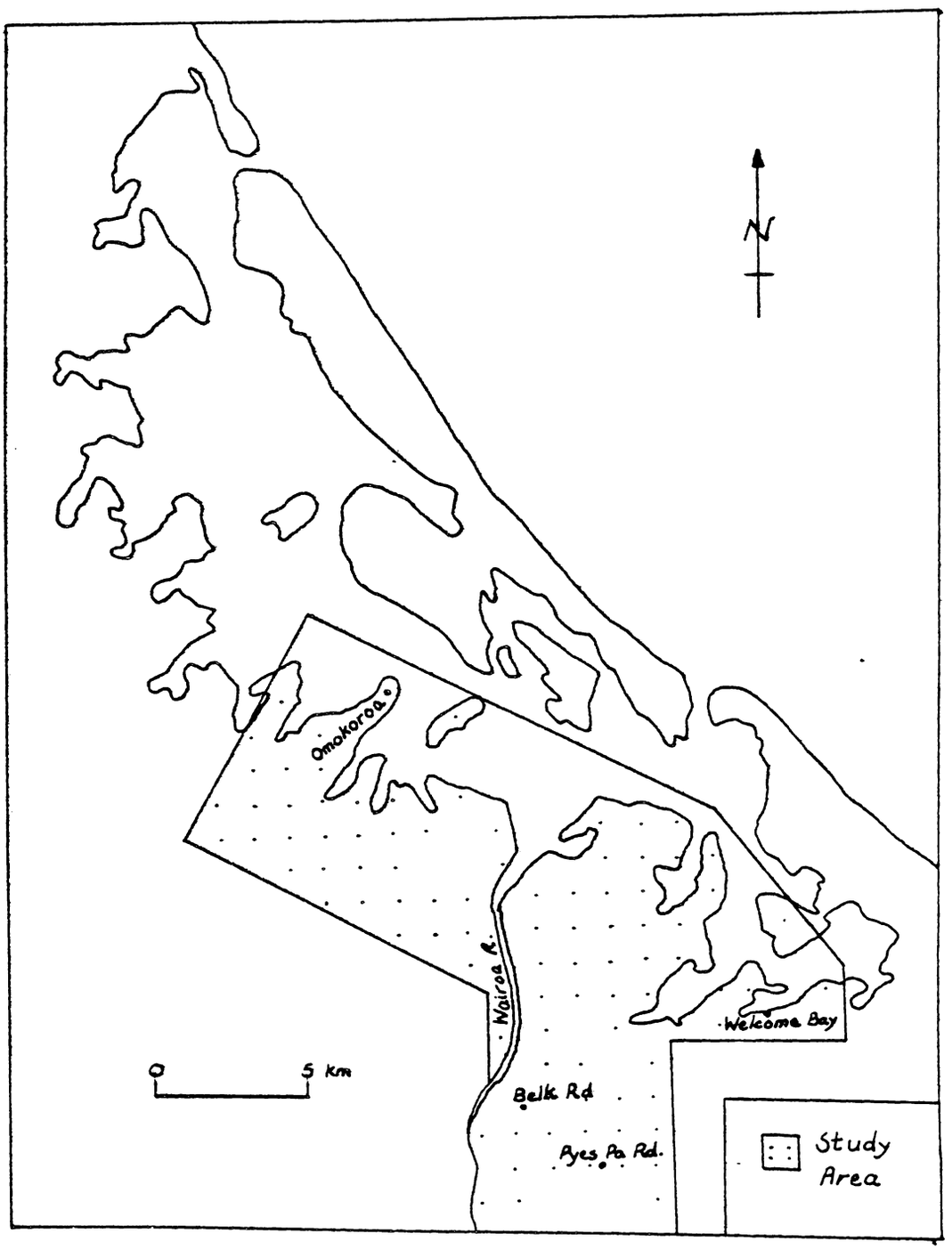


Fig. 1.3 Study area.

lagoon of Tauranga Harbour. This coastal drowning is typical of a ria complex.

Two plateau features are recognised. The Whakamarama Plateau is an old feature (∿ 0.84 m.y. B.P.) and dips gently into the Tauranga Harbour (Fig. 1.4) beneath sedimentary strata. The Mamaku Plateau is a younger feature (∿ 0.14 m.y. B.P.) and approaches the Basin as a near horizontal surface entrenched by numerous valleys. Many Peninsulas extend into, and islands dot, the Tauranga Harbour which is confined by Matakana Island, a barrier island complex forming the entire north east seaward coastline. Stratigraphic evidence suggests that the topographically higher part of the Island in the vicinity of Matakana Point (Fig. 1.1), as well as Rangiwaea Island, were once joined to the mainland in the vicinity of Aongatete/Omokoroa and Te Puna respectively. The island is now completely separate with tidal entrances at either end. Tidal channels are confined by Bowentown in the north and Mt Maunganui in the south, both of which are volcanic domes of Minden Rhyolite with tombolos connecting them to the mainland.

Drainage patterns (Fig. 1.5) have been most effective in moulding the landscape in the Basin and active downcutting by the many NE flowing streams during the last (∿ 18000 - 20000 yr B.P.) glacio-eustatic low (-120 m) sea level has given rise to the present highly irregular inner harbour coastline. Most of the streams now entering Tauranga Harbour have developed tidal swamps and wide flared estuaries at their mouths. Streams in areas south of the Wairoa River have also developed terraces and levees at their lateral margins, particularly in valleys which run northwards in the Basin. Terraces occur in remnant valleys, and were produced in most instances by lateral erosion of graded streams. Downcutting at several sites was accompanied by floodplain construction (e.g. localities from Wairoa River to Cambridge Road).

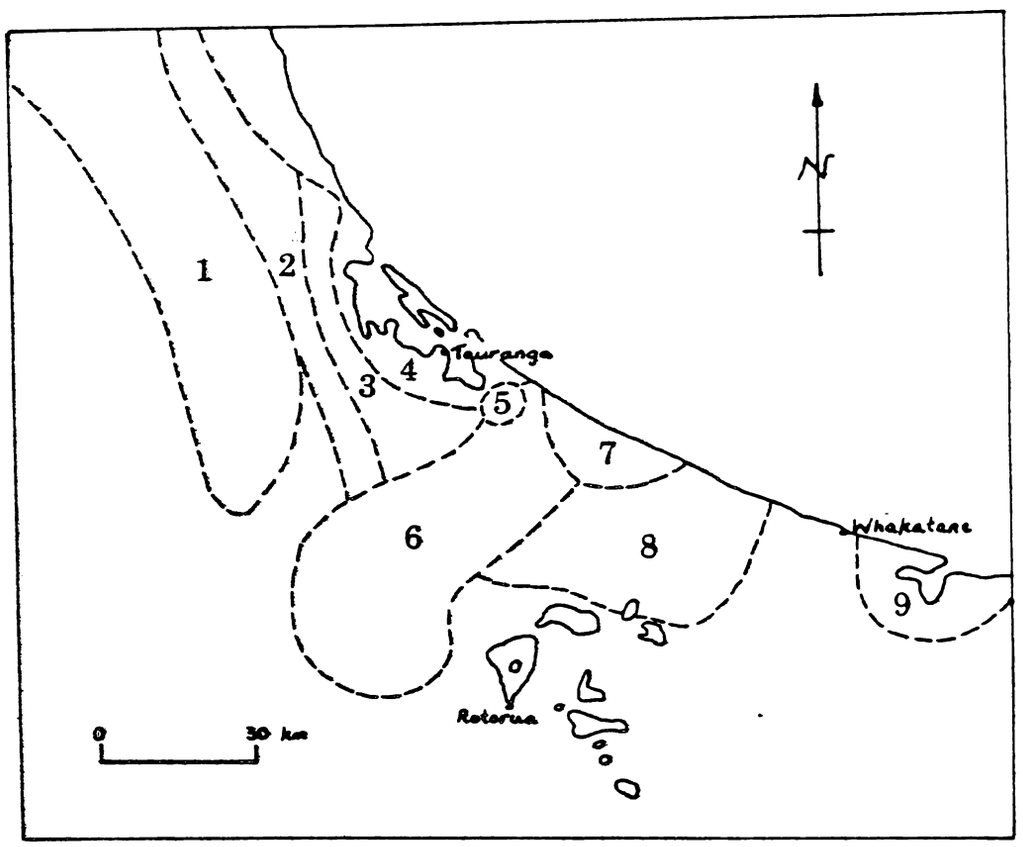


Fig. 1.4 Physiography of the Tauranga area.

1 - Hauraki Plains;

2 - Kaimai Range;

3 - Whakamarama Plateau;

4 - Tauranga Basin;

5 - Papamoa Hills;

6 - Mamaku Plateau;

7 - Maketu Basin;

8 - Kaharoa Plateau;

9 - Opotiki Basin.

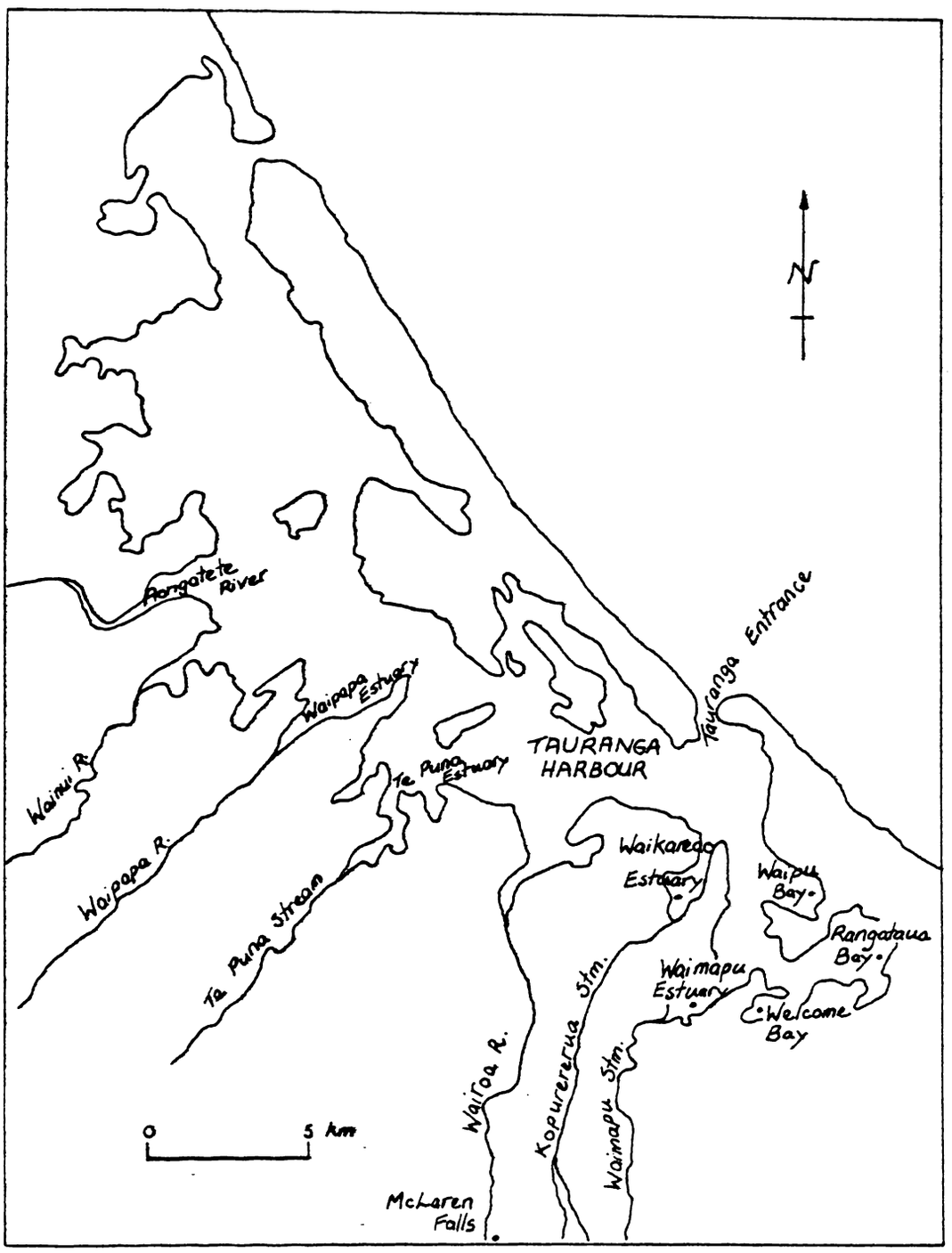


Fig. 1.5. Drainage characteristics of the Tauranga Basin.

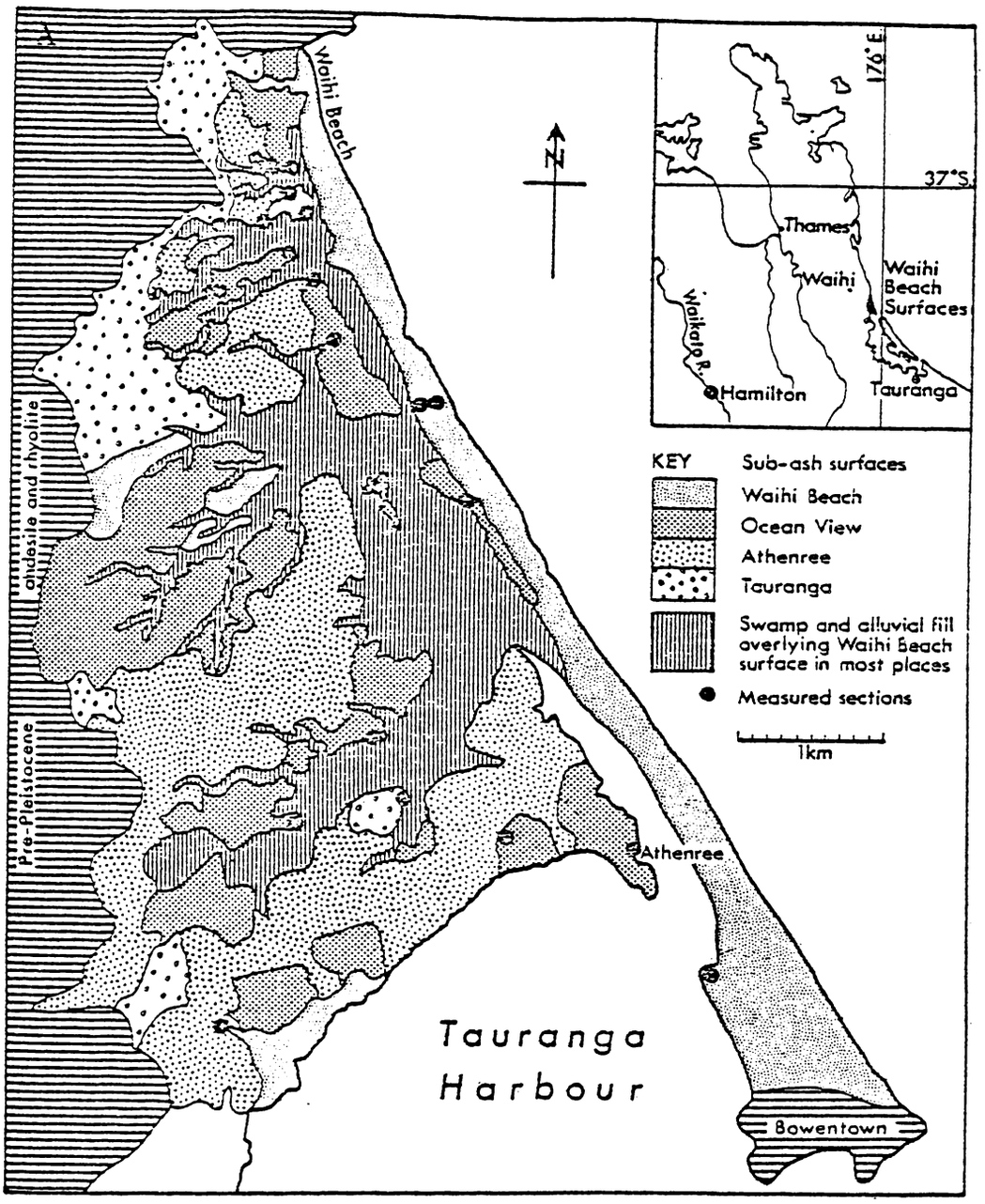
1.3.1 Terraces

Along the northern coastline of the Tauranga Basin a series of glacio-eustatic terraces occurs (Fig. 1.6). Four terraces were identified and mapped at Waihi Beach (Kear and Waterhouse, 1961; Selby *et al.* 1971) and correlations with terraces further south have been suggested (Chappell, 1975). The terrace surfaces at Waihi were estimated at 1.8 to 3.0 m a.s.l., 4.6 to 6.1 m a.s.l., 18.3 to 21.3 m a.s.l., and 33.5 to 35.0 m a.s.l. (Selby *et al.*, 1971), and were assumed to be the result of "terrestrial aggradation as a consequence of the rise of sea level" (Kear and Waterhouse, 1961). The validity of mapping glacio-eustatic terraces south from Waihi is questionable. Terrace heights in the Tauranga Basin proper are variable and owe their present form to a number of processes (see below), so that correlation with terraces outside the Basin is difficult.

The landscape of the Tauranga Basin consists of many gently dipping to horizontal concordant height surfaces*. Some are variably dissected but preserving concordant heights, suggestive of terrace levels (Fig. 1.7). However detailed study shows that these flat surfaces are underlain by a variety of deposits and that they have formed in several different ways.

Several terrace levels are evident in the southern parts of the Tauranga Basin (map area of this study, Fig. 1.8; Healy *et al.*, 1964). Terraces have been recorded at various seaward elevations, >70 m, 30 - 60 m, 12 - 22 m, 5 m, and 1.0 - 0.1 m above present sea level (Healy *et al.*, 1964), and most have dips of between 1^{o} and 4^{o} NE or N. Many of the terraces are intersected by broad shallow valleys and terminate seawards in low cliffs or steep slopes.

* Surface is used in this study to describe the uppermost level of the terrace.



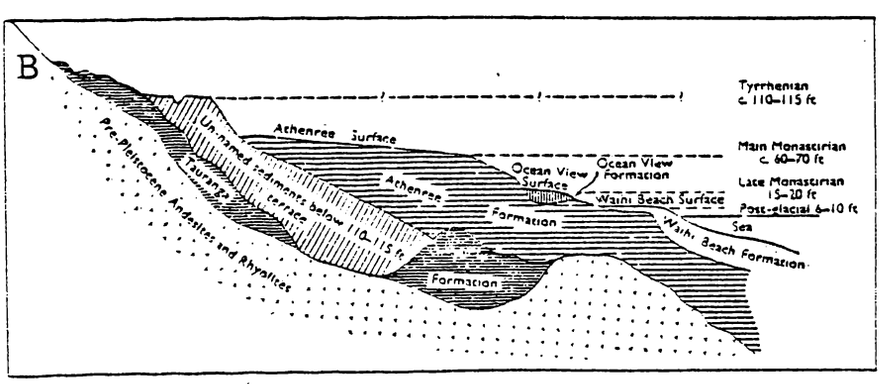


Fig. 1.6 Terraces at Waihi (from Selby *et al.*, 1971; Kear and Waterhouse, 1961).

A - distribution of the Waihi Beach sub-ash surfaces.

B - surfaces together with indicated sea levels and heights.

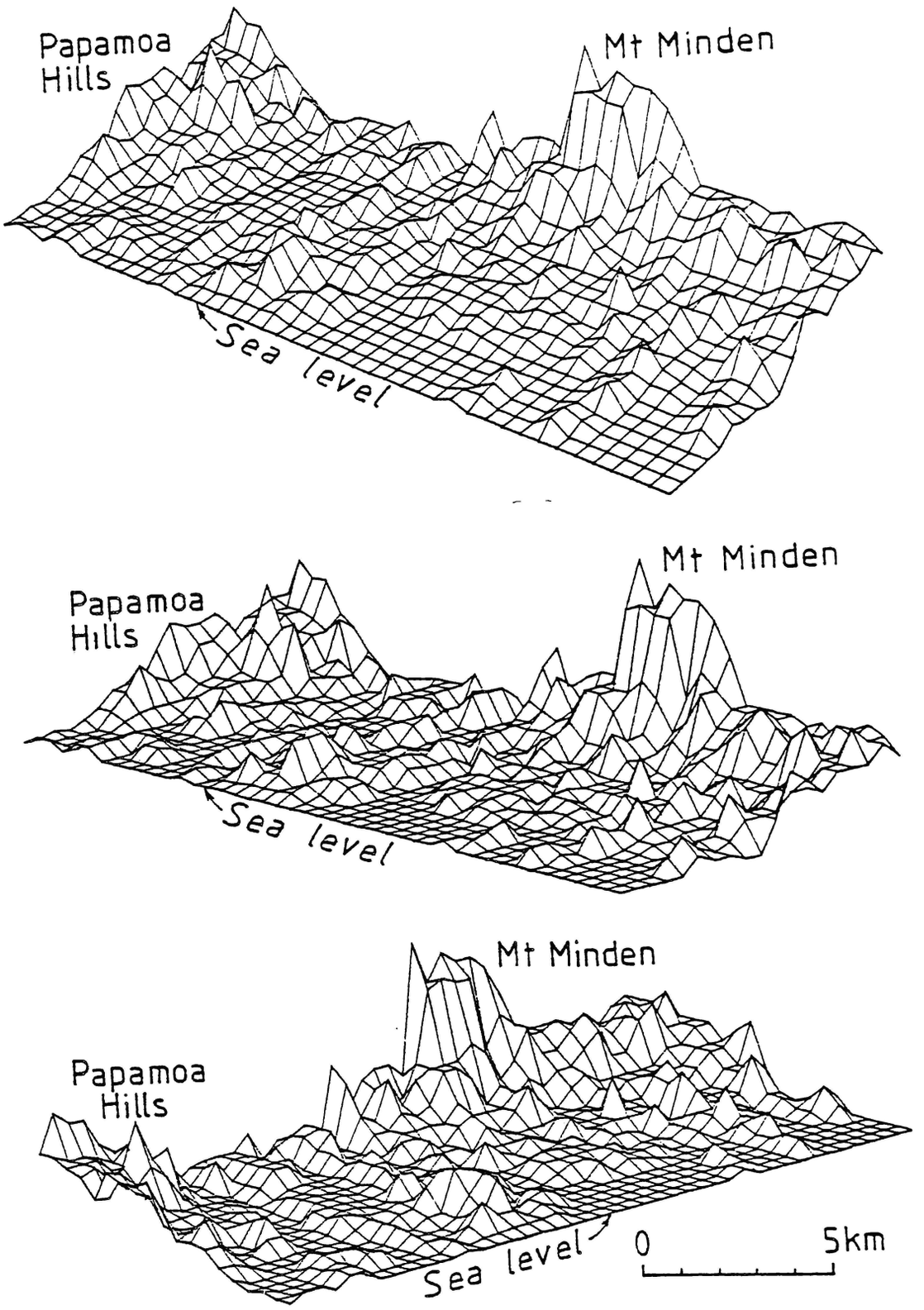


Fig. 1.7 A series of oblique views looking southward into the Tauranga Basin, are shown by these three dimensional models. These models serve to emphasize the contrast between the lowlying flat surfaces and more prominent (highest elevation) features such as Mt Minden and the Papamoa Hills.

The terraces in the area of study (Fig. 1.8, map folio) are polygenetic. Terraces are attributed to four major origins:

(1) Volcanic constructional surfaces*: the tops of lobes of pyroclastic flow deposits, often variably degraded (Fig. 1.9).

(2) Volcanic and/or fluvial degradation surfaces modified by air-fall tephra (Fig. 1.10).

(3) Fluvial terraces formed by either aggradation or lateral erosion, and variably degraded.

(4) Terraces formed by marine aggradation as a consequence of a higher than present sea level: the lowest terrace surface* (1.0 to 0.5 m a.s.l.) recorded in the Tauranga Basin, corresponds to the most recent post-glacial marine transgression (possibly correlates to the Waihi beach surface; Selby *et al.*, 1971). A blue-grey muddy sand interpreted as belonging to estuarine facies is found 0.2 to 3 m below the terrace surface*.

Most terraces in the Basin contain an ash increment. Variations in the thickness of specific air-fall tephra deposits, or missing units at different localities within the Basin appears to be a function of degradation and in some instances to regional undulation and/or warping. The terraces represent different periods of fluvial deposition and subsequent channel erosion. The stratigraphy beneath the terrace surface therefore records channel cut and fill episodes, the consequence being that specific air-fall tephra deposits have been removed in some areas. Some of the highest terraces in the Basin have formed atop pyroclastic flows which have ponded in topographic depressions or represent concordant upper surfaces of flows deposited in valleys. Terraces constructed of sequences of fluvial and air-fall tephra deposits occur on many of the peninsulas throughout the Basin (e.g. Maungatapu, Matua, Katikati). Terraces of fluvial origin which occur in paleostream



Fig. 1.9 A volcanic constructional surface formed atop of the Te Puna Ignimbrite is ∿30 m high. This terrace represents the concordant upper surface of the pyroclastic flow deposited in a valley at Te Puna (U14/823854).



Fig. 1.10 Fluvial degradation surfaces modified by air-fall tephra adjacent to the Wairoa River (U14/842825) reach a height of 30 to 40 m. The Wairoa Ignimbrite crops out beneath several fluvial sequences near this area.

valleys often reflect the longitudinal profile of the stream which formerly flowed in them.

1.4 GEOLOGICAL SETTING

The Tauranga Basin is a late Cenozoic sedimentary basin partially infilled by a sequence of volcanic deposits and fluvial and estuarine strata with a maximum thickness of ∿500 m (Fig. 1.11).

The oldest rocks exposed just outside the Basin are Miocene volcanic rocks (Beeson's Island Volcanics) cropping out in the Kaimai Range. These are overlain by dacite (Waitawheta Dacite) domes and flows of Pliocene age (Adams *et al.*, 1974, 1975). Early volcanic activity in the Basin is indicated by a number of Pliocene rhyolite domes and flows which project through (e.g. Mt Minden, Mt Maunganui) or are buried beneath ignimbrites and sedimentary strata of Pleistocene age.

In the Basin, local basement consists of Minden Rhyolite (∿ 4.34 m.y. B.P.) and extensive Aongatete Ignimbrite (∿ 1.26 m.y. B.P.). The Aongatete Ignimbrite is subaerially exposed in western areas marginal to the Basin (e.g. in the headwaters of the Aongatete River; Fig. 1.5)., although outcrops are limited, and is part of a sequence of volcanics which testify to an early Pleistocene period of volcanic activity in the Coromandel region. The Aongatete Ignimbrite is unconformably overlain by the Waitearíki Ignimbrite (∿ 0.84 m.y. B.P.) throughout most of the Tauranga area. An arbitrary local basement for this study consists of two welded ignimbrite sheets of Pleistocene age, the Waitearíki Ignimbrite which extensively covers the Whakamarama Plateau, and the Papamoa Ignimbrite (∿ 0.84 m.y. B.P.) which crops out in the Papamoa Hills along the southern margins of the Basin. Both ignimbrites dip gently eastward.

KEY

SEDIMENTARY

	fo	fixed foredunes
	fm	moving dune sand
	h_1, h_2, h_3,	fluviatile terrace deposits
	fa	undifferentiated alluvium
	hn	Hinuera Formation
	ha	fluviatile sands and silts underlying terrace 5 m above base level (interbedded pyroclastic deposits)
Hawera Series	hl	fluviatile sands, silts underlying terraces at 15 m and 22 m above base level (interbedded pyroclastic deposits)
Hawera Series	h_z	fluviatile silts, sands and interbedded pyroclastic deposits underlying terraces at 30 m and 60 above base level
Castlecliffian	Wf + h_z	zst, sst and conglomerate with interbedded pyroclastic deposits underlying terraces older than h_z
Pleistocene/ Pliocene		Te Puke Breccias
	fs	Peat
	h	undifferentiated terrace and fan deposits

VOLCANIC	Age (m.y. B.P.)
Mamaku Ignimbrite	0.14
Waitearikiki Ignimbrite	0.84
Papamoa Ignimbrite	?0.84
Omahia Andesite	-
Minden Rhyolite	4.34
Waitawheta Dacite	∿4.0
Beesons Island Volcanics	16 - 7

OTHER SYMBOLS

- Fault
- Concealed Fault

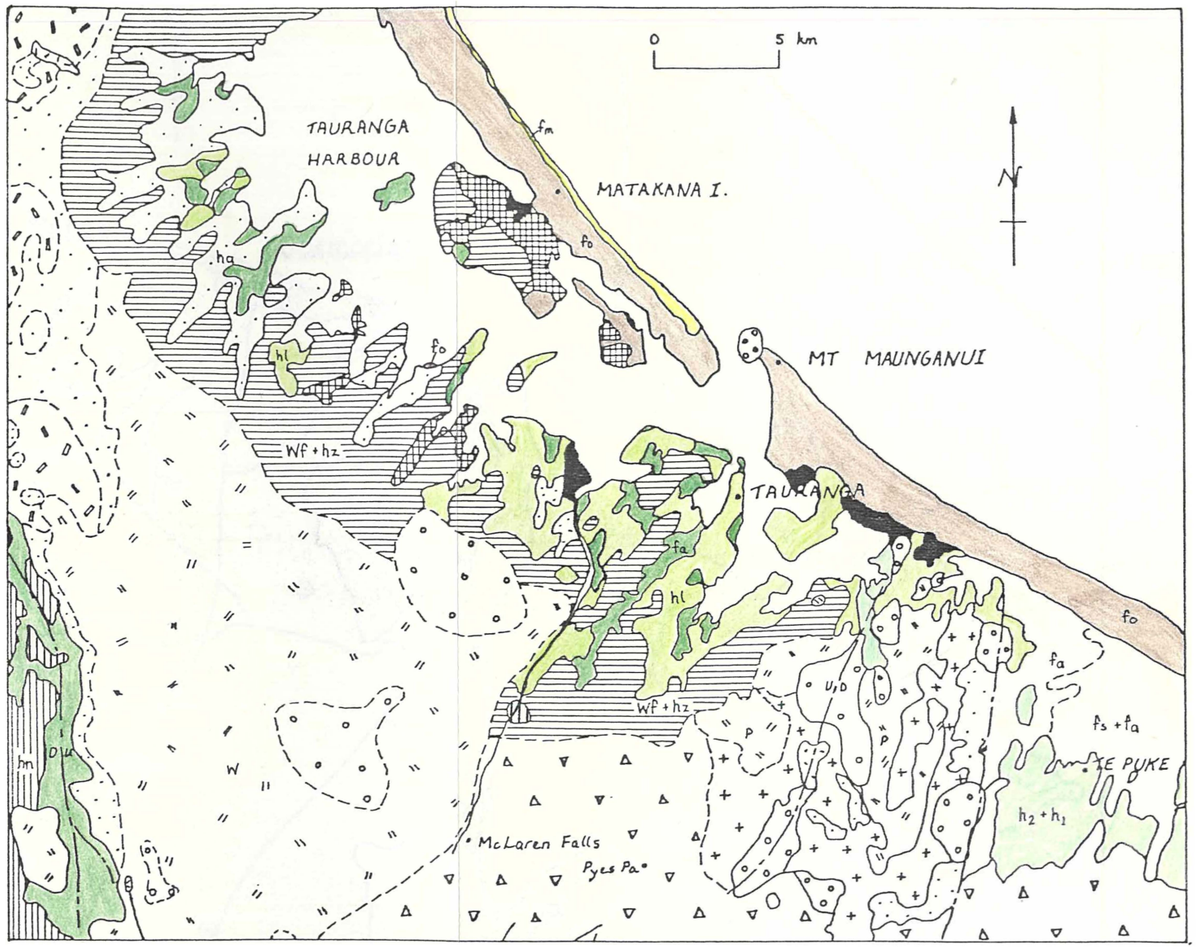


Fig. 1.11: Geology of the Tauranga area

TABLE 1.1 Summary table of geological events in the Tauranga Basin

ERA	SYSTEM/PERIOD	SERIES/EPOCH	AGE	GEOLOGICAL EVENT			
				Volcanic		Sedimentary	
				Pyroclastic air-fall	Pyroclastic flow deposits	Tauranga Basin	Areas outside of Tauranga Basin
			ky. B.P.				
Cenozoic	Quaternary	Holocene	1	Taupo Pumice Lapilli Rotorua Ash			Piako Subgroup
			30 40	Mangaone Lapilli Rotoehu Ash			
			m.y. B.P.				
		Pleistocene	0.10	Hamilton Ash Formation	Mamaku Ignimbrite	upper Matua Subgroup	Tauranga Group: Walton Subgroup
			0.18	Pahoia tephras & tuffs	Waimakariri Ignimbrite		
			0.30		Te Ranga Ignimbrite		
			0.40		Te Puna Ignimbrite		
			0.50			Matua Subgroup *Fluvial and Estuarine* *- silts* *- sands* *- gravels* *Reworked - tuffs* *- tephras*	
			0.60		Wairoa Ignimbrite		
			0.70				
			0.80		Waitearikiki & Papamoa Ignimbrites		
			1.0		Aongatete Ignimbrite		
	Tertiary	Pliocene	2.5				Tauranga Group: Frankton Subgroup
			4.0		Minden Rhyolite		
			5.0				
		Miocene	10.0		Beesons Island Volcanics	Volcaniclastic deposits	Volcaniclastic deposits
			16.0				
Mesozoic		Jurassic				Argillites + Greywackes	Argillites + Greywackes

Volcanic activity has profoundly influenced the type of sedimentation in the Basin throughout the Pleistocene. Several unwelded distal ignimbrite's occur, contributing large quantities of volcaniclastic sediment and becoming intercalated with air-fall tephra and sedimentary units. Late Quaternary ignimbrites have formed the Mamaku Plateau. The sediments infilling the Tauranga Basin are time correlatives of the Tauranga Group (Kear and Schofield, 1978). This group comprises of a thick sequence of Late Cenozoic deposits in the Bay of Plenty, Hauraki and Waikato regions. In the Tauranga Basin, the sediments overlying the Waitepariki Ignimbrite are Castlecliffian and younger in age. However, sediment of a much older age, is presumably intercalated with several volcanic deposits beneath the Waitepariki Ignimbrite.

A summary of major geological events since the Mesozoic is presented in Table 1.1.

1.5 SOILS

Soils of the Tauranga Basin (Fig. 1.12) are derived from weakly to moderately weathered accumulations of rhyolitic ash (Table 1.2). Two main soil types occur (Gibbs and Pullar, 1961), the yellow-brown pumice soils developed on Kaharoa Ash and Taupo Lapilli Ash, and yellow-brown loams developed on a mixture of Late Pleistocene ashes (< 42 ky) named the Waihi Ashes (discussed in detail in Chapter 3). Soils in the Te Puna and Omokoroa areas have been mapped as Katikati black sand loams (Table 1.3; Taylor, 1954). Soils in the Maungatapu area (Fig. 1.12) and south of this area are yellow-brown pumice soils.

1.6 PREVIOUS WORK

Cox (1887) made first note of the Tauranga sediments by referring to them as the "brown Tauranga sands". He believed that they occurred at various localities along the Bay of Plenty coast and made special

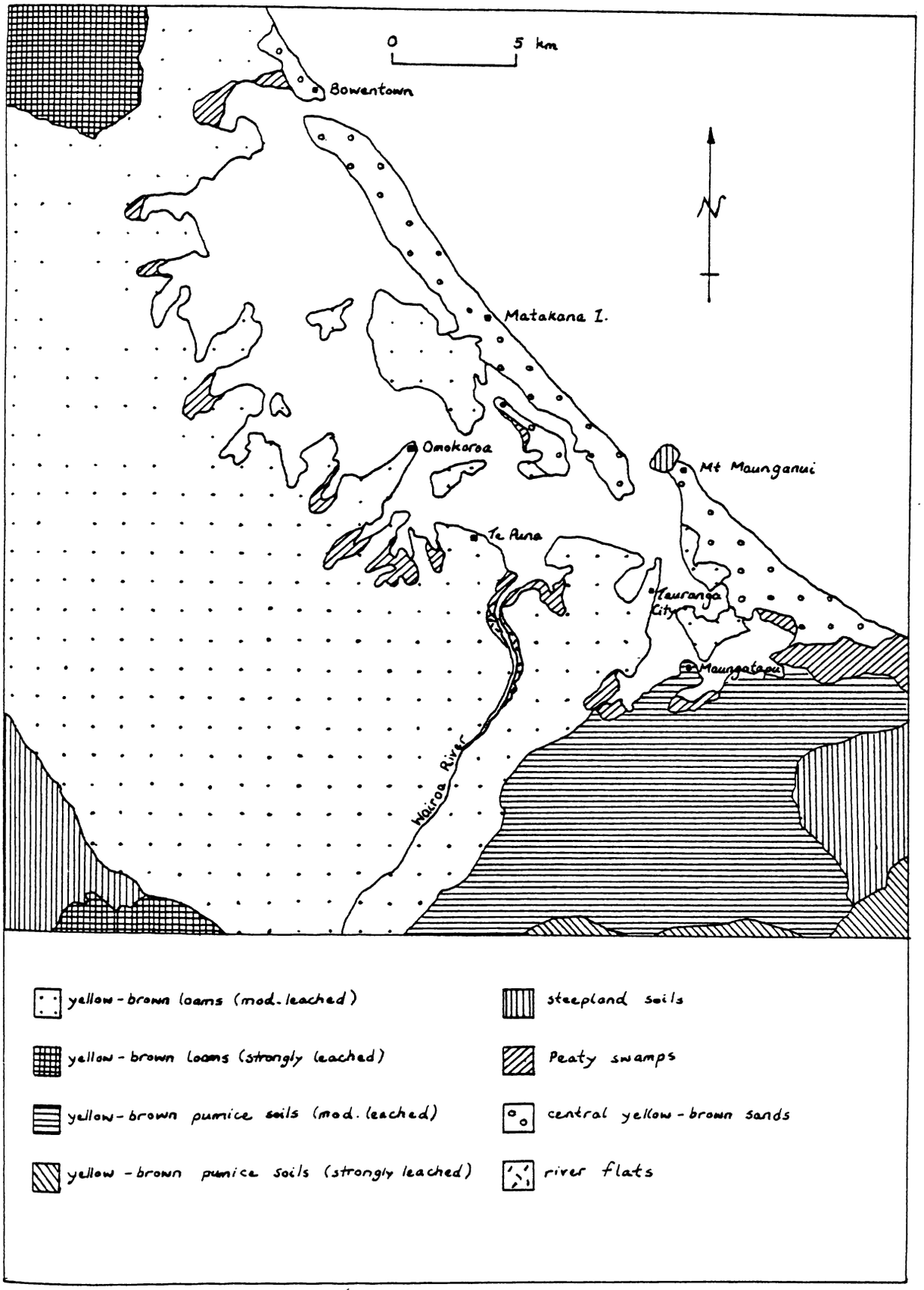


Fig. 1.12 Soil types of the Tauranga area. The distinction between yellow brown loams and yellow brown pumice soils is improved because of recognition of andesitic ash as an inclusion in some rhyolitic tephras (from Gibbs and Pullar, 1961; and Gibbs *et al.*, 1968).

TABLE 1.2 Soil types within the map area and areas adjacent to the Tauranga Basin (after Gibbs *et al.* 1961 and Gibbs *et al.* 1968)

CLASSIFICATION		TOPOGRAPHIC SETTING	AGE	NAME	COMPOSITION	SOIL FORM OF ASH BEDS AND PRINCIPAL EFFECTS	POSITION OF SOIL FORMING PARENT MATERIAL	CLAYS IN SOIL
YELLOW BROWN LOAMS	mod. leached	undulating to flat	~<20 ky	Waihi ashes	rhyolitic and andesitic ashes	gradual deep - rejuvenation	surface and near surface	Allophane Gibbsite Halloysite
	strongly leached	undulating to flat				rapid deep - regeneration	<100 cm	
YELLOW BROWN PUMICE SOILS	mod. leached	undulating to flat	0.94 ky	Kaharoa ashes	rhyolite lapilli and ash	rapid deep - regeneration	surface and near surface	Allophane
	strongly leached	undulating to flat	1.9 ky	Taupo ashes	rhyolite lapilli and ash	rapid deep - regeneration	<100 cm	
STEEPLAND SOILS		steep to undulating	Late Pleist.	sandy loam	rhyolite and andesitic ash and rock		surface and near surface <40 cm	
RECENT SOILS	DUNES	flat (barrier island, low lying peninsulas and islands)	Holocene	yellow brown sands	sand		surface and near surface	
	PEATY SWAMPS	flat (lowlying swamps - mangrove swamps	Holocene	sandy loams to clays (dark brown peaty loams)	estuarine sands and muds and some ash; some alluvial sand	Comment: high organic matter content	surface and near surface	
	RIVER FLATS	flat (estuarine and river terraces)	Late Pleist. to Holocene	deep friable loams, sandy loams, loamy sands	alluvial sands and silts and some ash		surface and near surface	

TABLE 1.3 Soil types within the Tauranga Region (from Taylor 1954)

Name (Parent Material)	Classification	Profile page reference - Taylor 1954	Topographic setting
* Katikati sandy loam [1]	Yellow-Brown Loam	p. - 122	Easy rolling to rolling
* Katikati sandy loam, hill soil [1]	Yellow-Brown loam	p. - 124	Moderately steep to rolling
* Katikati black sandy loam [1]	Yellow-Brown Loam	p. - 124	Flat to easy rolling
* Whakamarama sandy loam [1]	Yellow-Brown Loam	p. - 124	Rolling and strongly rolling
* Whakamarama sandy loam hill soil [3]	Yellow-Brown Loam	p. - 124	Moderately steep
Waitekauri sand and coarse sandy loam, hill soil [2]	Yellow-Brown Loam	p. - 124	Moderately steep to steep
Waitekauri sandy loam, hill soil [4]	Yellow-Brown Loam	p. - 124	Moderately steep to steep
* Te Manaia sandy loam [3]	Yellow-Brown Loam	p. - 124	Rolling to moderately steep
* Oropi shallow sand, hill soil [5]	Primary Podzolic Soil	p. - 78	Moderately steep, broken
* Oropi shallow sand [6]	Primary Podzolic Soil	p. - 78	Easy rolling to rolling
Paengaroa shallow sand [6]	Primary Podzolic Soil	p. - 76	Undulating
Paengaroa sand [6]	Primary Podzolic Soil	p. - 74	Undulating

Parent Material -

1 Waihi Ash
2 Taupo - Kaharoa Ash on Waihi Ash
3 Waihi Ash over rhyolite
4 Waihi Ash on Rhyolite and andesite
5 Kaharoa and Waihi Ash
6 Kaharoa Ash on Waihi Ash

* Soil types within the Tauranga Basin.

reference to Opotiki. This was followed by more extensive geological investigation in the Tauranga Basin by Henderson and Bartrum (1913). Their report concentrated on field descriptions of the sediments, an analysis of "coal" in the area, and a geomorphological outline of the Tauranga Basin. They defined the "Tauranga beds" as a poorly consolidated succession of sands with a "good deal of pumice" included, as well as conglomerates, clays and lignite, all of shallow water origin. The beds were estimated to cover an area of 82 $mile^2$, extending as far north as the Waiau Stream, near Waihi. Kear (1957) noted the pumiceous nature of the Tauranga beds, and assigned a Mid-Pleistocene age of what he described as "richly pumiceous sediments" on the basis of a fossiliferous-marine sequence at Ohope, 90 km to the southeast. The inferred source of the sediments was the Rotorua-Taupo region, Kear adding that "Castlecliffian pumice was deposited in abundance" throughout the North Island and that this rhyolitic source has remained into the Holocene.

Kear and Waterhouse (1961) recognised several terrace levels at Waihi, north of the Tauranga Basin. Pumiceous sediments (i.e. "Tauranga Formation") underlying the oldest aggradational terrace (? 33.5 - ? 35.0 m) were suggested to be correlatives of the "Tauranga beds" of Henderson and Bartrum (1913). They attempted to correlate these terraces with the classical European surfaces of similar altitude, but their investigations did not extend into the Tauranga Basin proper. Healy *et al.* (1964), in their regional 1 : 250,000 scale geological map, gave no group name to the Pleistocene sediments in the Tauranga Basin, but separated them on the basis of lithology and occurrence beneath terraces of different heights. A geological report on the then proposed (1967) Kaimai Railway Tunnel (Healy J., 1967; unpublished report, NZGS, Rotorua) gave a detailed description of volcanic rocks in the area.

The terrace work of Kear and Waterhouse (1961) was extended by Selby *et al.* (1971) using volcanic ashes to distinguish, date and correlate the terraces. They recorded Late Pleistocene ash beds overlying Hamilton and Kauroa Ash beds in the highest surface (? 33.5 - ? 35.0 m) at Waihi. Underlying these ash beds was *in situ* weathered rhyolite. Pullar *et al.* (1973) interpreted a collective unit of older deposits in the Bay of Plenty below the Rotoehu and Hamilton Ashes as undifferentiated white tuffs and named them "Pahoia Tuffs". The type section at Pahoia is situated in the Tauranga Basin. They were described on the basis of colour and texture, and were mapped in the Tauranga Basin with thicknesses totalling 20 m. The relationship between these tuffs and the terrace remnants in the Basin were uncertain and the "tuffs occurred on or were associated with constructional surfaces" (Chappell, 1975). It was reported by Pullar *et al.* (1973) that the Pahoia Tuffs covered pumiceous deposits of Castlecliffian age, and because of their highly weathered nature, were considered to be older than the Hamilton and Kauroa Formations. Investigations of Quaternary warping and uplift rates in the Bay of Plenty by Chappell (1975) involved mapping tephras and tracing these along the coast. By using tephrostratigraphy Chappell (1975, 1978) attempted to date and correlate coastal terraces at Waihi with those in the Tauranga Basin, and at other Bay of Plenty localities. He attributed variations in terrace elevation along the coast to warping.

The Pahoia Tuffs (Pullar *et al.*, 1973) has remained a portmanteau term for tephras beneath the Hamilton Ash along the Bay of Plenty coast. Chappell (1975) referred to undifferentiated pumice in the Tauranga Basin and referred to two new stratigraphic units south of the Tauranga Basin (Little Waihi Formation and the undifferentiated pumice beds) both of which are included in the Pahoia Tuffs. Further investigations of these tuffs were carried out south of the Tauranga Basin at Opotiki

by Kirkman and Pullar (1978) who suggested an age range of 125 ky - 220 ky for the sequence of beds investigated. Vucetich *et al.* (1978) extended their previous work of the lowermost members of the Hamilton Ash Formation (Ohinewai Tephra Formation) into the Tauranga Basin and concluded that the Pahoia Tuffs were older.

The term Tauranga Group (Kear and Schofield, 1978) has been used by many workers, and it was originally proposed by Kear and Schofield (1978) that this term be used for Late Cenozoic terrestrial, estuarine and marine sediments found in the Bay of Plenty, Hauraki and Waikato regions. The reason for producing a collective term such as this was defended by authors (Kear and Schofield, 1978; Stevens, 1980) because a time break and a lithological change occurred at the beginning of the Pliocene in the northern part of the North Island. The Tauranga Group has included Holocene sediments and has been defined such that correlation with the Kaihu Formation of Brothers (1954) is inferred. This latter formation of Pleistocene strata (sands banked locally against an old valley topography cut partly in Pliocene beds) represents a period of submergence in the SW Auckland area where several coastal terraces have been mapped (Brothers, 1954; Chappell, 1970).

More recent work (1979 - 1982) in the Tauranga Basin has included several unpublished reports (NZGS, Rotorua) which record aspects of the stratigraphy of the Tauranga Basin. A continuous cored drillhole at Otumoetai (Houghton, B.F., 1982) and a number of drill-cutting descriptions have provided much scattered data on the subsurface geology of the region. Vucetich *et al.* (1980) described the stratigraphy of a section at Omokoroa and attempted to correlate tephras at this site with those outside the Basin at Tirau. A brief description of processes modifying the geomorphology of the Tauranga area was given by Bird (1981) in a study examining landsliding in coastal areas in the Basin.

Soils in the Tauranga Basin have been mapped by the New Zealand Soil Bureau (Taylor, 1954) and by Gibbs and Pullar (1961), the latter authors describing tephras and associated soil horizons.

CHAPTER TWO

METHODS

2.1 FIELD METHODS

2.1.1 Introduction

After preliminary reconnaissance studies, detailed field examinations were begun in the southern parts of the Tauranga Basin. A number of well exposed coastal cliff sections were chosen for detailed stratigraphic logging (Fig. 2.1), the main sections being at Omokoroa, Te Puna, Matua and Te Ranga on the Pyes Pa Road. Representative samples were collected following completion of stratigraphic columns. Additional sediment data came from other subaerial exposures and drillhole reports (NZGS, Rotorua).

Field work involved:

(1) Mapping of major lithological units and geomorphological features.

(2) Erection of stratigraphic columns from both field exposures and drillhole reports.

(3) Describing a number of lithofacies (based on structure/texture/composition) for paleoenvironmental data.

2.1.2 Mapping Method

Field mapping was carried out from December 1981 to March 1982. Aerial photographs of 1 : 18,300, 1 : 25,000, and 1 : 50,000 scales were used to locate outcrops and for the mapping of terraces and other geomorphological features (e.g. paleochannels) within the Basin. A large number of samples were collected at inland sites with the intention that their sedimentological and mineralogical properties might enable correlation with samples from the coastal sections.

Several distal ignimbrites were recognised in the Basin and a major part of the study was designed to map both pyroclastic flow and airfall

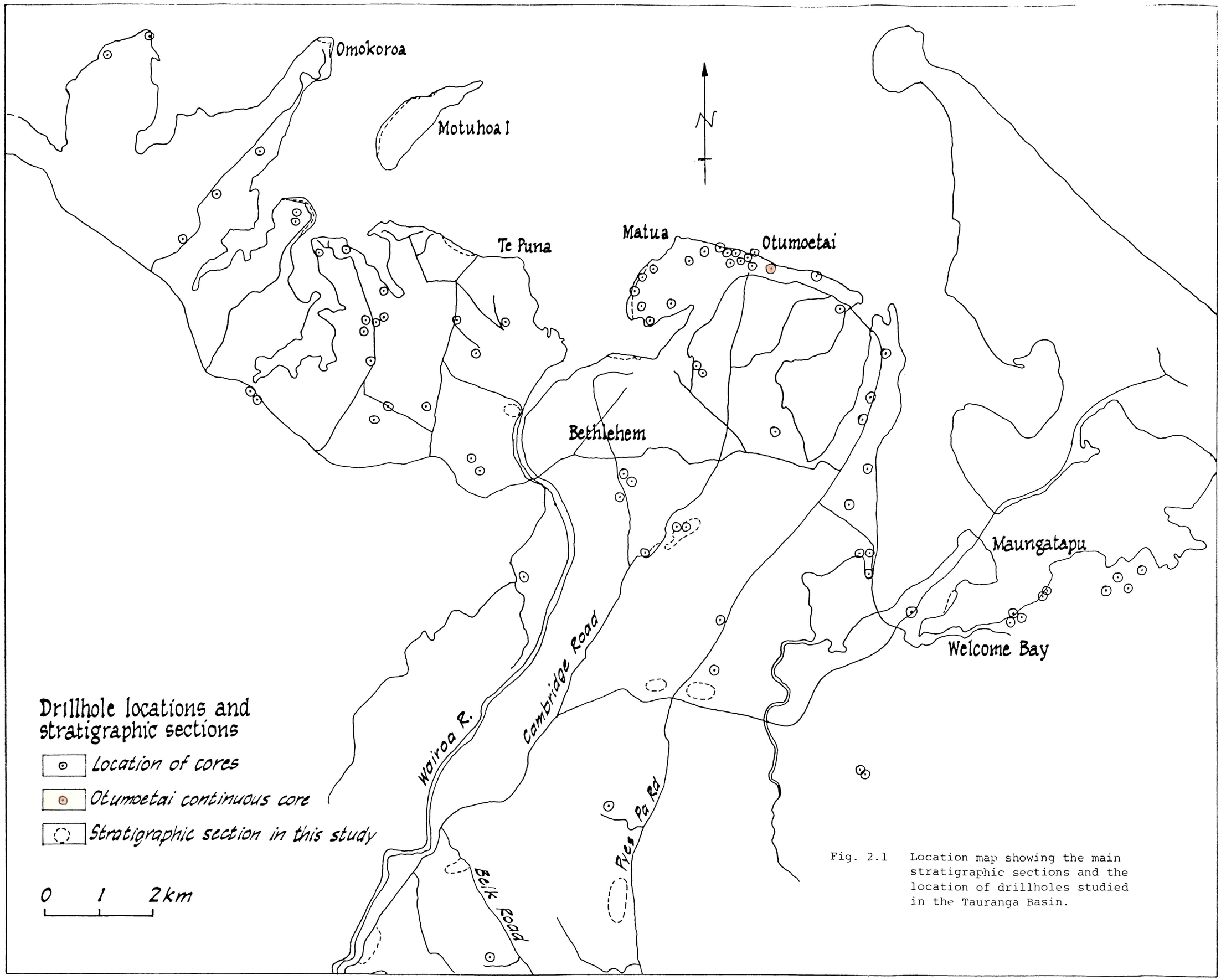


Fig. 2.1 Location map showing the main stratigraphic sections and the location of drillholes studied in the Tauranga Basin.

deposits and to establish the provenance of the fluvial sediments in areas proximal to, and at the coast. Initial mapping was carried out using a 1 : 12,500 scale base map and field data were subsequently transferred onto a 1 : 25,000 map covering an area from Omokoroa to Welcome Bay along the coast and extending inland along the Wairoa River and across to Belks Road and Pyes Pa Road (map folio at back of thesis). A large part of the field work concentrated on describing structures in the sedimentary and pyroclastic deposits.

(i) References for maps used in this study

Maps referenced in this study are:

(i) N.Z. Geol. Map, 1 : 250,000, Sheet 5, Healy *et al.* 1964.

(ii) NZMS (topographical) 260, Sheet U14, Tauranga, 1 : 50,000, Lands and Survey, 1980.

2.1.3 Mapping of terraces

A number of methods was employed to map terraces in the Tauranga Basin:

(1) A 3 m staff rod and measuring tape were used to establish terrace heights < ∿30 m in areas near the coast.

(2) A contour map of the area was drawn using 1 : 50,000 and 1 : 12,500 maps. The aerial extent and elevation were checked using aerial photographs with scales of 1 : 18,300 and 1 : 25,000 and further mapping was undertaken using a stereoscope.

(3) Contour data were plotted onto a 30 cm x 20 cm table divided into 1 cm grids. At the intersection of each grid line, a contour value was entered and digitised for computer analysis. These digitised contour values were then entered into the computer using TOPOGRAPHY (FORTRAN 77 + NCAR Graphics

modelling programme (W. de Lange, pers. comm. 1982, University of Waikato). The three dimensional models which can be viewed obliquely enabled a check to be made on terraces with similar elevation.

2.2 LABORATORY METHODS

2.2.1 Introduction

Samples collected in the Basin ranged from consolidated to unconsolidated and, except for those with a high clay content, most could be disaggregated using only moderate to light pressure. Because of the highly pumiceous nature of these sediments, slight modifications were made to some analytical methods which otherwise follow the standard procedures (Fig. 2.2) outlined by Müller (1967), Folk (1968), and Carver (1971).

2.2.2 Textural analysis

Disaggregation of harder sediments was achieved by soaking samples for 48 hr in distilled water. All samples were then wet sieved through a 4ϕ mesh screen and muds were collected and weighed by a decantation process. Grain size analysis of this mud fraction was made using the pipette method (Carver, 1971). The weight of the mud was also established by removing 20 ml of the fluid after 20 sec. at 20 cm depth, and then drying before weighing (Carver, 1971).

Size fractions coarser than 4ϕ were dried at 50^{o}C and dry sieved at 0.25ϕ intervals on an Endecott (T.S.) sieve shaker. Samples were split into sand and gravel fractions for textural classification (Table 2.1). Because of the high proportion of pumice in most samples sieving time was reduced to 3 minutes to prevent excessive size modification (Walker, 1971). Raw data were converted into a representative form by

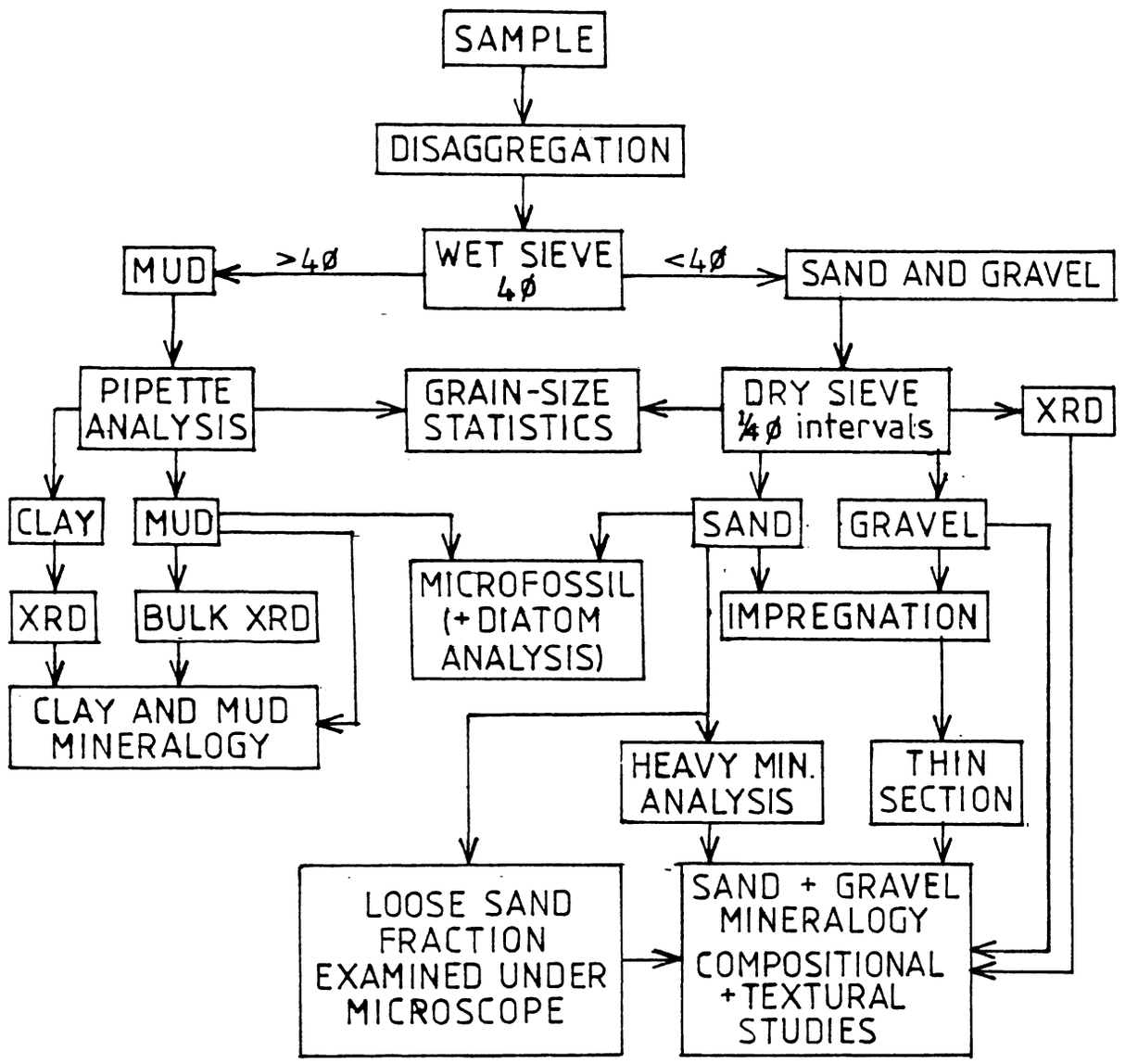


Fig. 2.2 Laboratory techniques for sample analysis.

Limiting particle diameter					
mm	φ units		Size class		
2048	−11		Very large	Boulders	GRAVEL
1024	−10		Large		
512	− 9		Medium		
256	− 8		Small		
128	− 7		Large	Cobbles	
64	− 6		Small		
32	− 5		Very coarse	Pebbles	
16	− 4		Coarse		
8	− 3		Medium		
4	− 2		Fine		
2	− 1		Very fine	Granules	
1	0		Very coarse	Sand	
1/2	+ 1	500 μm	Coarse		
1/4	+ 2	250	Medium		
1/8	+ 3	125	Fine		
1/16	+ 4	62	Very fine		
1/32	+ 5	31	Very coarse	Silt	MUD
1/64	+ 6	16	Coarse		
1/128	+ 7	8	Medium		
1/256	+ 8	4	Fine		
1/512	+ 9	2	Very fine		
				Clay	

Table 2.1 Grain-size scale (after Wentworth 1922) showing the millimeter and equivalent phi (ϕ) unit limits to each size class (after Folk *et al.*, 1970).

statistical analysis following procedures described by Folk (1968), Walker (1971), Carver (1971) and Pettijohn (1975). The parameters determined included the graphic mean, inclusive graphic standard deviation, inclusive graphic skewness, and graphic kurtosis (Fig. 2.3). Data are summarised on grain size distribution plots.

2.2.3 Compositional analysis

Petrographic analysis involved separating samples into three size fractions, -2 to 0ϕ (gravel and very coarse sand), 0 to 2ϕ (medium and coarse sand), and 2 to 4ϕ (fine and very fine sand). A microsplit of the sediments was then made and thin sections were prepared using an impregnation technique (Bergin, S., pers. comm., 1982, University of Waikato). Approximately 500 grains were then point counted in slides. A loose sand fraction sample, -1 to 4ϕ (very coarse sand to very fine sand), was also retained for point counting. 500 grains were analysed (e.g. surface texture and shape) and counted on a grid under a binocular microscope (x 10 and x 40 magnification). Total phenocryst content (calculated as whole rock) was then compared to that calculated from thin sections.

Rock fragment analysis was conducted separately with selected samples but followed a similar procedure, using size classes < -1ϕ and -1 to 2ϕ. Splits of non-pumiceous material were impregnated and 300 grains counted (Carver, 1971) under a petrographic microscope to establish rock fragment compositional types. Comparative analysis again was conducted using loose sediment samples under a binocular microscope.

Heavy mineral assemblages were concentrated by passing a weighed 2 - 4ϕ fraction through tetrabromoethane (T.B.E.) liquid (S.G. = 2.96). Following separation, the sample was washed and dried and grains were weighed and mounted in Canada Balsam. Detrital slides were then examined under a petrographic microscope and 500 point counts recorded. For

Graphic Mean

$$M_z = \frac{\phi 16 + \phi 50 + \phi 84}{3}$$

Inclusive Graphic Standard Deviation

$$\sigma_I = \frac{\phi 84 - \phi 16}{4} + \frac{\phi 95 - \phi 5}{6.6}$$

Verbal Classification:

σ_I under 0.35ϕ	very well sorted (vws)
0.35 to 0.50ϕ	well sorted (ws)
0.50 to 0.71ϕ	moderately well sorted (mws)
0.71 to 1.0ϕ	moderately sorted (ms)
1.0 to 2.0ϕ	poorly sorted (ps)
2.0 to 4.0ϕ	very poorly sorted (vps)
over 4.0ϕ	extremely poorly sorted (eps)

Inclusive Graphic Skewness

$$Sk_I = \frac{\phi 16 + \phi 84 - 2\phi 50}{2(\phi 84 - \phi 16)} + \frac{\phi 5 + \phi 95 - 2\phi 50}{2(\phi 95 - \phi 5)}$$

Verbal Classification:

Sk_I from +1.00 to +0.30	strongly fine-skewed (sfs)
+0.30 to +0.10	fine-skewed (fs)
+0.10 to -0.10	near-symmetrical (ns)
-0.10 to -0.30	coarse-skewed (cs)
-0.30 to -1.00	strongly coarse-skewed (scs)

Graphic Kurtosis

$$K_G = \frac{\phi 95 - \phi 5}{2.44(\phi 75 - \phi 25)}$$

Verbal classification:

K_G under 0.67	very platykurtic (vpk)
0.67 to 0.90	platykurtic (pk)
0.90 to 1.11	mesokurtic (mk)
1.11 to 1.50	leptokurtic (lk)
1.50 to 3.00	very leptokurtic (vlk)
over 3.00	extremely leptokurtic (elk)

Fig. 2.3 Statistical Parameters (after Folk, 1968)

comparative study, pumice blocks were extracted from selected samples (collected at stratigraphic sections) and crushed. Heavy minerals in the pumice were then subject to the same analytical procedure outlined above, with the intention of elucidating provenance.

(i) X.R.D.

The mineralogy of the sand and mud fractions was determined by X-ray diffraction using a Philips P.W. 1050 X-ray diffraction spectrometer (Hume and Nelson, 1982). Samples were prepared by grinding sediments in a 12 cm twin head Gilko (model LRM) ring mill for 10 sec. so that the material became reduced to a particle size between ∿8 - 40 μm (Nelson and Cochrane, 1970). The powder was loaded into sample holders by the back-filling technique. Machine settings used were kV 35.0, mA 15.0, rate meter setting 400 cps, time constant 4 sec.

Semi-quantitative estimates of abundances were obtained for plagioclase, quartz and clay minerals using crushed bulk samples, bulk mud samples and separate grain size class samples. Determinations of wt% quartz were made using the peak at 4.26 Å, of wt% plagioclase at 3.20 Å and wt% clay at 4.46 Å. The weight percent of each mineral was established by measuring the peak height above background and reading the value off intensity-concentration curves (Hume, 1978; Hume and Nelson, 1982; this study; Figs. 2.4 and 2.5). Because of the high glass content (Lister, 1978; Hume and Nelson, 1982) in many of the Tauranga Basin deposits, intensity concentration curves were drawn in this study using known wt% of glass, quartz and feldspar (Figure 2.5). It is known that amorphous materials have a significant absorption effect on X-rays (Hume and Nelson, 1982) so that the I - C graphs of Fig. 2.4 typically underestimate the actual wt% of minerals in such samples.

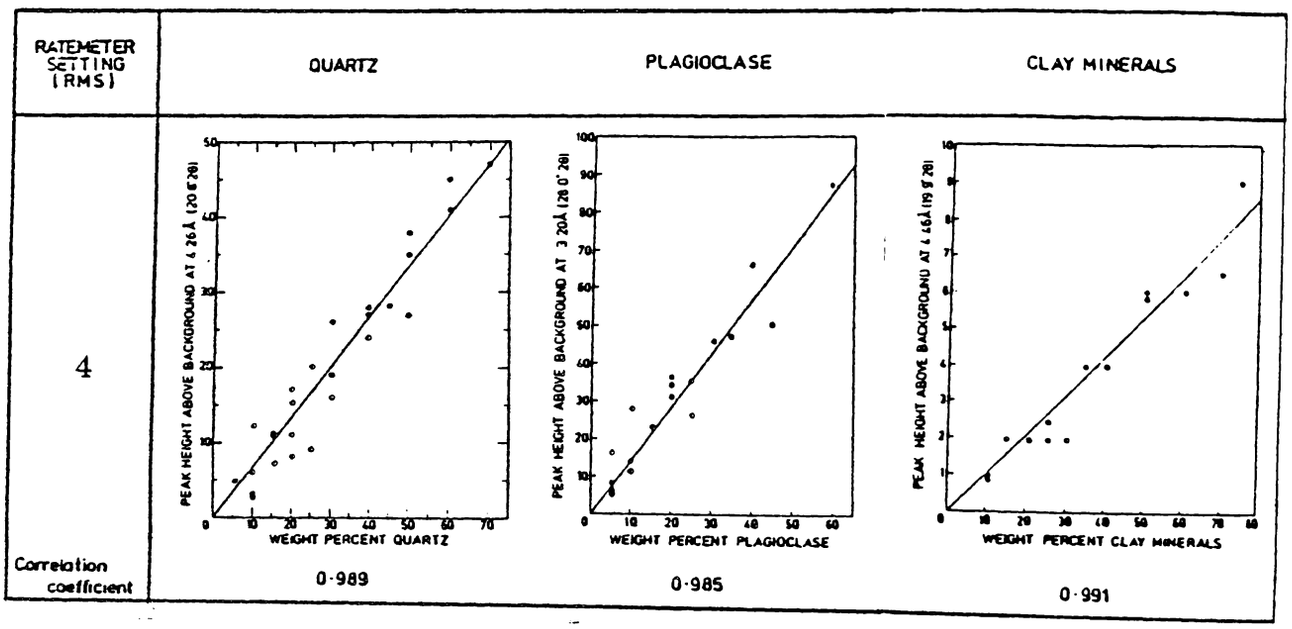
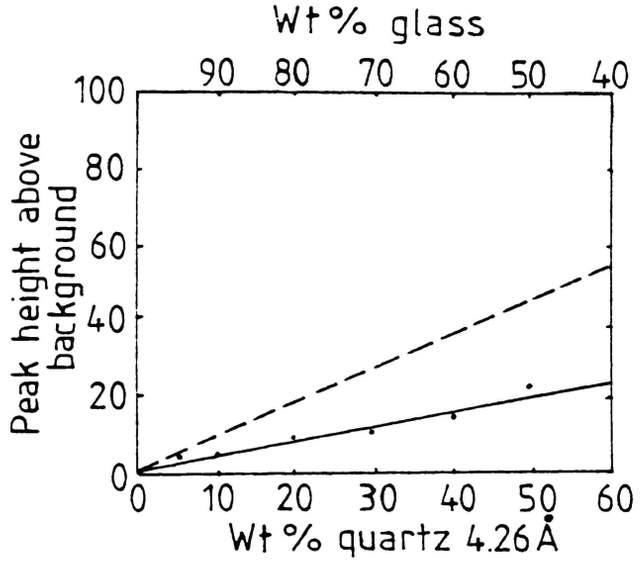
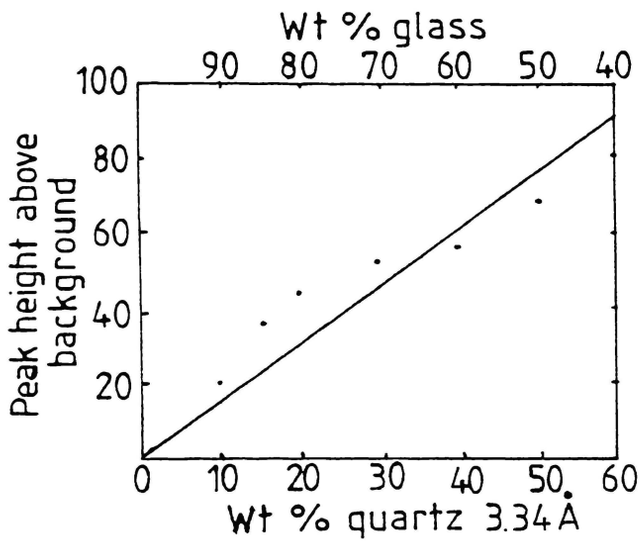
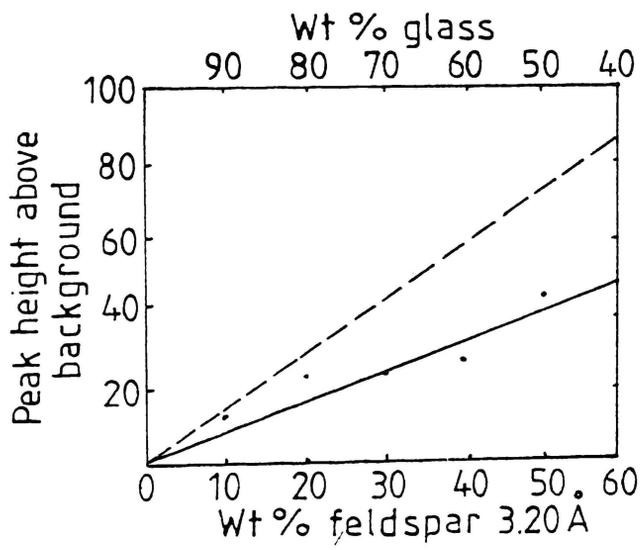


Fig. 2.4 XRD intensity-concentration plots for quartz, plagioclase feldspar and clay minerals at rate meter settings of 4.0. Linear coefficients are at the 95% significance (Hume and Nelson, 1982).









Dashed line corresponds with the curves produced in Fig. 2.4.

Fig. 2.5 XRD intensity-concentration curves for quartz and plagioclase feldspar from the Tauranga Basin deposits. These curves were produced following mixing of each mineral with crushed (<30μm) pumice, in weight percent ratios from 0-60% mineral at 10% intervals.

The possibility existed that the grains within each sample may have been derived from a number of potential sources. Therefore multiple and single clast samples were analysed and compared with size classes <2.0ϕ and between 2ϕ - 4ϕ. Bulk samples were scanned from 4^{o} to 36^{o} 2θ following calibration with a quartz standard prepared by Hume (1978).

(ii) X.R.D. Clay mineralogy

Estimates of clay mineral abundances were interpreted using the average background level of intensity concentration curves (Hume and Nelson, 1982). Clay fractions concentrated during the pipette analysis were mounted onto glass slides using the dropper technique (Hume and Nelson, 1982). Samples were dried under an infrared lamp and placed in a desiccator containing H_2O before being scanned. Untreated samples were scanned from 3^{o} - 29^{o} 2θ and rescanned from 3^{o} - 20^{o} 2θ after glycolation and again after heating to 550^{o}C for 1 hour. Diffractometer traces were then compared for observable shifts and differences in peaks and peak heights. This followed methods described by Hume (1978) and Hume and Nelson (1982) and enabled identification particularly of halloysite, kaolinite, and mixed-layer clays, along with their relative abundances.

2.2.4 Microfossil analysis

Fossils give an indication of previous environments and conditions prevailing after sediment deposition. Sample splits were gently broken down in water and the mud fraction was separated using a 75 µm mesh sieve.

(i) For diatom analysis selected samples were taken from this mud fraction, diluted ten times and passed through a millipore filter (0.45 µm) before being examined under a binocular microscope at x 40, x 100 and x 400 magnifications. Analysis required the use of an eyepiece grid and stage micrometer.

A second method used involved drying a few drops of diluted mud solution onto a circular glass coverslip, the "precipitate" being kept to sediment thickness of 1 grain. The coverslip was then immersed in Pleurax resin which has a high refractive index. If diatoms were detected a 50 cc fraction was retained for identification purposes.

(ii) For foraminiferal analysis, the sand fraction was dried at room temperature and a 100 cc microsplit made (Dr B.W. Hayward, pers. comm., Micropaleontology Section, NZGS, Lower Hutt, 1982). However no microfossils were found in the sediments analysed.

CHAPTER THREE

STRATIGRAPHY OF THE TAURANGA BASIN AND ADJACENT AREAS

3.1 INTRODUCTION

A major aim of this thesis was the compilation of detailed stratigraphic columns of coastal exposures in the Tauranga Basin, as well as construction of columns using information from inland borehole data (NZGS, Rotorua); these columns are reproduced in Appendix I. To accompany these stratigraphic descriptions a 1 : 25,000 geological map with associated cross sections has been produced for a part of the Tauranga Basin (see map folio). The ultimate goal was to establish a general history of geological events in the Basin and to place these events within the framework of an evolving sedimentary model.

3.2 STRATIGRAPHIC USAGE

Conventional stratigraphic terminology is used except that the formal name Matua Subgroup is proposed for the Quaternary deposits in the Tauranga Basin (see section 3.4.13). A lower time constraint of (0.84 m.y. B.P.) is imposed on this sequence by the local arbitary basement Waitea riki Ignimbrite. The Matua Subgroup comprises all those deposits above the Waitea riki Ignimbrite. It is dominated by fluvial and pyroclastic flow deposits but includes also a number of air-fall tephra deposits, particularly in the upper parts of the subgroup (∿ the upper 40 m). Air-fall tephra deposits which are intercalated with or overlying fluvial sediments in the upper part of the Matua Subgroup but beneath the Hamilton Ash Formation (Ward, 1967) are referred to as the Pahoia tephras. The name Pahoia tephras is used principally for air-fall tephra deposits which include some pyroclastic-flow deposits, the collective sequence being previously referred to by Pullar *et al.* (1973) as the Pahoia Tuffs in the Tauranga Basin.

The informal name upper Matua Subgroup is used for those deposits which are subaerially exposed in the Basin, especially those described in some detail from the coastal stratigraphic sections.

3.3. STRATIGRAPHY

A generalised stratigraphic column for the Tauranga Basin (Fig. 3.1) shows a varied sequence of sediments, ignimbrites and air-fall tephras.

A number of ignimbrites are subaerially exposed in or at the margins of the Tauranga Basin and/or recorded in the subsurface stratigraphy of the Basin. The Aongatete Ignimbrite (∿ 1.26 - 0.86 m.y. B.P.) was previously described by Healy (1967) as being a member of a set of volcanics (i.e. Aongatete Volcanics). This ignimbrite is recorded at or near the base of drillholes (∿ 200 m depth) throughout the Basin and is subaerially exposed west of the Basin. The Papamoa Ignimbrite (∿ 0.84 m.y. B.P.) bounds the Basin to the South (Healy *et al.*, 1964). The Waitearíki Ignimbrite (0.84 m.y. B.P.) forms the Whakamarama Plateau west of the Basin (Healy *et al.*, 1964), and stratigraphically overlies the Aongatete Ignimbrite as shown by borehole data, and subaerial stratigraphy.

In the study area (map folio at back of thesis) three new subaerially exposed unwelded ignimbrites have been identified and named according to their geographic locality : the Wairoa Ignimbrite, the Te Puna Ignimbrite and the Te Ranga Ignimbrite. A fourth new moderately welded ignimbrite identified in the area, is the previously named, Waimakariri Ignimbrite (Fransen, 1982). They are interpreted as distal ignimbrites and are intercalated with Matua Subgroup fluvial and air-fall deposits. Based on stratigraphic association with the dated Waitearíki Ignimbrite and the degree of weathering and paleosol

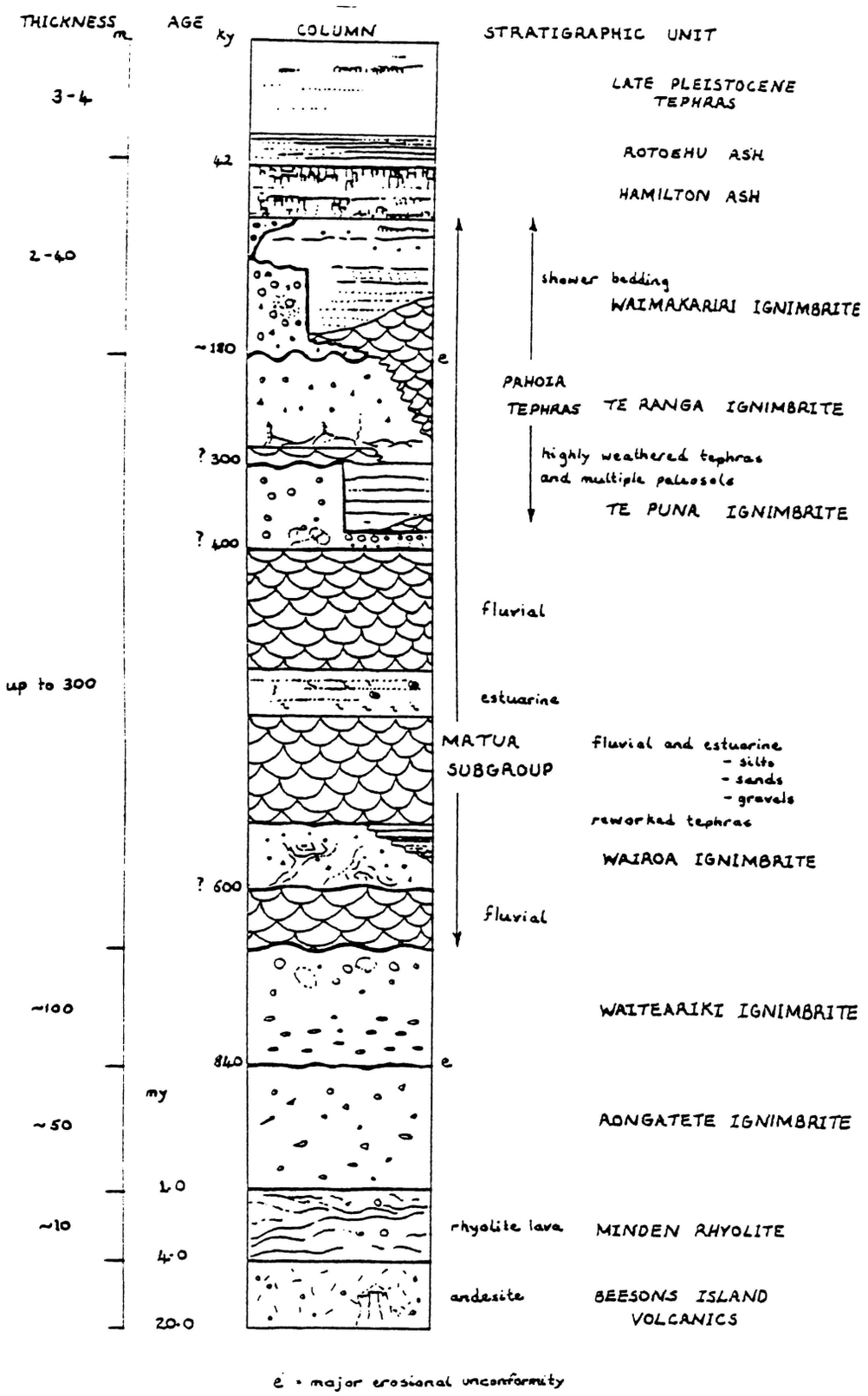


Fig. 3.1 Stratigraphic column for the Tauranga Basin showing a number of ignimbrite formations intercalated with fluvial sediments within and below the Matua Subgroup.

development at Sharp Road (N35/4171) and at the Tauranga dump (N35/6056), the Wairoa Ignimbrite is considered the oldest of the three units. An age of between ∿ 0.30 m.y. B.P. and ∿ 0.50 m.y. B.P. is suggested for the Te Puna Ignimbrite. This is based on air-fall tephra cover, paleosol development and a chalazoidite bed exposed at a number of sites in the Basin. The Te Ranga Ignimbrite is separated from the overlying Waimakariri Ignimbrite (Fransen, 1982) by an erosional unconformity, and is therefore considered to be the youngest (> ∿ 0.18 m.y. B.P. an age suggested for the Waimakariri Ignimbrite, Fransen, 1982).

The pyroclastic and sedimentary deposits exposed in the Tauranga area are described in the following section (Table 3.1). The major distinguishing features of principal ignimbrites exposed within the Tauranga Basin are presented in Table 3.2.

3.4 LITHOLOGIC DESCRIPTIONS

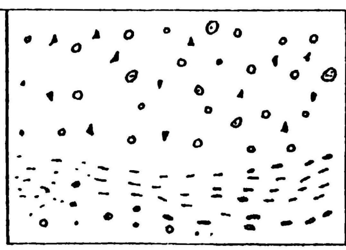
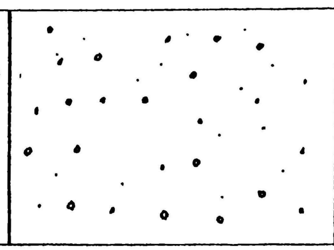
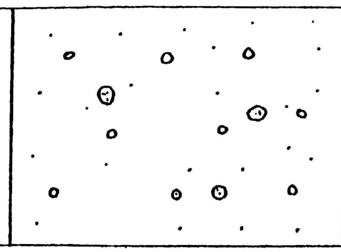
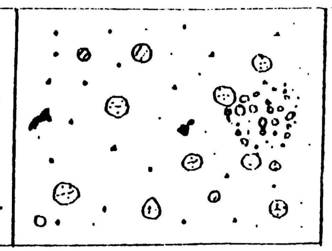
3.4.1 BEESONS ISLAND VOLCANICS

The Beesons Island Volcanics (Healy *et al.*, 1964; Schofield, 1973) or Coromandel Group (Skinner, 1976) are of Mid-Miocene to Late-Miocene age, and stratigraphically underlie the Minden Rhyolite in the Tauranga Basin (Healy *et al.*, 1964; Schofield, 1973). K-Ar ages range from about 16-7 m.y. B.P. (Richards *et al.*, 1966; Adams 1975; Rutherford, 1978; Cole, 1979). The Volcanics comprise of an extensive pile of andesitic to dacitic flows and plugs, volcanic epiclastics as breccias and lacustrine sediments and less common pyroclastics (Skinner, 1976). Andesites, some of which are propylitised, crop out west of the Basin in the Kaimai Range and to the south in the Papamoa Hills. Rocks are often red-grey and are dominantly hornblende-bearing hypersthene andesites, usually with some augite; however, hornblende

TABLE 3.1 Stratigraphy of the Tauranga Region

AGE m.y. B.P.	SYSTEMS/PERIOD	SERIES/EPOCH	VOLCANIC UNITS	MEMBER	SEDIMENTARY UNITS	
					Group	Subgroup
0.01	QUATERNARY	HOLOCENE			Tauranga Group	Matua Subgroup
0.1		PLEISTOCENE	Mamaku Ignimbrite (0.14)			
0.2			Waimakariri Ignimbrite (0.18)			
0.3			Te Ranga Ignimbrite (∿0.3)			
			Te Puna Ignimbrite (∿0.4)			
0.6			Wairoa Ignimbrite (∿0.6)			
0.8			Waitetariki Ignimbrite (0.84)	Upper Sheet (iv) (iii)		
1.0			Papamoa Ignimbrite (∿0.84)	Lower Sheet (ii) (i)	?	
1.2			Aongatete Ignimbrite (1.26)	(iii)		
			Aongatete Volcanics	(ii)		
1.6				(i)		
1.8	TERTIARY	PLIOCENE				
2.0						
3.0			Waitawheta Dacite (3.75-4.0)			
4.0			Minden Rhyolite (4.34)			
5.0		MIOCENE				
10.0						
15.0			Beesons Island Volcanics (7.0 - 16.0)		Beesons Island Volcaniclastic deposits	
22.5						

TABLE 3.2 Major distinguishing features of principal ignimbrites subaerially exposed within the Tauranga Basin

	Old ———	———	———	———	———► Young
Ignimbrite	Waiteariki	Wairoa	Te Puna	Te Ranga	Waimakariri
Welding condition	strongly welded to nonwelded	nonwelded	nonwelded	nonwelded	nonwelded to moderate
Outcrop characterisation	nonwelded upper breccia and sheetlike strongly welded lenticulite exposes in streams	consolidated deposits showing leisegang phenomena	forms thick lobes and thin pyroclastic flows	consolidated but very permeable material cropping out in valleys	high white to yellow coloured cliffs
Colour (matrix)	reddish brown to grey	yellow to brown	yellow to white	grey	yellow; tan
Colour (pumice)	white to brown	yellow to brown	white	white to red	yellow
Pumice (size)	variable	medium sand to fine gravel	variable	variable	variable
Pumice (state)	vitric	vitric	vitric	vitric	vitric
Total phenocryst abundance	? 15%	18.20	7.43	10.33	5.96
plag.		9.85	5.41	7.61	4.21
quartz.		6.38	1.11	1.74	0.74
hyp.		0.36	0.20	0.18	0.36
horn.		0.67	0.30	.05	0.12
mag.		0.93	0.35	0.74	0.53
biotite		0.06	0.07		tr
Other features	andesitic lithics	rhyolitic lithics	rhyolitic lithics	elutriation channels segregation structures charcoal	segregation structures textural concentration zones; charcoal
Texture					

is rare in basal members (Skinner, 1976). Quartz and biotite are present in uppermost members where the rock is crystal-rich.

3.4.2 MINDEN RHYOLITE

Minden Rhyolite of Pliocene age (Healy *et al.*, 1964; Schofield, 1967; Skinner, 1976) stratigraphically overlies extensive andesitic eruptives (Beensons Island Volcanics) and drillhole information (Fig. 3.7) indicates that the Minden Rhyolite flows stratigraphically underlie the Aongatete Ignimbrite (0.86 - ∿ 1.26 m.y. B.P., Healy, 1967). The Minden Rhyolite in the Tauranga Basin has an age of ∿ 4.34 m.y. B.P. based on a fission track date on obsidians from Mt Maunganui (Rutherford, 1978). In some areas west of the Basin, the rhyolites are locally intruded and overlain by Waitawheta Dacite of Early-Pliocene age.

The subgroup name "Minden Rhyolite" (Skinner, 1976) has been used by Healy *et al.* (1964) and Schofield (1967) to include all lithoidal and spherulitic, hypersthene-hornblende-biotite rhyolites north of the Taupo Volcanic Zone. In the Basin the subgroup includes conspicuous domes, rhyolite flows and pumice breccias (Healy, 1967). Phenocrysts (slide WT 18487) are dominated by quartz and plagioclase with subordinate hornblende and hypersthene. The groundmass also consists of these minerals.

Rhyolite domes protrude through the ignimbrites and sedimentary deposits at several localities in the Tauranga Basin. For example, Mt Minden (286 m; N.Z. Geol. Map 1 : 250,000, Sheet 5 GR N35/5357) dome occurs on the western margin of the study area where the pale red-grey fine-grained rhyolite containing visible quartz is well exposed in a quarry at Te Puna. Exposures in road cuttings around the mountain are highly weathered. Rhyolite domes within the Tauranga Basin (i.e. Mt Maunganui and Mt Minden) are possibly part of a large

volcanic complex extending north and south of the Basin and west of the Whakamarama Plateau. Numerous glassy and spherulitic rhyolite clasts (0.1 - 8 cm diameter) occur in streams and in fluvial deposits in the vicinity (5 km radius) of the rhyolite dome. Indeed, rhyolite clasts (banded, lithoidal and spherulitic varieties) occur in fluvial deposits throughout the Basin and may be derived from several sources to the west of the Basin and from within the Basin (e.g. ignimbrite sheets and rhyolite domes).

3.4.3 WAITAWHETA DACITE

The Waitawheta Dacite (Healy *et al.*, 1964) of Early Pliocene age (Rutherford, 1978) is a series of dacitic lavas and pyroclastic (ignimbrite) deposits which overlie Beesons Island Volcanics cropping out west and northwest of the mapped area. They are exposed in the headwaters of a number of streams which discharge into the Katikati area (N.Z. Geol. Map 1 : 250 000, Sheet 5 GR N35/3875). The dacites contain phenocrysts of plagioclase, hypersthene, hornblende and corroded quartz and show spherulitic, glassy and perlitic textural varieties (Healy *et al.*, 1964; Healy, 1967).

3.4.4 AONGATETE VOLCANICS

Stratigraphic definition

The Aongatete Volcanics (e.g. see Table 3.1) comprise of tuffs, breccias and ignimbrite (Healy, 1967). The term is synonomous with the Aongatete Ignimbrite, which is the main member. The Volcanics which overlie Beesons Island Volcanics west of the Basin, and stratigraphically overlie Minden Rhyolite in the Basin, have fission track ages between 1.26 and 0.86 m.y. B.P. (Healy, 1967). The volcanics dip eastward, and are considered to have been derived from a Coromandel source, as suggested by thickening away from the Basin towards the

west. They are exposed west and northwest of the mapped area in streams which cut through the Whakamarama Plateau and are separated from the overlying Waitea riki Ignimbrite (c. 0.84 m.y. B.P.) by an erosional unconformity. The Aongatete Ignimbrite occurs at or near the base of several drillholes in the Tauranga Basin and overlies Minden Rhyolite in some drillholes. Drillhole data also confirm thinning of the ignimbrite over the Minden Rhyolite (Houghton, 1982).

Lithology

The volcanics have a variable composition, predominantly dacitic, but also rhyolitic and andesitic. Healy (1967) has subdivided them into three main units:

(i) Lower tuffs and breccias

(ii) Aongatete Ignimbrite

(iii) Upper tuffs and breccias

The Aongatete Ignimbrite possibly consists of a number of flows.

Petrography

Mineralogically they are quite similar to the overlying Waite-ariki Ignimbrite, but they have a lower crystal content and quartz may be absent or rare. In the Aongatete Ignimbrite (middle unit) and basal units of the volcanics the dominant phenocryst is plagio-clase, with subordinate hypersthene and minor augite and magnetite. In upper members of the volcanics, hornblende occurs with minor magnetite. The dominant xenolith is pumice (Healy, 1967).

3.4.5 WAITEAKIRI IGNIMBRITE

Stratigraphic definition

Crystal tuffs of the Whakamarama plateau were mapped separately from the Waitawheta Dacites by Healy *et al.* (1964) and given the name

Waiteariki Ignimbrite. The ignimbrite was given a fission track age of 0.84 m.y. B.P. (Kohn, unpublished). The Waiteariki Ignimbrite was thought by Briggs (1973) to have flowed from a source near the crest of the present Kaimai Range, but mapping evidence and coarsening of lithics away from the Basin suggest a more southerly source (B.F. Houghton, pers. comm. 1982). Upon entering the Tauranga Basin the ignimbrite flowed firstly north and then east and its present form abuts against the Kaimai Range (Chapter 4). Borehole data (Fig. 3.7) and subaerial exposure shows that the Waiteariki Ignimbrite overlies the Aongatete Ignimbrite and is in turn overlain by a thick (∿ 150 m) sequence of fluvial sediments, estuarine deposits, and pyroclastic deposits. As such it is convenient to regard the Waiteariki Ignimbrite as a local basement rock in the Tauranga Basin.

Lithology

The Waiteariki Ignimbrite consists of a number of crystal-rich dacitic flows which have been informally divided into four lithologic units (Healy, 1967), the middle two of which are hard and have a characteristic lenticular texture:

(i) A poorly compacted pumice breccia and soft ash (basal ash) with a thickness of 5 m.

(ii) The main unit comprising welded lenticulite with a max. thickness of 120 m.

(iii) A well compacted to hard ignimbrite 20 - 35 m thick.

(iv) An upper pumice breccia (poor to well compacted) 70 m thick.

The hard ignimbrite and parts of the welded ignimbrite contain light coloured (light grey to light brown) coarse lithics (∿ 1 to 20 mm) set in a dark blue-grey to brown matrix. Flow textures are often indicated by characteristic elongated pumice clasts (> ∿ 4 mm). Parts of the upper breccia have a cavernous appearance in outcrop and

Healy (1967) attributed this to complete recrystallisation of pumice fragments so that they have become loose aggregates of cristobalite and feldspar. Glass in the matrix is usually devitrified in this unit.

The main unit consists of densely welded lenticulite containing dark grey flattened pumice and occasional lithic inclusions of andesite and rhyolite set in a grey or pink matrix. Some of the andesitic fragments may be accessory and incorporated into the ignimbrite as it flowed over Beesons Island Volcanics. The harder parts of the ignimbrite are often exposed as near horizontal or slightly undulating sheets in streams in the vicinity of the Wairoa River, and in the more northern parts of the Whakamarama Plateau, where pothole scouring is a characteristic feature.

Petrography

Dominant phenocrysts in the Waitearíki Ignimbrite include plagioclase and quartz, which are frequently fractured, with subordinate magnetite, hypersthene and augite (slide R-44, NZGS, Rotorua); biotite occurs in the upper parts (the breccia) of the ignimbrite. Flow units are indicated by variations in the size of lenticles in the welded part of the sheet (Healy *et al.*, 1964, Healy, 1967).

Distribution

The Waitearíki Ignimbrite forms an extensive easterly dipping ($\sim 10^{\circ}$) surface covering most of the Whakamarama Plateau and is characterised by a basal welded lenticulite and an upper moderately to poorly welded breccia (cross section in map folio). The harder and more welded parts of the ignimbrite crop out in streams which dissect the plateau northwest of Omokoroa, at McLaren Falls (N.Z. Geol. Map 1 : 250,000 Sheet 5 GR N35/5345) and along parts of the

Wairoa River. An upper breccia unit with a characteristic pinkish-red to grey colour crops out in streams and in several road cuttings in the Whakamarama Plateau and along the Waihi-Tauranga highway (Fig. 3.2) in the vicinity of Apata (N35/4664). The ignimbrite reaches a thickness of 120 m on this plateau (Healy, 1967) but has been eroded to a thickness of 30 m in the Otumoetai and Matua areas (Fig. 3.7) where it is found in drillholes at over 100 m depth. Drillhole data and subaerial exposure indicate that the Waitearíki Ignimbrite also thins to 60 m against underlying breccias of the Aongatete Volcanics and Beesons Island Volcanics west of the Basin while thinning over Minden Rhyolite and Aongatete Ignimbrite within the Basin. In areas northwest of Omokoroa the breccia unit is covered by a thick (∿ 4 m) sequence of Pahoia tephras, in turn covered by Hamilton Ash beds.

3.4.6 PAPAMOA IGNIMBRITE

Stratigraphic definition

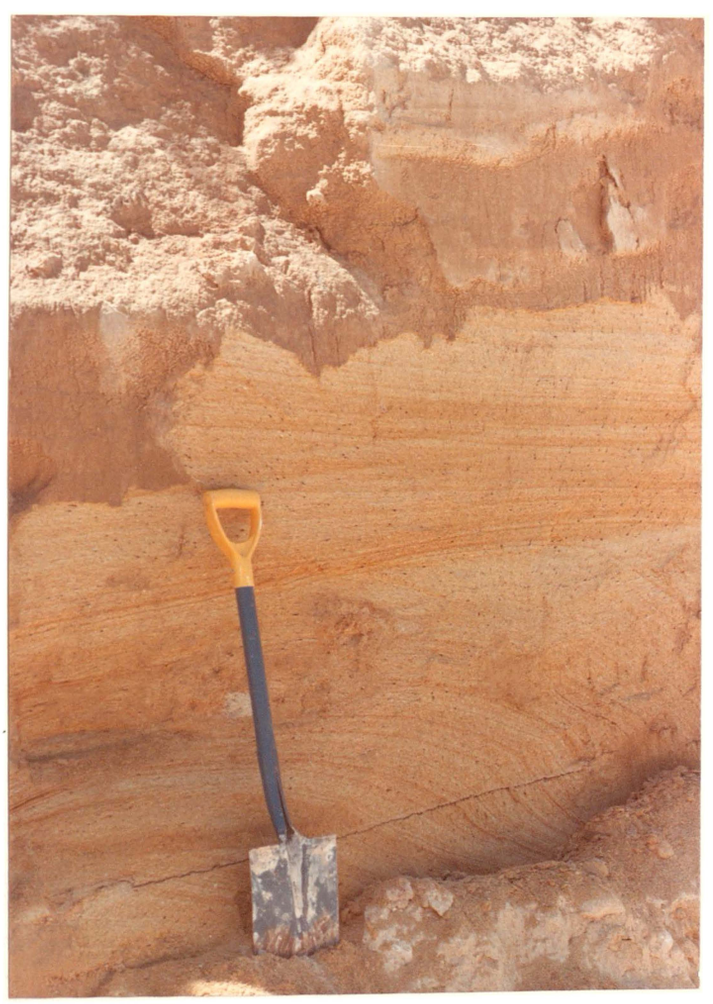
The Papamoa Ignimbrite is considered to be of Middle Pleistocene age (∿ 0.84 m.y. B.P.; Healy *et al.* 1964; B.F. Houghton, pers. comm. 1982). Because of similarities (e.g. field characteristics, texture, mineralogy) with the Waitearíki Ignimbrite, the Papamoa Ignimbrite may either be an earlier emplaced flow unit of the Waitearíki Ignimbrite (i.e. predates Waitearíki Ignimbrite) or synonomous with the Waitearíki Ignimbrite. The Papamoa Ignimbrite is faulted in the Papamoa Hills which bound the Basin to the south and southeast. Although it dips eastward (∿ 8°) generally, subisdence in the Tauranga Basin has caused the ignimbrite to dip northwards beneath Matua Subgroup deposits, and form basement rock (= Waitearíki Ignimbrite) in the Welcome Bay area.

The source of this ignimbrite remains purely speculative but an origin in the Taupo Volcanic is suggested because of its thickening in

Fig. 3.2 Upper breccia member of the Waitearikl Ignimbrite cropping out near the Waipapa River (U14/752893). The exposure is pale red to grey, unwelded, and contains abundant pumice lithics 1 - 5 cm across.

Fig. 3.3 The crystal rich Wairoa Ignimbrite (Type F4 deposit) exposed at the Tauranga Dump (U14/858835) showing leisegang phenomenon.





the south away from the Basin and similarities with the Waiteariki Ignimbrite.

Lithology

The Papamoa Ignimbrite is sub-divided into two informal field units:

(i) A lower welded lenticulite

(ii) An upper poorly welded breccia with a basal hard ignimbrite zone.

It resembles the Waiteariki Ignimbrite in being dacitic,crystal rich, having flattened pumice lenticles in the hard parts of the ignimbrite and a lenticular texture in the lower (beneath the hard ignimbrite) welded parts of the ignimbrite. The hard to welded parts of the Papamoa Ignimbrite are grey to brown. In the basal part of unit (ii), weakly compressed pumice inclusions are set in a grey tuffaceous matrix (sample R-30; NZGS, Rotorua), while in the lower more welded parts of the ignimbrite, grey black lenticles are set in a buff grey ash (Sample R-52; NZGS, Rotorua). The rock type ranges from dacitic in the lower welded unit to andesitic in the poorly welded upper breccia.

Petrography

Dr J. Healy, 1980, has described the following thin sections:

Specimens from unit (i) (slide R52, NZGS, Rotorua) show dark brown lenticles and phenocrysts of plagioclase and quartz, subordinate hornblende and less common Fe-Ti oxide, hypersthene and biotite pheocrysts set in a densely welded isotropic matrix in which the outline of individual shards is obliterated by welding. Upper breccia (unit ii) specimens show textural changes, the pumice is less compressed (although pumice lenticles are still characteristic)

and the shards in the matrix are undeformed and/or uncompressed (slide R-30; NZGS, Rotorua).

Distribution

The Papamoa Ignimbrite is exposed in the southern margin of the Basin, covering the Papamoa Hills. Outcrops of the upper breccia and lower welded unit occur in road cuttings along the Welcome Bay Road, Waitao Road and Reids Road (N.Z. Geol. Map. 1 : 250,000 Sheet 5 GR N35/6853).

3.4.7 WAIROA IGNIMBRITE (new name)

Stratigraphic definition

The Wairoa Ignimbrite (0.5 m.y. B.P. < Wairoa Ignimbrite < 0.84 m.y. B.P.) is included in the Matua Subgroup. Based on air-fall tephra stratigraphy, the highly weathered appearance of the ignimbrite and its stratigraphic position overlying sediments derived from the Waitea riki Ignimbrite, it is considered to be the oldest of a number of newly identified ignimbrites subaerially exposed in the Tauranga Basin.

Lithology

At the Tauranga dump (U14/858835) it forms a pumiceous lapilli ash tuff which is crystal and lithic rich and displays leisegang banding (Fig. 3.3). The glass in pumice clasts is not devitrified and rhyolitic lithics commonly range from 1 - 4 mm.

Petrography

Dominant phenocrysts of plagioclase and quartz occur in a 2 : 1 ratio, with subordinate hornblende, magnetite and limonite, minor hypersthene, and traces of zircon.

Distribution

The Wairoa Ignimbrite crops out at the Tauranga dump (U14/858 835). Investigation outside the study area indicates that this ignimbrite occurs 5 km north of the mapped area (i.e. Sharp Road). At the Sharp Road locality the ignimbrite is exposed at the sides of an old protruding terrace remnant which lies adjacent to the lowest marine cut surface exposed a.s.l. in the Tauranga Basin. A correlation between that deposit exposed at Sharp Road and that exposed at the Tauranga dump is based on compositional and textural similarities. At the Tauranga dump (Fig. 3.3) the ignimbrite is covered by at least 15 m of fluvial sediment derived from the erosion of the Wairoa Ignimbrite. The sediment includes 4 dark brown interbedded paleosols (dipping at $\sim 30^{\circ}$, 15 cm thick) and each paleosol is separate by $\sim$ 1 m of fluvial sediment. The dip of the paleosols suggests that air-fall tephra mantled a hill at this site which has since been truncated by erosion. Overlying this thick sequence of fluvial sediment and interbedded paleosols is a thick sequence (to 3 m) of highly weathered ashes supporting light brown paleosols, which are preserved at higher elevations along Cambridge Road. At Sharp Road, near Katikati (Fig. 1.1) the Wairoa Ignimbrite is covered also by a thick ($\sim$ 2 m) sequence of deeply weathered air-fall tephra and again by a number of paleosols. However, fluvial sediment derived from erosion of the Wairoa Ignimbrite at this location is exposed at the sides of the deposit. It is considered in this study that the Wairoa Ignimbrite was once more laterally extensive in the Tauranga Basin, particularly in the Cambridge Road area and northwestwards from this area.

3.4.8 TE PUNA IGNIMBRITE (new name)

Stratigraphic definition

It is suggested from mapping and air-fall tephra stratigraphy that

the Te Puna Ignimbrite stratigraphically overlies the Wairoa Ignimbrite and stratigraphically underlies the Te Ranga Ignimbrite. The Te Puna Ignimbrite is considered in this study to be older than 0.30 m.y. B.P. but younger than 0.50 m.y. B.P. This approximate age range is suggested from a thick (∿ 8 m) sequence of Pahoia tephras, a number of interbedded paleosols and ∿ 2.5 m of Hamilton Ash covering the ignimbrite at Omokoroa. A chalazoidite bed underlying the Waimakariri Ignimbrite (∿ 0,18 m.y. B.P., Fransen, 1982) at Ruahihi and overlying a post-depositional slump deposit derived from the Te Puna Ignimbrite on Motuhoa Island indicates an age > ∿ 0.18 m.y. B.P. (see section 3.5.3).

Lithology

Te Te Puna Ignimbrite is an unwelded but consolidated lapilli ash tuff breccia, light grey to yellow, and containing grey to white pumice clasts (up to 8 cm). Lithic inclusions of rhyolite are abundant to common, while andesite is less common.

Petrography

Phenocrysts are dominantly plagioclase and quartz with subordinate hornblende and minor hypersthene and biotite. The groundmass consists mainly of glass shards, plagioclase and quartz, and pumice inclusions are not divitrified.

Distribution

Te Te Puna Ignimbrite crops out in cliff sections adjacent to Te Puna Station Road (U14/826 855) and the Wairoa River. Limited exposure occurs along Clarkes Road (U14/825 855), and in a road cutting along the Wairoa Road (U14/831 845) close (∿ 50 m) to the Waihi-Tauranga main highway. Further along (∿ 200 m) the Wairoa Road, are exposures of Waitearikí Ignimbrite in banks at the sides of the

Wairoa River. The Te Puna Ignimbrite has formed a thick remnant (∿ 30 m) tongue of material, producing a constructional but variably degraded terrace at Te Puna (Fig. 3.4). Thinner (< 6 m thick) pyroclastic flow deposits are found at Omokoroa (Fig. 8.10) and a post-depositional deposit (∿ 6 m thick) derived from the Te Puna Ignimbrite crops out in cliffs in the southern part of Motuhoa Island. These deposits are discussed in detail in Chapter 8.

3.4.9 TE RANGA IGNIMBRITE (new name)

Stratigraphic definition

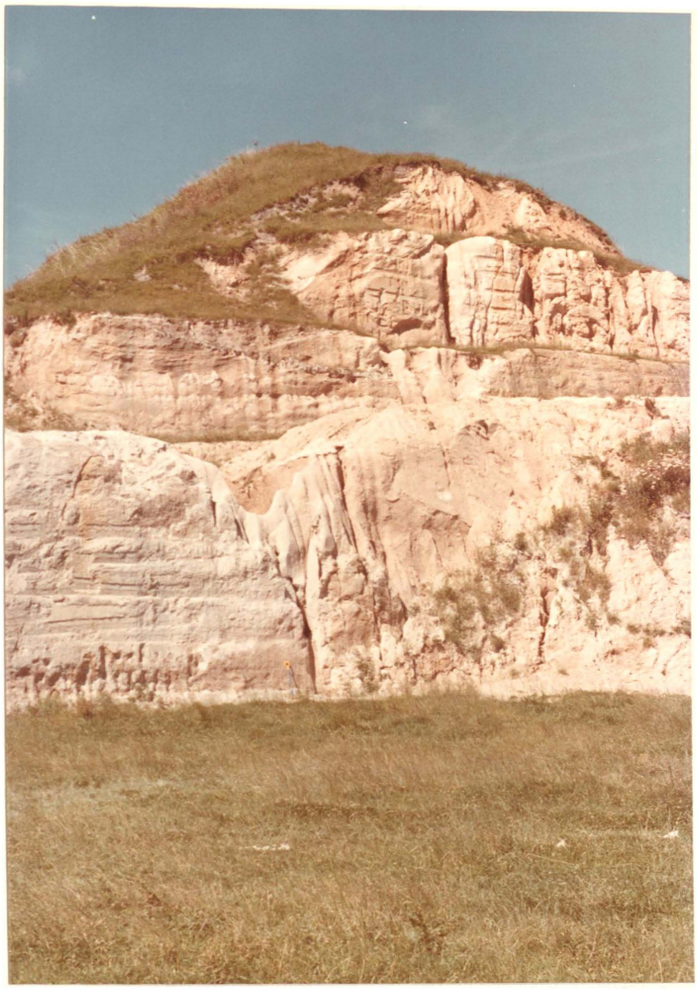
The Te Ranga Ignimbrite stratigraphically overlies the Te Puna Ignimbrite and stratigraphically underlies the Waimakariri Ignimbrite within the Matua Subgroup. An erosional unconformity which separates the Te Ranga Ignimbrite from the Waimakariri Ignimbrite indicates an age > ∿ 0.18 m.y. B.P. for the Te Ranga Ignimbrite (i.e. 0.18 - 0.16 m.y. B.P. was an age for the Waimakariri Ignimbrite suggested by Fransen, 1982). The Te Ranga Ignimbrite is considered to be ∿ 0.30 m.y. B.P., an age based on the severe erosion of the ignimbrite in the Basin before emplacement of the Waimakariri Ignimbrite and from air-fall tephra stratigraphy. The Te Ranga Ignimbrite is covered by ∿ 2 m of Hamilton Ash in the Pyes Pa Road area (U14/846 773).

Lithology

The ignimbrite (Fig. 3.5) forms a dark grey to grey, poorly consolidated to consolidated slightly gravelly sand which has been the source of a large proportion of the fluvial sediment exposed throughout the Tauranga Basin. Segregation channels, basal cross bedded structures and charcoal fragments are characteristic of this deposit, these features being discussed in detail in Chapter Eight. Vesicular glassy pumice clasts, 4 to 20 mm, and obsidian and rhyolitic rock

Fig. 3.4 The Te Puna Ignimbrite exposed in an ~30 m thick section along the Te Puna Station Road (U14/828859). The spade at the base of the cliff is 1 m.

Fig. 3.5 The glass rich Te Ranga Ignimbrite cropping out at the Melame Street quarry (U14/861805). Note the convolutions which appear beneath fluvial sediment at the top of the deposit. Spade is 1 m.





fragments (1 to 8 mm) are abundant throughout the Te Ranga Ignimbrite.

Petrography

Glass is very prevalent in the ignimbrite and occurs in two forms, vitreous flakes and brown to black obsidian flakes. Dominant phenocrysts are plagioclase and quartz with subordinate magnetite and hypersthene, and minor hornblende.

Distribution

Te Te Ranga Ignimbrite (Figs. 3.5 and 8.3) occurs in the map area in the form of two lobes. One extends eastwards from Pyes Pa Road (U14/846 762) to Greerton (U14/867 815), and crops out in a quarry near Te Ranga (U14/845 769), in a quarry adjacent to Keenan Road (U14 /846 763), and is exposed in cliffs at the end of Melame Street (U14/856 805). The other lobe extends towards Belk Road (U14/820 770) and the main highway 29 (U14/840 776). At Belk Road the Te Ranga Ignimbrite is covered by the Waimakariri Ignimbrite, which infills an old (> ∿ 0.18 m.y. B.P.) valley cut into the Te Ranga Ignimbrite.

3.4.10 WAIMAKARIRI IGNIMBRITE

Stratigraphic definition

The Waimakariri Ignimbrite was previously identified in the Mamaku Plateau by Fransen (1982) and an age of 0.16 to 0.18 m.y. B.P. suggested for the ignimbrite was based on the sharp contact and the thin (∿ 10 cm) depositional infill separating the overlying Mamaku Ignimbrite from the Waimakariri Ignimbrite. Based on a stratigraphic relationship with the Mamaku Ignimbrite (0.14 m.y. B.P., Murphy and Seward, 1981), and on a thick (∿ 2 m) sequence of Hamilton Ash covering the Waimakariri Ignimbrite in the Pyes Pa Road/Keenan Road area (U14/836 765), and along Joyce Road (U14/853 739), an age of ∿0.18

m.y. B.P. is suggested for the Waimakariri Ignimbrite in the map area. The Waimakariri Ignimbrite overlies the Te Ranga Ignimbrite in the map area, but underlies the Mamaku Ignimbrite just outside the map area in the Pyes Pa Road/Oropi gorge Road area (U14/855703). The Waimakariri Ignimbrite was previously regarded as the lower Mamaku Ignimbrite but several characteristic features give it separate name status (e.g. lithologic and mineralogic differences).

Lithology

The Waimakariri Ignimbrite exposed in the Belk Road quarry (U14/830 770) and in cliffs adjacent to the Wairoa River is a moderately to poorly welded, white to yellowish-grey, pumiceous breccia. Moderately welded parts of the ignimbrite occur in vertically jointed (i.e. columnar jointed; Fig. 3.6) cliffs which run perpendicular to the main highway 29 (U14/795 759) in the southern margins of the Basin. Pumice clasts (up to 15 cm) protrude from the outcrop face of moderately welded ignimbrite exposed in cliffs along Belk Road. Other characteristic features include, charcoal fragments and segregation structures (discussed in detail in Chapter 8, Table 8.3). Rhyolitic lithics are commonly found throughout the ignimbrite.

Petrography

The dominant phenocrysts are plagioclase and quartz, with subordinate hypersthene and magnetite and minor hornblende.

Distribution

The Waimakariri Ignimbrite is exposed in an extensive area which extends from the Wairoa River eastwards to the Papamoa Hills. The ignimbrite is exposed in cliffs at the sides of broad valleys which run north-south into the southern parts of the Tauranga Basin (i.e. the Mamaku Plateau area). The ignimbrite crops out in cliffs (Fig. 3.6)

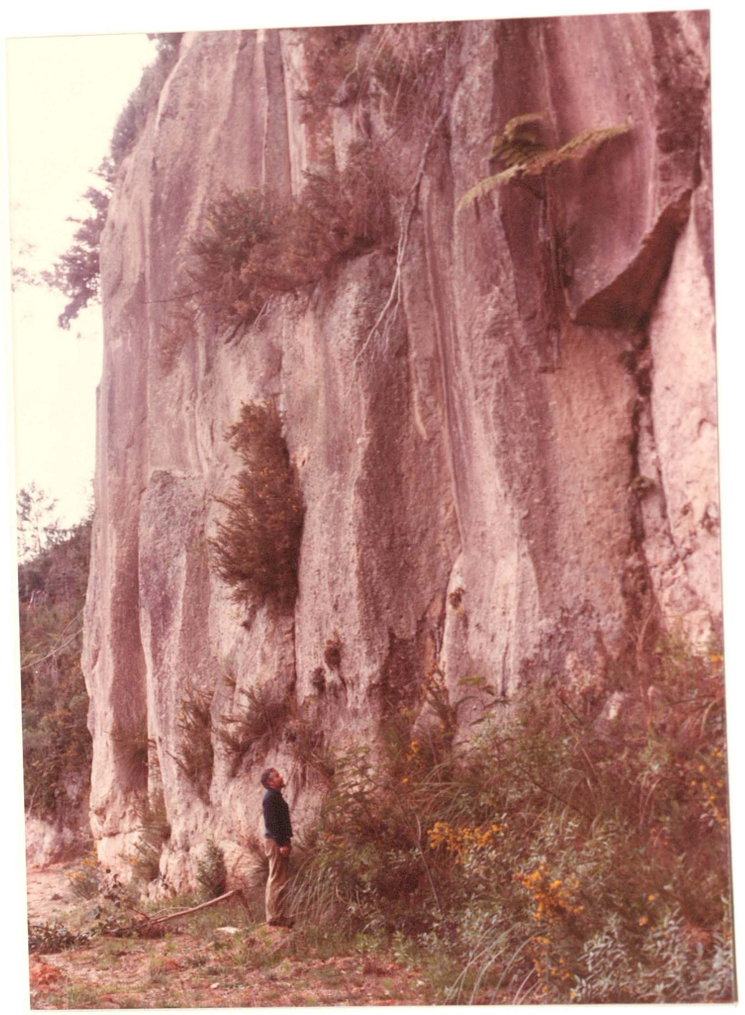


Fig. 3.6 Columnar jointed Waimakariri Ignimbrite exposed in 40 m high cliffs near the Wairoa River (U14/795760).

along the Wairoa River, at Belk Road (U14/820 770), Omanawa Road (U14/810 745) and in the Merrick Road/Pyes Pa Road area (U14/842 740). Investigation outside the map area, suggests that the ignimbrite thickens southward, and was once extensive in the Tauranga Basin and probably reached a thickness of ∿60 m. The ignimbrite reaches a thickness of ∿ 30 m in the Belk Road area.

3.4.11 MAMAKU IGNIMBRITE

The Mamaku Ignimbrite overlies the Waimakariri Ignimbrite just outside the map area in the Pyes Pa Road - Oropi gorge Road area (U14/857 700) where it has a thickness of ∿ 40 m. The ignimbrite is extensive south of McLaren Falls (U14/784 728), and Pyes Road (U14/856 705). It is probable that the Mamaku Ignimbrite was once a thick deposit in the Tauranga Basin but has subsequently been completely eroded out. Field work in the Ruahihi area (U14/805 740) indicates that sediment overlying the Waimakariri Ignimbrite is Mamaku Ignimbrite derived. Much of this sediment is overlain by ∿ 0.5 m of Hamilton Ash.

3.4.12 TAURANGA GROUP

Kear and Schofield (1978) proposed the name Tauranga Group for Late Cenozoic deposits found in the Bay of Plenty, Hauraki Lowland, Hamilton Lowland, Lower Waikato and Manakau Harbour areas. They described them as "..... mainly pumiceous, terrestrial, estuarine and marine sediments" with a probable source being the Taupo Volcanic Zone. In the Hamilton and Hauraki Lowlands, Kear and Schofield (1978) divided the Tauranga Group into the Frankton, Walton and Piako subgroups (Table 1.1). However geographic restriction on these names prevents their usage in the Tauranga Basin. Partial time correlatives (i.e. younger than the Waiteariki Ignimbrite of 0.84 m.y. B.P.) of these subgroups in the Tauranga Basin are here placed in a new single subgroup, the Matua Subgroup, as defined in the next section.

3.4.13 MATUA SUBGROUP

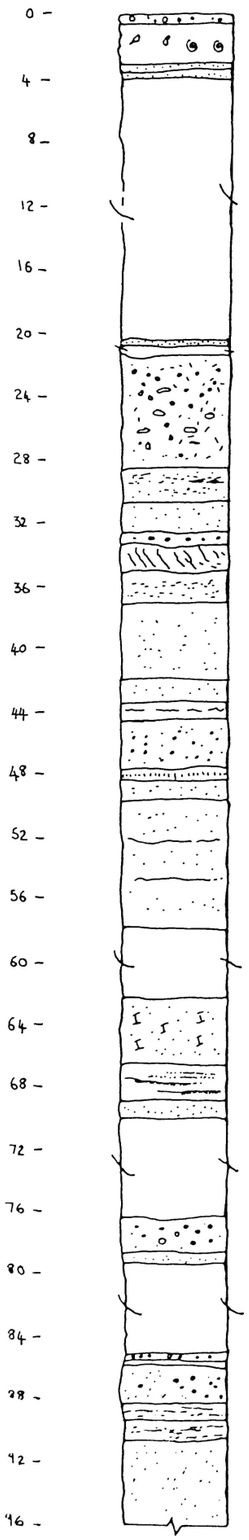
The formal name Matua Subgroup is proposed for the Pleistocene sediments (and associated lithologies) which overlie the Waitea riki Ignimbrite (c. 0.84 m.y. B.P.) within the Tauranga Basin. The Subgroup includes a sequence of fluvial and estuarine strata as well as several ignimbrites and air-fall tephras. Matua Subgroup deposits infill the Tauranga Basin to a depth of ∿ 150 m (Fig. 3.7 represents part of this thickness). A wide range of lithologies occurs: pumiceous gravels; moderately and well sorted cross-bedded gravelly sands and sands; moderately to poorly sorted horizontally stratified pumiceous sediments; clays; fossiliferous sands; peats; carbonaceous and/or diatomaceous silts; breccias; and massive silts and sandy silts. The source for most of these sediments is a rhyolitic volcanic terrain. The upper parts of the Matua Subgroup are exposed in a number of coastal cliff sections (much of this study concentrated on describing subaerial exposures), and are referred to informally as the upper Matua Subgroup. The upper Matua Subgroup, which is representative of much of the Matua Subgroup is discussed in detail in Chapter Five onwards. Sketches of the three main sections studied are given in Figs. 3.8, 3.9 and 3.10.

Lignite within the Matua Subgroup

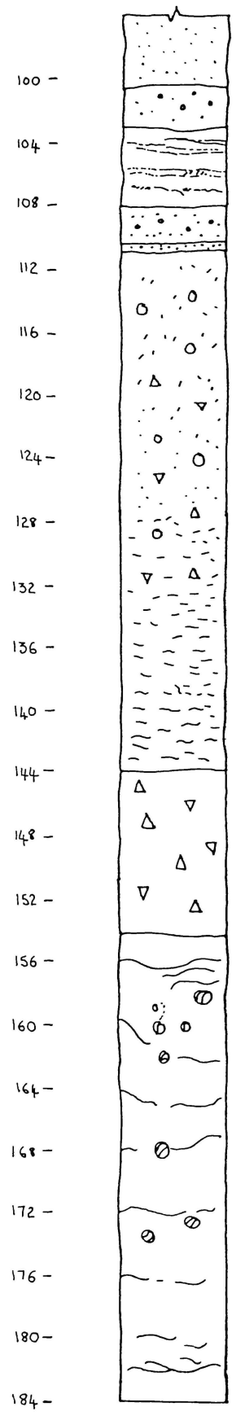
(a) Stratigraphic definition

Lignite is exposed at low tide on the beach surface at Omokoroa (Fig. 3.11) and Motuhoa Island, stratigraphically underlying the Te Puna Ignimbrite at Omokoroa. A very approximate age for the lignite is therefore older than the Te Puna Ignimbrite (∿ 0.30 - 0.50 m.y. B.P.).

IDEALISED STRATIGRAPHY OF OTUMOETAI CONTINUOUS CORE



Depth (m)	Lithology	Interpretation
0 – 4	pebbly sandy mud	modern soil
	shelly muddy sand	deposits of most recent post-glacial marine transgression
	clean well sorted feldspathic sand	beach deposit
	fine rhyolitic ash, small arcuate shards	air-fall ash
4 – 20	NO RECOVERY	coastal cliff stratigraphic sections indicate fluvial, pyroclastic flow and air-fall deposits
20 – 24	rhyolitic ash NO RECOVERY	air-fall ash
24 – 28	coarse rhyolitic ash – fibrous long tube pumice	air-fall and pyroclastic flow deposits
28 – 32	fine rhyolitic ash	air-fall ash
32 – 36	clean well sorted sand	beach or river channel
	silty sand	lower energy fluvial deposit
	carbonaceous silt	estuarine or swamp deposit
36 – 40	white rhyolitic ash	tephra (? reworked)
40 – 44	clean coarse plagioclase rich sand, rounded pumice pebbles	major river environment channel deposit
	fine rhyolitic ash	tephra
44 – 48	ferromag-rich well sorted sand	river channel deposit
48 – 52	plagioclase-rich sand containing pumice bands	river channel deposit
	mud sized rhyolitic? ash	tephra interbedded with terrestrial sediments
52 – 56	finely interbedded rhyolitic ash and sand/gravel	
	fine sand containing thin ash layers	
56 – 60	NO RECOVERY	probably as above
60 – 64	indurated fine sand	fluvial
64 – 68	bedded sand with peat	fluvial
	rhyolitic ash, biotite bearing	air-fall tephra
68 – 72	NO RECOVERY	
72 – 76	rhyolitic pumiceous sands	air-fall tephra
76 – 80	bedded sand and gravel	fluvial
80 – 84	NO RECOVERY	
84 – 88	gravelly sand	fluvial
	fine rhyolitic ash	air-fall tephra
	coarse sand-gravel	fluvial
88 – 92	bedded sand and rhyolitic ash	reworked air-fall
	bedded sand	fluvial
92 – 96	silt and sand	air-fall and fluvial



Depth (m)	Lithology	Interpretation
100 – 104	silt and sand	air-fall and fluvial
	sand and gravel	fluvial
104 – 108	banded pumiceous ash and finer beds	
108 – 112	pumiceous tuff breccia	– upper Waitekariki breccia
	fine-grained ash	– upper Waitekariki ash
112 – 124	unwelded to welded crystal rich tuff breccia	Waitekariki Ignimbrite
124 – 136	lenticulite	
136 – 152	unwelded pumice-rich tuff breccia	Aongatete Ignimbrite
152 – 184	spherulitic and flow-banded rhyolitic lava	Minden Rhyolite

Fig. 3.7 Stratigraphic column for the Otumoetai area. Information for the column has been derived from drillhole reports. (Adapted from borehole data, N.Z.G.S., Rotorua).

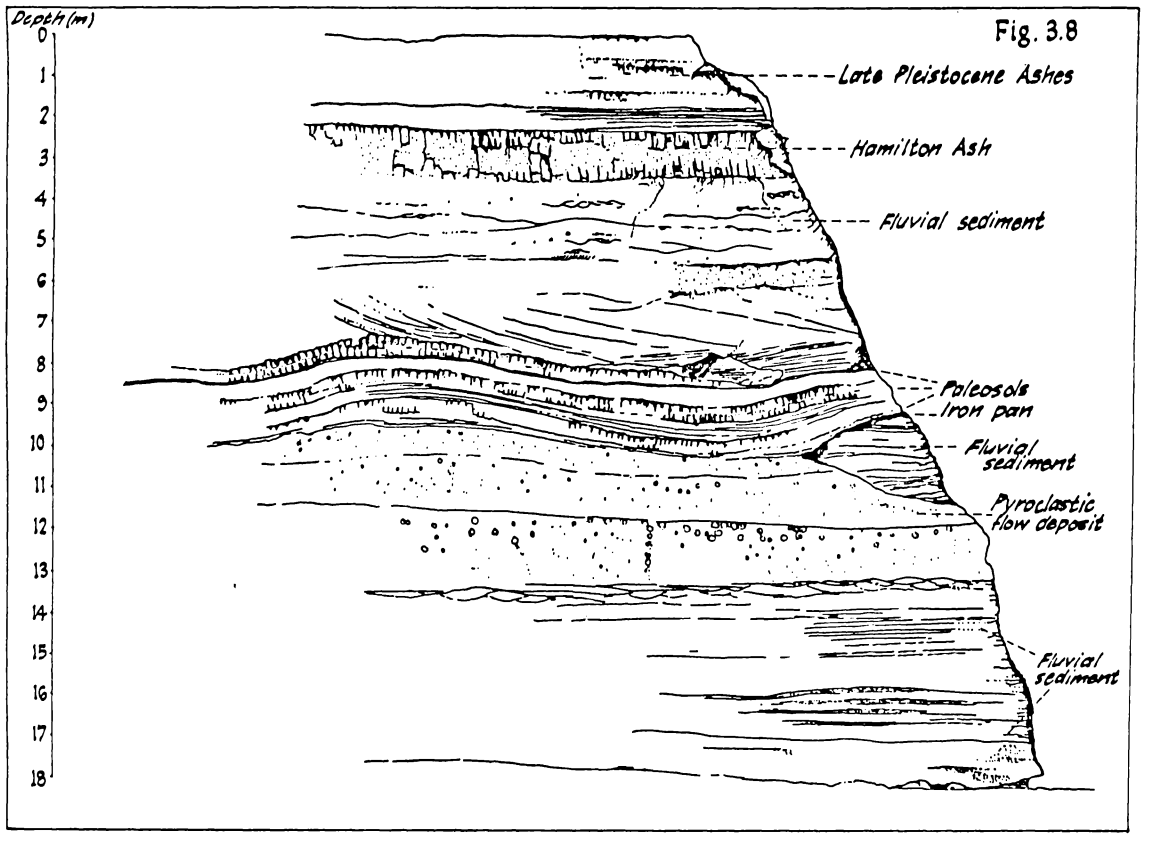


Fig. 3.8

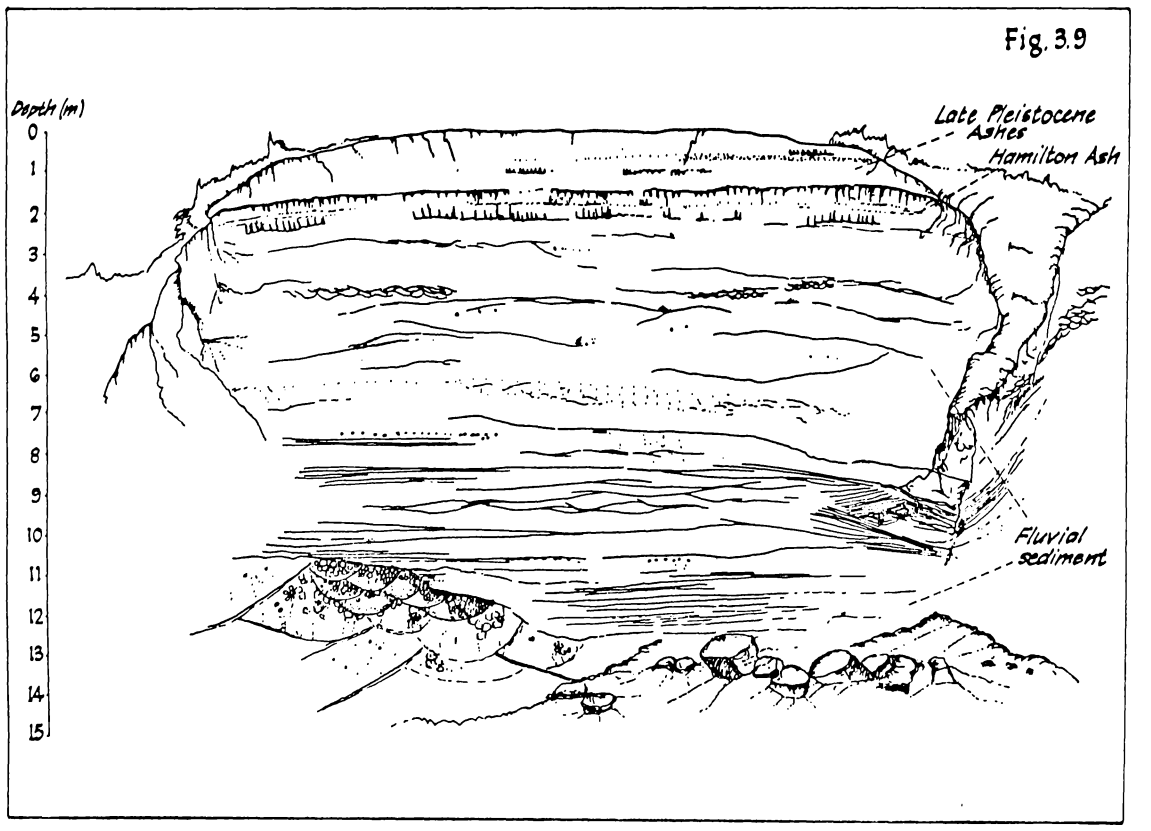


Fig. 3.9

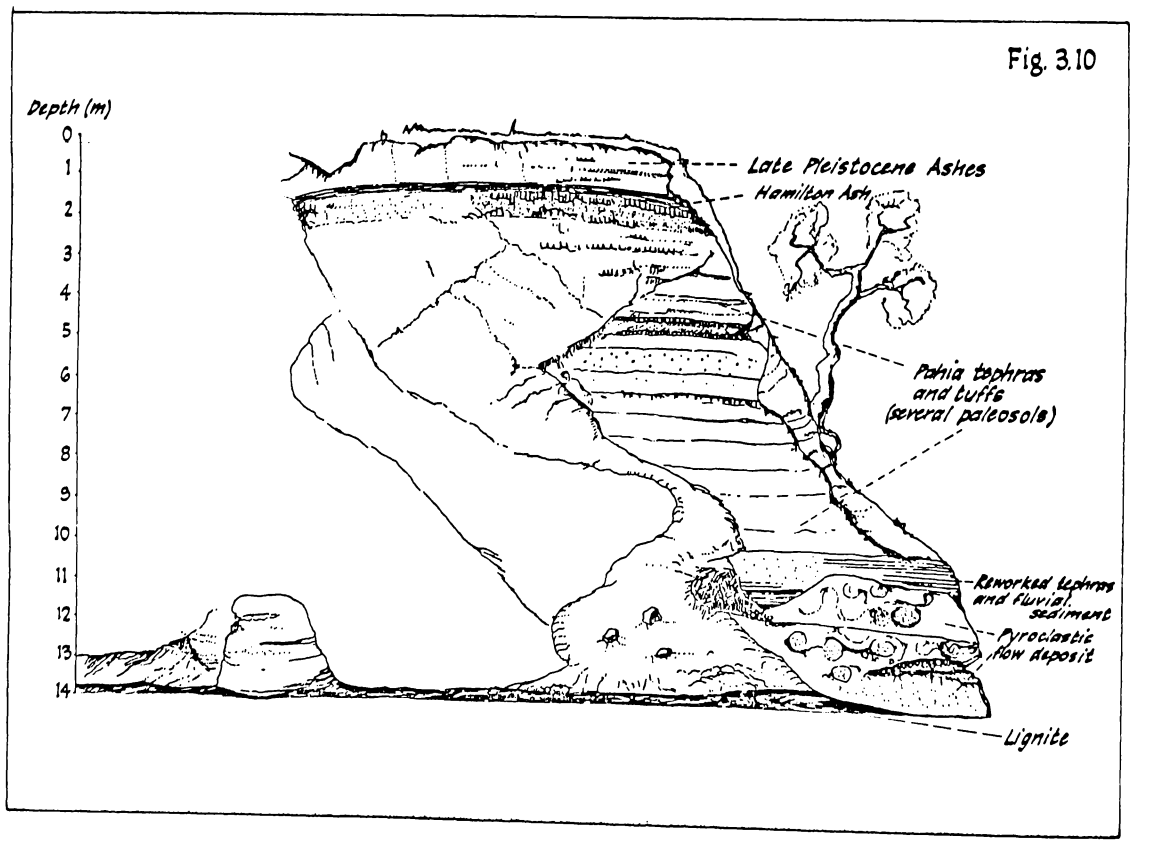


Fig. 3.10

Figs. 3.8 - 3.10 Sketches of the three main sections which were studied in the Tauranga Basin: the Kings Avenue section of Matua, Fig. 3.8; the Te Puna Section, Fig. 3.9; the Omokoroa section, Fig. 3.10.

(b) Description

The lignite at Omokoroa (Fig. 3.11) is 5 m thick but thins markedly to 0.6 m at Matakana Island, and 3 m at the Te Puna estuary. It is characteristically black and obvious structures include numerous branches and logs up to 0.5 m long and 0.06 m in diameter. The lignite exposed on the Omokoroa beach displays several concentric radial patterns with intervening ridges (2 cm high) spaced 4 - 6 cm apart and separated by flattened troughs. These concentric patterns appear to have developed around a central core, perhaps the more resistant stump of trees and shrubs which were once abundant in the swamp, and may be due to differential compaction about these centres.

(c) Distribution

The lignite exposed at Omokoroa is covered by two pyroclastic flow units and a thick (∿ 10 m) sequence of air-fall tephra. It extends east to Motuhoa Island where it is exposed on the beach surface and southeast to Te Puna West where it forms at low tide, a saturated, densely bored and current scoured shore platform in the Te Puna estuary. The lignite has an average thickness of 2 to 3 m. It is assumed from ash cover correlation and pollen analysis (Hull, 1977) that the same seam crops out ∿ 3.7 m above low tide level on Matakana Island. Another seam is exposed 6 m above low tide but represents a later period of swamp development. The surface of the lignite dips (4 - 8°) north and northeastwards away from Omokoroa Point (U14/798 927), and northwestwards away from Motuhoa Island and thins towards Matakana Island. This form may be suggestive of a raised bog (Hull, 1977; M.S. McGlone, pers. comm. 1982) or of differential compaction and/or tectonics.



Fig. 3.11 An ∿3 m thick black lignite deposit exposed above low tide level at Omokoroa (U14/798928). Overlying the lignite is the Type F5a deposit (Chapter 8) showing iron pans near the base of the deposit and fluvial sediment intrusions near the top of the deposit.

(d) Palynology

Pollen analysis (Hull, 1977) of lignite samples from Omokoroa and Matakana Island were carried out by Dr M. McGlone, Botany Division D.S.I.R., Christchurch.

Results

In terms of total pollen and spore content, the dominant swamp pollen is *Calorophus* and *Gleichesia* species (acid bog sedges). Gremineae (grass) pollen is absent. The main types of ferns present throughout the lignite are *Dicksonia squarrosa* and *Cyathea smithii*.

Tree and shrub pollen composes the majority of the lignite. The restricted variety of shrubs include *Lyptospermum* (Manuka and Kanuka), *Dacrydium bidwilli/bioforme group* (bog or pink pine) and *Epacris pauciflora* (acid soil or bog shrub). The occurrence of Podocarp/ hardwood forest types are identified throughout the lignite. Tree pollen is made up by *Dacrydium colensoi* (silver pine) and the*Notho-fagus fusca* group (all of the beeches except silver beech). Towards the top of the lignite the relative abundance of *Dacrydium cupressinum* (rimu), *Podocarpus spicatus* (matai) and *Podocarpus ferrugineus* (miro) increases.

(e) Significance of observations

The lignite acts as a stratigraphic marker and a potential paleo-environmental indicator. Comparison of the vegetation types in the lignite exposed in the Tauranga Basin with modern swamps having similar vegetation types allows several paleoenvironmental interpretations to be made (Hull, 1977; M.S. McGlone, pers. comm. 1982):

(i) The swamp grew in stadial conditions, probably when temperatures were 3°C lower than the present mean annual temperature of 14°C recorded in Tauranga.

(ii) Rainfall was possibly 800 to 900 mm higher than the present mean annual precipitation in Tauranga of 1348 mm.

(iii) An increase in podocarp pollens relative to Beech pollen in the upper part of the lignite suggests a climatic warming. This could signify stadial conditions when sea level was rising.

3.5 AIR-FALL TEPHRA SEQUENCES

Introduction

Tephrostratigraphy has been an essential chronological tool in providing a geological framework for the Tauranga Basin. It has also been important as a means of establishing former land surfaces and for correlating terrace heights (Selby *et al.*, 1971; Kamp, 1978; Kennedy, 1980; Vucetich *et al.*, 1980). Tephra marker beds are of considerable value as instantaneous time planes, but limitations arise from problems with regional identity and reliable dates (Kamp, 1978; Kennedy, 1980). The potential for tephra correlation with younger tephras (less than 42 ky) is usually greater than with older beds (> 42 ky). Limitations occur in correlating older ash beds outside the Tauranga Basin, mainly because of the high degree of weathering and loss of primary components and because of limited exposures which make "hand over hand" correlation difficult (Vucetich *et al.*, 1980). This obviously necessitates care in compositional analysis and textural description.

Tephra distribution (Fig. 3.12)

The tephrostratigraphy overlying or within the Matua Subgroup may be grouped broadly into 2 sequences (Table 3.3):

(i) older (pre-Rotoehu Ash) tephras (i.e. structured and structureless deposits)

(ii) younger (Rotoehu Ash and post-Rotoehu Ash) tephras

Together these tephras can range from 2 - 20 m thick in the Tauranga Basin. The older tephras [Hamilton Ash beds, Pahoia tephras

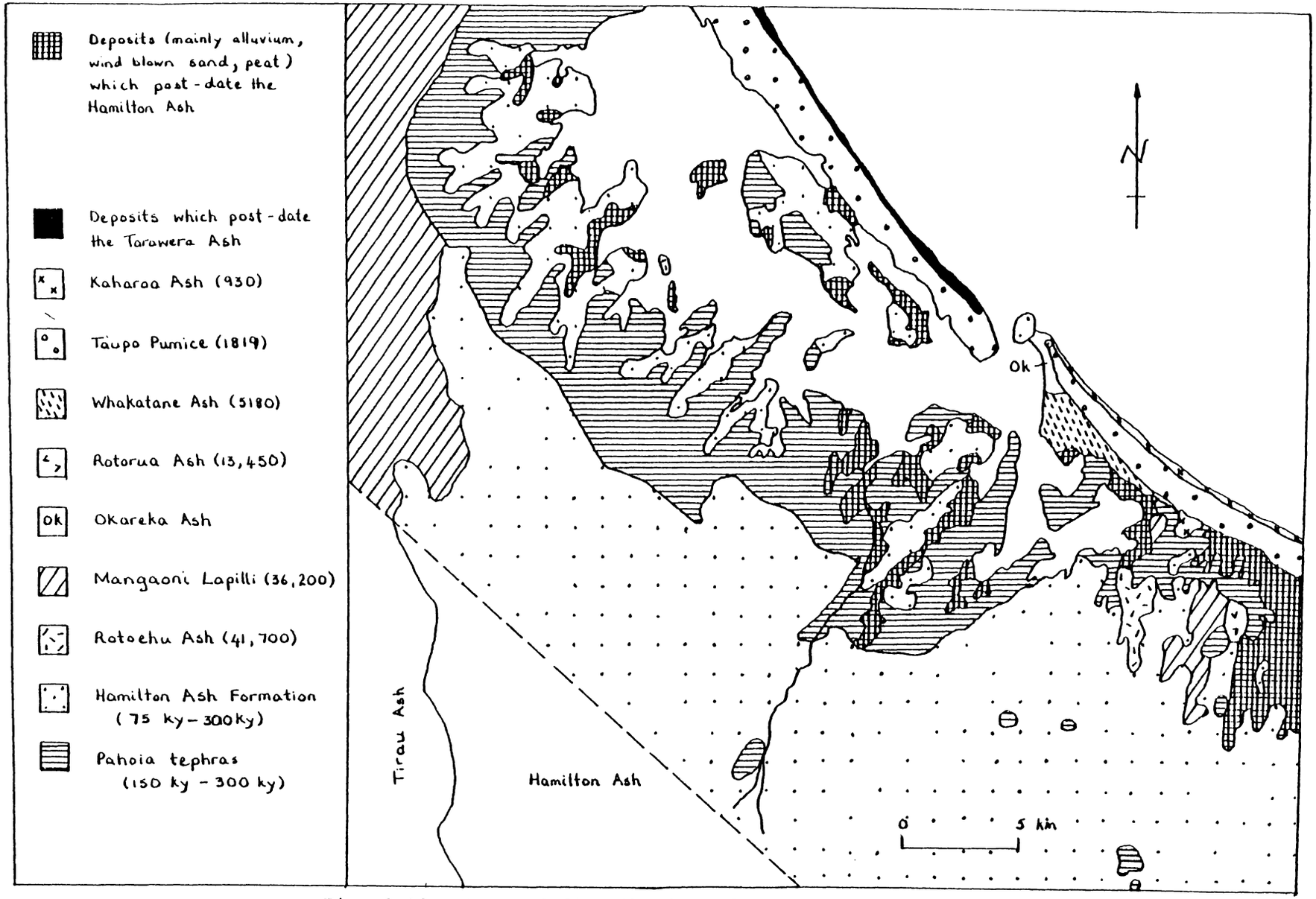


Fig. 3.12 Age and distribution of tephra marker beds in the Tauranga Basin (from Pullar and Birrell, 1973).

TABLE 3.3

TEPHRA (Volcanic Centre)	AGE (yrs)	REFERENCES	COMPOSITION	CLAYS		POSITION AS SOIL FORMING PARENT MATERIAL	SOIL CLASSIFICATION
				SOIL	PALEOSOL		
Kaharoa Ash (Okataina)	930 ± 70	Vucetich and Pullar (1964)	Rhyolitic	Allophane	Allophane	At surface and near surface	Yellow-brown pumice soil (sub-alvic)
Taupo Pumice Formation Taupo Lapilli (Taupo)	1,850 ± 100	Vucetich and Pullar (1964)	Rhyolitic	Allophane		At surface and deep	Yellow-brown pumice soil (sub-alvic)
Rotorua Ash (Okataina)	13,450 ± 250	Vucetich and Pullar (1964)	Rhyolitic		Allophane	Near surface and deep	Yellow-brown loams
Okaraka Ash (Okareka)		Pullar and Birrell (1973)					Yellow-brown loams
Oruanui Formation	19,850 ± 310	Pullar and Birrell (1973)	Rhyolitic				Yellow-brown loams
Mangaoni Lapilli Formation (Okataina)	30,100 ± 1300	Vucetich and Pullar (1969) Pullar and Heine (1971)	Dacitic-Rhyolitic		Halloysite	Near surface and deep	Yellow-brown loams
Rotoehu Ash (Okataina)	41,700 ± 3500	Vucetich and Pullar (1969) Pullar and Heine (1971) Nairn (1972) Howorth (1975) etc.	Rhyolitic		Halloysite Allophane	Deep	Yellow-brown loams
Hamilton Ash (unknown)	>42,000 or >42 ky	Ward (1967) McCraw (1975) Vucetich *et al.* (1978) Vucetich *et al.* (1980)	Andesitic and Rhyolitic	Halloysite Gibbsite Allophane	Halloysite Gibbsite Allophane	Deep	Brown granular loam (spadic)
Pahoia tephra (this study) or Pahoia Tuffs (unknown)	∿125-220 ky	Pullar and Birrell (1973) Kirkman and Pullar (1980) Vucetich *et al.* (1980)	Rhyolitic		Halloysite	Deep	
Undifferentiated brown tuffs (unknown)	<∿220 ky	Pullar and Birrell (1973) Kirkman and Pullar (1978)	Andesitic and Rhyolitic	Halloysite	Halloysite Allophane	Deep	
Kauroa Ash (unknown)	∿200-800 ky	Ward (1967) McCraw (1975) Kirkman (1980)	Andesitic and Rhyolitic	Halloysite Allophane Gibbsite	Halloysite Allophane Gibbsite	Deep	

(Kauroa Ashes), (Selby *et al.*, 1971; Pullar *et al.*, 1973; Vucetich, 1978; Kirkman and Pullar, 1978)] are typically highly weathered and lack prominent distinguishing characteristics. The Pahoia tephras are intercalated with fluvial sediment and include pyroclastic flow deposits. For this reason they are included within the Matua Subgroup. A number of paleosols are interbedded within the Pahoia tephra sequence which contains several unconformities representing missing time. The name Pahoia tephras is used in this study for all tephras below the Hamilton Ash Formation in the Tauranga Basin, and possibly includes tephra correlatives of the Kauroa Ash, found in areas outside of the Bay of Plenty. It is assumed in this study that the Kauroa Ash and Pahoia tephras are of similar age, and that tephras within the Pahoia tephra sequence possibly represent eruptive association with a number of the ignimbrites presently subaerially exposed in the Tauranga Basin.

3.5.1 OLDER (PRE-ROTOEHU ASH) TEPHRAS

Pahoia tephras

The name Pahoia tephras (Pahoia Tuffs, Pullar *et al.*, 1973) is used in this study as a portmanteau term for highly weathered white tephras (dominated by halloysite) including some brown to grey undifferentiated beds, forming ∿1 to 15 m thick sequences beneath the Hamilton Ash beds in the Tauranga Basin (Fig. 3.13). The term tephra is used both because shower bedding is prevalent in less weathered exposures, and because thin (< ∿ 2 m) pyroclastic flow deposits are included in the sequence. The ash is distinctly rhyolitic and normally graded. The Pahoia tephras are intercalated with white pumiceous fluvial sediment at several exposures (e.g. Matua), and deposits with characteristics which pertain more to a volcanic flow-type origin are interbedded with or immediately underlie Pahoia tephras at Omokoroa



Hamilton Ash

Pahoia tephras

pyroclastic flow deposit

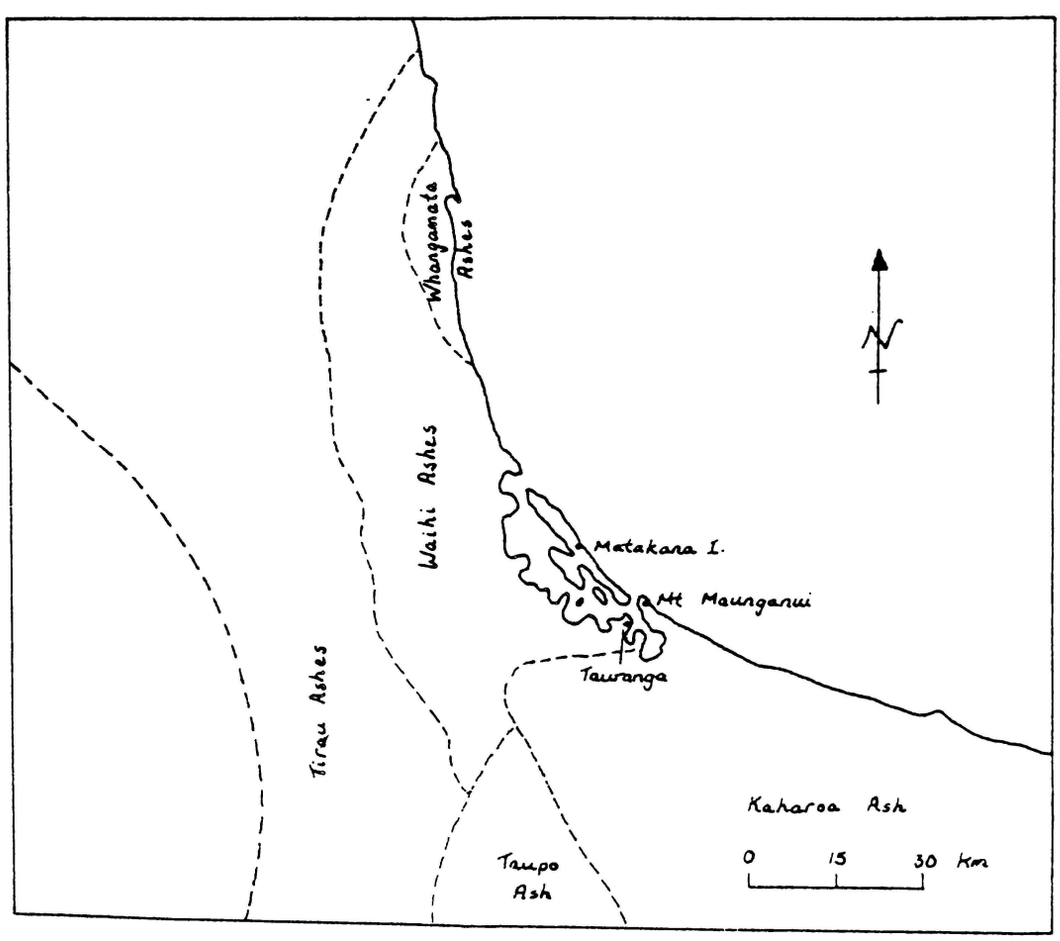


Fig. 3.13 The Omokoroa section (U14/798928) exposing the yellow to grey Pahoia tephras overlying an inversely graded pyroclastic flow (Type F5; Chapter 8) deposit. A channel scour occurs in the centre of the photo, above the pyroclastic flow deposit. The dark brown Hamilton Ash beds occur above the Pahoia tephras, and below white Rotoehu Ash. The trowel is 30 cm long.

Fig. 3.14 Distribution map of the soil forming ash showers in the Tauranga area, showing the extensive Waihi Ashes.

and at Matua (e.g. Type F7, Type F6, and Type F5 deposits described in Chapter 8).

An age range from 125 ky to 300 ky has been suggested for the Pahoia tephras (Kirkman and Pullar, 1978; Vucetich *et al.*, 1980). The Pahoia tephras (Pahoia Tuffs, Pullar *et al.*, 1973) are described outside the Tauranga Basin at several localities in the Bay of Plenty (Pullar *et al.*, 1973; Chappell, 1975; Kirkman and Pullar, 1978). Kirkman and Pullar (1978) noted a minimum of 12 beds each containing a basal ash and an associated paleosol within the Pahoia Tuffs at Opotiki, 120 km southeast of the Tauranga Basin, and multiple paleosols exist within the Pahoia tephras in the Tauranga Basin.

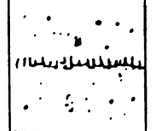
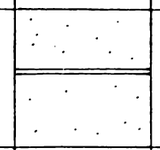
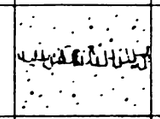
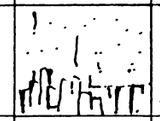
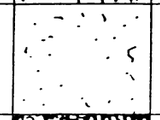
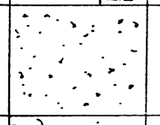
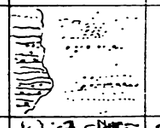
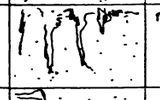
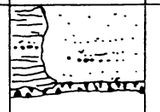
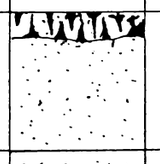
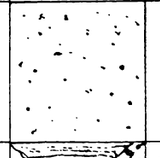
The Pahoia tephra sequence, although highly weathered, is well exposed at Omokoroa (U14/797 927; Fig. 3.13). The term bed is adopted at the Omokoroa site for descriptive purposes. The beds described from the Pahoia tephra sequence are informally named Oa to On (Table 3.4) and form a sequence ∿ 5 m thick. The rhyolitic tephras range from prominently bedded to massive with upper contacts defined by colour and slight textural changes and/or commonly by pale brown clay rich (halloysite) paleosols (2 to 15 cm thick; Fig. 3.16). At the Matua coastal section (U14/849 877) the Pahoia tephras include paleosols up to 40 cm thick.

All tephras except Oa contain at least 97% by weight of rhyolitic glass, pumice and felsic minerals. Tephra Oa contained 7% heavy minerals, this concentration being due to fluvial reworking. The ferromagnesian mineral assemblages comprise green hypersthene, hornblende and biotite.

(a) Kauroa Ash

The name Kauroa Ash Formation was given by Ward (1967) to 17 discrete tephra beds occurring immediately below the Hamilton Ash

TABLE 3.4 PAHOIA GROUP TEPHRAS and basal flow deposits (described from the Omokoroa section)

Pahoia group tephra code	Thickness (cm)	Texture	Colour	Consistence	Structure	Column	Comment
On	60	silty sand	7.5YR 8/2 light yellow to orange	friable	massive		weakly developed paleosol
Om	40	sandy clay	7.5YR 7/2 dull orange to brown	friable	massive		thin clay bed
Ol	5	clay	7.5YR 8/2 light grey	firm to friable	massive		weakly developed paleosol
Ok	5	clay	N8/0 white	friable to plastic	prismatic		white to light brown paleosol
Oj	15	sandy silt	N8/0 to N7/0 greyish white	compact	massive		white ash (creamy)
Oi	60	silt	N8/0 to N7/0 greyish white	compact	massive		weakly developed paleosol
Oh	30	silt	N7/0 grey	compact	massive		manganese oxide staining (prominent manganese nodules) shower bedding at base
Og	40	sandy silt	N7/0 to N6/0 grey	hard to compact	massive		dark grey indurated unit
Of	35	silt	7.5Y 7/1 light yellow to grey	compact	massive		partly shower bedded — normally graded. Pumice grains > than the Md 1φ sand size were present in poorly sorted sands
Oe	40	silt	7.5Y 6/1 grey	compact	massive		root channel deformation + reworked areas shower bedding
Od	30	sandy silt	7.5Y 7/1 light grey	compact	massive		shower bedding light brown paleosol
Oc	20	sandy silt	7.5Y 7/2 yellow to light grey	compact	massive		light brown paleosol
Ob	50	sandy silt	7.5Y 7/2 yellow to light grey	compact	massive		
Oa	90	sandy silt	N7/0 grey	compact	massive		fluvial reworking of tephra Oa represented by sheet wash infilling a channel scour
Unit 2	350	slightly gravelly gravelly to gravelly sands	7.5Y 7/1 to 7.5Y 7/2 light grey	consolidated	inversely graded to homogenous		pyroclastic flow deposit
Unit 1							

Formation, west of the Bay of Plenty, in the Central North Island. [although it consists of a group of ashes with missing time existing between some of the beds (Ward, 1967)].

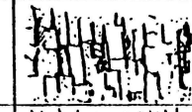
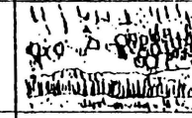
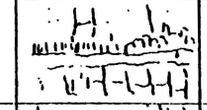
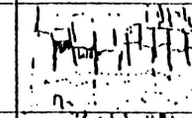
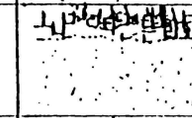
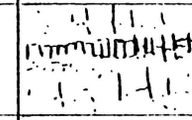
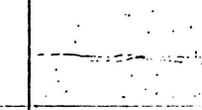
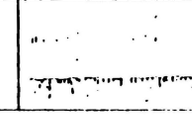
The beds possibly span a period of 500 ky as determined from stratigraphic associations with dated basalts (McCraw, 1975; Kirkman, 1980), while an age estimate for a lower member, the Oparau Tephra (Pain, 1975), is 750 ky (Vucetich *et al.*, 1978). In the Tauranga Basin undifferentiated brown tephras of andesitic and rhyolitic composition interbedded with Matua Subgroup fluvial deposits, beneath the Hamilton Ash Formation, are placed into the Pahoia tephra sequence.

Hamilton Ash

Hamilton Ashes occur immediately below the easily recognised Rotoehu Ash (c. 42 ky; Nairn, 1972). The Ohinewai Tephra, the lowermost member of the Hamilton Ash Formation (Ward, 1967) was recognised by Vucetich *et al.*, (1978) in the Tauranga Basin, although positive identification has proved difficult. These workers suggest an age for the tephra of 150 ky. Hendy *et al.*, (1980) gave an estimated mean age for the H-1 bed of the Hamilton Ash Formation at 200 ky (± 75.0 ky) using a Uranium/Thorium dating technique. Coastal terrace correlation (Chappell, 1975) gives an age for the Hamilton Ash Formation of between 120 ky and 210 ky, McCraw (1975) however suggests an age range of between 100 ky and 300 ky based on stratigraphic associations with dated ignimbrites and basalts.

The Hamilton Ash Formation in the Tauranga Basin forms a thick (usually > 0.9 m) yellow brown to dark reddish brown deeply weathered sequence in which paleosols are developed. Most beds show a well developed nutty to blocky structure. At Omokoroa (Fig. 3.13) this sequence is ∿ 2.5 m thick (Table 3.5) while at Te Puna and at Matua it is < 1.2 m.

TABLE 3.5 HAMILTON ASH FORMATION (described from the Omokoroa Section)

Bed	Thickness (cm)	Texture	Colour	Consistence	Structure	Column	Comments
A	30	sandy clay loam	10YR 4/4 deep brown	firm	strongly developed coarse nuts and blocks		
B	30	sandy clay	10YR 5/6 yellow brown	firm	strongly developed coarse nuts and blocks		allophane rich
C	20	silty clay	10YR 6/6 yellow brown	firm	weakly developed medium nut		allophane rich clay matrix
D	20	sandy clay	10YR 4/6 brown	friable	weakly developed medium to fine nut		well developed paleosol allophane layer
E	30	silty clay	10YR 5/6 yellow brown	firm	strongly developed coarse nuts		well developed paleosol
F	40	silty clay	10YR 5/6 yellow brown	firm	massive		well developed paleosol
G	40	silty clay	10YR 5/6 yellow brown	firm	massive		clay beds
H	10	sandy clay	10YR 5/4 yellow brown	friable	massive to weakly developed nut		halloysite rich fine ash

3.5.2 YOUNGER (ROTOEHU ASH AND POST-ROTOEHU ASH) TEPHRAS

Rotoehu Ash

The Rotoehu Ash (c. 42,000 yrs B.P.) is a very conspicuous white ash layer occurring typically at a depth of 120-218 cm over much of the Tauranga Basin, lying above Hamilton Ash beds. It is distinctly shower bedded in units ranging from 2 - 20 cm (i.e. multiple white to greyish yellow beds) and has a predominantly sandy texture.

Post-Rotoehu tephras

The younger tephras are red to dark brown, firm to friable and form a composite (i.e. mixture of ashes, and in parts of the Basin the ash column is described as collapsed) < 42 ky column. They have been derived from Rotorua, Okataina, Taupo and Mayor Island eruptive centres (Healy *et al.*, 1942; Pullar *et al.*, 1973; Hogg, 1979).

Post-Rotoehu tephras are important because they are surficial and hence are the major soil forming ashes of the region. The name Waihi Ash is used to describe an intimate mixture of at least two of these younger tephras (< 42 ky) which occur in variable proportions depending upon geographic location (Hogg, 1979), east of the Kaimai Ranges (Fig. 3.14). Tirau Ash is used for a mixture of younger tephras west of the Kaimai Range (Fig. 3.14). The definition (Taylor, 1953) of Waihi Ash, was made to include components of many tephras (e.g. including the Taupo Pumice, Rotorua, and Oruanui tephras; Table 3.4) which may range from Taupo Pumice to Rotoehu Ash (H.S. Gibbs, 1983, pers. comm.). Tephras > 20 ky may or may not be contained in the bed and identification of older tephras > 20 ky is complicated by mixing and the degree of weathering at different localities. Post-Rotoehu tephras may reach a thickness up to $\sim$ 3 m

in the Basin, but a thickness of ∿ 1 m is common throughout the Basin. Southeast of the Tauranga region the Taupo and Kaharoa Ashes can be distinguished separately (Figs. 1.12 and 3.14).

3.5.3 STRATIGRAPHIC RELATIONSHIPS OF TEPHRA SEQUENCES

The stratigraphy of air-fall deposits in the Tauranga Basin is presented in Figure 3.15.

Pahoia tephras describe a collective sequence of air-fall deposits, paleosols, and possibly loess beds and pyroclastic flow deposits beneath the Hamilton Ash Formation. The Pahoia tephras are included in the Matua Subgroup, which is overlain by the Hamilton Ash Formation. However at Te Puna (U14/821 887), Matua (U14/849 878) and Waimapu (U14/879 799) there is evidence which indicates that the Hamilton Ash beds have been reworked, and fluvial sediments underlie and are interbedded with Hamilton Ash beds.

(a) Age of Pahoia tephras

A chalazoidite bed exposed ∿ 30 cm below the Waimakariri Ignimbrite (separated from the Waimakariri Ignimbrite by fluvial sediment) in a road cutting near the Ruahihi powerhouse (U14/792 760; Fig. 8.14) also crops out at the base of a thick (∿ 10 m) Pahoia tephra sequence (containing several unconformities) in a coastal cliff exposure (Fig. 3.16) near Omokoroa (U14/790 898). The chalazoidite bed is also exposed overlying a post-depositional deposit derived from the Te Puna Ignimbrite, on Motuhoa Island. The Pahoia tephras overlie the Te Puna Ignimbrite at Omokoroa Point (U14/798 928). Some Pahoia tephras may however stratigraphically underlie the Te Puna Ignimbrite, but overlie the Wairoa Ignimbrite (∿ 0.84 - ∿ 0.5 m.y. B.P.). Borehole data indicates that rhyolitic ashes occur intermittently at depth throughout the Matua Subgroup. Fluvial sediment underlying the Waimakariri

KEY

- LP — Late Pleistocene and Holocene Ashes
- Rr — Rotorua Ash (13,450)
- Ok — Okareka Ash (20,700)
- Ou — Oruanui Formation (19,850)
- Mn — Mangaoni Lapilli (36,200)

} Late Pleistocene Ashes

- Re — Rotoehu Ash (41,700)
- H — Hamilton Ash (75 - 300 ky)
- P — Pahoia tephras (150 - 400 ky)
- H — Fluvially eroded and reworked Hamilton Ash
- Matua Subgroup (fluvial sediments interbedded with paleosols, pyroclastic air-fall and flow deposits)
- f — Matua Subgroup fluvial sediments
- M — Fluvial sediment derived from the erosion of the Mamaku Ignimbrite
- * Similar fluvial petrofacies
- Undifferentiated Ignimbrite
- W — Waimakariri Ignimbrite
- TI — Te Ranga Ignimbrite
- TP — Te Puna Ignimbrite
- WI — Wairoa Ignimbrite
- Waitetariki Ignimbrite
- Paleosols
- Chalazoidite bed
- Major unconformity

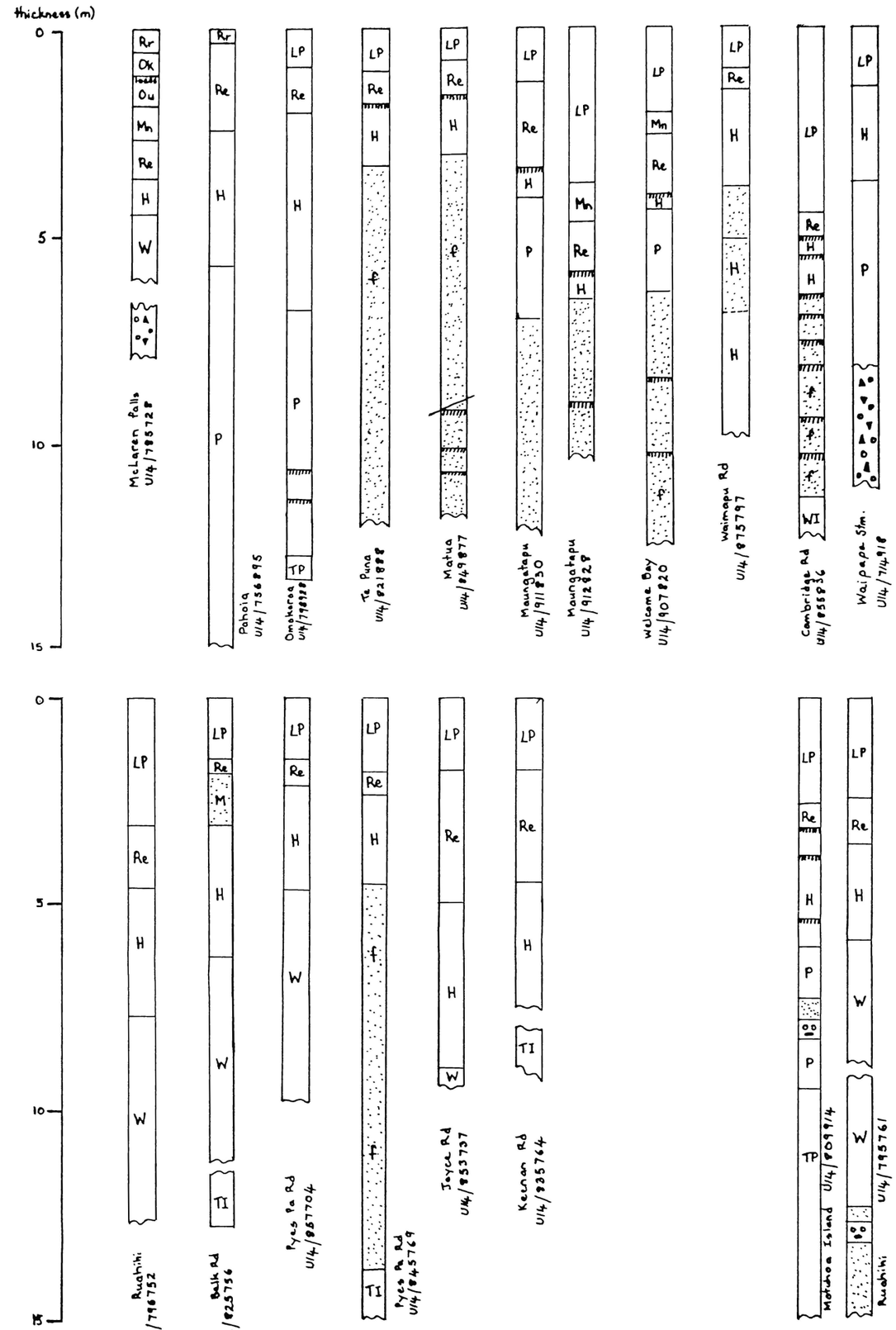


Fig. 3.15 : Stratigraphy of air-fall cover deposits in the Tauranga Basin

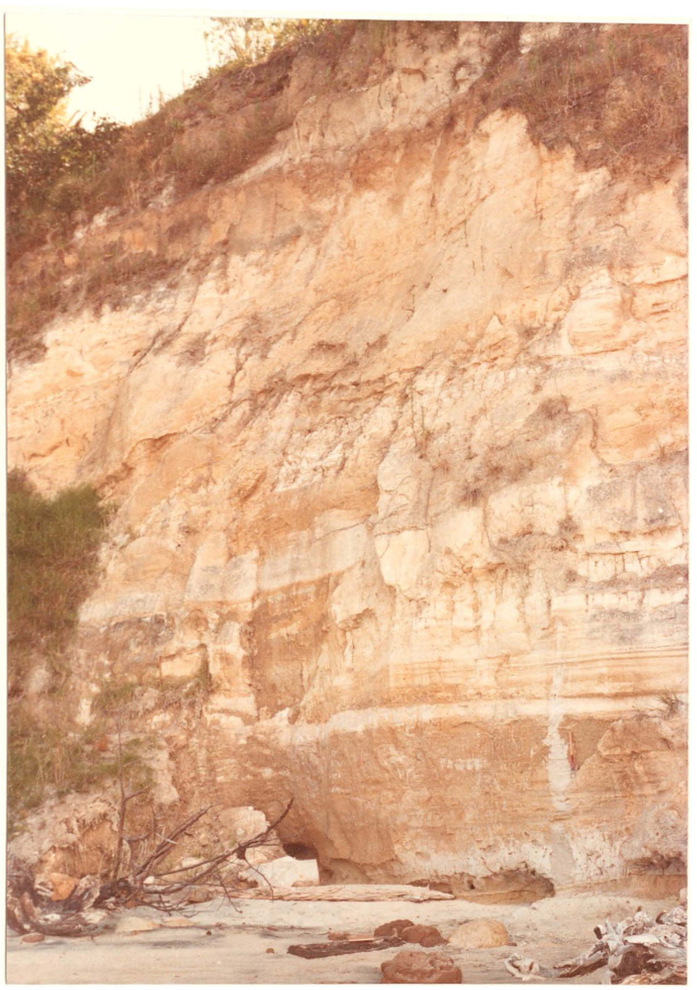


Fig. 3.16 The Pahoia tephras exposed in a coastal cliff section at Omokoroa (U14/790899). Several paleosols occur in the section, and a grey chalazoidite bed is exposed at the base above the beach surface. The trowel is 30 cm long.

Ignimbrite at Ruahihi (U14/792 760) may represent a period (> ∿ 0.18 m.y. B.P.) of channel erosion, which removed a large quantity of sediment from this site before the Waimakariri Ignimbrite was emplaced.

Age equivalence of the Pahoia tephras (i.e. tephras subaerially exposed throughout the Tauranga Basin in sequences up to 15 m thick) with the Waimakariri Ignimbrite (∿ 0.18 m.y. B.P.) and an age younger than the Te Puna Ignimbrite (∿ 0.4 m.y. B.P.) is therefore suggested from stratigraphic evidence in the Tauranga Basin.

Associations outside of the Tauranga Basin

Attempts to correlate ashes from the Tauranga Basin with those in the Waikato and King Country are difficult because of both loss of primary components by weathering and limited exposures. The Ohinewai Ash, (i.e. lowermost member of the Hamilton Ash Formation; Ward, 1967) has not been positively correlated with an ash bed lying immediately above the Pahoia tephras in the Tauranga Basin. However, work by Vucetich *et al.*, (1978; 1980) has tentatively established by stratigraphy and description some tephra correlation between the Omokoroa section in the Tauranga Basin and a section near Tirau, 55 km south of the Basin. Similarities between the section at Tirau and the section at Omokoroa (Vucetich *et al.*, 1980) are:

(i) a basal tephra flow ∿ pyroclastic flow deposit

(ii) a collective sequence of tephras and paleosols dominated by halloysite above the basal pyroclastic flow deposit which are referred to as the Pahoia Tuffs (= Pahoia tephra). [(i.e. multiple bedded, weakly developed paleosols with interbedded acidic tephras, sandy clay (medium/coarse ash) (Vucetich *et al.*, 1980)]

(iii) air-fall tephra units overlying (i) and (ii) deposits dominated by allophane and apparently paraconformable to basal deposits [i.e. (i) and (ii)]. Yellow brown friable tephras (= Hamilton Ash).

Attempts have also been made to define and correlate tephra and fluvial sequences occurring within the Pahoia Tuffs (= Pahoia tephras

in the Tauranga Basin) in the Bay of Plenty. At Little Waihi, 15 km southeast of the Tauranga Basin the Pahoia Tuffs are intercalated with fluvial sediment and possibly with pyroclastic flow deposits. Chappell (1975) defined the tuffs as including the Little Waihi Formation (i.e. a sequence of air-fall tephra and fluvial deposits beneath the Hamilton Ash Formation) and the informally defined undifferentiated pumice beds (i.e. below the Little Waihi Formation).

At the northern end of the Tauranga Basin at Waihi, the Kauroa Ash (Ward, 1967) was described as a "brown ash directly underlying the Hamilton Ash in the Anthenree deposits (Selby *et al.*, 1971). White, pumiceous fluvial sediment and air-fall tephra deposits beneath this ash at Waihi are correlated to the Pahoia tephras in the Tauranga Basin. Chappell (1975) positioned the Kauroa Ash, identified at Waihi as resting conformably beneath the Little Waihi Formation at Ohiwa, 100 km southeast of the Tauranga Basin.

Discussion of previous work

At the southern end of the Basin, Pullar *et al.* (1973) and Birrell *et al.*, (1977) recorded "undifferentiated brown tuffs" beneath both Rotoehu and Hamilton Ash beds and overlying highly weathered white tephras (= Pahoia Tuffs, Pullar *et al.*, 1973). These "undifferentiated brown tuffs" which are differentially eroded, probably include some of the Hamilton Ash beds, and some of the Kauroa Ash beds (Pullar *et al.*, 1973).

In the central areas of the Tauranga Basin, several dark brown firm ash beds and paleosols intercalated with fluvial sediments and Pahoia tephras (i.e. unconsolidated and consolidated tephra deposits below a sequence of Hamilton Ash beds) may possibly include older Hamilton Ash beds and some beds may be correlatives of Kauroa Ash. Therefore all white to grey tephras (dominant in halloysite) beneath

brown, more friable (many units are particularly dominant in allophane) tephras (= Hamilton Ash) are collectively grouped and given the name Pahoia tephra.

The Little Waihi Formation (Chappell, 1975) and the Pahoia Tuffs (Pullar *et al.*, 1973) were provisionally correlated by Vucetich *et al.*, (1978) to an informally defined late ignimbrite period (< ∿ 0.3 m.y. B.P.) with age equivalence to the Matahina, Waimakariri and Mamaku Ignimbrites. It is suggested however from this study that age equivalence for the Pahoia tephras, be extended back in time to encompass the emplacement of a number of newly identified ignimbrites and associated air-fall tephra in the Tauranga Basin. Namely, the Te Puna Ignimbrite (∿ 0.4 m.y. B.P.) and the Te Ranga Ignimbrite (∿ 0.3 m.y. B.P.).

CHAPTER FOUR

STRUCTURE

4.1 INTRODUCTION

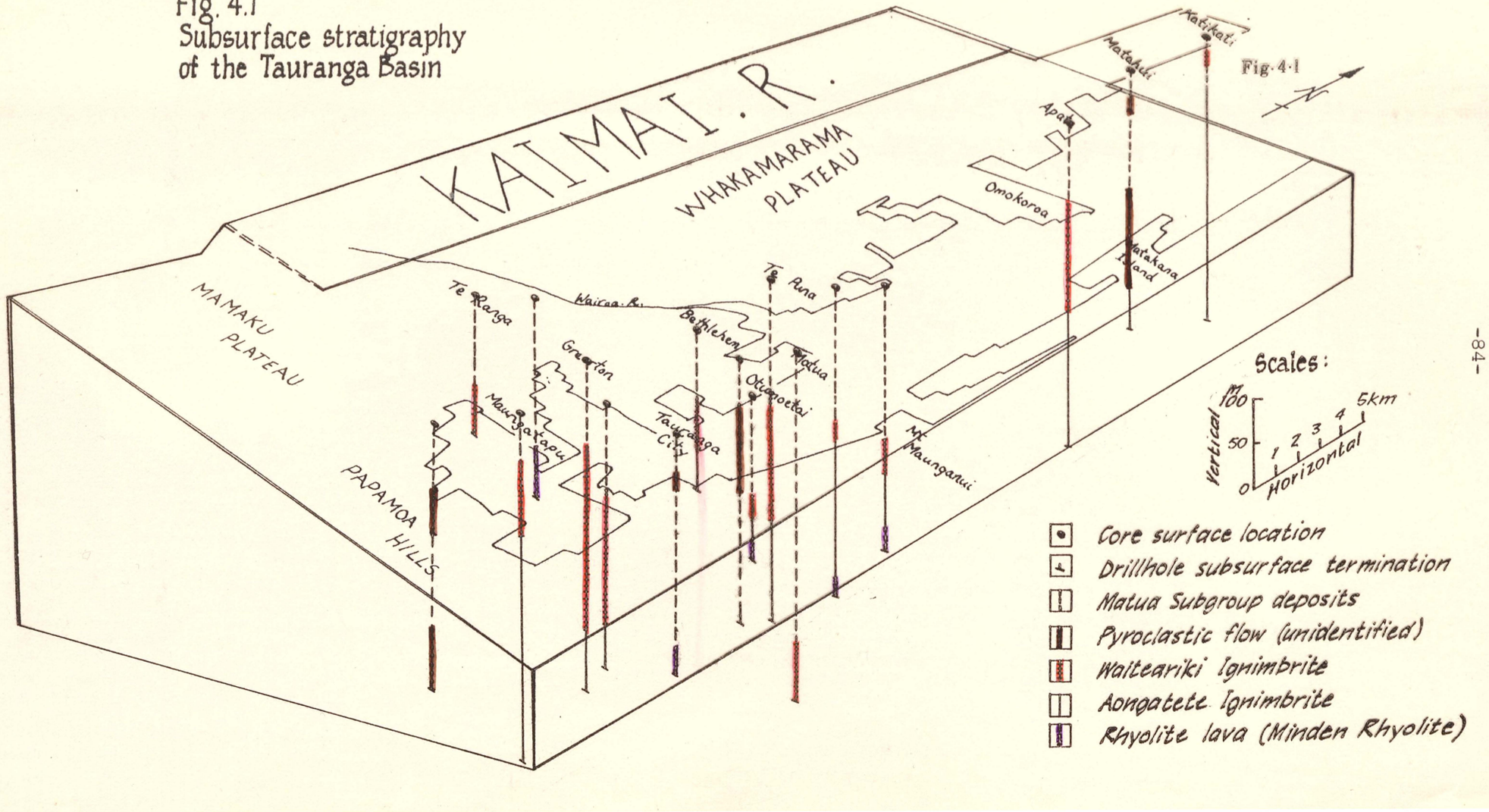
This study indicates that very little faulting has occurred within the Tauranga Basin in the last million years or so. However deep-seated faulting may be obscured by the thick sedimentary cover. Drillhole evidence shows quite marked variations in the depth at which specific rock units are found (Fig. 4.1) but this appears to be due to erosion rather than faulting. Volcanic rock units are dipping eastward into the Basin and therefore it is assumed that step faulting may have developed at depth in the Basin, or further north-east of the Basin (Fig. 4.2).

The Basin is a slowly subsiding depression ($\sim$ 0.12 mm/yr; Table 4.1 and 4.2) formed by uplift of the Kaimai Range to the west (major uplift began $\sim$ 0.84 m.y. B.P.) and by tilting of this horst towards the east and northeast. Since about the mid-Quaternary subsidence of the Basin associated with this tilting has accommodated a sedimentary pile up to 300 m thick. Cross-sections through the Tauranga Basin are shown in Figure 4.3 (map folio at back of thesis). Cross sections through the Coromandel Range are presented in Figure 4.4 (i), (ii) and (iii) and suggest that rock units of Miocene age (e.g. Beesons Island Volcanics) and older, extend underneath the Basin eastwards.

4.2 STRUCTURAL RELATIONSHIPS AND SUBSIDENCE

Drillhole data (NZGS, Rotorua, 1978; 1979; 1980; 1981), sedimentation rates and stratigraphic evidence (this study) indicate that the Basin has been subsiding at least since emplacement of the Waitetariki Ignimbrite (0.84 m.y. B.P.; Fig. 4.5). It is inferred that the rate of subsidence was highest immediately after emplacement of that ignimbrite and decreased to a slower rate in the late Quaternary. An

Fig. 4.1
Subsurface stratigraphy
of the Tauranga Basin



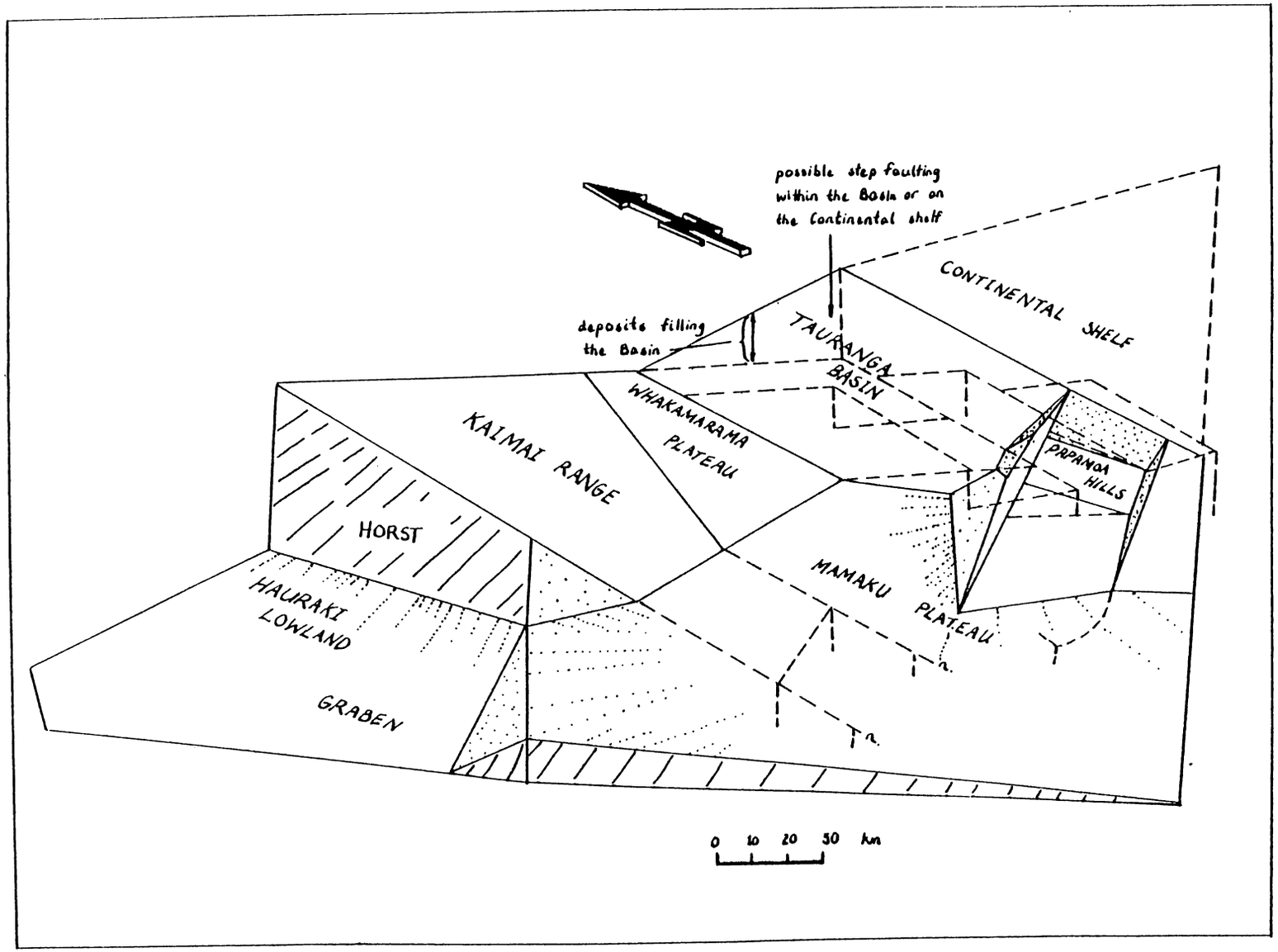


Fig. 4.2 Structural relationships between the Hauraki Lowlands and the Tauranga Basin. View is looking east towards the Tauranga Basin from the western Mamaku Plateau.

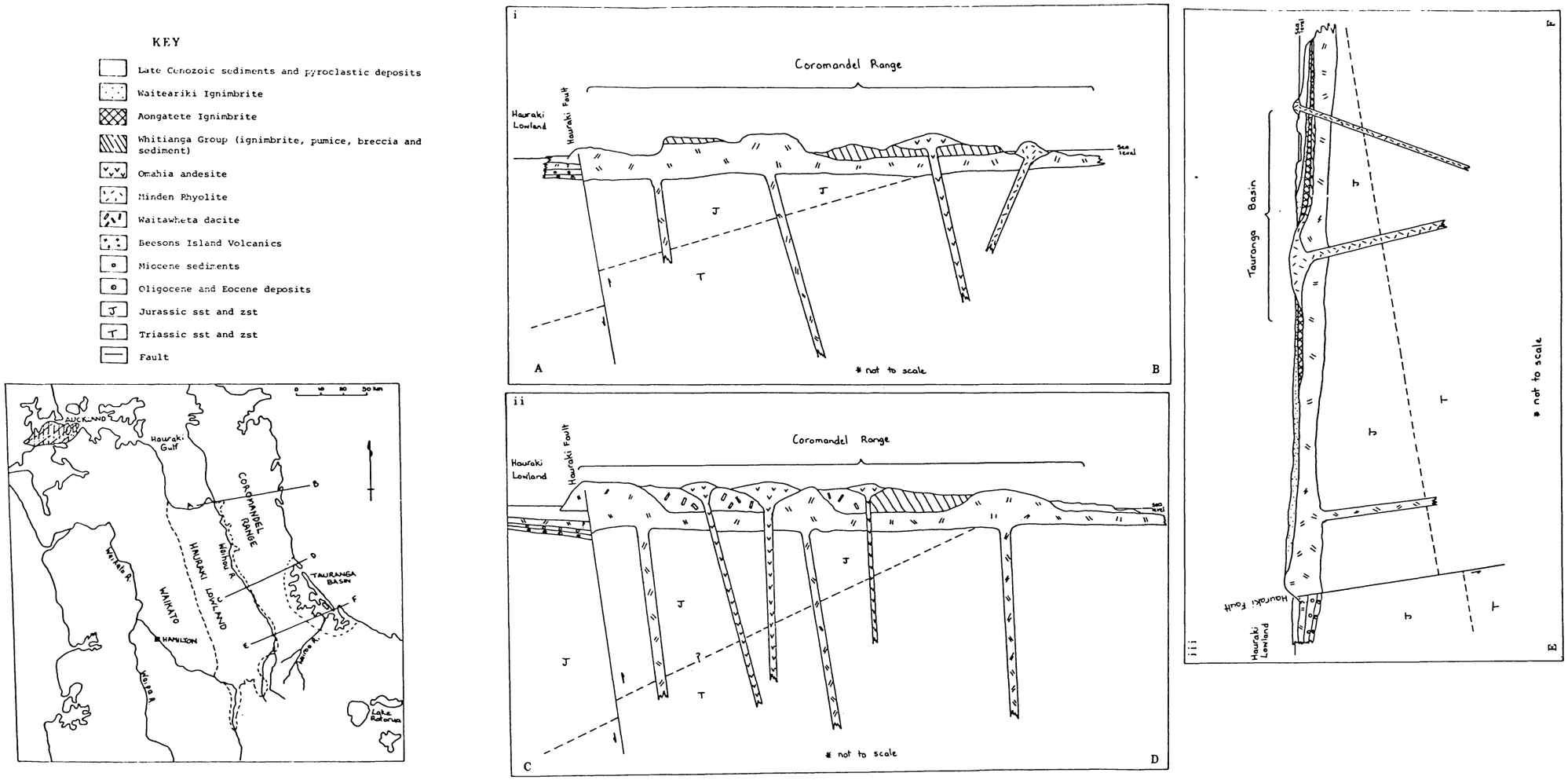


Fig. 4.4 Cross-sections through the Coromandel Range which indicate specific basement rocks in the Tauranga area (adapted from Healy *et al.*, 1964 and Schofield, 1973).

Fig. 4.5 Sketched cross-sections W-E across the Tauranga Basin representing various stages of geologic and structural development with time:

(a) Immediately after emplacement of the Waitetariki Ignimbrite (0.84 m.y. B.P.) in the Tauranga Basin. Cross-section through the Mt Minden rhyolite dome. In the northern parts of the Basin deposits older than Waitetariki Ignimbrite may have been tilted eastwards due to uplift of the present Kaimai Range in the north; prior to emplacement of Waitetariki Ignimbrite in the southern parts of the Basin, the surface was largely horizontal.

(b) After uplift of the Kaimai Range (and subsidence in the Basin) in the north and in the south, to present elevation. Cross-section through the Whakamarama Plateau - Te Puna area.

(c) After uplift of the Kaimai Range to present elevation (and subsidence in the Basin). Cross-section through the Kaimai Range - Katikati areas.

Legend



Matua Subgroup deposits

Wairoa Ignimbrite (∿0.6 m.y. B.P.)

Waitetariki Ignimbrite (0.84 m.y. B.P.)

Aongatete Ignimbrite (∿1.26 - 0.86 m.y. B.P.)

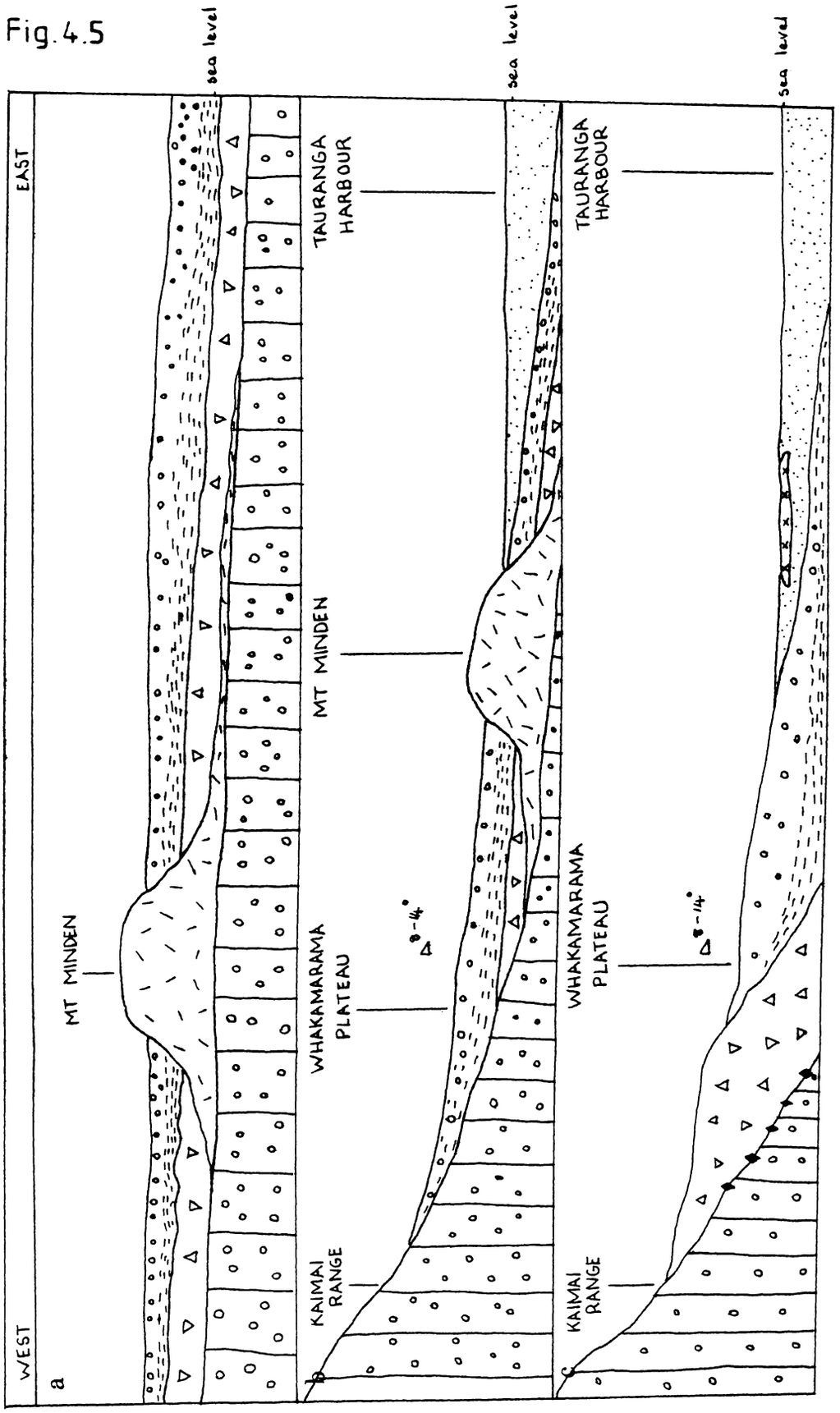
Minden Rhyolite (4.34 m.y. B.P.)

Beesons Island Volcanics (16 - 7 m.y. B.P.)

Carbonaceous material (3 cm thick)

Angle of dip of Waitetariki Ignimbrite

Fig. 4.5


WEST
EAST
a
sea level
MT MINDEN
WHAKAMARAMA PLATEAU
TAURANGA HARBOUR
KAIMAI RANGE
8-14°

assessment of this subsidence can be made by stratigraphic correlation and terrace levels, as is elaborated upon below.

Two Middle-Pleistocene ignimbrites, the Aongatete (∿ 1.26 m.y. B.P.) and Waitearikí, are recorded at, or near the base of the sedimentary succession in drillholes at depths between 100 m and 200 m throughout the Basin (e.g. Matua, Otumoetai, Te Puna, Greerton). The Waitearikí Ignimbrite, which forms the Whakamarama Plateau in the west, dips 8 - 14° E towards Tauranga Harbour, and in the southeastern parts of the Basin the Papamoa Ignimbrite dips 8 - 12° NE into the Welcome Bay area. The Te Ranga and Waimakariri Ingimbrites occurring in the southern parts of the Basin, have dips of only 1 - 4° towards the N and NE, and are part of a much younger topographic feature, the Mamaku Plateau. The Kaimai Range proper terminates by transition into this plateau (Fig. 4.6). Mapping in the Whakamarama Plateau (Houghton B.F., unpublished; this study) suggests that the Range has been uplifted to a greater extent in the north than the south. Some evidence based on the occurrence of conglomerates interbedded with pyroclastic deposits older than ∿ 0.5 m.y. B.P. in the northern parts of the Basin also suggests that the Range may have been uplifted in the north prior to elevation in the south (Fig. 4.7).

In the northern extremities of the Tauranga Basin the Kaimai Range causes the W - E lateral extent of the Basin to narrow. In the south the gradual transitional termination of the Kaimai Range into the Mamaku Plateau is probably related to the decreasing throw on faults on passing southwards in the Hauraki Depression. The throw on these faults possibly continues to decrease gradually underneath the Mamaku Plateau (Fransen, 1982). It is suggested that in areas adjacent to the southern parts of the Tauranga Basin this transitional termination results from the tilting of the Kaimai horst towards the east.

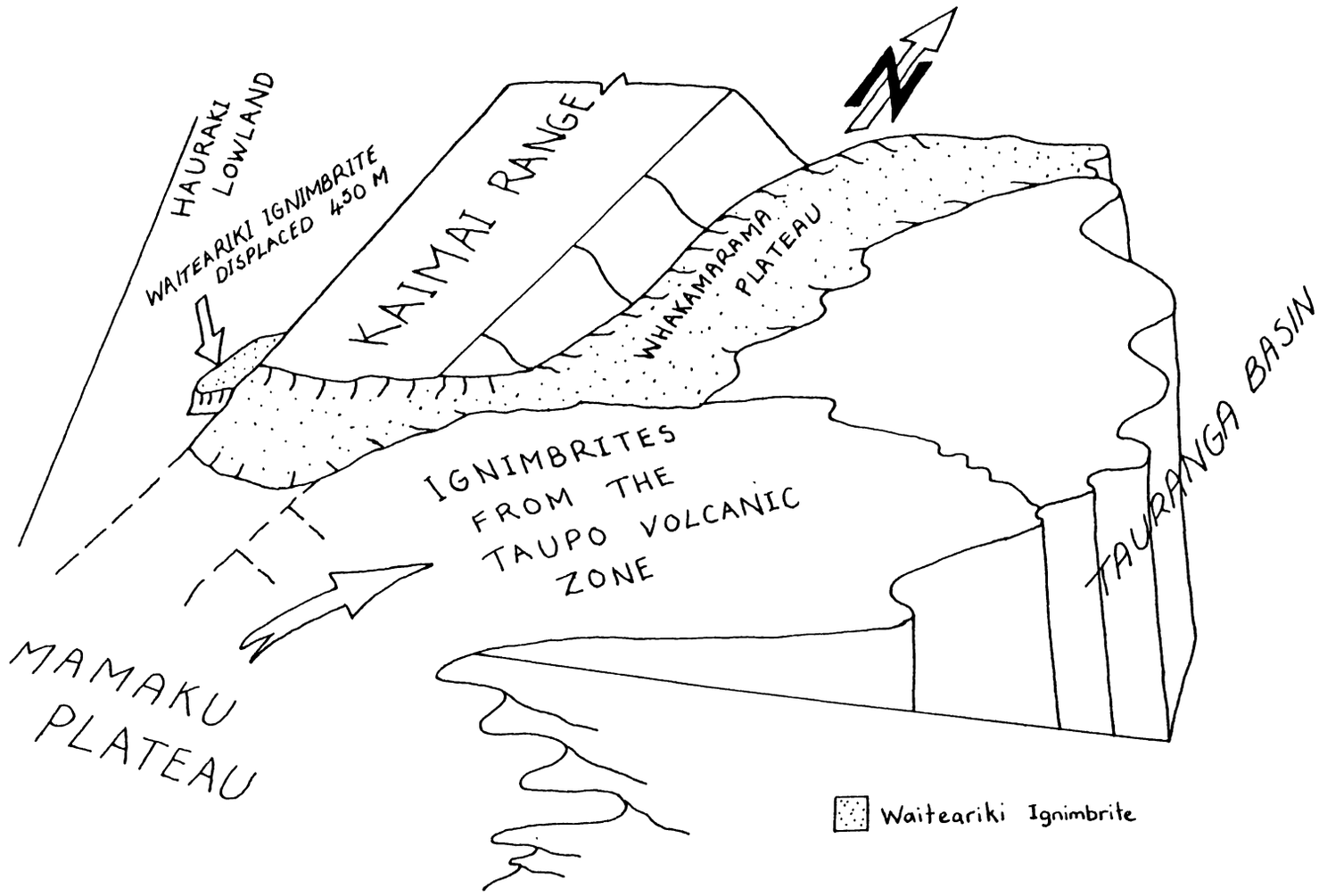


Fig. 4.6 A sketch showing distribution relationships between the older Waitearíki Ignimbrite (0.84 m.y. B.P.) underlying the Whakamarama Plateau and the younger (<0.84 m.y. B.P.) ignimbrites which have been deposited in the Tauranga Basin.

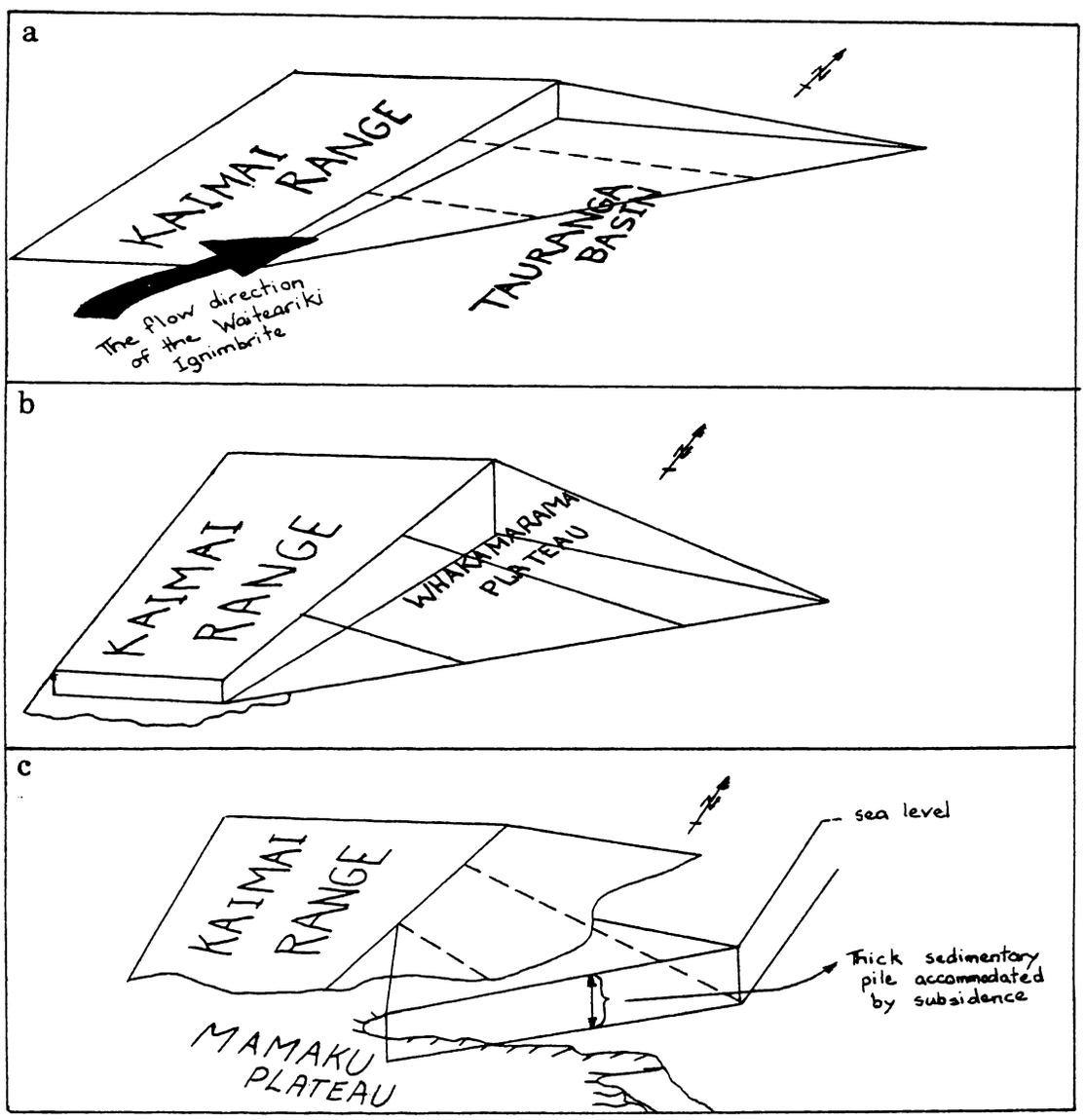
Fig. 4.7 Schematic sketches of the Tauranga Basin, looking northward from the present day Mamaku Plateau.

(a) Initial uplift of the Kaimai Range during Pliocene to mid Pleistocene time. At the end of this period (mid Pleistocene) Waitearíki Ignimbrite flows northwards into the Basin and is unrestricted in the south. In the northern parts of the Basin the ignimbrite flows eastwards. Major uplift (∿0.84 m.y. B.P.) of the Kaimai Range occurs after emplacement of the Waitearíki Ignimbrite.

(b) Subsidence in the Basin continues. Waitearíki Ignimbrite and older beds (Beeson's Island Volcanics, Aongatete lg.) are continually tilted eastwards.

(c) Subsidence continues in the mid to upper Pleistocene. Ignimbrites erupted from the Taupo Volcanic Zone are deposited in the Basin. A thick sedimentary pile begins to develop.

Fig. 4.7


a
KAIMAI RANGE
TAURANGA BASIN
The flow direction of the Waiteariki Ignimbrite
b
KAIMAI RANGE
WHAKAMARAMA PLATEAU
c
KAIMAI RANGE
sea level
Thick sedimentary pile accommodated by subsidence
MAMAKU PLATEAU

(i) Subsidence and sedimentation rates

In a continuous core at Otumoetai the Waitepariki Ignimbrite is recorded at a subsurface depth of ∿ 110 m which imposes a maximum time constraint of 0.84 m.y. B.P. on the sequence of sediments in the Matua Subgroup between this depth and 3.3 m, the depth of deposition resulting from the latest marine transgression. The recorded depths at which specific rock units (e.g. Waitepariki Ignimbrite) were identified in several cores is shown in Table 4.1. Comparative depths of the welded phases of the Waitepariki Ignimbrite in cores and where it crops out in the Whakamarama Plateau can be assessed in relation to information obtained from the Otumoetai core. The ∿ 106 m depth variation between the subsurface welded Waitepariki Ignimbrite at Otumoetai and the subaerially exposed welded Waitepariki Ignimbrite cropping out in streams near Aongatete (U14/714915) and McLaren Falls (U14/783727) gives an average subsidence rate of 0.12 mm/yr.

However, accurate sedimentation rates are extremely difficult to determine in that they need to take into account compaction and regional undulation and/or warping in the sedimentary pile. Sedimentation rates since emplacement of the Waitepariki Ignimbrite (0.84 m.y. B.P.) have been calculated by subtracting the thickness of the overlying sedimentary cover at several locations in the Basin (Table 4.2) to give an approximate minimum average rate/yr.

A Maori occupation site with an age of 180 ± 50 y, 45 cm below present sea level (Schofield, 1968b), suggests a subsidence rate of 2.5 mm/yr. Subaerial correlation of sediments at Matua and Te Puna indicates regional undulations and warping over a distance of 2 km. For example, sediments exposed in coastal cliffs at Matua, 20 m above the beach surface, occur only 1 m above the beach surface at Te Puna. It is probable that regional warping in the Tauranga Basin is related

TABLE 4.1 Recorded depths at which volcanic deposits were sampled in boreholes, from unpublished reports, N.Z.G.S. Rotorua

Grid Reference	Location	Rhyolite (m)	Waitеariki (unwelded) (m)	Aongatete (m)
U14/883881	Otumoetai	154 - 182	110.6 - 144	144 - 154
U14/798888	Te Puna (Wallace Rd)	271.25	170	256 - 207
U14/802876	Te Puna (Snodgrass Rd)		140 - 237	
U14/805878	Te Puna (Park Lane)	231	152 - 158	175 - 226
U14/856885	Matua		329	
U14/849844	Bethlehem (Moffat Rd)	155 - 177	128?	
U14/896866	Tauranga City (Willow Park)	246		
U14/892827	Tauranga City (Waimapu)		128 - 231	256 - 389
U14/897816	Maungatapu		57 - 149	149 - 408
U14/817759	Belk Rd (Griffin Rd)	183 - 262	170 - 183	

TABLE 4.2 SEDIMENTATION RATES IN THE TAURANGA BASIN

Grid Reference	Location	Sedimentation rate
U14/883881	Otumoetai	0.13 mm/yr
U14/802876	Te Puna	0.17 mm/yr
U14/892827	Waimapu estuary	0.15 mm/yr
U14/897816	Maungatapu	0.07 mm/yr
U14/862809	Greerton	0.12 mm/yr
U14/843784	Kennedy Road	0.17 mm/yr
U14/817759	Griffin Road	0.20 mm/yr
U14/736906	Apata	0.10 mm/yr
	Katikati	0.02 mm/yr
		Average = 0.12 mm/yr

to a combination of differential subsidence, variations in the thickness of sediment throughout the Basin, and possibly to readjustment towards a state of equilibrium due to loading by water in the estuary (Bowen, 1978).

Although subsidence has occurred since emplacement of the Waiteariki Ignimbrite the development of the Basin has also been affected profoundly by rhyolitic volcanism during the Pliocene (Fig. 4.8). Table 4.3 presents a summary of possible structural events in the Tauranga Basin since the Miocene.

4.2.1 Intrabasinal faulting

The only observed faulting in the study area is small scale (15 cm throw) N-S trending normal faults occurring immediately under a debris flow deposit of reworked Te Puna Ignimbrite on Motuhoa Island (Fig. 4.9). Fault displacement has resulted in synsedimentary deposition. This faulting suggests that some subsidence may have occurred after emplacement of the Te Puna Ignimbrite.

4.3 HAURAKI DEPRESSION : COMPARISON WITH THE TAURANGA BASIN

Hochstein and Nixon (1979) suggested that the Hauraki Depression (Healy *et al.* 1964) is a large fault-controlled tectonic feature which they named the Hauraki Rift. The structure comprises two interdepressional grabens separated by a median horst (Fig. 4.10), and horst-graben structures are also recorded southwards under the Mamaku Plateau (Fransen, 1982).

The Depression is thought to have developed since about 0.84 m.y. B.P. (Cuthbertson, 1981), subsidence being related to the uplift of the Kaimai Range; however, initial movement was possibly earlier (Cole, 1979). It has been suggested that the depression formed either in

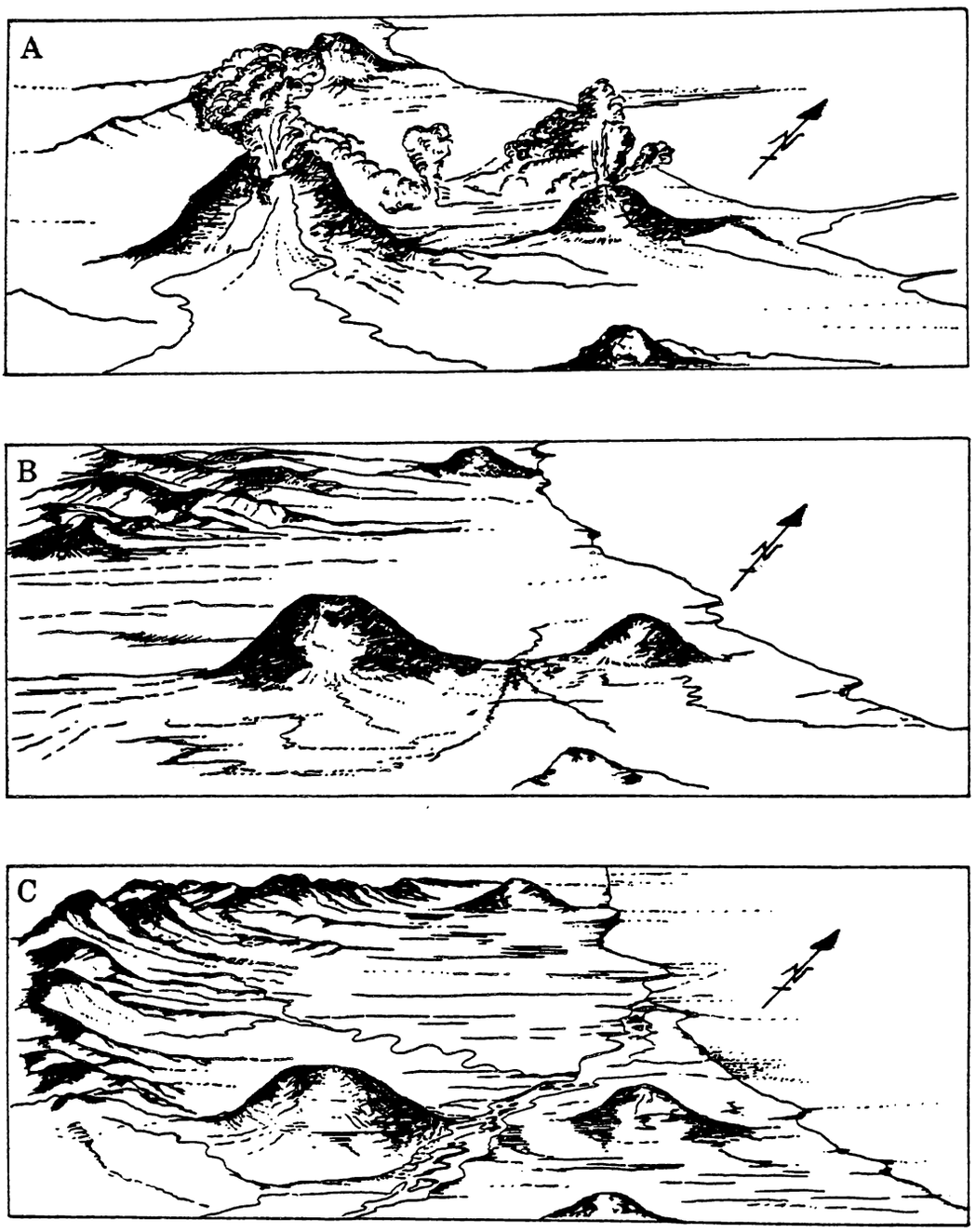


Fig. 4.8 Sketches showing possible structural events in the Tauranga area since the Pliocene. The sketches relate to events listed in Table 4.3.

TABLE 4.3

STRUCTURAL HISTORY OF THE

TAURANGA BASIN

Factors affecting subsidence	Age (m.y. B.P.)	Series/Epoch
(A) subsidence due to rhyolite volcanism in the Tauranga Region	5 - 2	Late Miocene to Pliocene
(B) uplift of Kaimai Range in the north	2 - 1	Pliocene to Early Pleistocene
(C) uplift of Kaimai Range in the south	1 - 0.8	Pliocene to mid Pleistocene



Fig. 4.9 Small scale normal faults exposed in a coastal cliff section on Motuhoa Island (U14/805914).

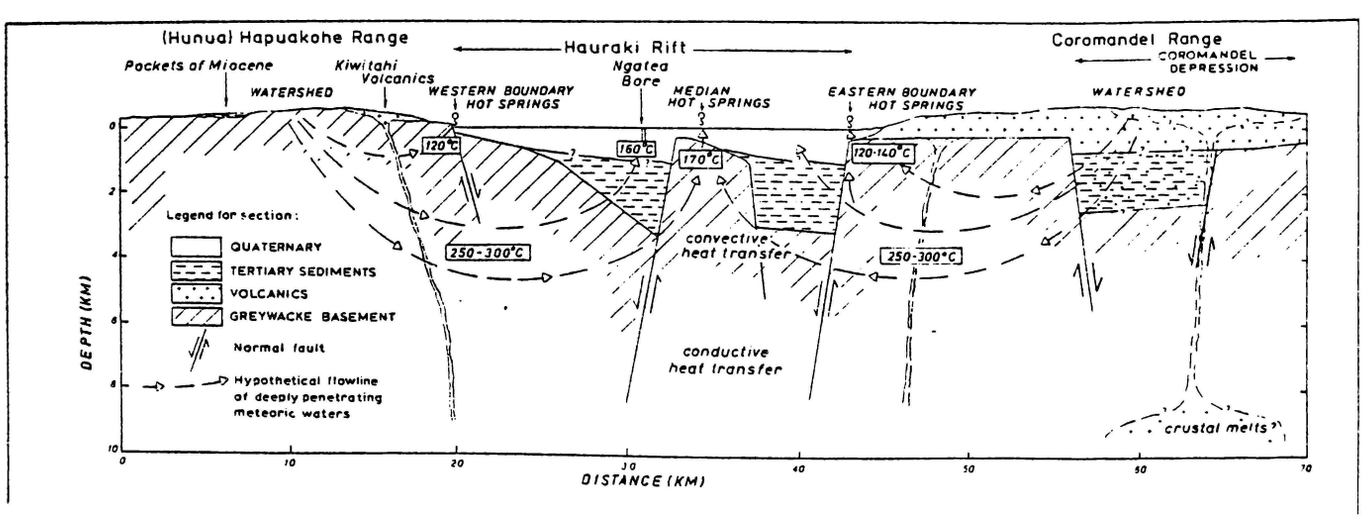


Fig. 4.10 Simplified geological section across the Hauraki Depression. (from Hochstein, 1979).

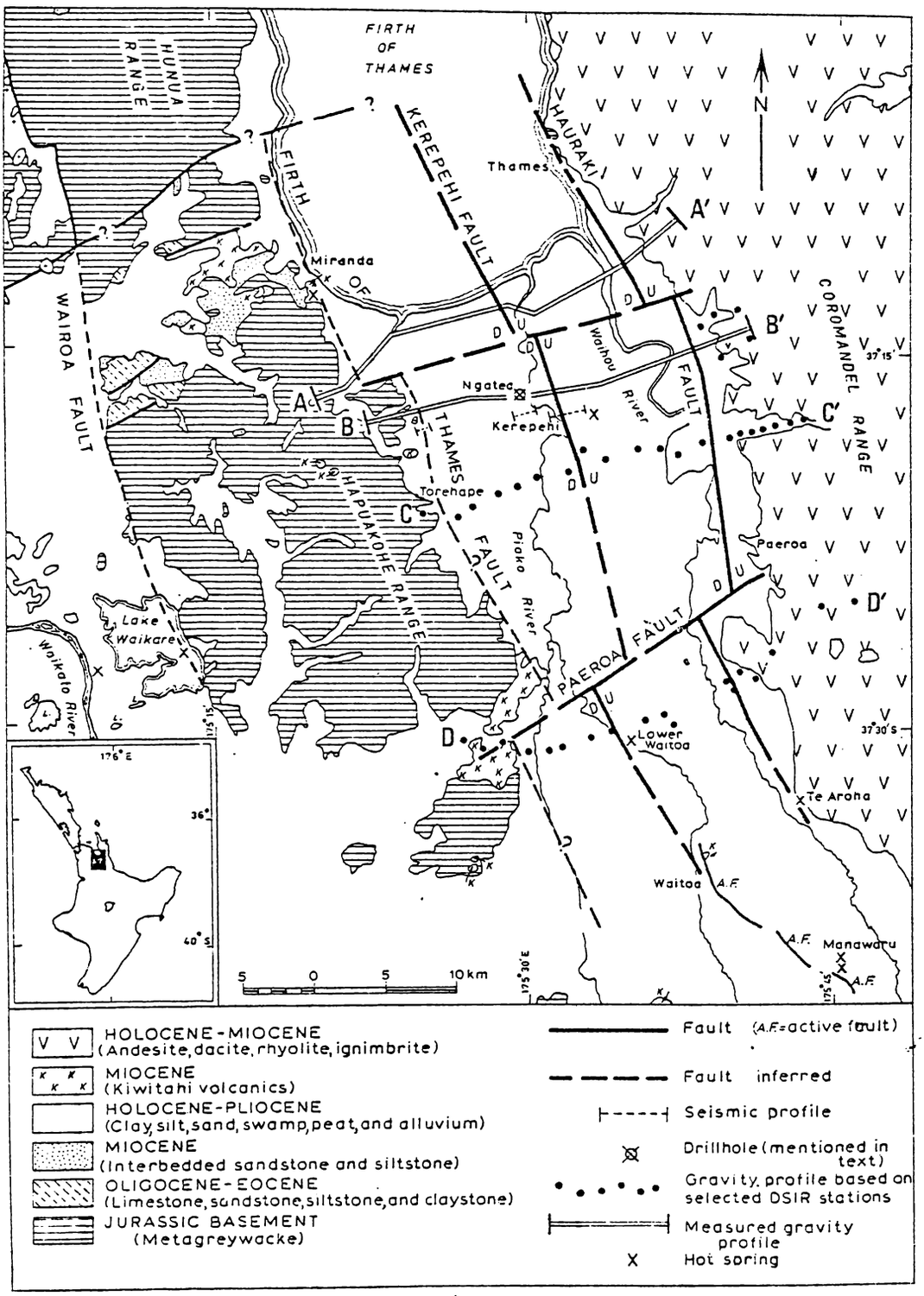


Fig. 4.11 General geology of the Hauraki Depression and the position of faults (from Hochstein, 1979).

relation to a major readjustment of the Indian and Pacific plates (Hochstein and Nixon, 1979) or because of a collapsed geanticline (Schofield, 1968a). The depression has since been filled with up to 1500 m of Quaternary sediments of the Tauranga Group (Tearney, 1981). Faulting was initiated in the Middle Tertiary (Hochstein, 1979) and two major fault systems exist in the depression (Fig. 4.11), one trending NNW-SSE and the other NE-SW (Hochstein, 1979). The throws on the faults are large (e.g. 3 km throw on the Kerepehi Fault; Hochstein, 1979) along with a deepening of the depression (Hochstein, 1979) away from the Mamaku Plateau (Fransen, 1982). Transverse faults cross the Depression causing large horizontal offsets (3 km near Paeroa) of the major NW-SE fault systems. Large-scale faulting has displaced several ignimbrites (e.g. the Ongatiti (0.75 m.y. B.P.) by more than 40 m, the Waitearíki (0.84 m.y. B.P.) by at least 450 m).

The Depression is unlike the Tauranga Basin in that it is directly fault-controlled. This has had an affect on the type of sedimentation, which is dominated by alluvial fan and braided river deposits (Cuthbertson, 1981).

Active faulting and shallow (c.12 km) earthquake activity indicate that the Hauraki Depression is still subsiding (Hochstein and Nixon, 1979).

4.4 TECTONIC SETTING OF THE TAURANGA BASIN

It has been suggested that a major readjustment of the Indian and Pacific plate margins occurred about 6 m.y. B.P. (Hochstein and Nixon, 1979; Cole, 1979). The Hauraki Depression (Hochstein and Nixon, 1979) and the Havre Trough (Feden *et al.* 1976) possibly developed in response to this plate movement about 5 m.y. B.P. Tensional faulting occurred

on the eastern side of Coromandel Peninsula and rhyolitic eruptions related to this faulting unleashed new activity in the Tauranga Region (Cole, 1979). About 2 - 3 m.y. B.P. the Tauranga Volcanic Zone is thought to have formed in relation to tensional graben structures (Cole, 1979) or active marginal basins (Karig, 1974).

Structural development in the Tauranga Basin has been due mainly to large scale tectonic subsidence. The uplift of the Kaimai Range ($\sim$ 0.84 m.y. B.P.) and evidence for the initiation of a rift system northeast of the Basin indicate large scale structural controls.

Work by the Gulf Research and Development Company (1972) and Carter (1976) indicates that the sea bed immediately northeast of the Tauranga Basin has a steep-sided graben structure named the Ngatoro Basin (Fig. 4.12). Lying on the western boundary of this graben is Mayor Island, 28 km NE of Tauranga. It is suggested that this isolated volcanic island, which differs chemically from other Cenozoic volcanoes in the North Island, is compatible with a tensional rift setting (Cole, 1978).

Karig (1970) and Hawkins (1974) suggest that the Ngatoro Basin represents a southward continuation of the late Miocene Lau Basin, an interarc basin between the Lau and Tonga ridges (Cole, 1979), and the Havre Trough.

The Ngatoro Basin then appears to form an extension of this system (i.e. Lau Basin) which is regarded by these authors as a relatively young extensional interarc basin. Extension of this structure south-eastwards intersects the Bay of Plenty coast at Tauranga.

This tectonic setting can be compared with that of the Ethiopian Rift (Cole, 1969; Gibson 1974; Cole, 1978) and of Pantelleria Island (Vilari, 1974; Cole, 1978).

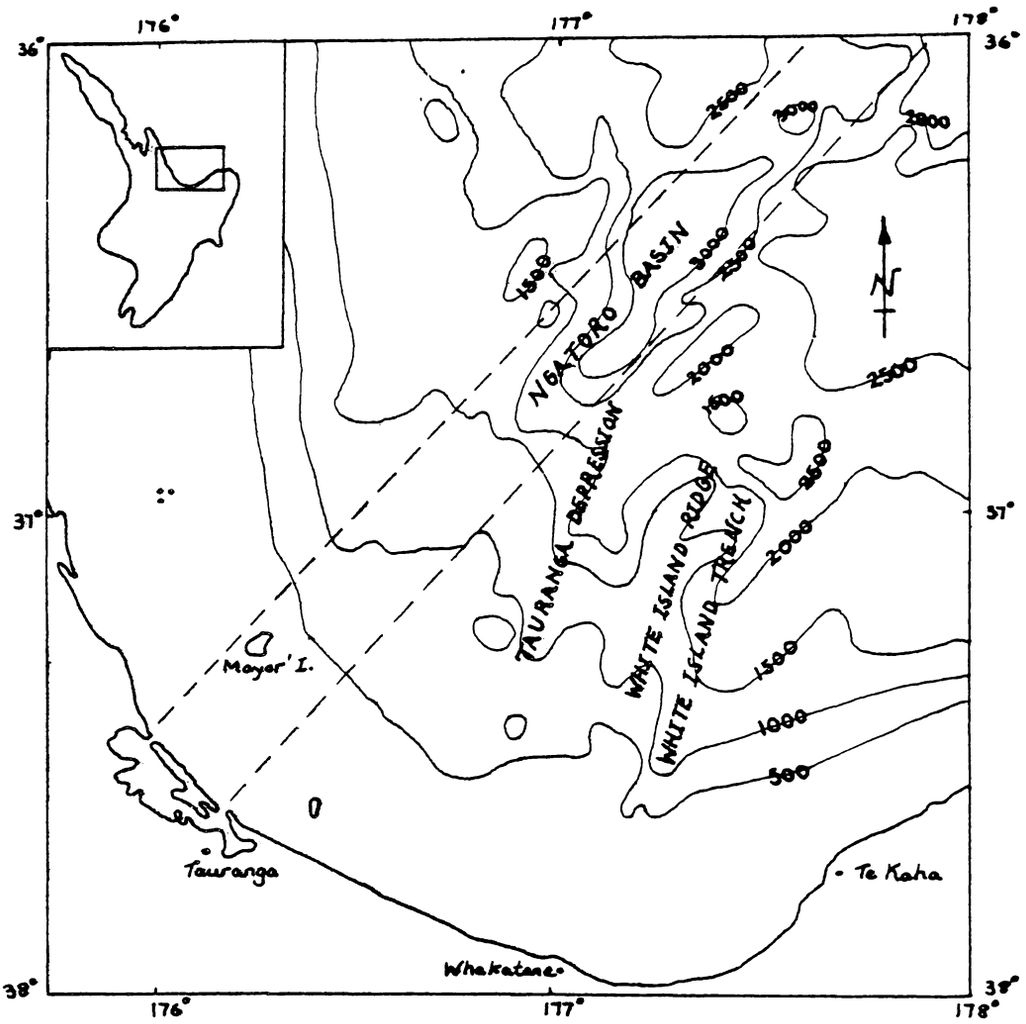


Fig. 4.12 Location of Mayor Island and its relationship to the Ngatoro Basin in the Bay of Plenty. Bathymetry in meters (from Cole, 1978).

CHAPTER FIVE

TEXTURAL PROPERTIES OF MATUA SUBGROUP DEPOSITS

5.1 INTRODUCTION

Considerable amounts of information may be obtained from sediment property studies. Of particular concern is the interpretative analysis of environmental conditions prevailing at the time of deposition as inferred from the textural characteristics of deposits. Textural analyses were carried out on 50 samples from the three main stratigraphic sections at Matua, Omokoroa and Te Puna, as well as on samples from elsewhere in the Tauranga Basin. Results are given in Appendix II.

Deposits in the Tauranga Basin have been emplaced by 3 major mechanisms : (a) Fluvial processes, (b) Pyroclastic flow, and (c) Pyroclastic fall. The textural characteristics of these deposits are described separately in the following sections with the intention of refining their modes of transport and deposition. The textural terminology used is shown in Figure 5.1 and a conclusions table is presented at the end of this chapter (Table 5.1).

5.2 TEXTURAL CHARACTERISTICS OF FLUVIAL DEPSOITS

5.2.1 Textural Plots (Figs. 5.1 and 5.2)

Three major textural groups are evident from textural plots, namely gravel -, sand -, (Fig. 5.2), and mud - dominated deposits (Fig. 5.3). The proportions of each of these lithotypes vary between each stratigraphic section and at different localities within the Basin.

A lateral variation in grain-size exists in some fluvial deposits and an overall decrease in grain-size is recorded away from source rocks, which are principally the distal ignimbrites subaerially exposed in the Basin (Chapter 6). For example, the central part of

Fig. 5.1 The textural terminology used in Figs. 5.2, 5.11 and 5.18, for : (a) Gravel-bearing detrital sediments and (b) Gravel-free detrital sediments (after Folk, Andrews and Lewis, 1970).

(a)

G = gravel

sG = sandy gravel

msG = muddy sandy gravel

mG = muddy gravel

gS = gravelly sand

gmS = gravelly muddy sand

gM = gravelly mud

(g)S = slightly gravelly sand

(g)mS = slightly gravelly muddy sand

(g)M = slightly gravelly mud

S = sand

mS = muddy sand

sM = sandy mud

M = mud

(b)

S = sand

zS = silty sand

mS = muddy sand

cS = clayey sand

sZ = sandy silt

sM = sandy mud

sC = sandy clay

Z = silt

M = mud

C = clay

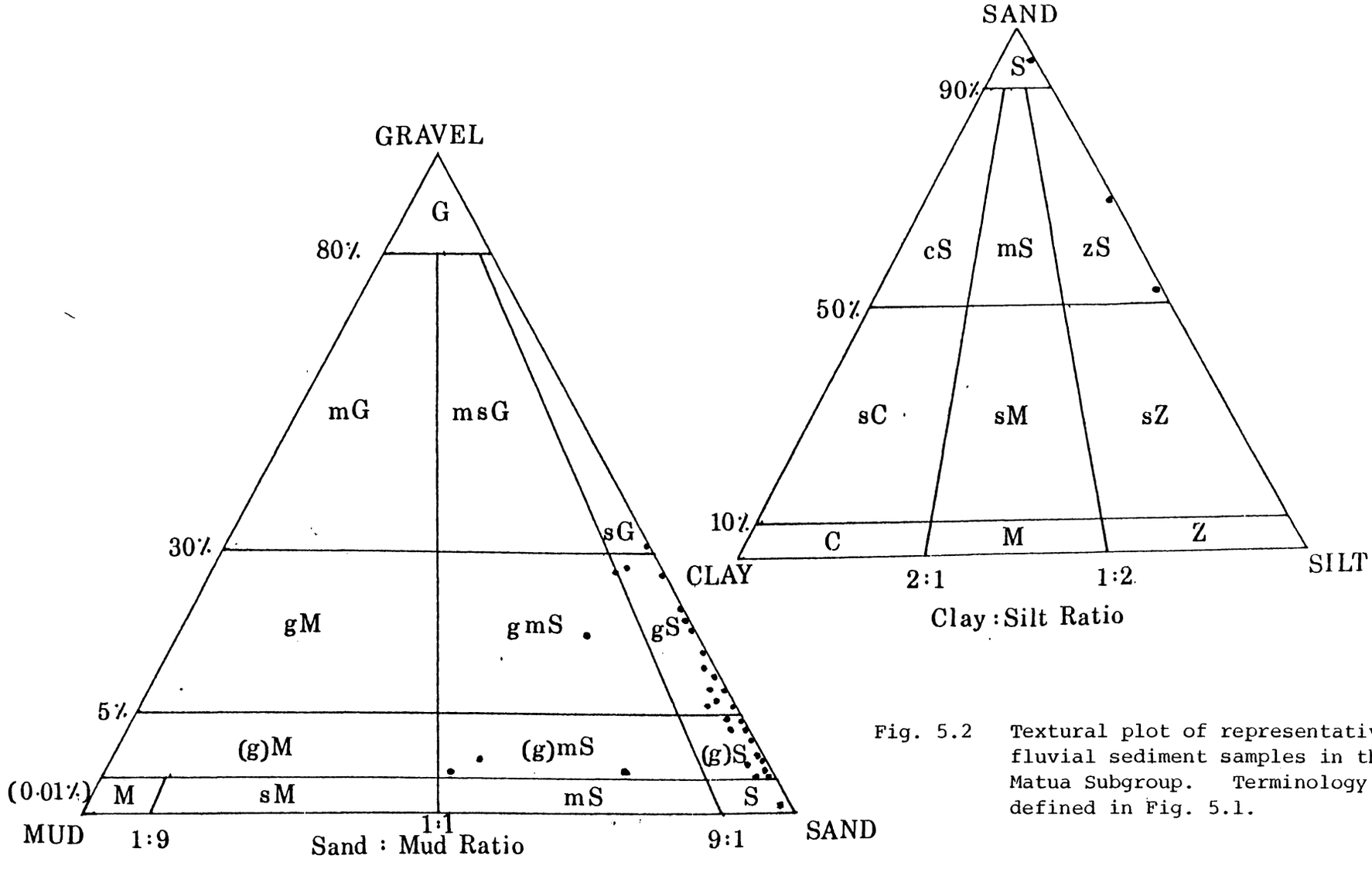


Fig. 5.2 Textural plot of representative fluvial sediment samples in the Matua Subgroup. Terminology is defined in Fig. 5.1.

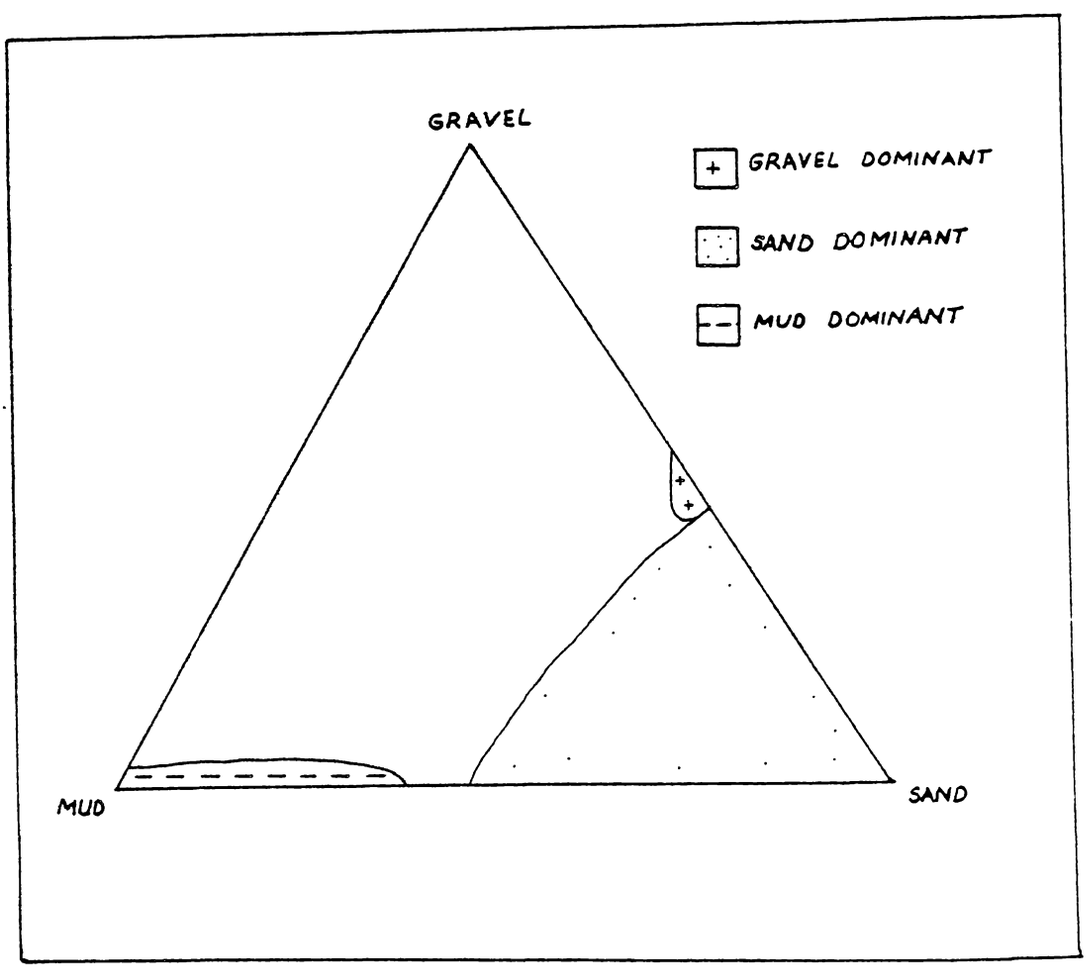


Fig. 5.3 Major textural lithotypes of fluvial sediments in the Matua Subgroup.

the map area from Pyes Pa Road to coastal cliff sections at Matua and Te Puna records a northerly decrease in grain-size in fluvial deposits from slightly gravelly sands to predominantly sandy sediments.

5.2.2 Grain-Size Distribution Curves

The characteristics of individual grain-size distribution curves provide a basis for environmental interpretation (Visher, 1969). Cumulative size frequency curves on log-probability paper commonly display two or three straight-line segments, each corresponding to separate log - normal subpopulations within the total sediment (Visher, 1969). Visher (1965, 1969) presumed that grading curves of all clastic sediments are composites of three basic modes of sediment transport with the straight-line segments in the log-probability plot corresponding to transportation by traction, saltation and suspension (Fig. 5.4). However, "any attempt to define precise limits for the slope, truncation points and percentages of the three basic populations for individual environments in impossible" (Visher, 1969) and grain-size distributions rarely conform to a simple log-normal law.

The grain-size distribution curves for the upper Matua Subgroup fluvial sediments (Fig. 5.5) are variable, and show that the samples range from poorly to well sorted. Most of the curves have two straight line segments and about 20% show three straight line segments (e g. similar to the sigmoidal curves of Visher, 1969). Comparison with the curves of Visher (1969) suggests that some of the Matua Subgroup deposits show no traction population, usually distinguished in the coarse, <0.0 ϕ range, of a log-normal subpopulation. In others a traction population is only weakly developed. However, about 60% of the samples analysed showed a traction population and it is evident that material of an appropriate grain-size (i.e. granules and pebbles)

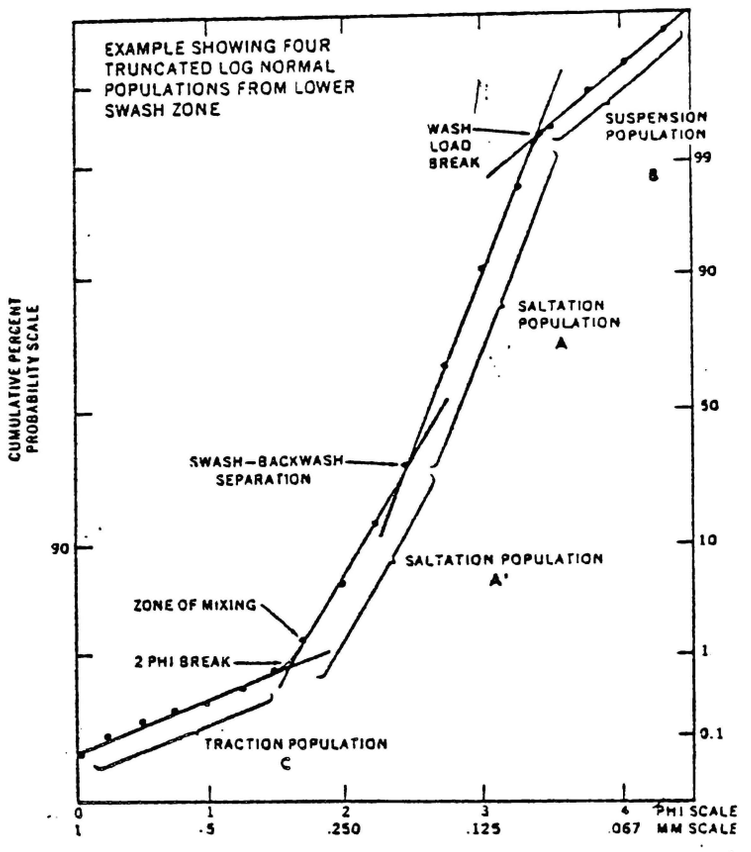


Fig. 5.4 Relation of sediment transport dynamics to populations and truncation points in a grain-size distribution (after Visher, 1969).

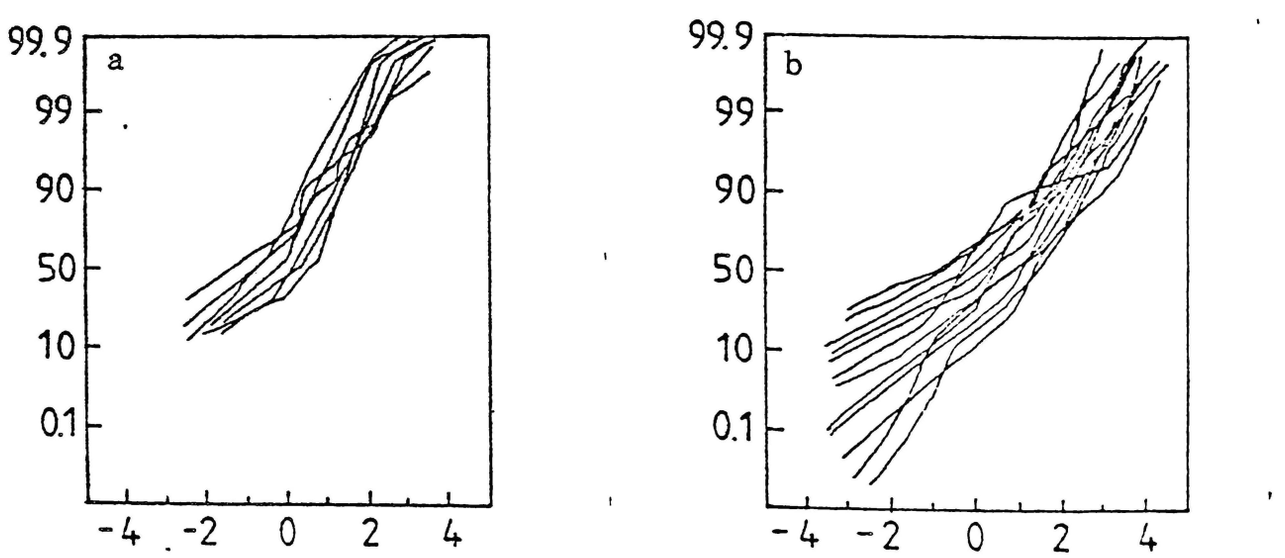


Fig. 5.5 Cumulative grain-size frequency curves for fluvial/sediments in the Matua Subgroup.

a) moderately to well sorted samples from Te Puna and Pyes Pa Road,

b) representative samples from Matua, Cambridge Road, Pyes Pa Road and Te Puna.

was avilable at the time of deposition. It is this size range, depending on the density of individual clasts, that is more consistent with a tractive mode of sediment transport. The greater proportion of sediment in the Matua Subgroup, show log-normal subpopulations which correspond to transportation by saltation. Curves showing a saltation population only, probably resulted from extreme mixing of suspension and saltation populations. Poorly sorted samples when plotted on log-probability paper showed simple curves with indistinct log-normal subpopulations. In moderately to well sorted sediment, the cumulative size frequency curves displayed more distinct subpopulations often showing three straight-line segments (Visher, 1969). Only one sample recorded a more complex curve (i.e. four straight line segments).

When compared with grain-size distribution curve characteristics given by Visher (1969) for modern fluvial sediments (Fig. 5.4) the upper Matua Subgroup curves show a coarser maximum limit for the saltation (-2.25ϕ cf. - 0.25) and suspension (2.0ϕ cf. 2.5ϕ) populations, and a wider range (i.e. similar to that in the Hinuera sediments, Hume *et al.*, 1975) in the slope (reflecting sorting) of the saltation population (28 to 64^{o} cf. 42 to 60^{o}), a generally coarser saltation population (-0.5 cf. 2.25ϕ), a consistently well developed saltation population (70% cf. 95%), a poorly sorted suspension population (up to 5% cf. up to 40%), and a greater degree of mixing between the saltation and suspension loads (significant cf. slight).

It is inferred from comparison of the distribution curves with Visher (1969) and Hume *et al.* (1975) that the upper Matua Subgroup grain-size curve characteristics indicate generally rapid deposition under turbulent, fluctuating energy conditions. The pumiceous nature of the Matua Subgroup fluvial deposits is regarded in this study as

a contributing factor to the poor sorting shown by the curves and to the dominance of a saltation mode of transport. The density of clasts and the flow regime must be considered when interpreting subpopulations as being related to a traction mode of transport. The hydrodynamic behaviour of pumice although not fully understood, shows variable differences in behaviour between waterlogged and dry vesicular clasts. Hydrodynamic experiments show that saturated pumice may still be susceptible to transportation by saltation up into the coarse, <0.0 ϕ, range of grain-sizes.

5.2.3 Statistical Parameters

(i) Grain-Size

The mean grain-size of deposits ranges from -0.1 ϕ (very coarse sand) to 3.3 ϕ (very fine sand) with the most common values in the coarse, medium and fine sand-grades (Figs. 5.6B and 5.7A). Most samples are bimodal or trimodal (Fig. 5.6C); gravel modes occur at -2.0 to -2.5 ϕ (small pebble), sand modes at 1.0 ϕ to 1.5 ϕ (coarse sand), 1.5 to 2.0 ϕ (medium sand and 2.0 to 3.0 ϕ (fine sand).

The gravel mode possibly represents blocks and lapilli sized material supplied from unwelded pyroclastic flow deposits. The sand modes represent poly- and monomineralic grains released during the physical disintegration of a number of source rocks, during glacio-eustatic changes which affected the Tauranga area, or through the direct action of fluvial erosion. The attrition of pumice fragments was an important source for sand modes. The first percentile, C, an approximation of the coarsest grain-size (Fig. 5.6A) in the sediment, indicates that clasts as large as -4.5 ϕ (pebbles) were incorporated in the upper Matua Subgroup sediments. The coarse-grained nature of fluvial sediments is partly a result of the hydrodynamic behaviour of pumice (i.e. low density).

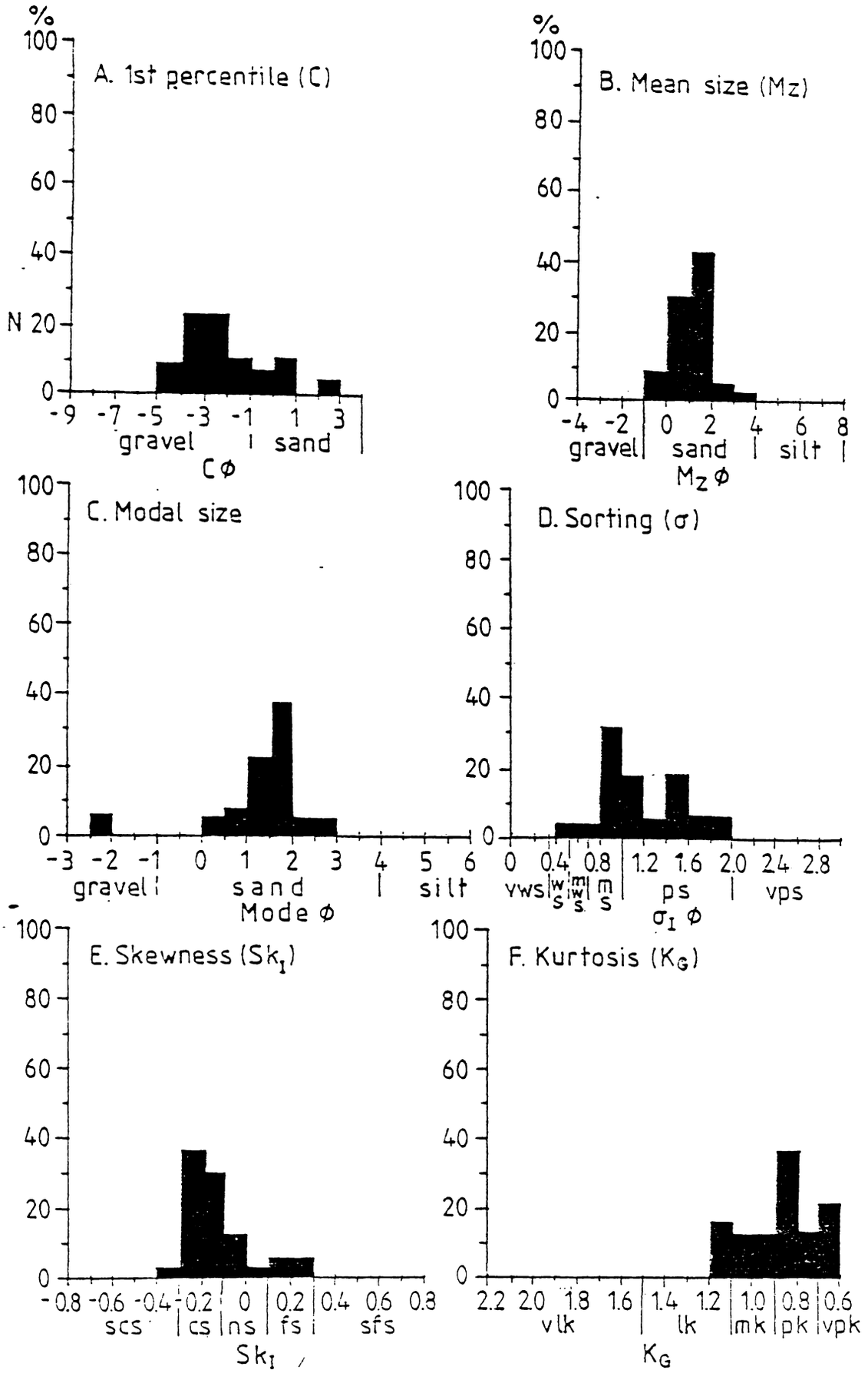


Fig. 5.6 Histograms of grain-size statistical parameters for fluvial sediments in the Matua Subgroup plotted as a function of numerical occurrence. Statistical parameters are defined in Fig. 2.3.

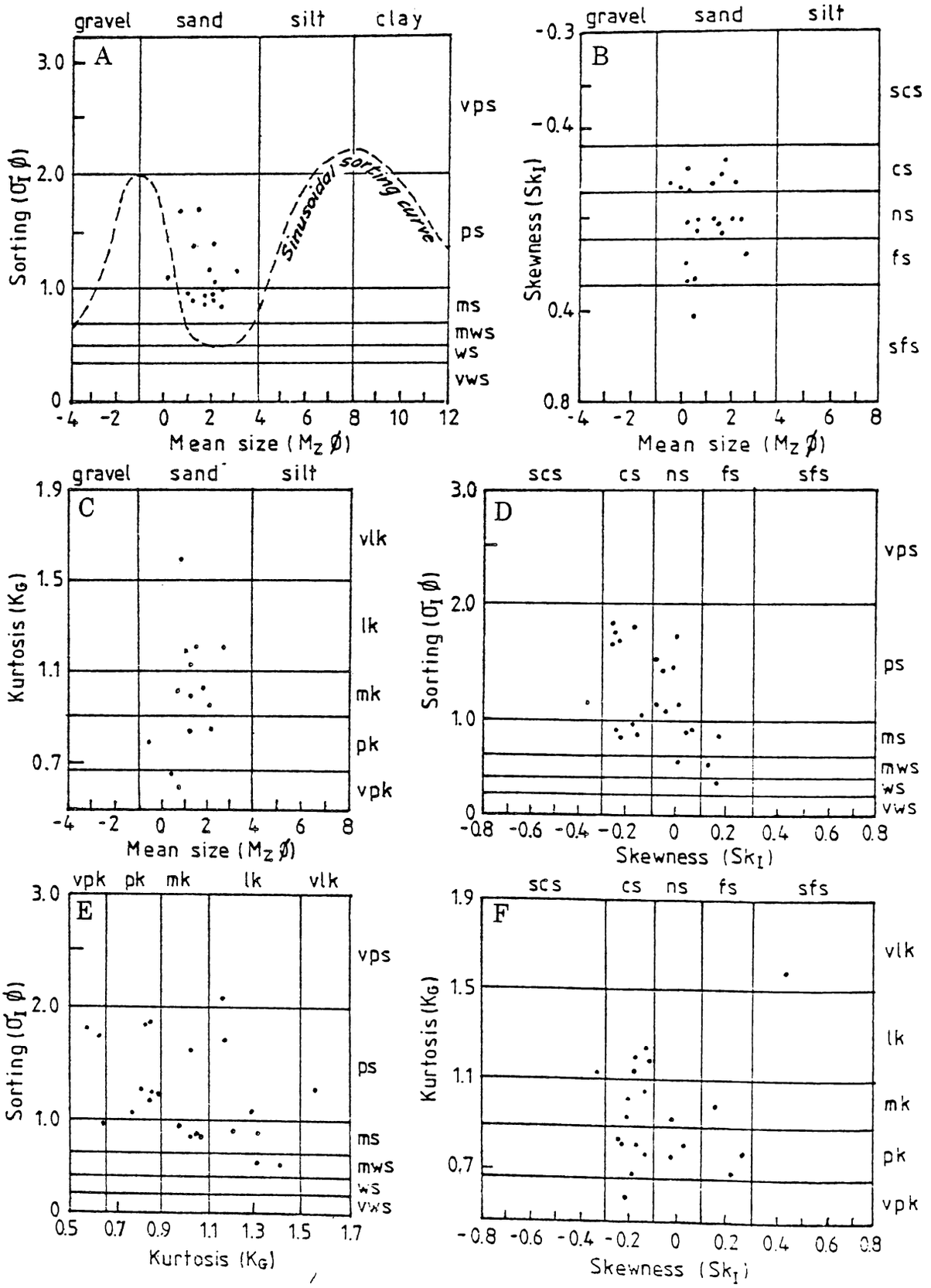


Fig. 5.7 Relationships between grain-size statistical parameters for fluvial sediments in the Matua Subgroup. Symbols as in Fig. 2.3. Sinusoidal sorting curve in A is after Folk (1968).

(ii) Sorting (Fig. 5.6D)

Fluvial sediments are poorly to well sorted. A large proportion (i.e. two thirds) of the samples are poorly sorted, indicative of a wide range of grain-sizes. Localities away from the coast become more poorly sorted in areas proximal to pyroclastic deposits. Source rocks, in particular distal ignimbrites, supplied a wide range of grain-sizes to the Matua Subgroup fluvial deposits. An increase in the mean grain-size of gravels is recorded in pyroclastic flow deposits. Information derived from sedimentary structures indicate that currents were often in the upper flow regime, and that the currents were competent to transport a wide range of grain-sizes. However, rapid deposition prevented the washing out of finer sediments and a poorly sorted assemblage resulted from strong fluctuating currents. Most of the upper Matua Subgroup sediments lie above the sinusoidal sorting curve (Fig. 5.7A) of Folk (1968) in the sand range and in a region which is predominantly poorly to moderately sorted. As the mean grain-size of sands increase the sediments become more poorly sorted above this curve (Figs. 5.7A and 5.7D). This relationship between mean grain-size and sorting possibly indicates the competence of the current velocity to transport a wide range of grain sizes and reflects rapid deposition.

(iii) Skewness (Fig. 5.6E)

Skewness values for the upper Matua Subgroup sediments show a tendency to be slightly coarse-skewed (i.e. negative value). About one third of the samples were nearly symmetrical or slightly positive. When skewness is plotted as a function of mean grain-size (Fig. 5.7B) a rough trend towards negative skewness with increasing grain-size is evident. The availability of gravel sized material and rapid deposition are probably important factors in explaining this negative skew-

ness, in particular the proximity of pyroclastic flow deposits to fluvial deposits. The hydrodynamic behaviour of pumice clasts is also important, and pumice because of its low denisty in water, even after saturation, is easily transported in a fluid medium.

(iv) Kurtosis

Samples range from leptokurtic (peaked) to very platykurtic (Fig. 5.6F). Kurtosis itself is not environmentally diagnostic but its relation to other grain-size parameters may be important. A plot of kurtosis against mean grain size (Fig. 5.7C) shows a slight tendency towards leptokurtosis with decreasing mean grain-size. A trend towards platykurtosis with increasing grain-size is therefore evident and many of the samples showing this characteristic had a wide range of grain-sizes, from pebble to very fine silt or clay size. Finer grain-sizes in poorly sorted platykurtic samples are attributed to rapid deposition and/or physical disintegration and weathering of fluvial deposits. A plot of kurtosis against sorting (Fig. 5.7E) verifies this tendency and more poorly sorted deposits are platykurtic. A plot of kurtosis against skewness (Fig. 5.7F) suggests that finer grades for example, fine sands to clays have an affect on shifting skewness towards more positive numerical parameters and towards a more platykurtic plot. However, this trend is related to the poor sorting of deposits, the wide range of grain-sizes principally eroded from pyroclastic source rocks, and reflects rapid deposition of the upper Matua Subgroup fluvial deposits.

(v) CM Patterns

Passega (1957, 1964) plotted samples from known environments using the distribution parameters : C, the coarsest one percentile, and M, the median grain-size (Fig. 5.8). It was presumed that the

particular CM pattern was indicative of the depositional agent or process. "The value of C is representative of the maximum competence of the transporting agent and M is a statistic characteristic of the total range of particle sizes undergoing transport by this agent" (Hume *et al.*, 1975). Passega (1964) interpreted the composite CM pattern by segregating certain areas within the pattern in terms of the relative importance of traction, saltation and suspension modes of sediment transport. Certain values were introduced at points of inflection between the traction, saltation and suspension segments (Fig. 5.8).

CM patterns for the upper Matua Subgroup sediments (Fig. 5.9) show certain exceptions to patterns established by Passega (1957, 1964; Fig. 5.8), and there is displacement towards the coarse end of the Cϕ axis. Figure 5.9 suggests that the maximum diameter of grains transported in suspension (Ca) and saltation (Cs) was 0.0 ϕ (coarse sand) and -1.3 ϕ (granule) respectively. The values are very coarse for these types of transportation modes and suggests that current speeds were probably high, perhaps as much as 0.8 - 1.0 m/sec. The optimum diameter at which grains are easiest to roll under conditions of sedimentation (Passega, 1964) corresponds to a value Cr for the Matua Subgroup deposits of -4.5 ϕ, or pebble size.

The situation is very similar to the patterns derived for the Hinuera sediments (Fig. 5.10) in the Waikato and Hauraki regions, which were also interpreted as very high energy deposits (Hume *et al.*, 1975; Cuthbertson, 1981). Passega (1964) developed certain curve-segment relationships for basic CM patterns (Fig. 5.8). If these are compared, the Q-P segment for the upper Matua Subgroup fluvial sediments forms a similar plot to Passega's pattern for bedload movement and a tail giving an NPQ pattern (bedload and graded suspension). This pattern for the fluvial sediments is a result of grain-sizes

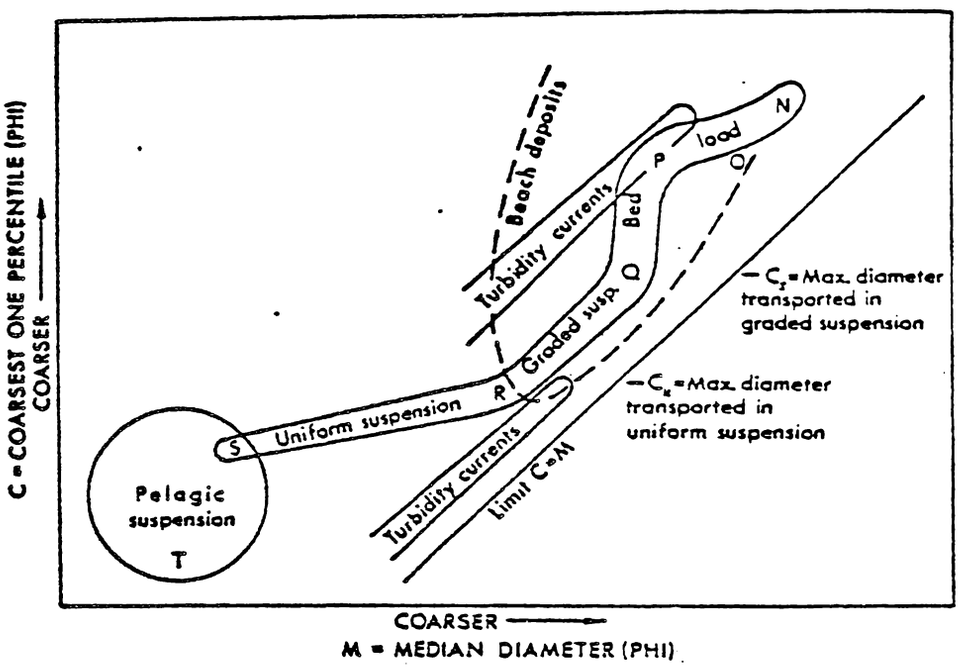


Fig. 5.8 Basic C-M patterns after Passega (1957).

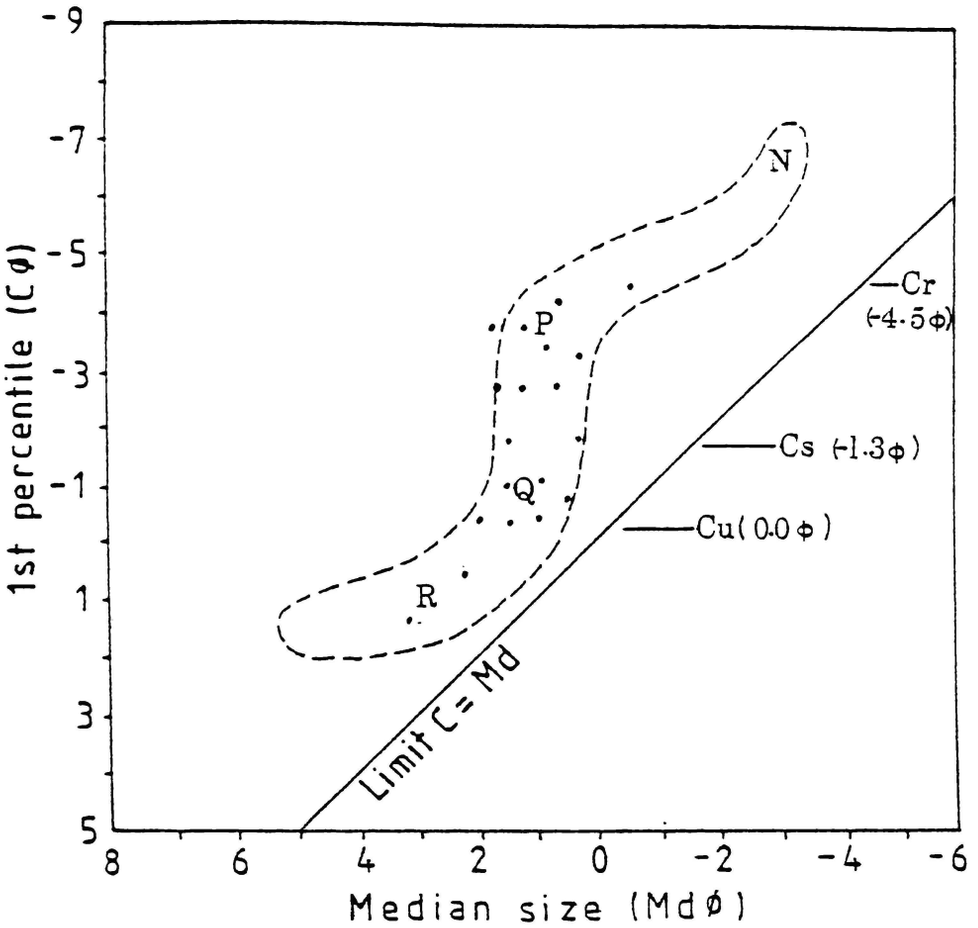


Fig. 5.9 CM pattern for representative fluvial sediment samples of the Matua Subgroup.

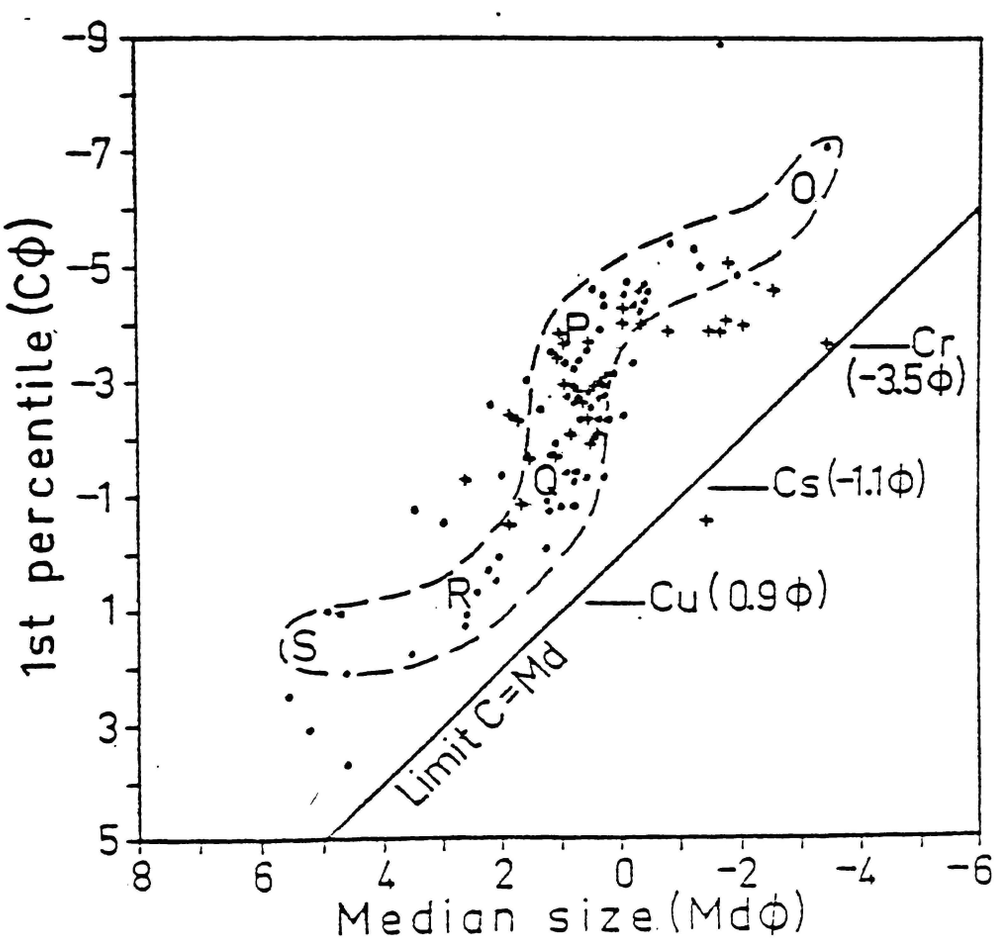


Fig. 5.10 CM pattern for sediments of the Hinuera Formation from both the southern Hauraki Lowlands and the Hamilton Basin (after Cuthbertson, 1981).

which were moved by saltation and those easiest to move by traction or rolling.

The shifting of the pattern towards the coarse end of the Cϕ axis, suggests that the Matua Subgroup fluvial deposits were deposited under high energy conditions. The hydrodynamic behaviour of pumice may also be a significant factor in this coarse distribution, because of its low density and partially to its commonly rounded shape increasing its ability to be transported by traction or by saltation.

5.3 TEXTURAL CHARACTERISTICS OF PYROCLASTIC FLOW DEPOSITS

5.3.1 Textural Plots (Fig. 5.11)

Pyroclastic flow deposits are everywhere characteristically coarse-grained, although particle sizes range from cobble to clay grade. Two major textural lithotypes occur, namely gravel- and sand- dominated (Fig. 5.12). Most deposits have a slightly gravelly sand texture.

5.3.2 Grain-Size Distribution Curves (Fig. 5.13)

Visher (1969) demonstrated that many sedimentary deposits were composed of several sub-populations formed by different depositional mechanisms active simultaneously to produce a polymodal population. A similar but cautious approach may be applied to pyroclastic flow deposits, and genetic implications are combined with criteria such as geometry and depositional structures (Sparks, 1976). In a pyroclastic flow unit or polycomponent deposit (Walker, 1971), the initial population - the entire assemblage of fragments coming from the vent - can be discussed in terms of pumice, lithic and crystal components each having a different grain-size distribution. It is not the intention of this study to fully examine grain-size charact-

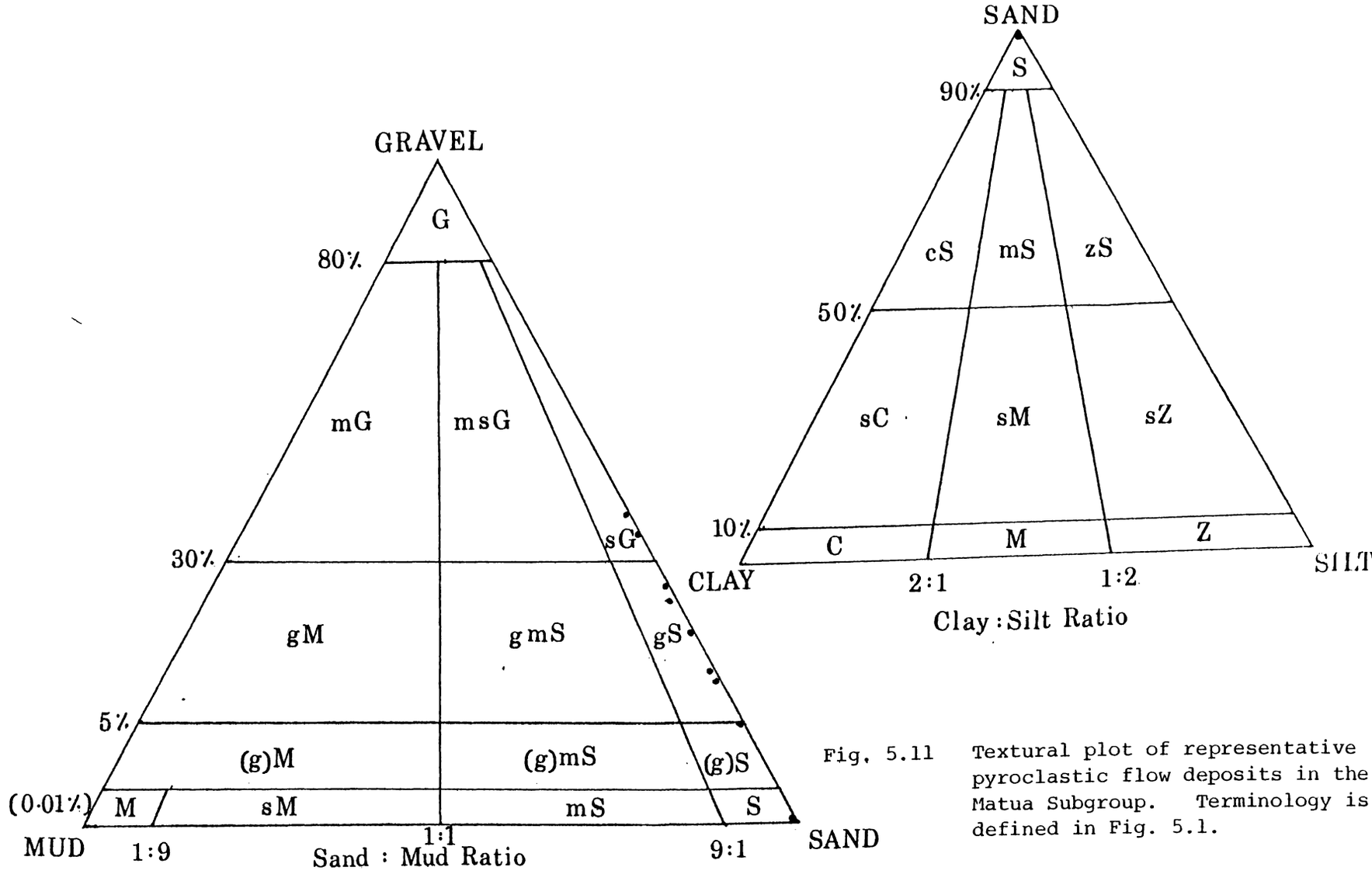


Fig. 5.11 Textural plot of representative pyroclastic flow deposits in the Matua Subgroup. Terminology is defined in Fig. 5.1.

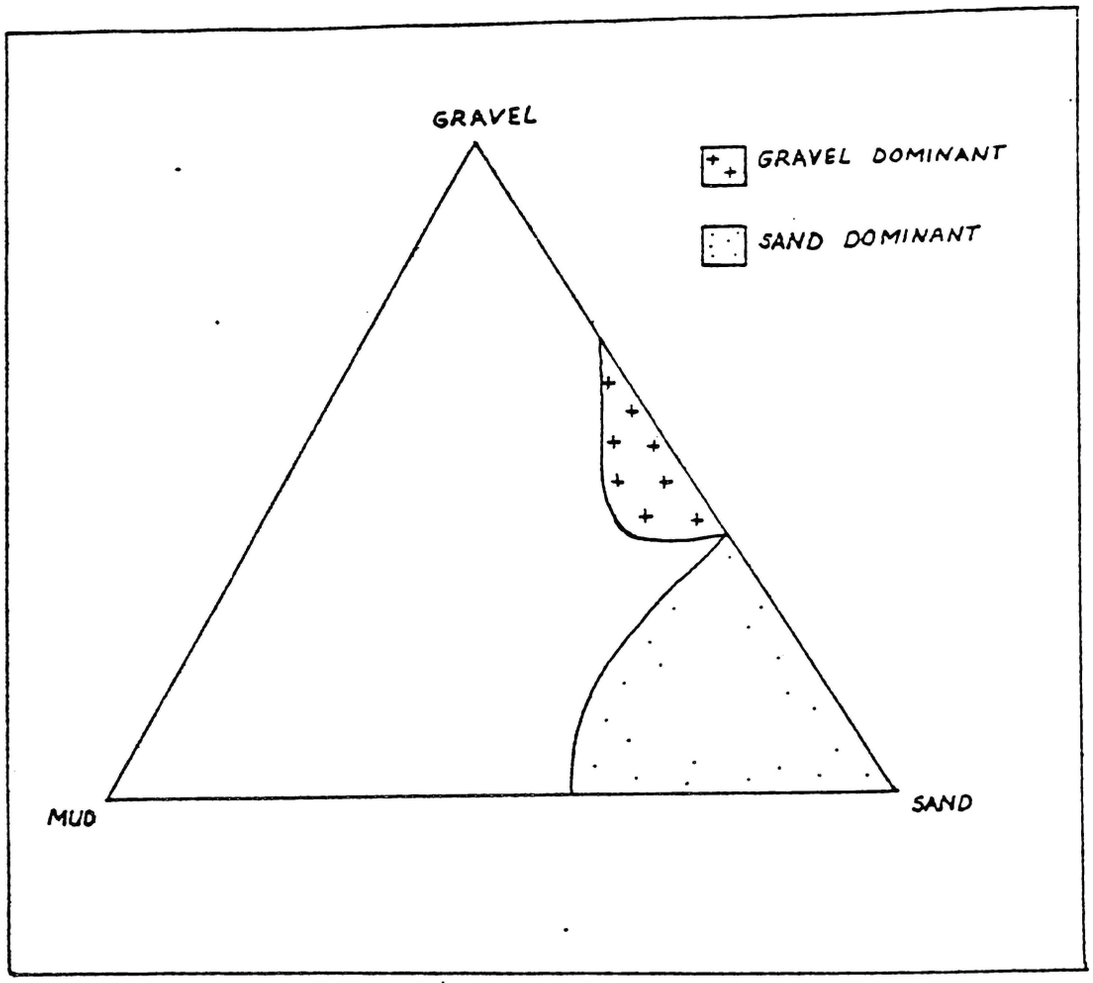


Fig. 5.12 Major textural lithotypes of pyroclastic flow deposits in the Matua Subgroup.

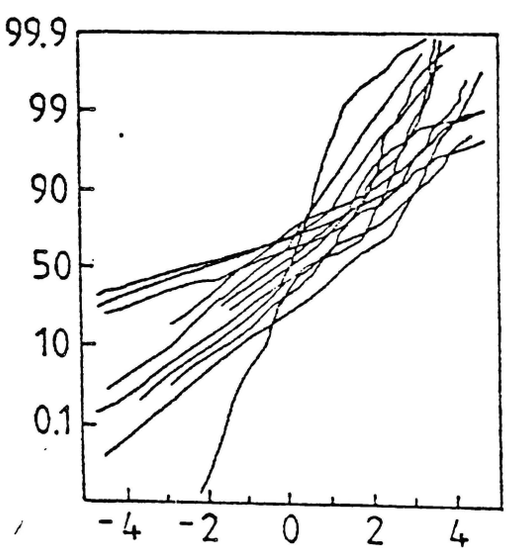


Fig. 5.13 Cumulative grain-size frequency curves for pyroclastic flow deposits in the Matua Subgroup.

ristics throughout individual deposits. The study has therefore been limited to discuss grain-size data as a means to interpreting some of the grain-size variations found in the Matua Subgroup deposits.

Many studies have established that pyroclastic flow deposits are poorly sorted and contain a continuous range of grain sizes from cobbles to clay (Walker, 1971; Sheridan, 1971; Sparks, 1976; Wright *et al.*, 1980). The wide range of size characteristics can be related to several factors, of which probably the most important is the relative proportions of the three constituents pumice, crystals, and lithics (Sparks, 1976).

Pyroclastic flow deposits of the Matua Subgroup exhibit relatively straight grain-size distribution curves with slopes of $\sim 18^{\circ}$ to $\sim 50^{\circ}$ indicative of generally poor sorting. The deposits contain a considerable ($\sim$ 85%) amount of pumice and grain-sizes are from large pebble to medium silt. Most deposits show a wide range of grain-sizes, and the grain-size characteristics represent both unimodal and polymodal populations. Variation in grain-size is attributed to subpopulations in different parts of the pyroclastic flow unit, in either the coarse range (very coarse sand to pebble) or in the finer range (medium sand to medium silt). Several deposits in the Matua Subgroup closely resemble parts of the standard ignimbrite flow unit (Sparks *et al.*, 1973; Sparks 1976, Fig. 8.1) in which the main portion of the flow unit is inversely graded and large pumice clasts are found at the top of the layer (layer 2b) while a finer grained basal layer, $< \sim 1$ mm and $> \sim 0.01$ mm, is found beneath layer 2b. However, an absence of grading in some Matua Subgroup deposits is also common. The main portion of the pyroclastic flow unit is poorly sorted, and cumulative curves for it cover a wide range of grain-sizes. The distribution

for most samples in this main portion was commonly unimodal but polymodal distribution occurred in some samples. In inversely graded deposits, the upper parts of the main portion showed a bimodal distribution, and a secondary mode often occurred in the coarse fractions. The basal layer is often finer grained and moderately sorted. The base of the flow unit lacks both the coarsest and finest grades and the cumulative curve for this region converges upwards towards the finer fractions. Other variations in grain-size occur within individual flow units, for example, segregation structures (Walker, 1971; Wilson, 1980) are characteristically coarser grained than the surrounding grain-size population, and reflect sorting in specific channels or bodies. Normal grading (Sparks, 1976) of lithics was evident in only two deposits in the Matua Subgroup, however lithics and crystals were abundant throughout most deposits, and crystal and/or lithic rich deposits may represent the basal parts of flow units (Walker, 1971; Sparks *et al.*, 1973; Sheridan, 1979; Wilson, 1980).

Poor sorting in ignimbrites is attributed to high particle concentrations, not turbulence (Sparks, 1976; Wilson, 1980). Sparks *et al.*, (1973) suggested that the cumulative curves for the upper and lower parts of the main portion of a pyroclastic flow unit, converge with the curve for the middle of the main portion, toward the finer fractions. This is indicative of enrichment of pumice at the top of the main portion and at the bottom bimodality is the result of an enrichment of lithics. A number of samples in the Matua Subgroup show enrichment of both pumice and lithics in different parts of the flow unit, however, crystals are largely abundant throughout the whole deposit. Variation in grain-size within pyroclastic flow units is related to various emplacement mechanisms (Sparks *et al.*, 1973; Sheridan, 1979; Wilson, 1980) which are discussed in Chapter 8.

Segregation structures were found to be fines depleted in the Matua Subgroup deposits, and grain-sizes < ∿ 0.05 mm were largely removed from these sites, possibly by gaseous flow processes (Sparks, 1978; Wilson, 1980). In one deposit fines enrichment by grain-sizes usually < 0.3 mm was significant near the sides of the deposit, where the particular flow unit had been scoured by an overlying but separate lithologic flow unit (Fig. 8.3). Gaseous flow processes were probably an important factor in sorting finer grain-sizes in this example. The finer grain-sizes appear to have been transported vertically through the deposit.

5.3.3 Statistical Parameters

(i) Grain-Size (Figs. 5.14A, B, C and 5.15A)

The mean grain-size ranges from -0.6 to 1.8 ϕ (very coarse sand to medium sand). Samples are unimodal, bimodal and polymodal; gravel modes occur at -2.0 to -2.5 ϕ and -2.5 to -3.0 ϕ (pebble), and sand modes at 0.5 to 1.0 ϕ (coarse sand), 1.0 to 1.5 ϕ (medium sand) and 1.5 to 2.0 ϕ (medium sand). The first percentile, Cϕ (Fig. 5.14A), an approximation of the coarsest grain-size in deposits, occurs typically in the -2 to -3 ϕ or -4 to -5 ϕ ranges for pumice, and -2 to -3 ϕ range for lithics (see C-M plots).

(ii) Sorting (Figs. 5.14D and 5.15A, D)

On the whole, ignimbrite flow units, particularly the main portion, are poorly sorted especially where the lithotype contains a high percentage of coarse sand to gravel pumice clasts in a coarse sand to clay matrix. However departures from generally poorly sorted values occurred in samples from specific areas within a flow unit. For example moderately sorted (σI = 0.71 to 1.0 ϕ) values occurred in a sample from a basal section which showed well developed cross bedding, as well as

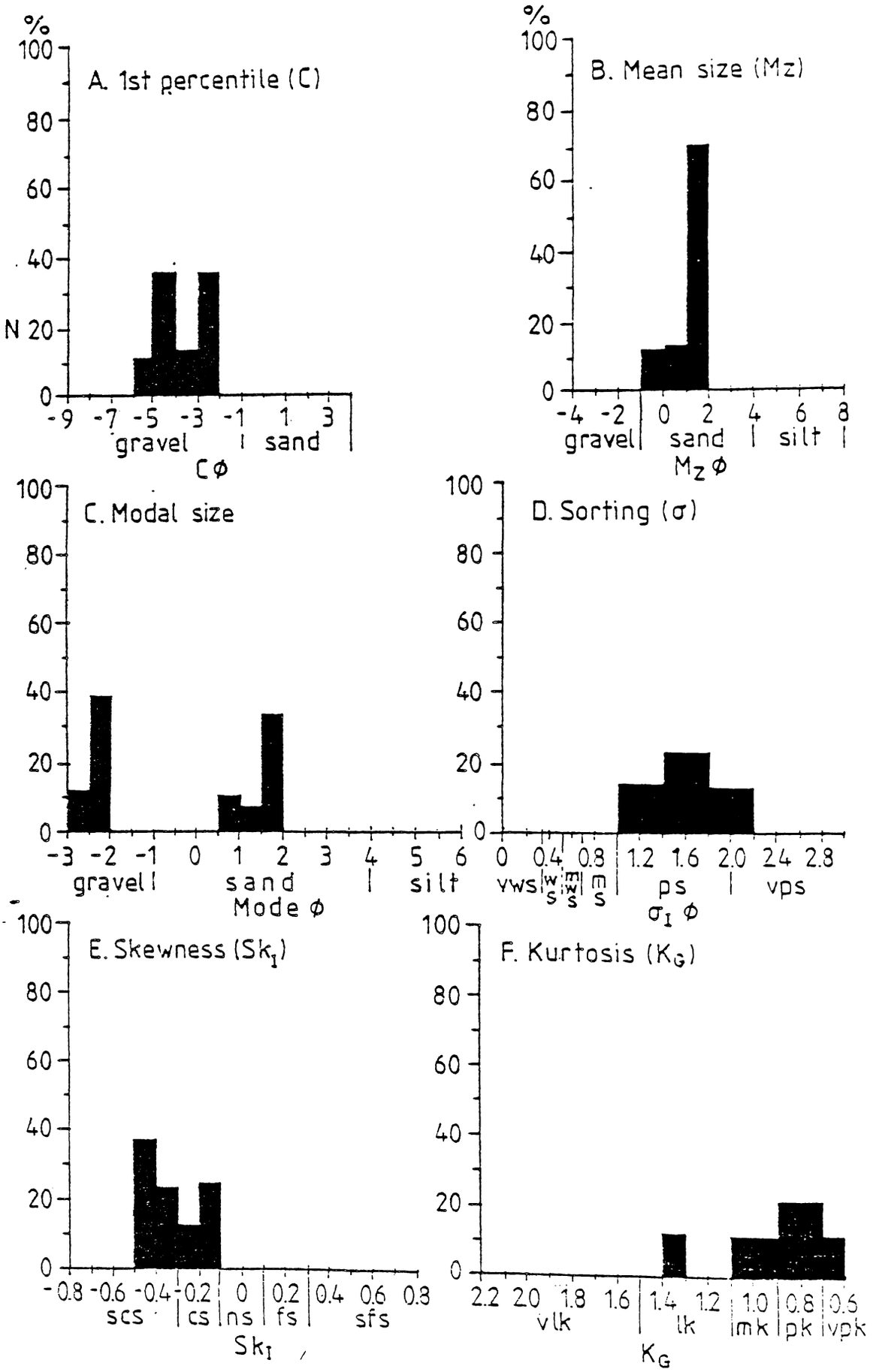


Fig. 5.14 Histograms of grain-size statistical parameters for pyroclastic flow deposits in the Matua Subgroup plotted as a function of numerical occurrence. Statistical parameters are defined in Fig. 2.3.

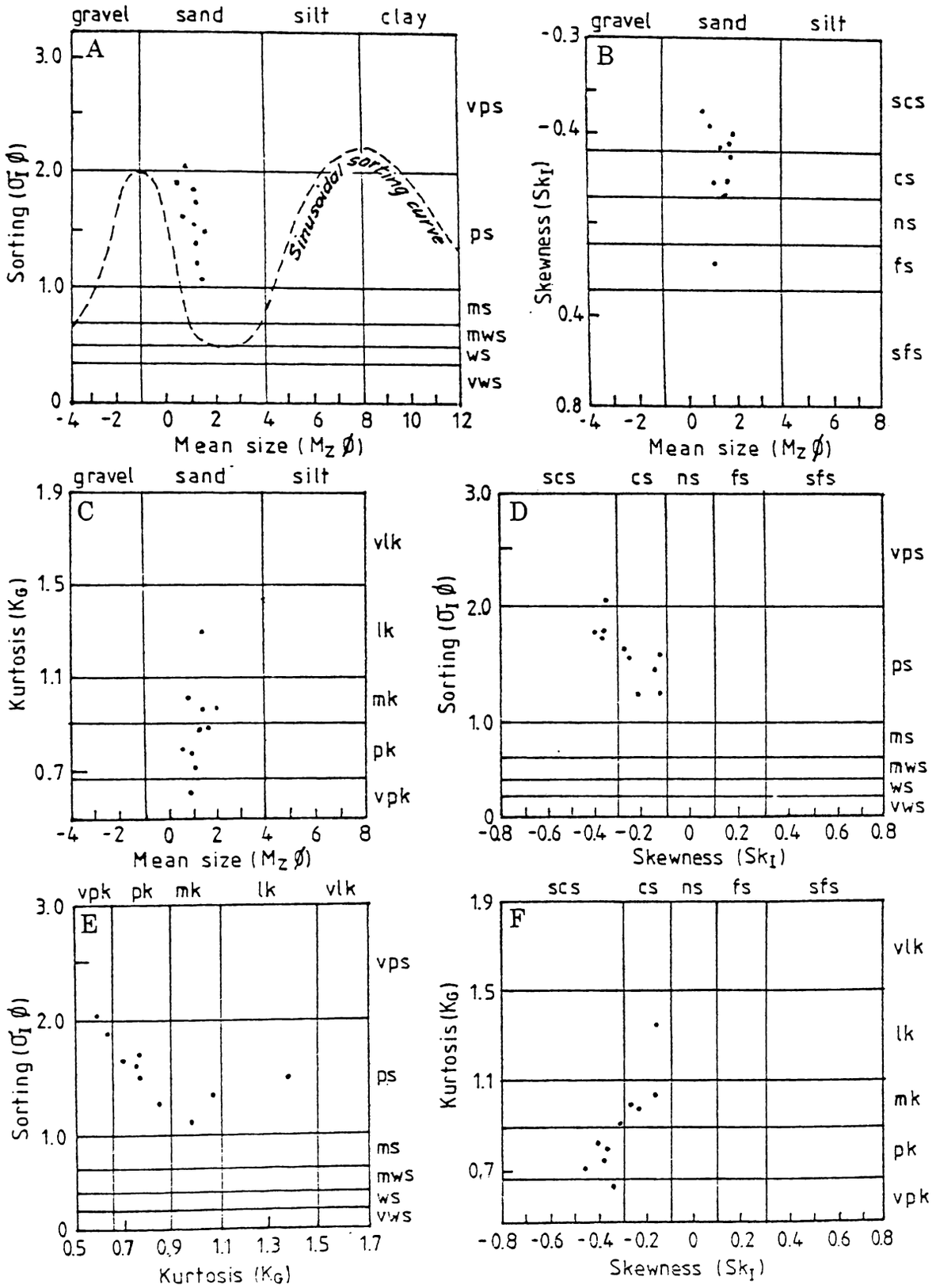


Fig. 5.15 Relationships between grain-size statistical parameters for pyroclastic flow deposits in the Matua Subgroup. Symbols as in Fig. 2.3. Sinusoidal sorting curve in A is after Folk (1968).

segregation structures which were enriched with a coarser median size than the surrounding deposit. These segregation structures commonly in the form of vertical sinuous channels (Walker, 1971) are composed of coarser pumice fragments and were richer in heavier constituents such as lithic fragments and crystals. Not uncommonly, zones of finer and better sorted components occurred adjacent to lateral contacts and near the base of many flow units. These zones showed a decrease in their median size compared to the immediately surrounding zones. Layers which were poorly sorted but showed enrichment of coarse to very fine sand lithic fragments and crystals possibly indicate more basal parts of particular flow units. When smaller flow units succeed one another the impression in the field is often one of stratification (Walker, 1971; Sparks *et al.*, 1973; Sparks, 1976). When sorting is plotted against mean grain-size (Fig. 5.15A) the plot shows a similar sinusoidal relationship to that found in fluvial sediments (Folk, 1968). This indicates that as the grain-size of pumice increases, for example in the main portion of the flow unit, the deposit becomes more poorly sorted.

Poor sorting reflects the wide range of grain-sizes transported, and possibly to the high particle concentrations (Wilson, 1980). In the Matua Subgroup deposits a lower $\sigma\phi$ value in the basal layer of the ignimbrite flow unit, and in segregation structures within the flow unit, may be attributed to gaseous flow processes (Walker, 1971; Wilson, 1980). This is probably related to the winnowing out of finer and lighter components especially gravel pumice clasts (Walker, 1971; Wilson, 1980). In a number of deposits the $\sigma\phi$ and Md ϕ values increased towards the top of the flow unit. The sorting characteristics of the segregation channels and bodies are possibly associated with gases streaming through the flow unit during emplacement (Walker, 1971). Walker (1971)

suggests that some channels may also be formed by post-emplacement processes during a cooling period. It is suggested that the grain-size characteristics in these types of channels is possibly due to a number of factors such as preferential cementation, welding, alteration or mineralization along channels. Another type of segregation structure found in the Matua Subgroup deposits, with a more circular form (Fig. 8.3), was poorly sorted and coarse skewed, this being attributed to the depletion of finer grain-sizes. The structure was partly clast supported and partly matrix supported, and contained numerous pumice gravels. Nevertheless grain-size characteristics of the structure suggest a gas streaming mechanism and removal of finer grains. Crystal enrichment near the base of the flow unit is also possibly related to the removal of finer and lighter components (Walker, 1971; Wilson, 1980). However, lithic concentration near or at the base of some flow units in the Matua Subgroup deposits increases the $\sigma\phi$ value. Lithic enrichment may be due in part to a "caterpillar track mechanism" (Wilson, 1980), whereby the coarse dense fraction is deposited at the base of the flow.

(iii) Skewness (Fig. 5.14E)

Pyroclastic flow deposits in the Tauranga Basin show a tendency to be coarse-skewed. When skewness is plotted as a function of mean grain-size (Fig. 5.15B) a trend towards negative skewness with increasing size is indicated. Coarse-skewed deposits also show a rough trend towards poor sorting (Fig. 5.15D). This can be attributed to matrix supported pumice gravels, and a wide range of grain-sizes from gravel to silt.

Negative skewness is the result of pumice blocks and lapilli existing in the flow unit. Within a particular flow unit, there is often an upward increase in negative skewness which is attributed to

inversely graded pumice. Towards the base of the flow, an increasing positive skewness accompanies a decreasing Md ϕ value. However, in many deposits in the Matua Subgroup, the base of the flow may be coarsely-skewed. This is partly due to some deposits having little grain-size variation within the flow unit or to an increase in granule to medium sand sized lithic fragments or coarse debris at the base of the flow unit.

(iv) Kurtosis (Fig. 5.14F)

Deposits range from leptokurtic to platykurtic, with a tendency towards platykurtic values. Platykurtic values indicate that a wide range of grain-sizes make up the deposit. If kurtosis is plotted against mean grain-size (Fig. 5.15C) a tendency towards platykurtosis with increasing grain-size is indicated. The only obvious relationship between skewness and kurtosis (Fig. 5.15F) is that as the grain-size and the percentage of grains greater than a particular grain-size increases, the ability to effectively sort out distinctive size classes diminsihes and a platykurtic distribution results. This is true of the main portion of the flow unit which has been described as homogenous (Walker, 1970; Sheridan, 1976; Wilson, 1980). A more leptokurtic value occurs towards the base of some deposits which are finer grained and moderately sorted, or in some segregation structures which are depleted of finer and lighter components, particularly pumice. Poor sorting in samples therefore corresponds to a more platykurtic distribution (Fig. 5.15E).

(v) CM Patterns

CM plots recording pumice clasts from pyroclastic flow samples were generally similar to those obtained for fluvial sediments and were comparable to the plots obtained by Sheridan (1971), for deposits interpreted as rhyolitic ash flows (Fig. 5.16 and 5.17). However, the

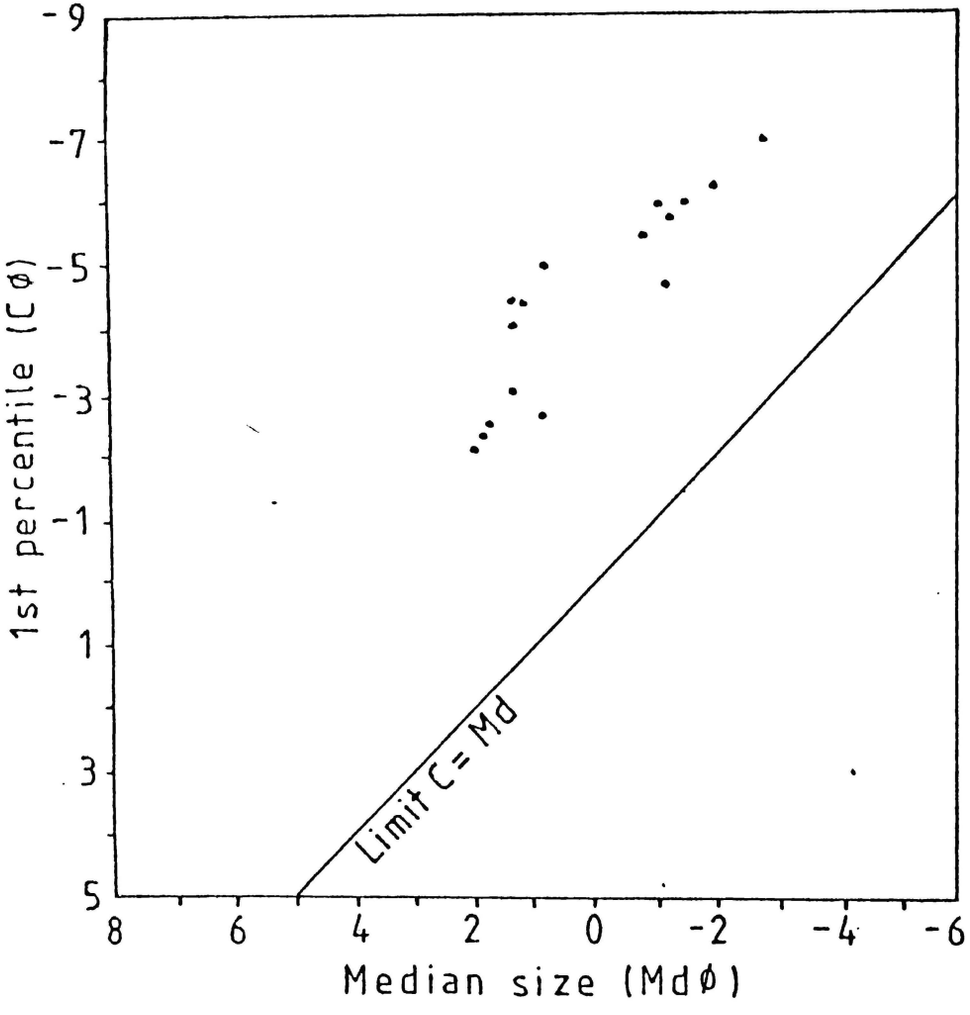


Fig. 5.16 CM plot for representative pyroclastic flow deposit samples of the Matua Subgroup.

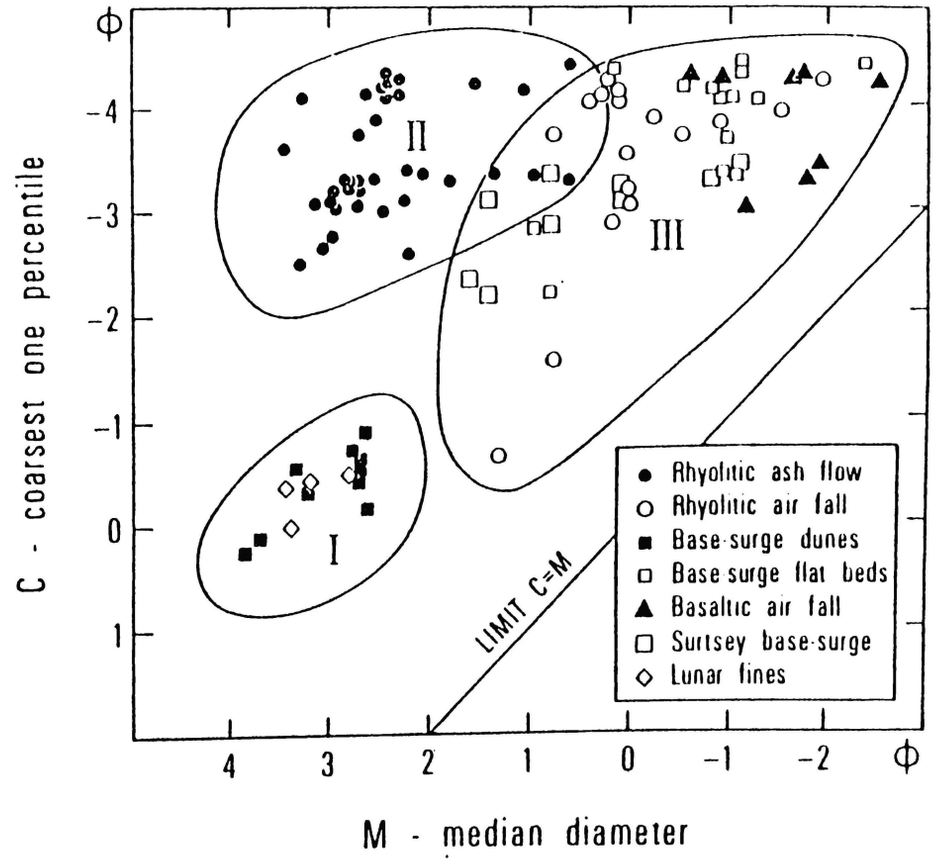


Fig. 5.17 C-M diagram for pyroclastic fall and pyroclastic flow deposits (from Sheridan, 1971).

pattern is moved upwards on the 1st percentile (C ϕ) axis, reflecting the increased competence of pyroclastic flows to transport very coarse grain-sizes and a greater proportion of gravel-sized clasts, but with a slightly increased mean value than the fluvial deposits. The competence of the flow may also be assessed by calculating the coarsest one percentile of denser lithic fragments. Most C ϕ values for lithics were typically in the -2 to 0.0 ϕ range with median grain-sizes ranging from - 2 to 4 ϕ. It is valid to interpret these results as indicative of certain energy values in pyroclastic deposits and the C-M diagram is useful for defining the mode of deposition for fluvial sediments (Passega, 1964; Yamazaki *et al.*, 1973). Any interpretation from the C-M plots for pyroclastic deposits, should be treated separately from fluvial deposits because of the complex interaction of processes existing in pyroclastic deposits (Walker, 1971; Wilson, 1980; Wright *et al.*, 1980). However, it may be useful to compare the distribution of populations for general identification of transport modes, for example, suspension and turbidity current deposits (Passega, 1964), and air-fall and ash flow deposits respectively (Sheridan, 1971).

5.4 TEXTURAL CHARACTERISTICS OF PYROCLASTIC FALL DEPOSITS

5.4.1 Textural Plots

Pyroclastic fall deposits are dominated by mud and sand lithotypes (Fig. 5.18) and are characteristically finer grained compared to fluvial and pyroclastic flow deposits (Fig. 5.19).

5.4.2 Grain-Size Distribution Curves

Walker (1971) suggested that many factors affect the form of the cumulative curve for pyroclastic fall deposits. This in turn affects other grain-size statistics, for example, the Mdϕ and $\sigma\phi$ values. The

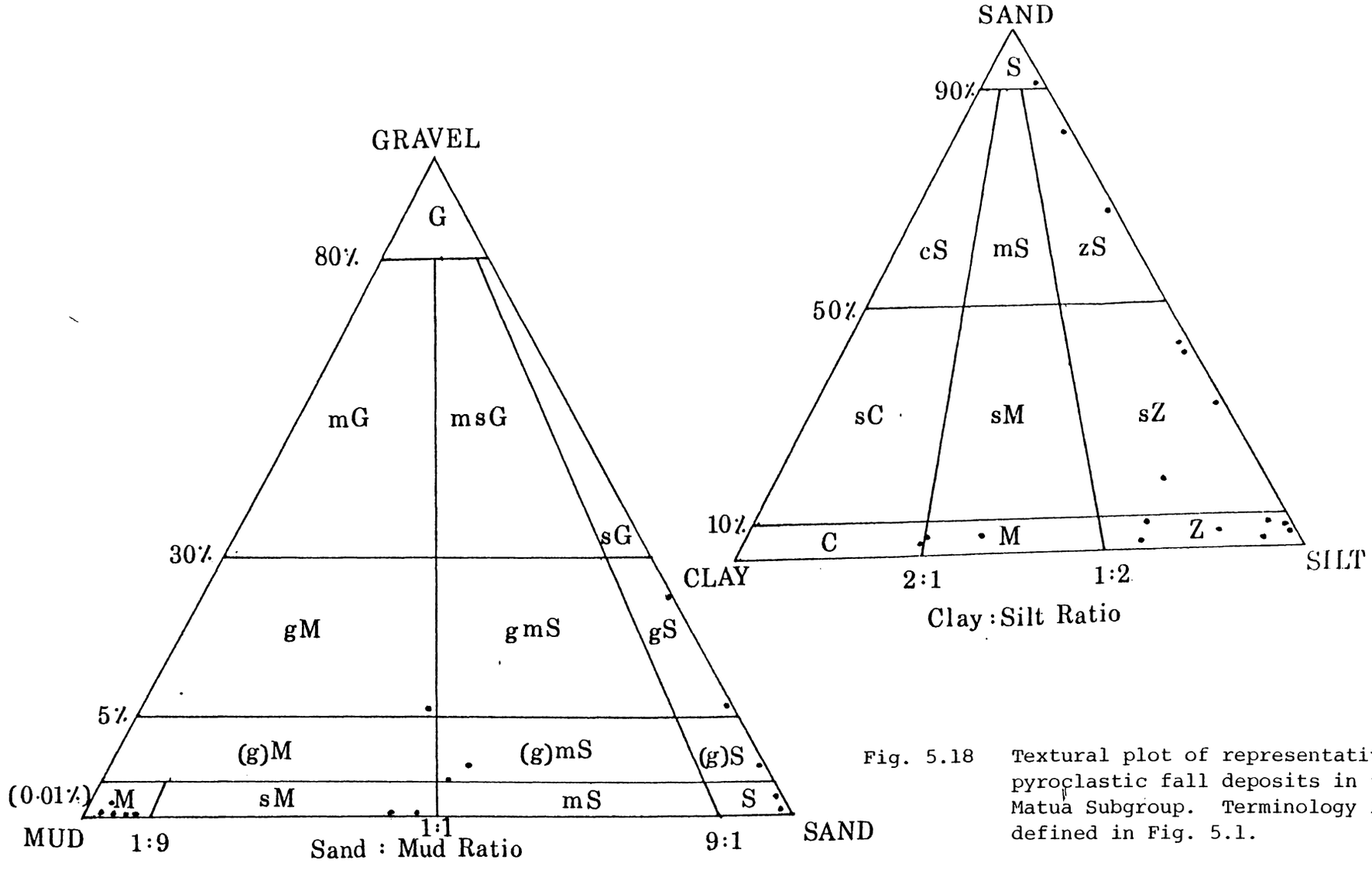


Fig. 5.18 Textural plot of representative pyroclastic fall deposits in the Matua Subgroup. Terminology is defined in Fig. 5.1.

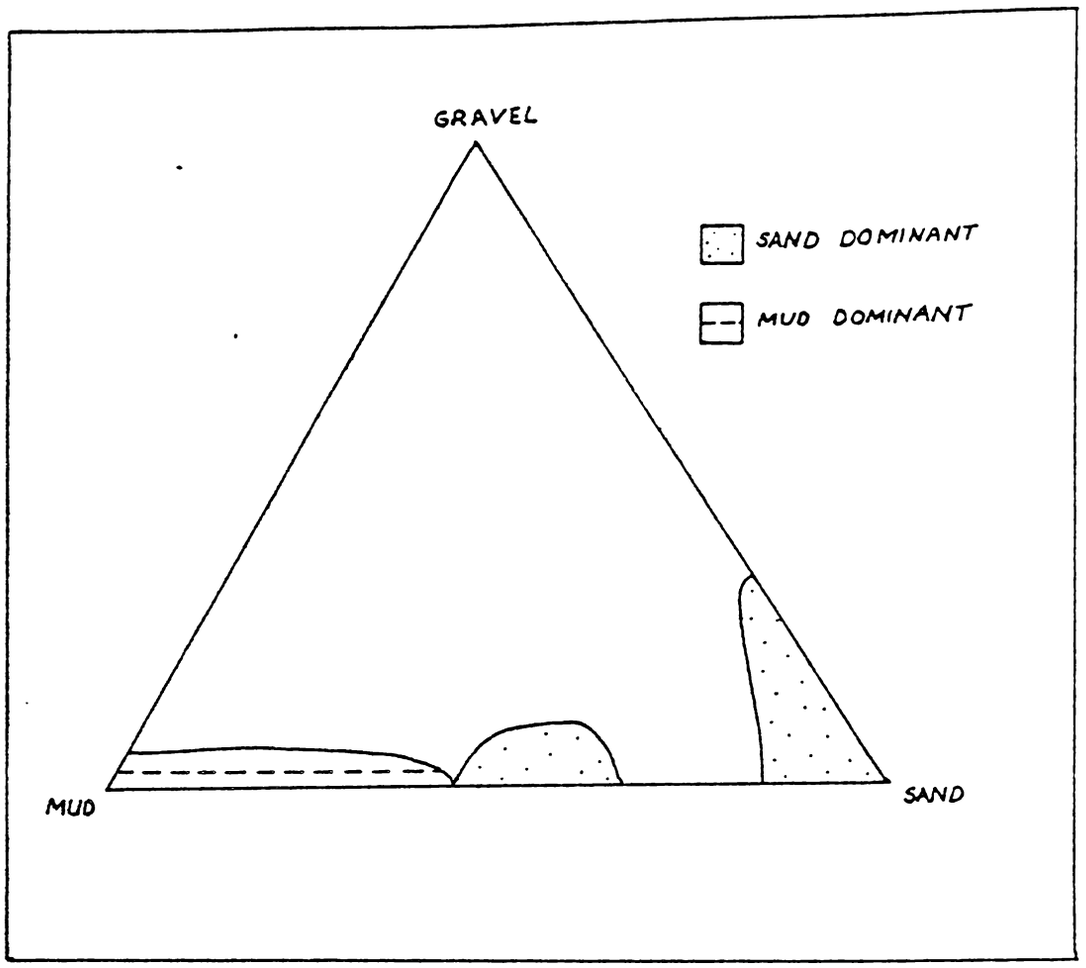


Fig. 5.19 Major textural lithotypes of pyroclastic fall deposits in the Matua Subgroup.

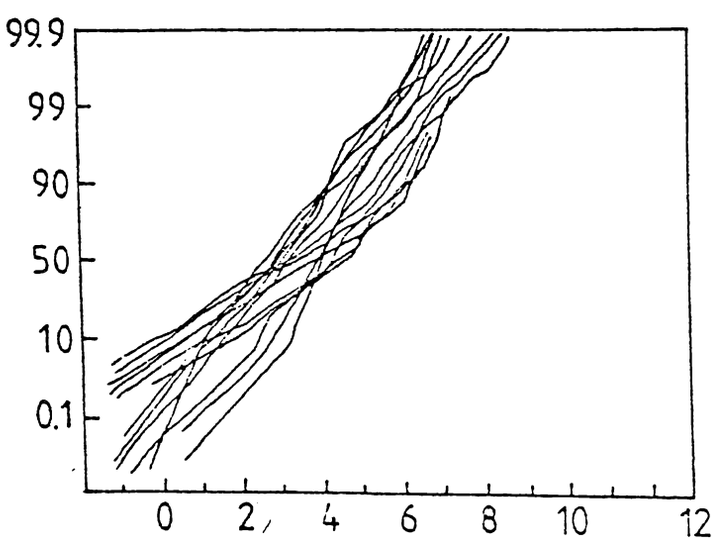


Fig. 5.20 Cumulative grain-size frequency curves for pyroclastic fall deposits in the Matua Subgroup.

initial population of a fall deposit - the material explosively ejected from the vent into the atmosphere - may be divided into three main components, namely, pumice and glass shards, crystals, and rock fragments. The latter includes dense glassy lithics representing non-vesiculated juvenile fragments and fragments derived from pre-existing country rock (Walker, 1971; Wright *et al.* 1980). The form of the cumulative curve given collectively by several components is a result of the particle size distributions of each component (Walker, 1971). The grain-size characteristics of the initial population of pumice or lithic fragments are different from crystals. Pumice is a product of breakage whereas the crystals are released during explosive disruption of porphyritic magmas and have a grain-size predetermined by conditions of growth in the magma. The crystals are modified only to a limited extent by breakage during ejection. After ejection from the vent, fragments settle through the air and are sorted according to their fall velocities.

Textural analyses of Matua Subgroup deposits were made on samples which were composed largely of pumice and glass shard, with a relatively low, $< \sim 5\%$, crystal content. The grain-size distribution curves for pyroclastic fall deposits form relatively straight lines with slopes of 40 to 65° (Fig. 5.20). When comparing curves from different units an increase in the content of finer grades (medium silt to clay) can be attributed to weathering. The steepness of the curves indicates that most pyroclastic fall samples are moderately to well sorted, and the curves move upward steeply towards the finer grained fractions. The latter suggests a preponderance of finer grain-sizes, $< 2\phi$, in most samples. However sorting values indicate that the samples range from well sorted to poorly sorted. The grain-size distribution of pumice is variable and is related to the fall

velocity of each grain, which is dependent mainly on fragment size (Walker, 1971), the density of pumice being measured at 1.00 g/cm^3 (Sparks, 1976). Other factors which may affect the fall velocity, are the shape of the grain and the surface roughness (Walker, 1971). The difference in the fall velocity between pumice grains and dense crystals and lithic fragments, has been demonstrated by Walker (1971). The mode values of dense fragments and pumice fragments indicated that the grain-size of the latter was greater, although both had accumulated at the same time. The cumulative curves for the Matua Subgroup deposits, therefore represent samples in which the individual pumice grains have stratified in deposits depending on their grain-size and therefore their individual fall velocities.

5.4.3 Statistical Parameters

(i) Grain-Size (Figs 5.21A, B, C and 5.22A)

The mean grain-size ranges from 0.71 to 5.45 ϕ (medium sand to medium silt) and samples are typically unimodal or bimodal. A unimodal distribution can be partly attributed to the grouping of particles which fall at the same rate. These samples are usually better sorted. A bimodal distribution may represent a mixing of two predominant grain-size classes. This may indicate weathering, bioturbation, or a combination of factors involving the aerodynamic behaviour of individual grains in the atmosphere, for example, shape, surface roughness and size. The main modes in the Matua Subgroup deposits are in the 3.0 to 5.5 ϕ (very fine sand to medium silt) range; this distribution is particularly characteristic of air-fall tephra and paleosols at Omokoroa and is indicative of weathering at this site. A coarser sand mode, from 1.0 to 1.5 ϕ and 1.5 to 2.0 ϕ (medium sand), is evident in $\sim$ 25% of the Matua Subgroup samples and may represent shower bedded units. The first percentile, C ϕ, and approximation

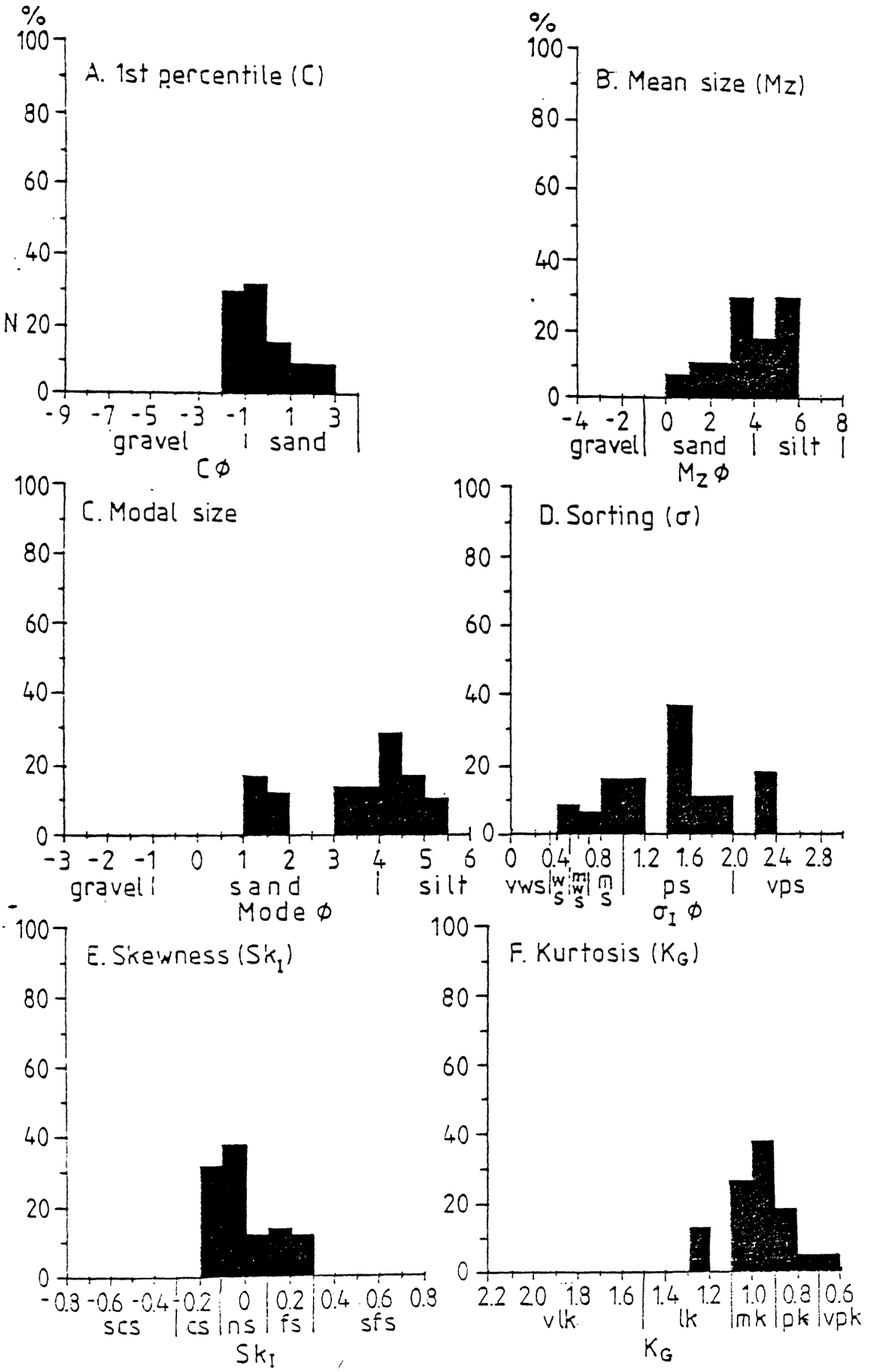


Fig. 5.21 Histograms of grain-size statistical parameters for pyroclastic fall deposits in the Matua Subgroup plotted as a function of numerical occurrence. Statistical parameters are defined in Fig. 2.3.

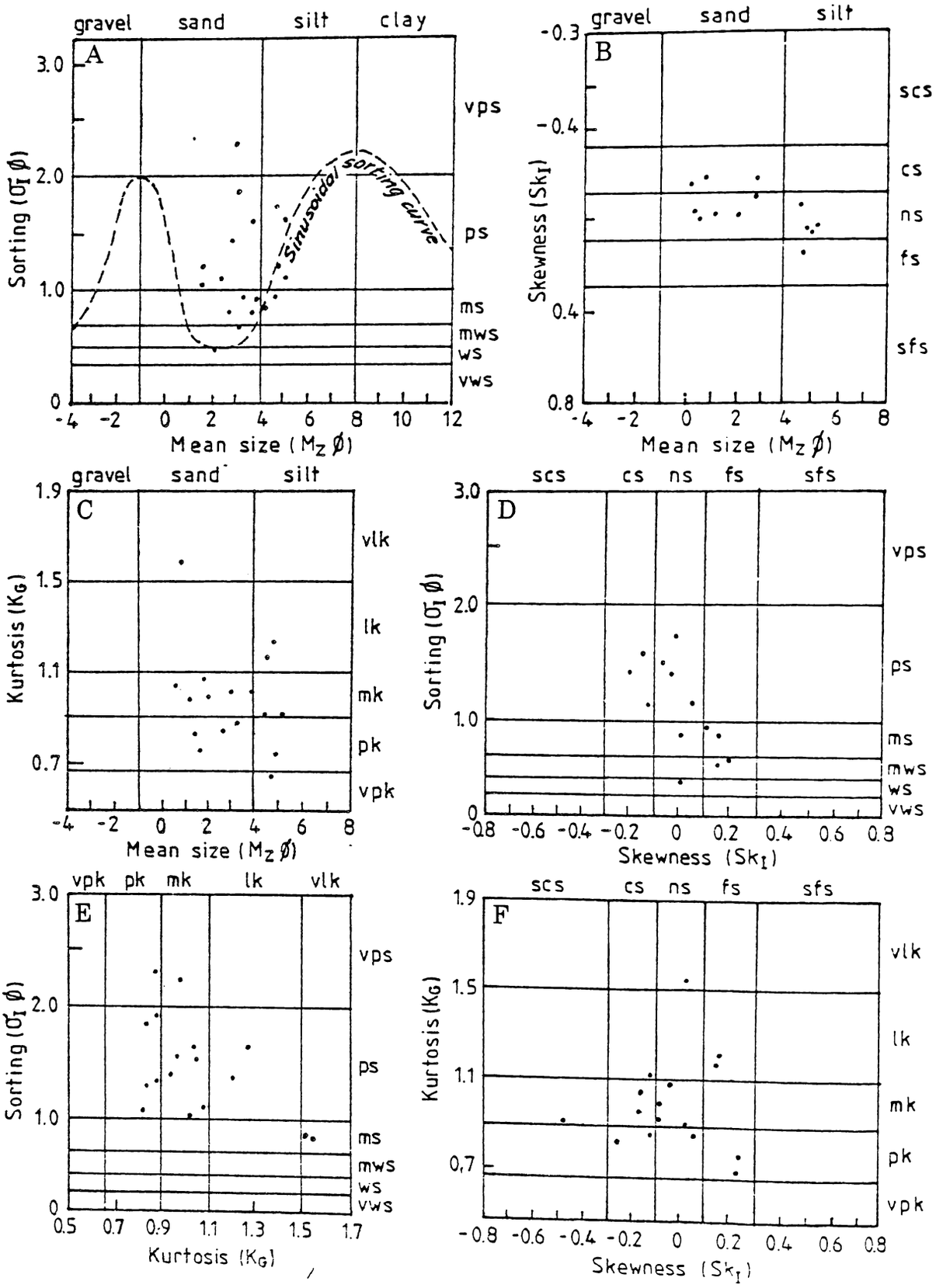


Fig. 5.22 Relationships between grain-size statistical parameters for pyroclastic fall deposits in the Matua Subgroup. Symbols as in Fig. 2.3. Sinusoidal sorting curve in A is after Folk (1968).

of the coarsest grain size, indicates that a few samples include grains of granule size (-1.75 ϕ), which may be attributed to large pumice clasts, with greater fall velocities, which have accumulated in normally graded deposits.

(ii) Sorting (Fig. 5.21D)

Pyroclastic fall samples are poorly to well sorted. In many samples poor sorting probably reflects processes such as weathering, which would increase the clay and possibly silt content, and bio-turbation, which is attributed to mixing the coarser pumice material (Walker, 1971). Moderate to well sorted samples are usually representative of internal stratification of shower bedding (Wright *et al.*, 1980).

A plot of sorting against mean grain-size is compared to Folks (1968) sinusoidal sorting curve (Fig. 5.22A). As the mean grain-size decreases, especially in the sand range, the sorting improves. However, in the silt range, a decrease in mean grain-size, indicates both well sorted and poorly sorted samples. Nevertheless, many fine-grained predominantly silty deposits with a smaller range of grain-sizes are generally well sorted. The plot suggests that material of a similar grain-size accumulating in specific parts of the deposit, for example in a stratified unit, are moderately to well sorted.

Moderately to well sorted samples (Fig. 5.23) possibly indicate sorting due to a number of factors, including fall velocities, wind strength the eruptive cloud dimensions and the eruptive column conditions (Walker, 1971, Wright *et al.*, 1980). Walker (1971) showed that when the weight percentages are plotted against fall velocity, samples usually show much lower sorting values.

(iii) Skewness (Fig. 5.21E)

Deposits range from coarse-skewed to fine-skewed. Two thirds of the deposits have a near symmetrical distribution, or a slight tendency to be fine-skewed. When skewness is plotted as a function of mean grain-size, a trend towards positive skewness with decreasing grain-size is evident (Fig. 5.22B). A plot of skewness against sorting shows a slight tendency towards positive skewness with a decreasing sorting value (Fig. 5.22D). Finer grain-sizes represent a number of factors, for example weathering, which increases silt and clay size fractions, and sorting which is partly attributed to the settling velocities of finer grain-sizes. The latter represents samples from normally graded, shower bedded units where grain-sizes are stratified. However, skewness may also reflect the height of the eruption column, conditions in the column and the effect of wind. These factors ultimately affect the rate of fall of individual grains and the efficiency of sorting. For example a strong wind should give a low $\sigma\phi$ value, while selective removal of specific grains depends partly on the eruption column conditions and distance from source.

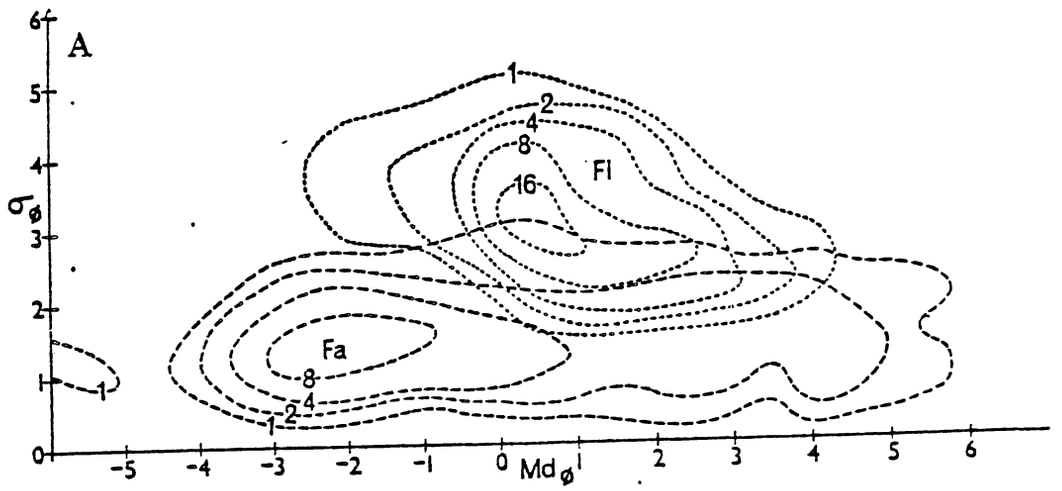
(iv) Kurtosis

Deposits range from leptokurtic to platykurtic; $\sim$ 80% are mesokurtic or leptokurtic (Fig. 5.21F). Kurtosis is probably more important when related to other grain-size parameters (Hume *et al.*, 1975). A plot of kurtosis against mean grain-size indicates a trend towards mesokurtic and leptokurtic values as the mean grain-size decreases (Fig. 5.22C). When plotted against sorting, poorly sorted samples show an increase in platykurtosis (Fig. 5.22E). A plot of kurtosis against skewness showed a trend towards more leptokurtic values when the samples were fine-skewed (Fig. 5.22F). Leptokurtic values indicate better sorted samples with a narrow range of grain-sizes.

Several samples are fine-skewed and leptokurtic, which indicates finer grain-sizes within the initial population. These values are possibly attributed to sorting of individual grains within the eruption cloud and during fall under the influence of gravity, and to weathering, with an increase in the silt and clay fractions. Platykurtic values often represent samples which are poorly sorted, with a wide range of grain-sizes between -1 and 9 ϕ. The grain-size distribution in some of these samples is attributed to weathering, while in others it may be due to a bimodal distribution with a coarse population mixed with finer grain-sizes.

(v) CM Patterns (Fig. 5.24)

Air-fall deposits plot in areas interpreted by Sheridan (1971) as deposits with dominant air-fall modes, or those interpreted as base surge dunes and lunar fines, and below the Matua Subgroup pyroclastic flow plots (Figs. 5.23 and 5.17). The plots are also comparable to Passega's (1964) segregated areas for suspended fluvial sediment. Compared to the Matua Subgroup pyroclastic flow and fluvial samples the pattern is shifted left along the Md ϕ axis because of the finer - grain-sizes deposited by air-fall mechanisms. This is partly because of the selective removal of coarser grains close to source. These plots possibly reflect wind velocity, distance from source and eruption cloud conditions which affect the grain-size, grain-size distribution and the geometry of deposits.



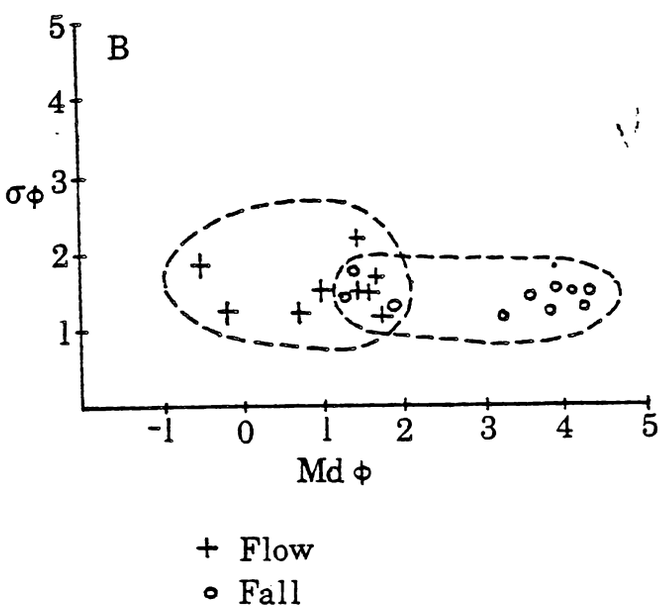


Fig. 5.23 A - Contoured plot of the data for pyroclastic fall (Fa) and pyroclastic flow (Fl) deposits (from Walker, 1971).

B - Plot of some of the Matua Subgroup pyroclastic fall and distal pyroclastic flow deposits. There is a trend in the fall deposits to finer and better sorted samples.

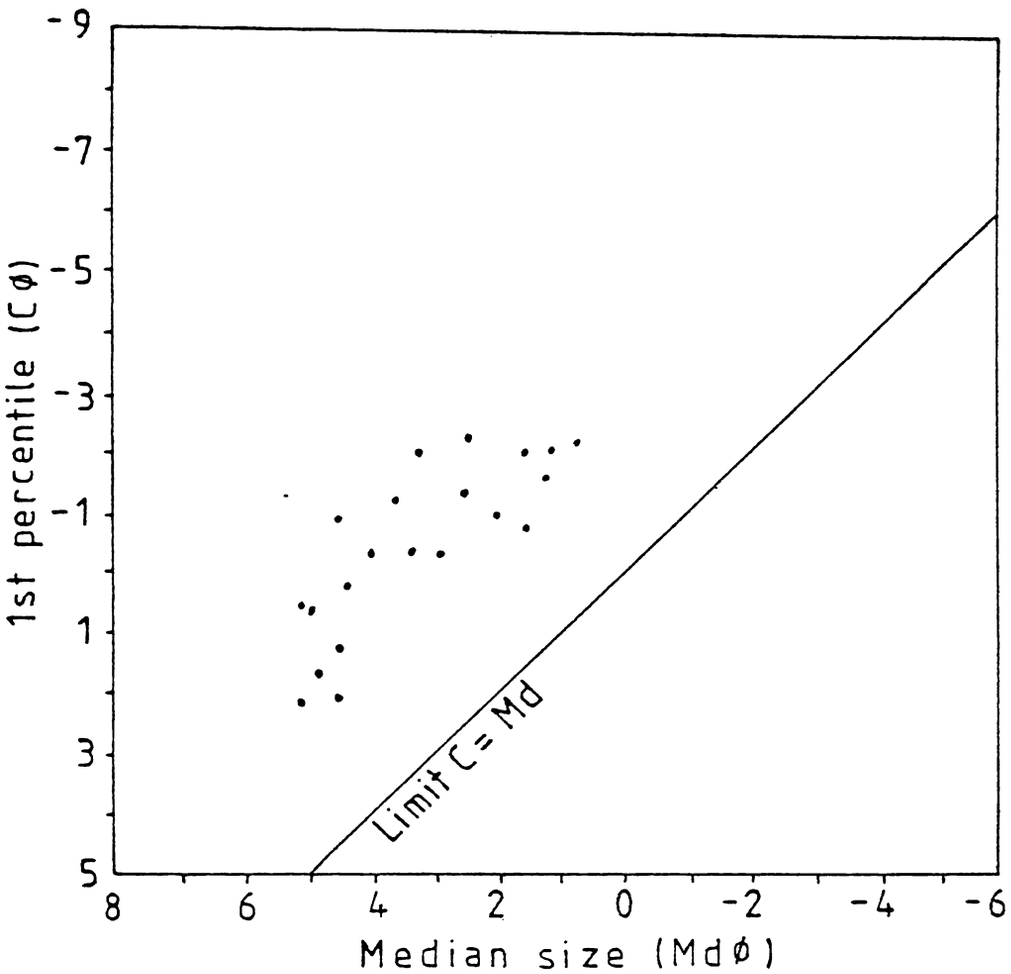


Fig. 5.24 CM plot for representative pyroclastic fall deposit samples of the Matua Subgroup.

TABLE 5.1 CONCLUSIONS

MAJOR TEXTURAL DIFFERENCES

Parameter		Fluvial	Pyroclastic flow	Pyroclastic fall
Grain-Size		gravels common, but predominantly sand sized	coarse clasts up to cobble size; gravels common	gravel uncommon, predominantly sands and silts
Statistical	Parameters skewness -	coarse to fine-skewed	coarse skewed	symmetrical and fine-skewed
	sorting -	poorly to well sorted	poorly sorted	moderately to well sorted
	kurtosis -	platykurtic to leptokurtic	platykurtic	mainly mesokurtic and leptokurtic
Structure		normally and inversely graded; inverse grading common, because of large quantities of pumice supplied to deposits	massive or inversely graded	stratified, shower bedded and normally graded

CHAPTER SIX

COMPOSITION OF MATUA

SUBGROUP DEPOSITS

6.1 INTRODUCTION

The composition of any clastic sedimentary deposit will reflect the nature of the source material and the inherent properties derived from transportation away from source. Analyses of the fluvial sediments in the map area were designed to investigate the composition by inferring that a number of potential source areas may have existed. Particular attention was paid to petrographic descriptions and to detailing detrital constituents. Evaluation is made of potential contributing sources and specific sources by a combination of analyses, including heavy and light mineralogy, and rock fragment types.

6.2 DISCUSSION OF BULK MINERALOGY

The mineralogy of 62 samples from stratigraphic sections within the Tauranga Basin was determined by standard techniques (see Chapter 2). Most of the material was pumiceous, and rhyolitic lithics were frequently numerous. Major components included abundant pumice, feldspar and quartz, glass shards, rock fragments, and occasional carbonaceous material. In addition, several ferromagnesian minerals and minor quantities of clay minerals were identified. Significant quantities of specific clay minerals were present in tephric material and in paleosols.

The bulk mineralogy recorded in the following diagrams (Figs. 6.1 and 6.2) is separated on the basis of mode of emplacement of the deposits.

6.3 COMPONENT COMPOSITION

Because of similarities between minerals studied in pyroclastic (especially ignimbrites) and fluvial deposits the following section

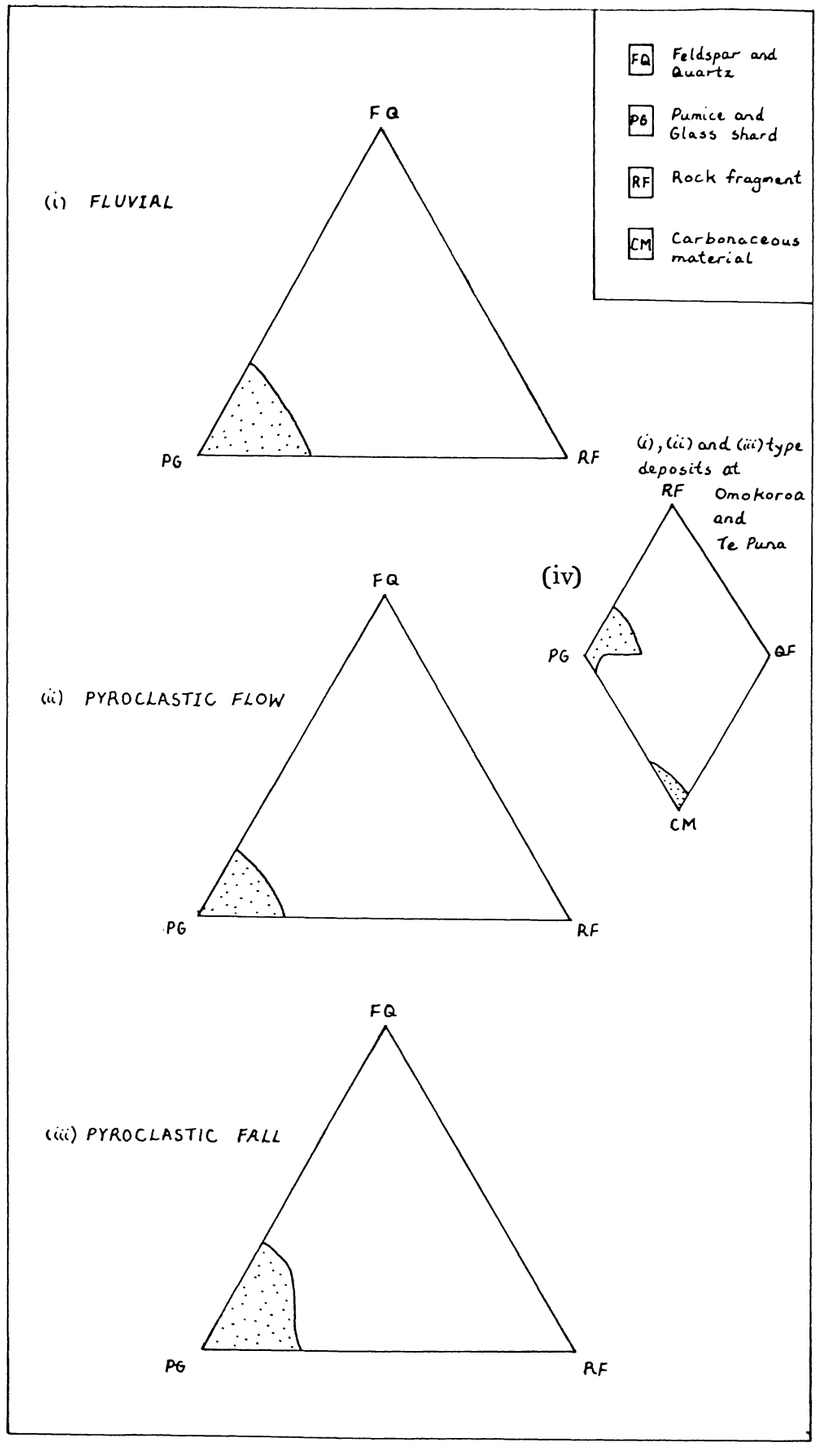


Fig. 6.1 Bulk mineralogy of representative samples from the Matua Subgroup. **(iv)** shows lignite and carbonaceous silts from subaerial sections which are intercalated with pyroclastic flow and fluvial deposits at Te Puna and Omokoroa.

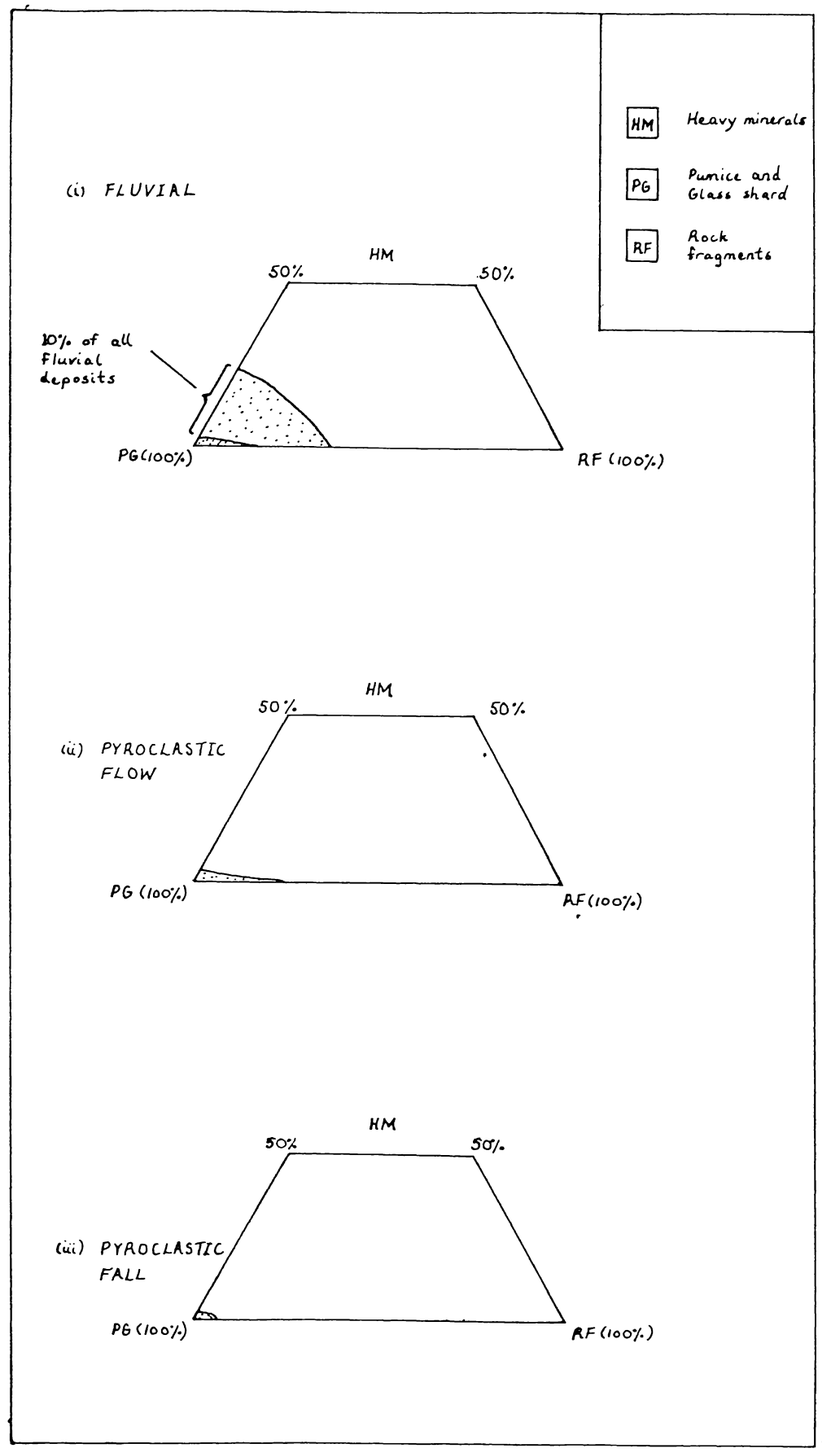


Fig. 6.2 Bulk mineralogy of representative samples from the Matua Subgroup including comparison of heavy mineral percentages.

details information concerning minerals in the Matua Subgroup deposits (i.e. excludes Hamilton Ash Formation mineralogy). Section 6.3.3 describes rock fragments found in pyroclastic flow, post-depositionally modified pyroclastic flow deposits and fluvial deposits, and the type of deposit examined is coded p, pd and f respectively. The following mineral descriptions are based on petrographic notes from thin section and they document the nature of the detrital constituents. Clay mineralogy has been determined by XRD analysis.

6.3.1 Light Mineralogy

Feldspar - Plagioclase feldspars are abundant (∿ 65% of total phenocrysts) in the Tauranga deposits, generally occurring as sand-sized (0.2 to 2.0 mm) subhedral crystals. Limonite staining occurs marginally on some grains. Inclusions are common and include minute pale yellow to brown glass blebs, black euhedral magnetite crystals, and prismatic hypersthene and hornblende crystals.

In thin section, the composition of the plagioclase feldspars ranged from An_{24} to An_{38} (i.e., sodic oligoclase to sodic andesine). Repeated lamellar albite twinning was common, ranging from narrow albite twin lamellae to relatively broad lamellae.

Quartz - varieties of quartz in the Tauranga Basin deposits were predominantly volcanic and include:

1 - vitreous, angular, elongate crystals are the dominant (∿ 75%) quartz type in most assemblages, occurring with feldspars and glass shards. Sizes ranged from coarse silt to granule. Inclusions are rare and are mainly volcanic glass and scarce fine-grained, opaque material. Much of this material had fractured-conchoidal surfaces, and was anhedral in this section.

2 - a more equidimensional, subhedral to euhedral (bipyramidal) form. This quartz was relatively fresh, occurring close to source, and had suffered less fragmentation and fracturing than varieties 1 and 3. Usually sand sized (0.4 - 2 mm). Relative abundance ∿ 15%.

3 - corroded quartz with iron-stained, fractured surfaces. Relative abundance ≈ 10%.

(i) Glass shards

Abundant in the Tauranga Basin deposits derived from both primary volcanic and epiclastic material. Glass shards assume forms which grade into one another and different forms occasionally occur in the same pyroclastic or fluvial sedimentary unit. Three main varieties

were found:

1 - curved in thin section. Commonly U- and Y-shaped, cuspate type shards which represent fragments of glass originally enclosing rounded bubbles. A significant (∿ 20%) proportion of glass in pumices was of vitreous globule form.

2 - fibrous shards occurred in sediments. Derived from framented pumice, colourless and fresh in appearance, fragments are angular - subangular and elongated. Tube-like pumice chambers and fibrous types indicate that these shards were derived from elongated vesicles.

3 - glass plates and flakes, colourless or iron-stained. Also abundant and often show angular, irregular outlines with spaced concave fractures and ragged shreds. Formed by fragmentation of walls of large, more compressed vesicles.

6.3.2 Heavy Mineralogy

Heavy minerals form 0.5 - 1.0% by weight of the Tauranga Basin deposits. They are dominated by hypersthene, magnetite, hornblende, limonite, zircon and biotite, with rare augite, and were most abundant in the fine and very fine sand fractions. Heavy minerals occurring in pumice clasts were dominated by the same minerals as above with the exception of limonite.

Weight percentages were generally (∿ 40%) lower in fluvial samples than in distal ignimbrite samples. This is possibly attributed to selective sorting and removal of heavier constituents at some sites. Sites recording low heavy mineral percentages, particularly those further from source (∿ >2 km) showed an increasing abundance of pumice and glass shards. However, fluvial samples collected from heavy mineral concentration zones, for example from sites close (< ∿ 1 km), to source, recorded very high (∿ 10%) heavy mineral percentages due to fluvial reworking. Heavy minerals generally were prismatic, angular and subhedral in the 2 - 4ϕ range, and were largely immature and fresh in both fluvial deposits and distal ignimbrites. Euhedral shapes were

particularly characteristic for magnetite and for most zircons. Most ferromagnesian minerals were subrounded to subangular in coarse sand, subangular in the medium sizes, and subangular to angular in the fine sand and silt range.

(i) Heavy mineral descriptions

Hypersthene - very subtle colours, almost colourless in some crystals; pinkish yellow-light green, prismatic and acicular crystals, 0.1 to 2.0 mm long, usually with dentations or hacksaw type ragged terminations often appearing to extend through elongate crystals. The ratio of prismatic to anhedral grains in the fine sand grade is about 1:1. Maximum interference colours are middle first order yellowish green to olive green. Inclusions are mainly blebs of glass in elongated prismatic crystals.

Magnetite - small opaque crystals with metallic lustre. Many euhedral grains. Crystals 0.06 to 1.0 mm in size ranging in shape from perfect octahedra to subrounded octahedra, giving square and hexagonal outlines. A few well developed faces are apparent in most grains. Reddish brown limonite stains from <5% - 80% of the grains in different assemblages from different localities. Magnetite occurs as inclusions in some feldspar grains, but is rare in hypersthene.

Hornblende - in hand specimen, crystals are black with a glassy lustre. Elongate, prismatic and pleochroic from deep green to green crystals 0.1 - 2 mm long with high positive relief. Most grains were bladed and translucent at the edges, many were cleavage plates (110) with frayed and ragged ends, others showed prismatic striae. Only about 5% of the grains were euhedral, the majority being subhedral, and a few fragments were angular.

Biotite - shows a brown-gold lustre. Thin platy six-sided crystals, 0.06 mm to 1.0 mm in size, about 90% are irregular but a few are subhedral. Most biotites are basal flakes with partial hexagonal outlines, rounded corners in many grains, or fractured with a concave to angular outline, and some ragged shreds. Brown-brownish green interference colours, but pleochroic from yellow to light brown, flakes sometimes showed ferrous-rich colours in more weathered samples.

Zircon - colourless, euhedral to subhedral crystals 0.4 to 0.8 mm with high relief, often showing pyramidal terminations. Interference colours are mainly pastel shades of pinks and blues. Some crystals show minute vacuole inclusions and blebs of glass. About 20% showed zoning.

Limonite - red-brown alteration product of magnetite grains. Irregular, 0.06 - 2.0 mm in size, with an earthy or powdery appearance, may be interstitial as a cement around other mineral grains.

Augite - elongated, anhedral grains with a dull colourless appearance, but showing pale yellow-green interference colours.

Vermiculite - fan-shaped platy minerals, 0.08 - 0.06 mm in size, altered from biotite. High interference colours

6.3.3 Rock Fragments

Many deposits in the Tauranga Basin were rich in fine sand to fine gravel sized lithics. The following rock fragment types occurred in pyroclastic flow deposits, post-depositionally modified pyroclastic flow deposits and fluvial deposits and are assigned p, pd and f respectively. The pd deposits show either pyroclastic flow and debris flow or pyroclastic flow and fluvial characteristics (see Tables 6.1 and 6.2):

1 - Obsidian - abundant. Occurred as black-brown glass shards, plates and as rock fragments. Subangular to angular fragments with conchoidal fractures. Vitreous lustre in hand specimen; p, pd and f.

2 - Rhyolite - abundant. Angular to subrounded pale-red to dark-grey, fine to medium grained fragments. In thin section, rhyolites were porphyritic containing plagioclase, quartz and minor magnetite and hypersthene. Some rhyolite fragments showed flow bandings; p, pd, f.

Three varieties were recognised:

(i) spherulitic sand-sized bluish grey fragments
(ii) flow banded, sand to gravel sized, brownish grey, blue grey to red fragments.
(iii) lithoidal and glassy, sand to gravel size, pink to pale grey clasts surrounded by a manganese oxide shell (i.e., Minden Rhyolite).

3 - Pumice - abundant. Subangular to rounded. Shapes are commonly oblate and equant. White - pale, grey - red, vesicular, spherical - ellipsoidal chambers often coarsely to finely cellular. Containing a high proportion of glass (e.g. globules) and fewer sand sized crystals of quartz and feldspar.

Pumices in the Te Ranga Ignimbrite were often glass-rich with a vitreous appearance. A few pumices show swirl structures, vesicles in the interior are often closed but chambers towards outside of pumice are more continuous with the exterior. Minor phenocrysts included quartz, feldspar, hypersthene, hornblende and magnetite; p, pd, f.

4 - Ignimbrite - common. Angular to rounded, pale, brown grey fragments. Mainly Waitea riki and Waimakariri fragments containing phenocrysts of pumice, feldspar and quartz. Fragments often contain varying amounts of hornblende and hypersthene; f.

TABLE 6.1 Locations of samples used for rock fragment compositional analysis (refer to Appendix II)

Sample No.	Grid Reference	Area
501	U14/849876	Matua
502	"	"
503	"	"
509	"	"
520	"	"
521	"	"
523	"	"
203	U14/819888	Te Puna
205	"	"
206	"	"
207	"	"
803	U14/854805	Greerton
106	U14/796927	Omokoroa
409	U14/854834	Cambridge Rd.

TABLE 6.2 Rock fragment types (%) in fluvial deposits in the Tauranga Basin.* based on pumice character (e.g. vesicular, fibrous, and nature of glass shards).

	501	502	503	509	520	521	523	203	205	206	207	803	106	409
Te Puna Ignimbrite pumice*								6					87	
Waimakariri I. (White to yellow) pumice*	80	76	89											
Te Ranga I. Yellow to white red grey pumice* + obsidian r.f.				86	91	74	4	52		84	87	85		
Minden Rhyolite lithoidal and spherulitic rhyolite						1	83		87					9
Spherulitic rhyolite						7								26
Banded rhyolite	2	1	1	4	3	6	4	4	4	7	1			
Pumiceous and lithic rich ignimbrite			6					28				6	2	32
Rhyolite lithics (red to bluish grey)	9	11	4	10	6	12	9	10	9	9	12	9	1	4
Andesite lithics	2													

5 - Andesite - rare. Fine - medium grained fragments, angular to subrounded. Phenocrysts of quartz, feldspar and hypersthene set in a fine-grained matrix. Dark grey to brown; p, pd, f.

6 - Silt - rare. Subrounded to rounded, pale white to brown. Fine-grained soft fragments; pd, f.

6.3.4 Clay Minerals

Because a large proportion of the deposits found in the Tauranga Basin are highly weathered and airfall tephra related, very fine material (<4μm) is quantitatively important either overlying or interbedded with fluvial and pyroclastic flow units. The most abundant clay mineral identified was halloysite. Metahalloysite, allophane, mixed-layer clays and kaolinite were also present in varying amounts. Because clay minerals were abundant in pyroclastic fall deposits, clay mineralogy is recorded separately for deposits interpreted as being airfall (section 6.6).

6.4 FLUVIAL DEPOSITS

6.4.1 Results:

Rock fragment and heavy mineral analyses were used in this study to ascertain associations between fluvial-fluvial and pyroclastic-fluvial deposits in the Matua Subgroup. The following tabulated results record characteristic individual or combination rock fragment types (Table 6.2 and Fig. 6.3) found in fluvial deposits throughout the southern part of the Tauranga Basin (Table 6.1). The results of heavy mineral analyses are shown in Tables 6.3 - 6.5 and Figs. 6.4 and 6.5.

TABLE 6.3 Locations of samples used for heavy mineral analysis (refer to Appendix II) of fluvial deposits

Sample No.	Grid Reference	Area
106	U14/796927	Omokoroa
409	U14/854834	Cambridge Rd.
6005	U14/845768	Pyes Pa Road
803	U14/854805	Greerton
501	U14/849876	Matua
502	"	"
503	"	"
509	"	"
521	"	"
522	"	"
523	"	"
205	U14/819888	Te Puna
207	"	"
203	"	"
206	"	"
207	"	"

TABLE 6.4 Heavy mineral content (%) of fine sand fractions in fluvial deposits in the Tauranga Basin

Sample No.	Hypersthene	Hornblende	Biotite	Zircon	Vermiculite	Magnetite	Limonite
106	-	10.2	1.6	4.0	8.8	72.4	3.0
409	0.2	17.2	0.8	4.4	0.2	50.4	26.8
6005	14.0	1.1	-	1.6	-	81.6	1.5
803	35.2	8.6	-	0.6	-	55.4	-
501	28.0	3.2	-	0.6	-	66.6	1.6
502	22.4	4.1	-	0.4	-	71.7	1.4
503	19.1	2.0	-	0.4	-	77.9	0.6
509	12.6	6.8	-	0.8	-	78.1	1.7
521	7.3	4.0	-	5.3	-	83.3	-
522	2.5	1.5	-	2.5	-	56.6	36.8
523	6.0	4.3	-	3.0	-	71.0	15.6
205	3.6	4.8	-	1.6	-	29.6	60.4
207	10.4	7.8	-	1.8	-	78.2	1.8
203	10.5	5.3	-	1.2	-	81.8	1.2
206	21.3	5.2	-	0.8	-	71.3	1.4
207	10.4	7.8	-	1.8	-	78.2	1.8

TABLE 6.5 Heavy mineral content (%) of pumice blocks in fluvial deposits

Sample No.	Hypersthene	Hornblende	Biotite	Zircon	Vermiculite	Magnetite	Limonite
501	20.2	2.0	-	0.1	-	77.7	
502	16.4	1.0	-	0.1	-	82.5	
503	14.6	1.0	-	-	-	84.4	
509	6.0	3.1	-	0.1	-	90.8	
203	5.2	1.6	-	0.1	-	93.1	
206	12.4	5.2	-	0.2	-	82.2	
207	6.4	4.2	-	-	-	89.4	

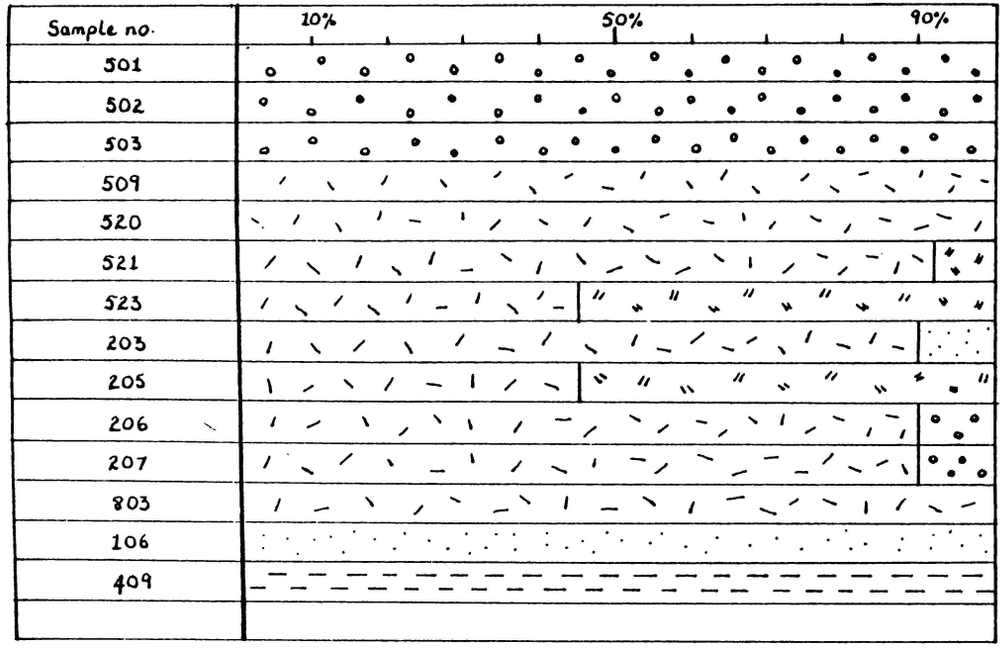


Fig. 6.3 Content (%) and possible source areas of rock fragment material in the fluvial deposits sub-aerially exposed in the Tauranga Basin.

Waimakariri Ignimbrite

Te Ranga Ignimbrite

Te Puna Ignimbrite

Wairoa Ignimbrite

Minden Rhyolite

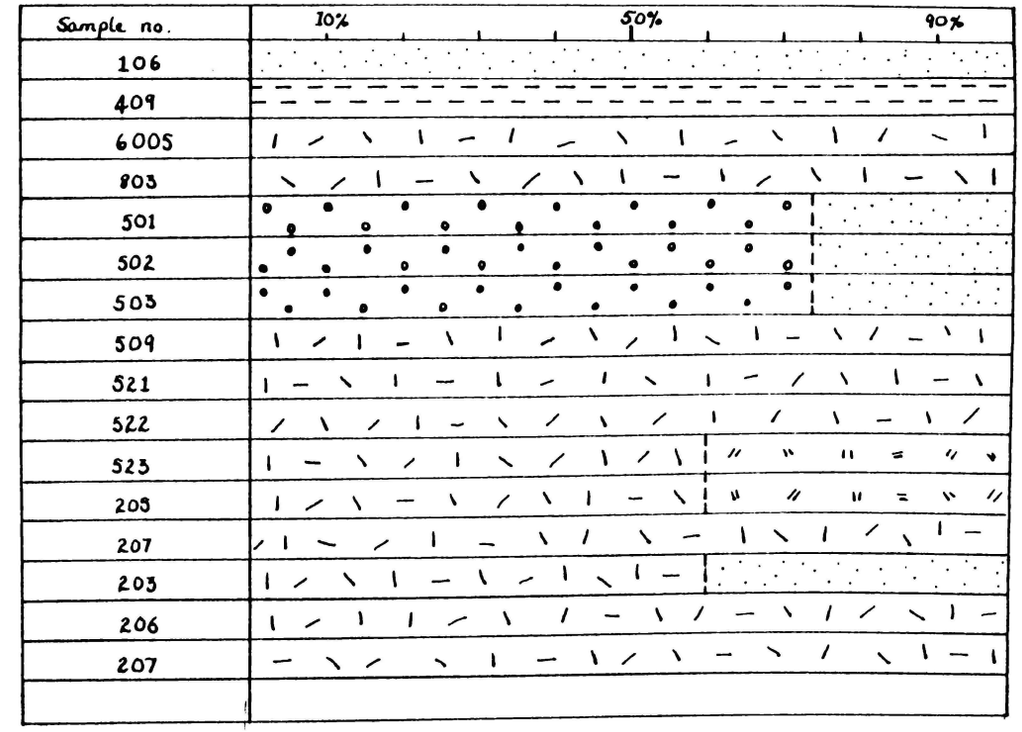


Fig. 6.4 Content (%) and possible source areas of heavy minerals in fluvial deposits.

Waimakariri Ignimbrite

Te Ranga Ignimbrite

Te Puna Ignimbrite

Wairoa Ignimbrite

Minden Rhyolite

Fig. 6.5 Average heavy mineral content (%) of the fine sand fraction from nine fluvial sediment samples in the Matua Subgroup.

(a) sample 207 - Te Puna
(b) sample 205 - Te Puna
(c) sample 521 - Matua
(d) sample 522 - Matua
(e) sample 523 - Matua
(f) sample 803 - Greerton (source rock = Te Ranga Ignimbrite)
(g) sample 6005 - Te Ranga (source rock = Te Ranga Ignimbrite)
(h) sample 106 - Omokoroa (source rock = Te Puna Ignimbrite)
(i) sample 409 - Cambridge Road (source rock = Wairoa Ignimbrite)

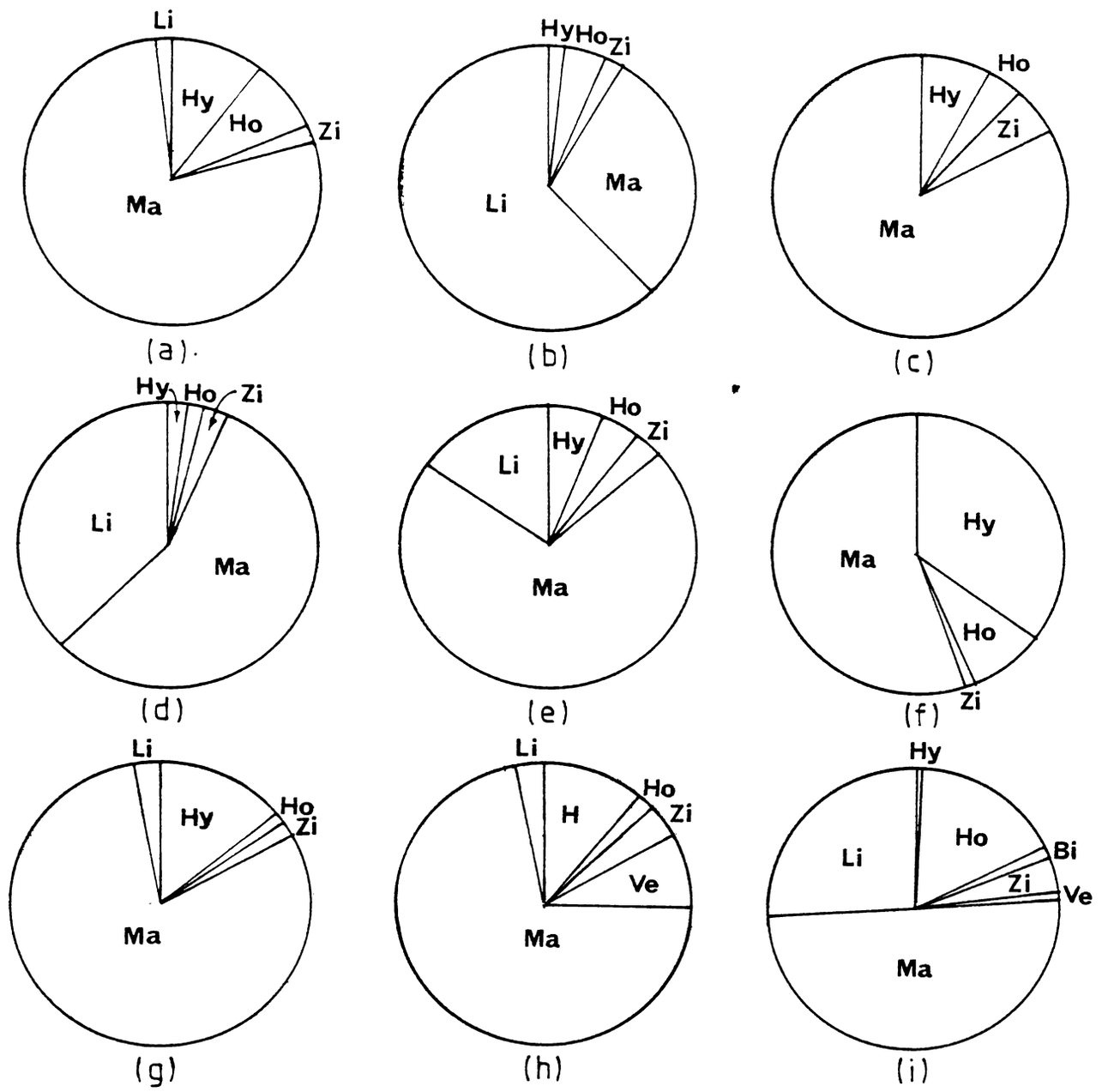

Li
Hy
Ho
Zi
Ma
(a).
Hy Ho Zi
Li
Ma
(b)
Ho
Hy
Zi
Ma
(c)
Hy Ho Zi
Li
Ma
(d)
Ho
Zi
Li
Hy
Ma
(e)
Hy
Ma
Ho
Zi
(f)
Li
Hy
Ho
Zi
Ma
(g)
Li
H
Ho
Zi
Ve
Ma
(h)
Hy
Li
Ho
Bi
Zi
Ve
Ma
(i)
Hy Hypersthene
Ho Hornblende
Bi Biotite
Zi Zircon
Ve Vermiculite
Ma Magnetite
Li Limonite

Fig. 6.5

6.5 PYROCLASTIC FLOW DEPOSITS

6.5.1 Results:

A. Petrographic description

Ignimbrites subaerially exposed in the Tauranga Basin are documented from thin section. Petrographic notes are given below. Descriptions for (i) and (ii) are for welded samples, while those from (iii) onwards are for impregnated unconsolidated samples with sand to sandy gravel textures; (vii) describes ignimbrite and ignimbrite derived fluvial sediment:

(i) Waitearíki Ignimbrite - (Houghton B.F.; slide R44; NZGS, Rotorua)

Rhyodacitic, dark grey, welded ignimbrite with lenticular texture. Phenocrysts are dominated by plagioclase, quartz and biotite. Microphenocrysts include Fe-Ti oxide, biotite, hornblende and rare hypersthene.

(ii) Papamoa Ignimbrite - (Healy, J., 1977; slides KT-16, R-30, R-52; NZGS, Rotorua)

Rhyodacitic, dark grey to brown, welded ignimbrite with lenticular texture. Phenocrysts are dominated by plagioclase, quartz, abundant hornblende, uncommon biotite, rare hypersthene and microphenocrysts of hornblende and Fe-Ti oxide.

(iii) Wairoa Ignimbrite - (slide WT 18520)

Brown to dark grey, crystal rich (∿ 15%) unwelded ignimbrite. Highly weathered slightly gravelly sand (iron-stained) containing spherulitic and flow banded rhyolitic blue to grey lithics. Phenocrysts are dominated by plagioclase and quartz (2 : 1) with minor hornblende, biotite, magnetite and limonite. Hypersthene is rare.

(iv) Te Puna Ignimbrite - (slide WT 18480, WT 18502, WT 18503)

Rhyolitic, unwelded, brown, slightly gravelly sand containing rhyolitic and common andesitic rock fragments. Phenocrysts are dominated by plagioclase, quartz (3:1) with minor hornblende, magnetite and biotite set in a glass shard matrix. Hypersthene and vermiculite are uncommon although the latter is more common in samples collected at coastal exposures.

(v) Te Ranga Ignimbrite - (slide WT 18528)

Grey unwelded porous ignimbrite, with sandy texture containing black angular obsidian and rhyolitic (red to bluish grey) rock fragments. Phenocrysts are dominated by plagioclase, quartz (3:1) with minor hypersthene and magnetite set in a glass shard matrix composed of colourless to brown glass flakes.

(vi) Waimakariri Ignimbrite - (slide WT 18529)

Brown to white, poorly to moderately welded porous ignimbrite containing phenocrysts dominated by plagioclase, quartz (3:1) with minor hypersthene and magnetite set in a glass shard matrix. Subordinate microphenocrysts of hornblende and pumice containing glass globules are also characteristic.

(vii) Fluvial sediments derived from ignimbrite (Te Ranga and partly Waimakariri and Wairoa) and Minden Rhyolite - (Slide WT 18487, WT 18498)

Weathered, slightly gravelly sand (manganese and iron oxide staining) containing pink to brown glassy and spherulitic, coarse sand to gravel size rhyolite, with pumice inclusions up to 2 mm diameter. Lithoidal rhyolite rock fragments are common. Phenocrysts are dominated by plagioclase, quartz, and magnetite, with subordinate limonite, and minor hornblende and hypersthene.

B. Heavy mineral results

Heavy minerals constitute about 1% of the weight of pyroclastic flow deposits and occur in coarse sand to gravel pumice clasts and in the coarse sand to silt grade matrix. The deposits are dominated by magnetite, hypersthene, hornblende and biotite and many deposits contain trace zircon. Biotite is often enriched in the upper parts of the pyroclastic flow unit while magnetite, hypersthene and hornblende occur throughout. The results of heavy mineral analysis are presented in Tables 6.6 and 6.7 and in Fig. 6.6.

C. Results of pyroclastic flow deposits exposed at Omokoroa and Matua

The results of petrographic description, rock fragment analysis and pumice character studies are shown in Fig. 6.7 for selected pyroclastic flow deposit samples. The table suggests possible correlatives for pyroclastic flow units intercalated with fluvial and airfall deposits at Omokoroa and Matua. Pyroclastic flow units exposed at the coast were often thin ($< \sim 3$ m), but showed mineralogic and textural similarities to distal ignimbrites subaerially exposed inland away from the coast.

TABLE 6.6 Locations of samples used for heavy mineral analysis (refer to Appendix II) of pyroclastic flow deposits.

Sample No.	Grid Reference	Area
301	U14/828859	Te Puna
302	U14/828859	Te Puna
103	U14/796927	Omokoroa
6701	U14/820770	Belk Rd.
603	U14/845768	Pyes Pa Rd.
7011	U14/820770	Belk Rd.
401	U14/857835	Cambridge Rd.
504	U14/849876	Matua

TABLE 6.7 Heavy mineral content (%) of fine sand fractions in pyroclastic flow deposits in the Tauranga Basin

Sample No.	Hypersthene	Hornblende	Biotite	Zircon	Vermiculite	Magnetite	Limonite
301	8.0	47.3	3.8	1.6	-	37.8	1.6
302	6.0	27.0	16.0	2.0	1.0	47.0	1.0
103	2.0	28.2	-	3.2	-	66.6	-
6701	13.3	2.0	-	1.0	-	76.3	7.3
603	20.0	3.3	3.3	-	-	66.6	6.6
7011	40.0	1.0	-	-	-	58.8	-
401	1.2	24.2	6.2	2.8	0.4	47.8	13.4
504	26.3	13.6	-	0.33	-	59.6	-

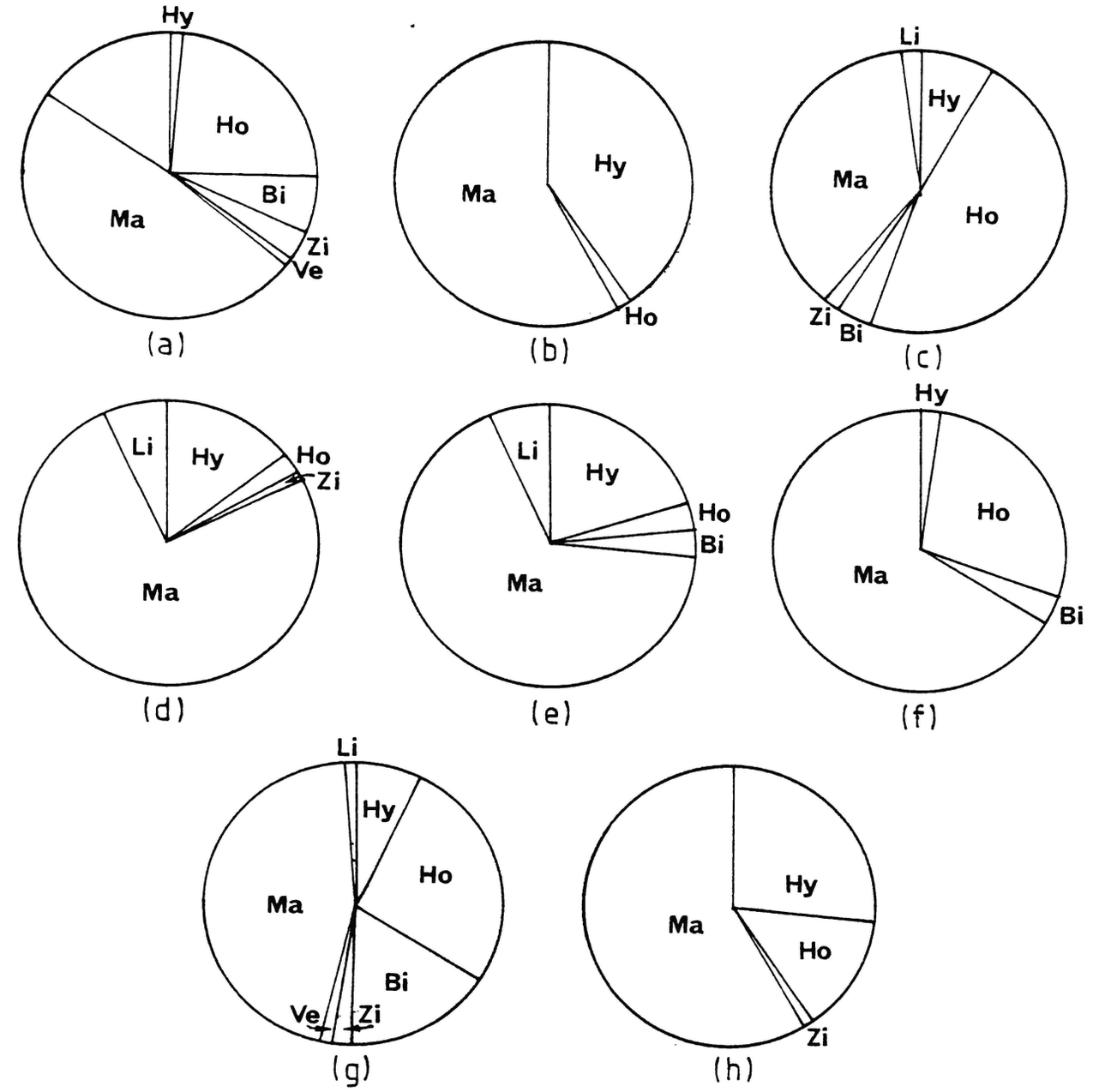


Fig. 6.6 Average heavy mineral content (%) of the fine sand fraction from selected pyroclastic flow deposits.

(a) sample 401 - Wairoa Ignimbrite
(b) sample 7011 - Waimakariri Ignimbrite
(c) sample 301 - Te Puna Ignimbrite
(d) sample 6701 - Te Ranga Ignimbrite (Belk Road)
(e) sample 603 - Te Ranga Ignimbrite (Pyes Pa Road)
(f) sample 103 - Pyroclastic flow deposit at Omokoroa
(g) sample 302 - Te Puna Ignimbrite
(h) sample 504 - Pyroclastic flow deposit at Matua

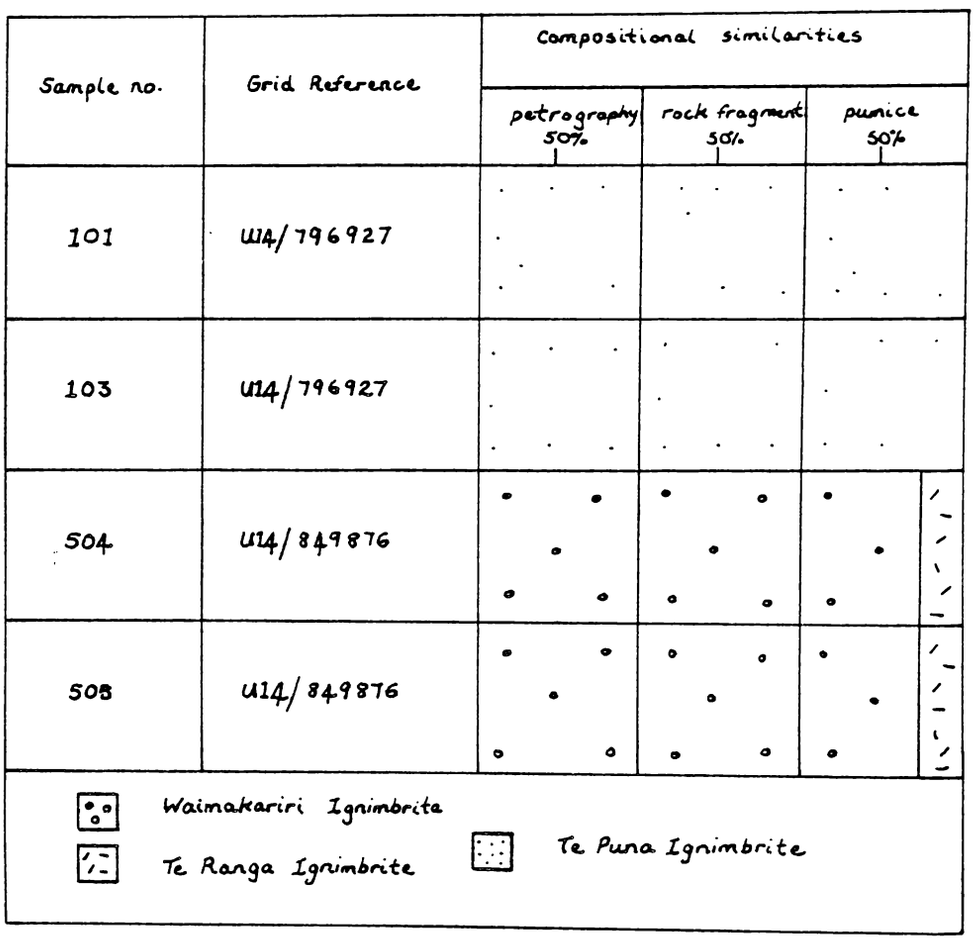


Fig. 6.7 Possible analogous pyroclastic flow deposits suggested from petrofabric, rock fragment and pumice type studies.

6.6 PYROCLASTIC FALL DEPOSITS

6.6.1 Results:

Primary mineral assemblages are dominated by glass shards, feldspar and quartz. Secondary minerals are represented by amorphous colloids, halloysite and allophane.

A. Results of heavy mineral analysis

Heavy minerals constitute about ∿ 1 to 0.5% by weight of air-fall deposits in the Matua Subgroup. Samples were selected from stratified units which were less weathered, containing a low proportion of clay (< ∿ 10%). The Pahoia tephras (see Chapter 3) were dominated by hypersthene, hornblende and biotite. Vermiculite was common in some deposits exposed in coastal cliffs. Results are shown in Tables 6.8 and 6.9 and in Fig. 6.8.

B. Results of clay mineralogy

Tephras were commonly highly weathered and contained varying amounts of clay minerals. Older tephras, such as the Pahoia tephras, were dominated by halloysite. The Hamilton Ash Formation overlying the Pahoia tephras was dominated by halloysite and allophane. Results of the clay mineralogy are presented in Table 6.10.

C. Summary

A compositional summary of specific tephras is presented in the following discussion. The Pahoia tephras are included in the Matua Subgroup (see Chapter 3) while the Hamilton Ash Formation overlies the Pahoia tephras. Some Hamilton Ash beds, however, have been reworked at some sites and fluvial sediments derived from and interbedded with Hamilton Ash are included in the Matua Subgroup. It is therefore necessary to briefly describe the composition of both the

TABLE 6.8 Locations of samples used for heavy mineral analysis (refer to section 3.5.1, chapter 3 and Appendix II) of pyroclastic fall deposits.

Sample No.	Grid Reference	Area
105	U14/796927	Omokoroa
1066	"	"
107	"	"
108	"	"
109	"	"
110	"	"
1101	"	"
1112	"	"
112	"	"
510	U14/849876	Matua
511	"	"
512	"	"
515	"	"

TABLE 6.9 Heavy mineral content (%) of fine sand fractions in pyroclastic air-fall deposits

Pahoia tephras (code)*	Sample No.	Hypersthene	Hornblende	Biotite	Zircon	Vermiculite	Magnetite	Limonite
Oa	105	14.6	26.4	1.0	3.1		54.9	
Oa	1066	-	14.2	3.6	2.0	9.6	68.6	2.0
Oe	107	31.4	20.6	14.8	1.0		32.2	
Of	108	22.3	19.7	4.9	0.8		40.6	
Og	109	23.7	26.8	20.2	0.6		28.7	
Oj	110	21.3	29.4	5.8	0.4		43.1	
Ol	1101	20.6	30.1	16.3	1.2		31.8	
Om	1112	11.5	12.9	18.5	0.8		56.3	
Oj	112	10.1	11.9	15.4	0.8		61.8	
	510	4.3	8.1	tr	0.66		84.3	3.1
	511	19.0	4.2		1.8		75.8	
	512	16.7	6.9		1.2		75.2	
	515	12.2	7.2		1.9		78.7	

* see Pahoia tephras - Chapter 3.

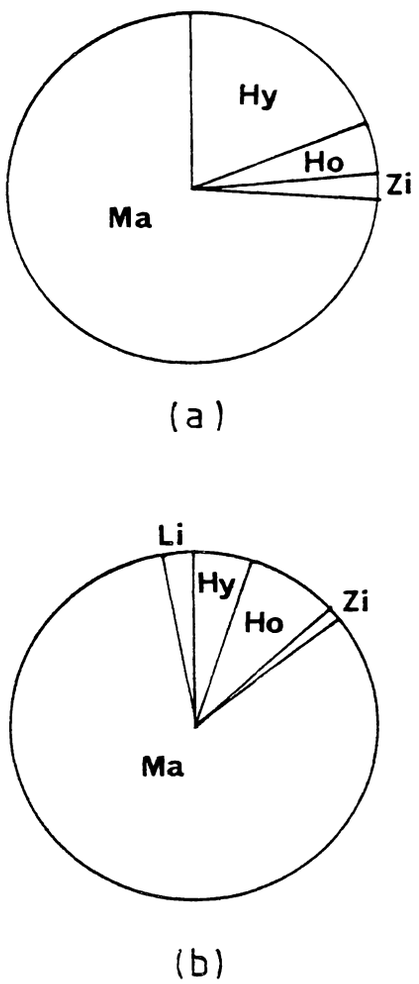


Fig. 6.8 Average heavy mineral content (%) of the fine sand fraction from two shower bedded pyroclastic fall units intercalated with pyroclastic flow and fluvial deposits at Matua.

(a) Sample 512

(b) Sample 510

TABLE 6.10 Clay Mineralogy

Area	Sample No.	WT No.	Halloysite	Allophane	Kaolinite	Mixed-layer clays	Vermiculite
Omokoroa	106l	WT 18406				m	c
"	105l	WT 18405	c				
"	108l	WT 18409	a				
"	109l	WT 18410	a			t	
"	110l	WT 18411	a			t	
"	111l	WT 18458	c	c	t		
"	112l	WT 18459	c	c	t		
Matua	506	WT 18424	a	t			
"	508	WT 18429	a	t			
"	5p1	WT 18438	a	m			
"	5p2	WT 18439	a				

a = abundant; c = common; m = minor; t = trace

Pahoia tephras and the Hamilton Ash Formation and to summarise and interpret their clay mineralogy:

(a) Pahoia tephras

The Pahoia tephras contain the following minerals in decreasing order of abundance : glass shards, halloysite, feldspar (plagioclase) and quartz. Heavy minerals constitute a small weight fraction of the whole deposit (∿ 1%) and the following decreasing order of abundance is recorded : magnetite, hypersthene, hornblende, and biotite.

Vermiculite (i.e. biotite → hydrobiotite → vermiculite) was recorded in fluvial and pyroclastic flow deposits which were intercalated with, or underlying, Pahoia tephras.

(b) Hamilton Ash Formation

Hamilton Ash deposits contain the following minerals in decreasing order of abundance : halloysite, allophane, glass shards, quartz, and feldspar. Dominant heavy minerals include magnetite, hypersthene and hornblende.

(c) Distribution of clay minerals

Halloysite was the dominant clay mineral identified in stratigraphically older deposits (i.e. Pahoia tephras) below the Hamilton Ash beds. Pahoia tephras were sampled from both highly weathered ash beds (e.g. those containing greater than ∿ 40% weight of clay) and from less weathered samples which are more mineralogically immature and are described as sands and silts (e.g. those containing a greater weight % of glass shards and pumice).

Stratigraphically younger ash deposits (i.e. those which overlie Pahoia tephras) are dominated by allophane, which is particularly common in Hamilton Ash beds (e.g. especially in the upper parts of the

Omokoroa section). Halloysite is present in varying proportions and is dominant to minor.

(d) Interpretation of composition in highly weathered deposits

The presence of a particular clay mineral in volcanic ash possibly reflects the original composition and the degree of weathering as a function of time and climate (Fields, 1955; Fieldes, 1968; Kirkman and Pullar, 1978).

Kirkman (1980) postulated that the morphologic form of halloysite in the Pahoia tephras indicates that it may have altered from feldspar (→ allophane → halloysite; Kirkman and Pullar, 1978), whereas in the Kauroa Ash deposits a more direct alteration is likely to have taken place (i.e. feldspar → halloysite). In many other ash deposits it is likely that an indirect alteration process passes from glass → allophane → halloysite (Kirkman, 1980).

The presence of allophane in the Hamilton Ash beds indicates initial weathering of glass to allophane (→ allophane B → allophane A; Hogg, 1974).

6.7 MINERALOGICAL GROUPS

Sediments in the map area contain a high proportion (∿ 85% of the total rock assemblage) of pumice and glass shards, with the minerals feldspar and quartz abundant (∿ 90% of total phenocrysts) in all samples. Feldspar (mainly plagioclase) usually dominates over quartz in the range 3:1 to 4:1, depending on location.

From the construction of stratigraphic columns, extensive mapping and from mineralogical analysis, seven major petrofacies are recognised The underlined components are particularly characteristic in specific petrofacies.

(A) Pumice - glass shards - hypersthene - obsidian

(B) Pumice - glass shards - quartz - feldspar - hypersthene

(C) Pumice - glass shards - feldspar - quartz - hornblende - biotite

(D) Pumice - quartz - feldspar - rhyolite - magnetite - limonite

(E) Pumice - glass shards - quartz - feldspar - rhyolite

(F) Quartz - feldspar - rhyolite - hornblende - hypersthene - biotite (i.e. crystal rich ∿ 20%)

(G) Carbonaceous deposits

The distribution of petrofacies is shown in Figs. 6.9 and 6.10.

(i) Petrofacies A occurs stratigraphically below petrofacies B. Both are important in the southern part of the study area. Petrofacies A occurs in sandy gravels, gravelly sands, slightly gravelly sands and sands. It forms the Te Ranga Ignimbrite and associated sediments. The Te Ranga Ignimbrite is exposed at Belks Road, Pyes Pa Road and the Melame Street quarry. Associated fluvial sediments make up paleochannel and bar deposits exposed above and to the sides of the ignimbrite and can be followed from Pyes Pa to Te Puna and Matua. Petrofacies A appears at the top of stratigraphic sections at Matua and just above (≃ 1 m) beach level at Te Puna. It is overlain conformably by petrofacies D at both these locations.

(ii) Petrofacies B makes up the Waimakariri Ignimbrite and associated fluvial sediments. It overlies petrofacies A and is confined to southern and central sections of the map area. It is exposed at Belk Road, Wairoa River, Ruahihi, Pyes Pa Road, and is extensive and forms a thick (up to 40 m) deposit from McClaren Falls back to the Waipapa Stream in the Mamaku Plateau.

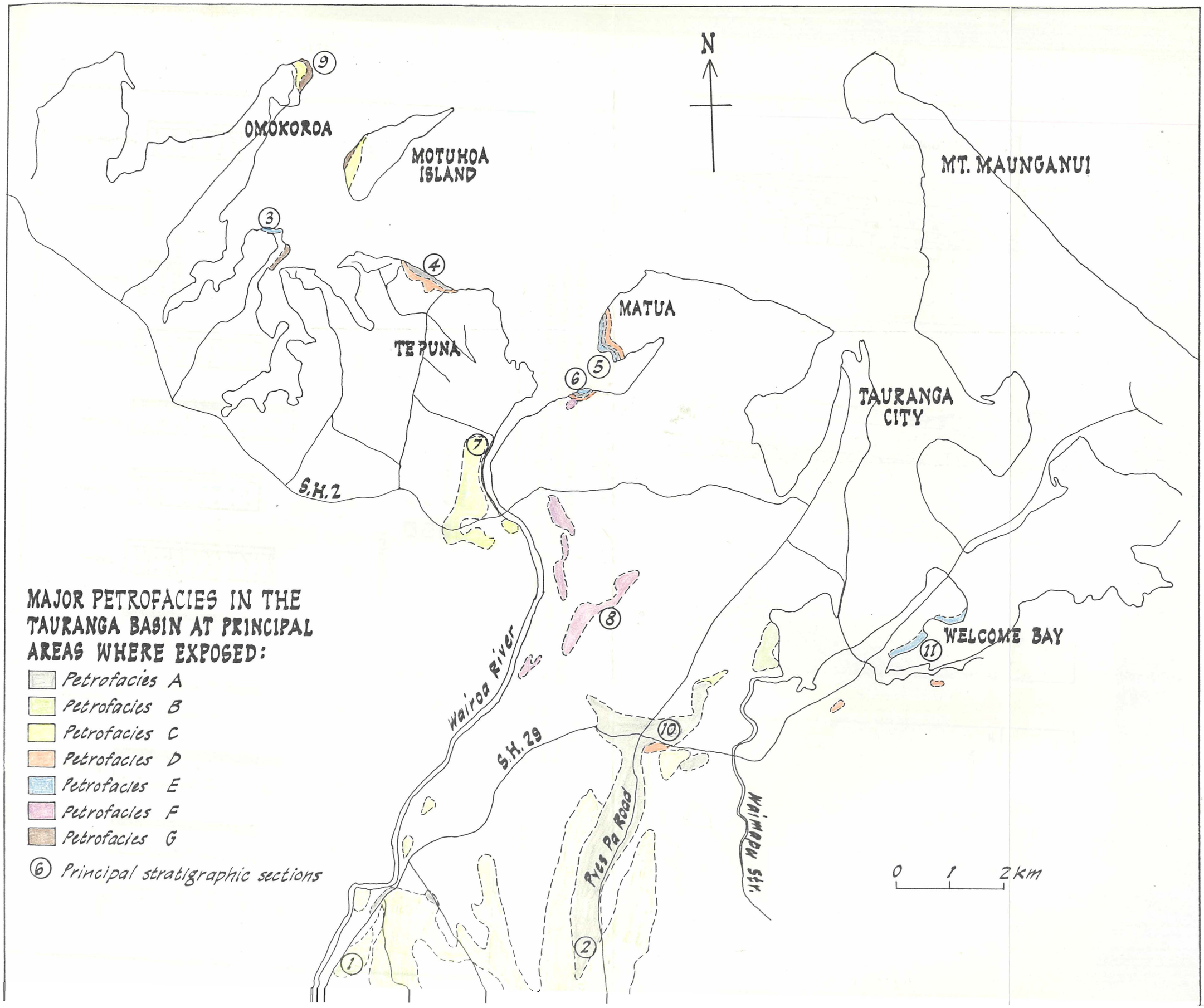


Fig. 6.9 Petrofacies distribution map showing the locality of the main subaerial sections studied.

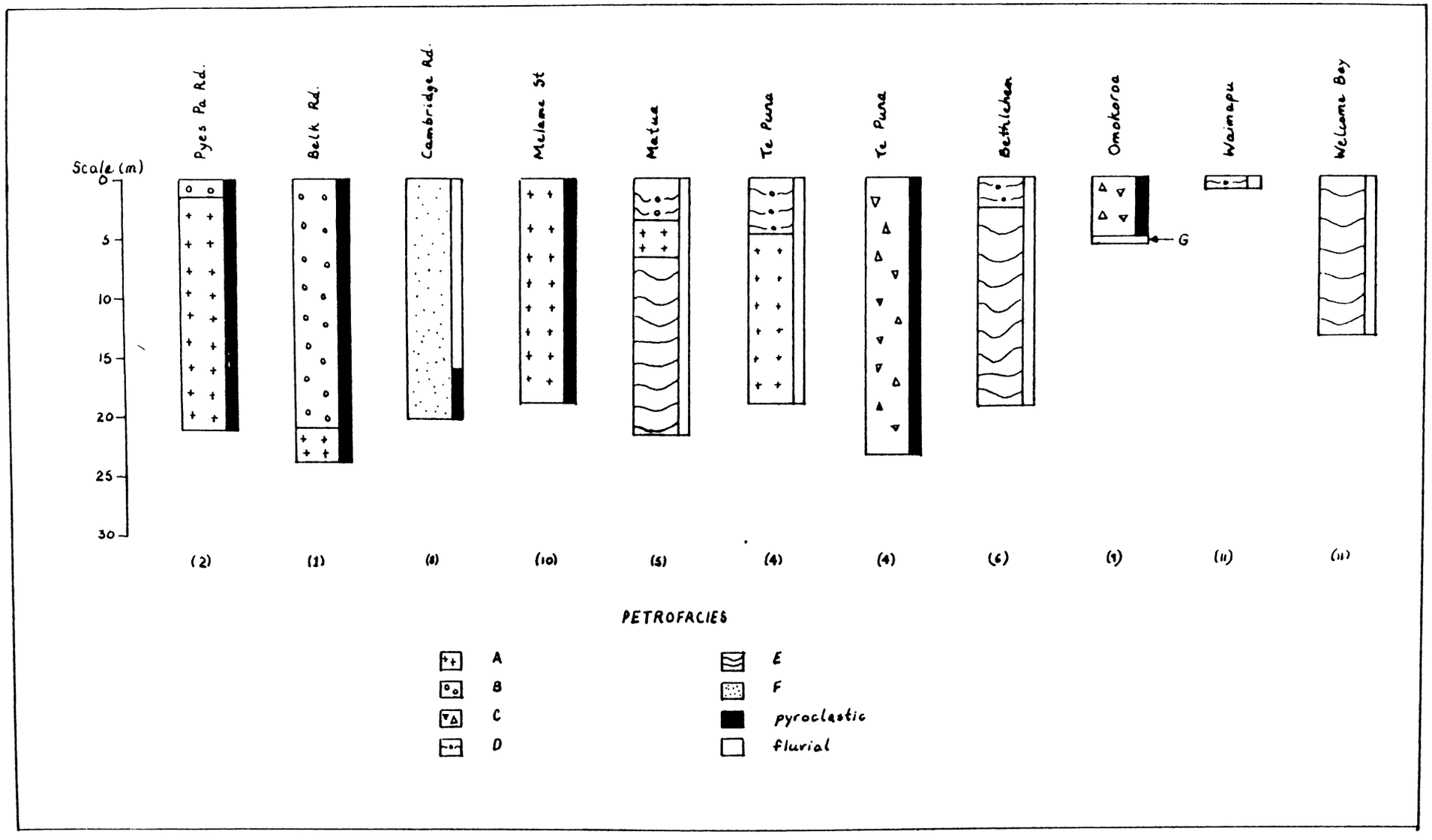


Fig. 6.10 Petrofacies diagrams showing the types of deposit which correspond with specific petrofacies at various localities within the Tauranga Basin. Numbers below block diagrams are related to those displayed in Fig. 6.9.

(iii) Petrofacies C is recognised in coastal exposures and underlies a thick sequence of Hamilton Ash, Pahoia tuffs and possibly Kauroa Ash and multiple paleosols at Omokoroa. It forms subsidiary pyroclastic flow/debris flow, alluvial fan and distal ignimbrite deposits. The petrofacies is important north of the Wairoa River at Te Puna, Motuhoa Island and Omokoroa.

(iv) Petrofacies D is important at Te Puna and Matua where it forms very extensive braided/ephemeral river deposits up to 4 m thick. Rhyolite clasts within the deposit have been derived from Mt Minden. Much of the material appears to have been reworked, possibly from alluvial fan/debris flow deposits and is exposed throughout the Basin beneath Hamilton Ash beds. Other locations include exposures at Welcome Bay and at Waimapu Road, where petrofacies D thins considerably to less than 5 cm and 50 cm respectively. At Welcome Bay and at Waimapu Road, petrofacies D becomes interbedded with ash units and may incorporate ash. Petrofacies A is only recognisable north of these sections.

(v) Petrofacies E is recognised extensively in the map area, and at Matua it underlies petrofacies A and D deposits and is intercalated with pyroclastic flow material. At Welcome Bay, Mangatapu and at Bethlehem these deposits are below the Pahoia tuffs and often contain interbedded tuffaceous and unconsolidated ash deposits and paleosols. Stratigraphic evidence at coastal cliff exposures indicates that these deposits are older than petrofacies A and D but younger than petrofacies B, C and F. However, in areas away from the coast to the west stratigraphic evidence indicates petrofacies E is younger than petrofacies A suggesting an inverse relationship in age correlation between areas at the coast and away from the coast. This can be related to periods of fluvial erosion and deposition after ignimbrite emplacement

(see section 6.9). Texturally the deposits are sandy gravels, slightly gravelly sands and sands and are interpreted as alluvial braided/ ephemeral deposits.

(vi) Petrofacies F is important in central parts of the study area, extending from Ruahihi to Bethlehem and is well exposed at the Tauranga Dump (U14/856835). It is characteristically highly weathered by iron and manganese oxides, is associated with several intercalated paleosols, and stratigraphically underlies petrofacies A, B, C, D, and E. The petrofacies forms alluvial wash, gravel lag and braided river sediments and pyroclastic flow/alluvial fan deposits; texturally these deposits are gravelly and slightly gravelly sands to sands.

(vii) Petrofacies G is important in the Omokoroa, Motuhoa Island, Matakana Island and Te Puna areas. Lignite disconformably underlies pyroclastic flow, air-fall tephra and fluvial deposits. Carbonaceous silts exposed at Omokoroa and On Motuhoa Island are also interbedded with these deposits.

6.8 PETROFACIES DISTRIBUTION AND INTERPRETATION; with emphasis on fluvial deposits

It is concluded from this study that fluvial deposits subaerially exposed in the southern parts of the Tauranga Basin are derived mainly from a number of local pyroclastic flow deposits (Figs. 6.11 and 6.12), with minor contributions of sediment derived from the Pahoia tephras. Figure 6.9 should be consulted during reading of this section. In the Matua, Otumoetai, Maungatapu and Tauranga City areas, fluvial sediment (petrofacies A and E) has been derived principally from three sources:

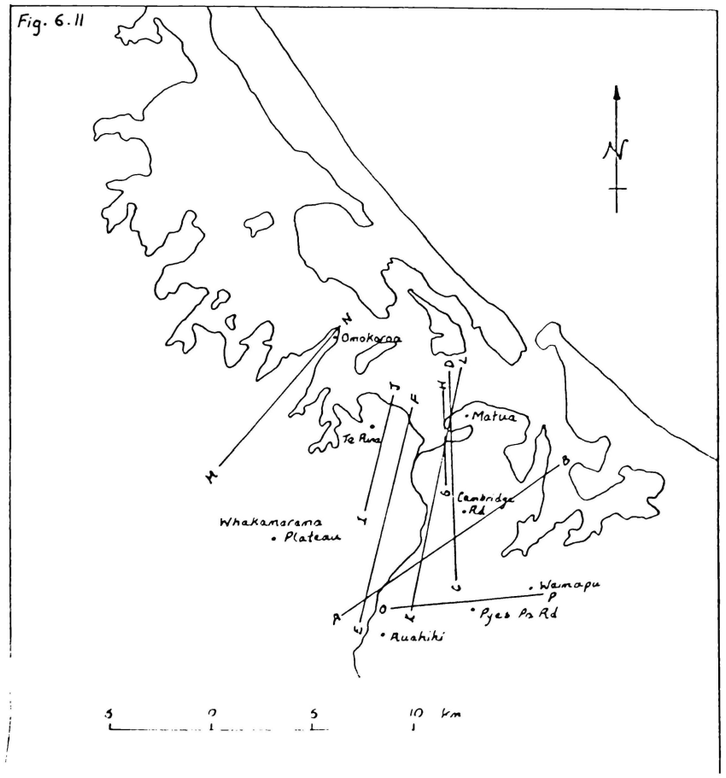
(a) Te Ranga Ignimbrite,

(b) Waimakariri Ignimbrite, and

(c) Pahoia tephras.

LEGEND

- A — Petrofacies A
- B — Petrofacies B
- C — Petrofacies C
- D — Petrofacies D
- E — Petrofacies E
- F — Petrofacies F
- Petrofacies G
- Matua Subgroup deposits (mixture of petrofacies and sediment derived from a number of sources)
- Hamilton Ash Formation
- Waitepariki Ignimbrite
- Aongatete Ignimbrite
- Minden Rhyolite
- Andesite (Beesons Island Volcanics)
- Interdigitating sediment intercalated with and/or associated with pyroclastic deposits



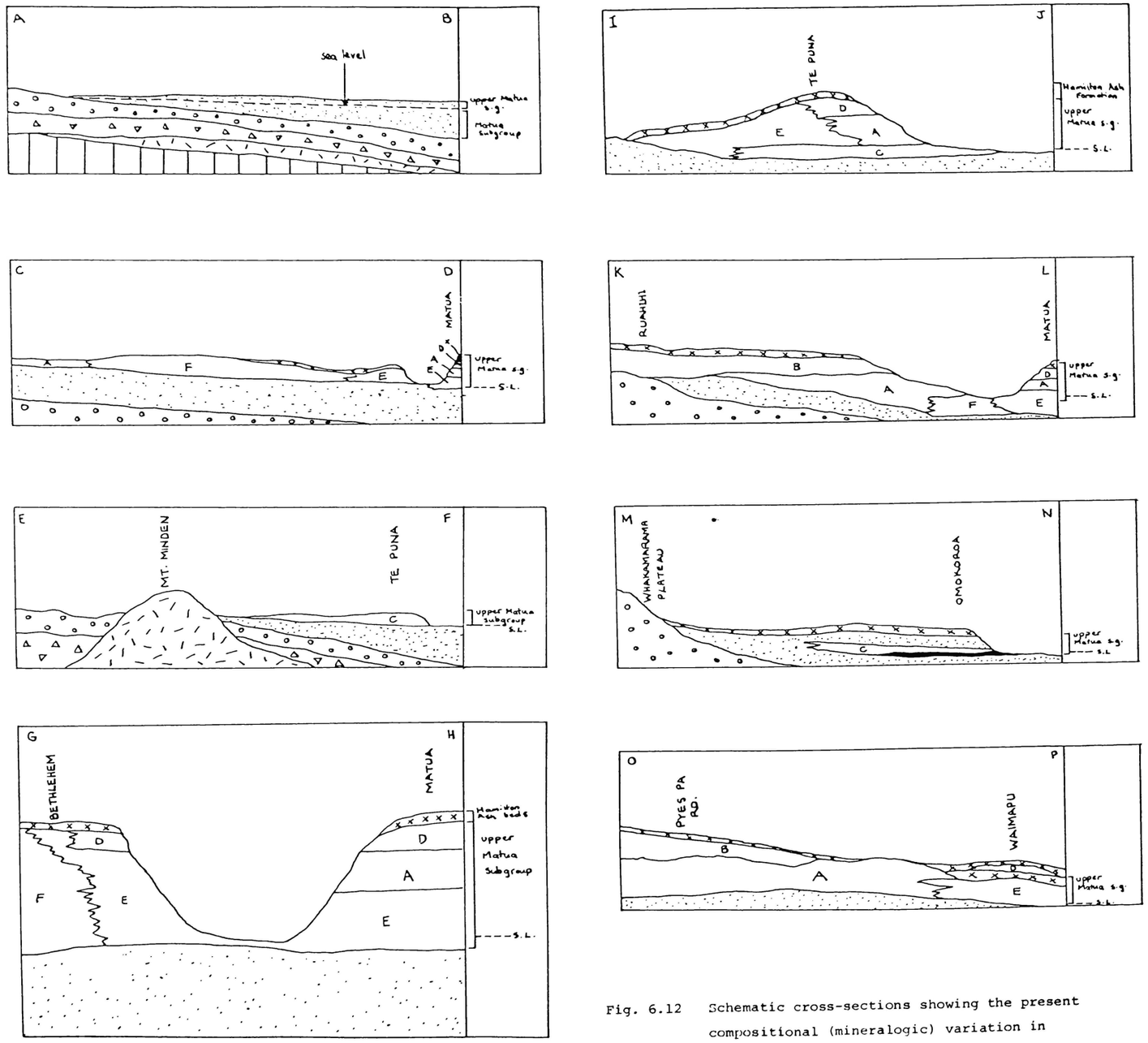


Fig. 6.12 Schematic cross-sections showing the present compositional (mineralogic) variation in deposits in the Matua Subgroup.

An intermixing of fluvial sediment derived from the above three sources and that derived from the Te Puna Ignimbrite (petrofacies C) occurs northwest of the Wairoa River throughout the Te Puna area. In this area a lobe of the Te Puna Ignimbrite has been laterally truncated by fluvial erosion.

Further north in the Omokoroa area, petrofacies C crops out as fluvial, post-depositionally modified pyroclastic (e.g. slump deposits) and pyroclastic flow deposits above petrofacies G. Petrofacies G is intercalated with petrofacies E material at some site localities exposed along the coast in the Omokoroa and Te Puna areas. Pahoia tephras and Hamilton Ash beds are preserved to a greater extent in the northern parts of the map area, particularly at Omokoroa.

Petrofacies D (e.g. exposed at Te Puna, Bethlehem, Matua and Welcome Bay) consists of reworked material of rhyolitic (i.e. Minden rhyolite) and ignimbritic origin. It (i.e. petrofacies D) is stratigraphically younger than the other petrofacies deposits but is highly weathered. Stratigraphic and mineralogical evidence would suggest it partly consists of reworked Hamilton Ash beds, Te Ranga Ignimbrite, Minden rhyolite and Pahoia tephras and this is substantiated by its distribution and stratigraphic position.

Petrofacies F consists mainly of fluvial sediment derived principally from the Wairoa Ignimbrite and crops out in a narrow belt extending from Bethlehem in the north, along Cambridge Road and southward to the Ruahihi area. It is partially mixed with sediments derived from the Waitеariki and Waimakariri Ignimbrites in an area south of Cambridge Road. At Bethlehem, the composition of petrofacies F again becomes mixed with sediment derived from the Waimakariri and the Te Ranga Ignimbrites. Petrofacies D is also partially interbedded with petrofacies A, B, and F in the Bethlehem area.

6.9 PROVENANCE

The relative proportions of mineral components in the Matua Subgroup fluvial deposits suggests that they were derived principally from the erosion of ignimbrite, pumice, rhyolite and andesite source rocks and their air-fall equivalents (see Fig. 6.13 and Table 6.11). The petrology of Quaternary volcanics from the Central Volcanic Region has been reviewed by Cole (1979).

Pyroclasts deposited in the Tauranga Basin which result from volcanic extrusion (probable source is the CVR) are characterised by abundant rhyolitic pumiceous fragments and glass shards and by the following phenocrysts : plagioclase (An 0% - An 30%), magnetite (abundant), quartz, hypersthene, hornblende (common), biotite (less common) and augite (rare). Fluvial deposits in the upper Matua Subgroup duplicate this mineralogy. Evidence presented in this study indicates that fluvial deposits are mineralogically similar to specific distal ignimbrites subaerially exposed in the Tauranga Basin (section 6.7). A number of distal ignimbrites cropping out in the Basin or showing thick deposits at the margins of the Basin are therefore considered the major source rocks for the upper Matua Subgroup fluvial sediments. The proximal nature of source rocks is evidenced by the freshness and immaturity (e.g. poor sorting and angularity of grains) of detrital sand grains in fluvial deposits. Specific fluvial deposits showing a mineralogical relationship with specific pyroclastic flow deposits also record textural similarities. Comparative mineralogy of ignimbrites and fluvial deposits subaerially exposed in the Tauranga Basin indicates that only minimal chemical weathering has affected most deposits, in particular source rocks (e.g. the Te Ranga Ignimbrite). This may be attributed to several factors, including the high permeability of the unconsolidated distal ignimbrites and associated fluvial deposits, and cool climatic periods since emplacement of ignimbrites.

Fig. 6.13 Schematic W-E cross-sections (cartoons) through the Te Puna-Wairoa River areas showing compositional variations within the Tauranga Basin with time; see Fig. 6.13 (1) (1) for location and Fig. 6.12 for legend.

(1) Immediately after emplacement of the Waitearikí Ignimbrite (0.84 m.y. B.P.).

(2) The Waitearikí Ignimbrite was eroded and contributed thick sequences of fluvial sediment into the subsiding Basin. The Wairoa Ignimbrite (petrofacies F) was emplaced over the sediment derived from the Waitearikí Ignimbrite.

(3) The Wairoa Ignimbrite was eroded and thick sequences of fluvial sediment were supplied to the Matua Subgroup.

(4) The Te Puna Ignimbrite (∿0.4 - 0.3 m.y. B.P.), or petrofacies C was deposited in the Basin.

(5) The Te Puna Ignimbrite was eroded, and fluvial sequences were again deposited in the Matua Subgroup.

(6) In the early stages of erosion and sediment supply after emplacement of the Te Ranga Ignimbrite and the Waimakariri Ignimbrite. Deposition of petrofacies E; * see Fig. 6.13B for explanation of petrofacies sequences.

(7) Deposition of petrofacies D over petrofacies A, B and E.

Fig. 6.13B *Explanation of No. 6 schematic cross-section*

(a) Emplacement of Te Ranga Ignimbrite (petrofacies A).

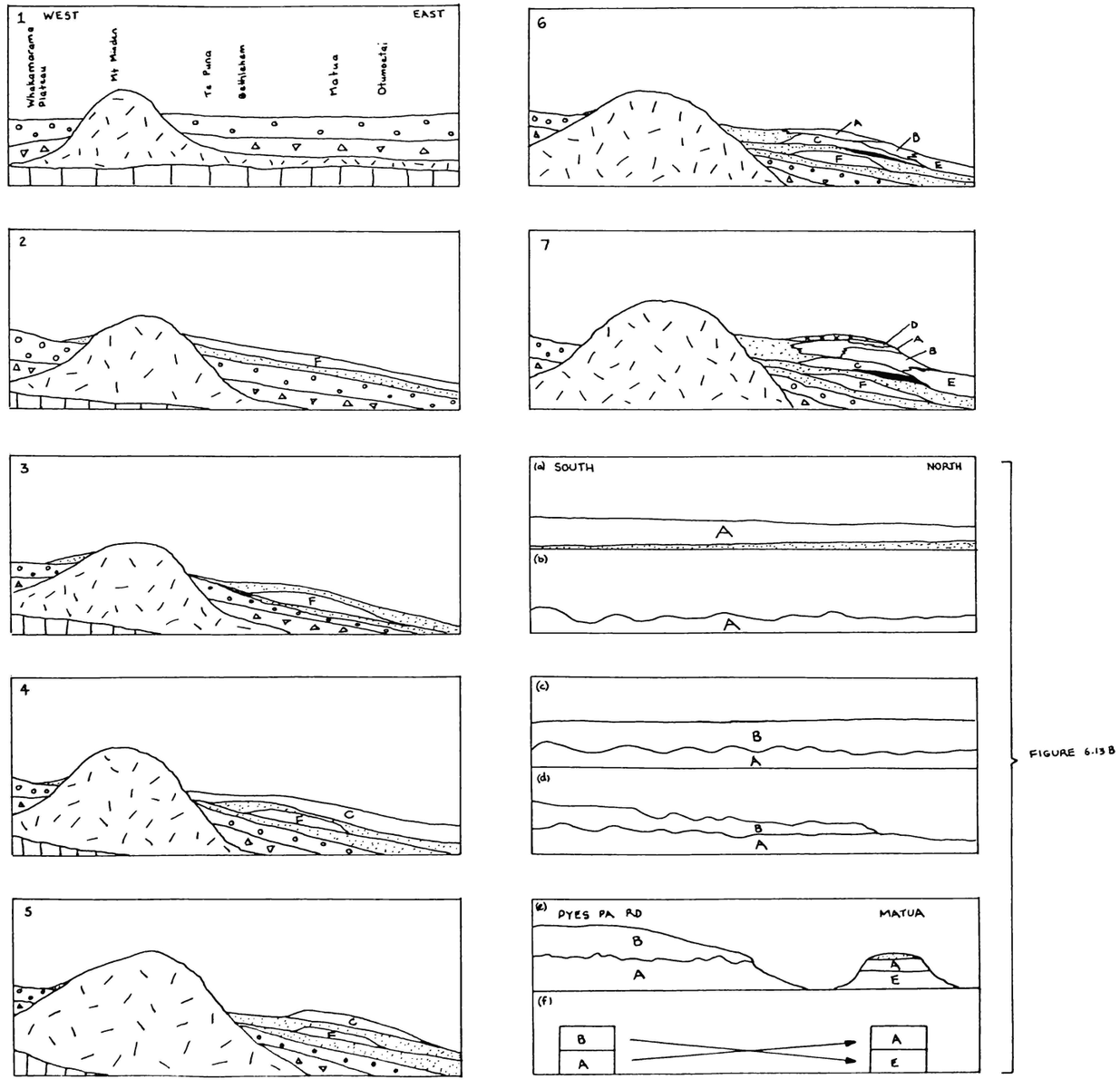
(b) Erosion of Te Ranga Ignimbrite.

(c) Emplacement of Waimakariri Ignimbrite over an eroded surface.

(d) Erosion of Waimakariri Ignimbrite.

(e) Removal of parts of the Waimakariri Ignimbrite. Renewed erosion and supply of sediment from the Te Ranga Ignimbrite.

(f) Petrofacies E is derived from several sources (e.g. Waimakariri, Te Puna and Wairoa Ignimbrites) but the greater proportion of sediment is derived from the Waimakariri Ignimbrite.



The freshness of minerals in a number of samples also suggests the renewed erosion effect on deposits previously buried by a thick sedimentary cover. The mineralogy of fluvial deposits partially reflects depositional processes. Because source rocks (i.e. ignimbrites) are largely nonwelded, erosion of the deposits was probably rapid (e.g. indicated by thick sequences of fluvial sediment and by a thickening of pyroclastic deposits away from the Basin) producing a high sediment input into the Basin and therefore high sedimentation rates during short intervals (e.g. sedimentary structures suggest this episodic nature). Minor contributions of both fluvial sediment and primary volcanic material have also been derived from the Kaimai Range and the remainder of the Mamaku and Whakamarama Plateaus.

The mineralogy of the upper Matua Subgroup deposits has been grouped into a number of major petrofacies which reflect the mineralogy of distal ignimbrites, fluvial deposits and reworked air-fall tephra deposits (Fig. 6.9). A large proportion ($\sim$ 60%) of this primary volcanic material has been reworked. Fluvial deposits contain a high proportion ($\sim$ 95%) of acid volcanic detritus and it is likely that most of the pyroclastic material subaerially exposed in the southern parts of the Basin but north of the Papamoa Hills originated from a Central Volcanic Region source. It is suggested however that Matua Subgroup deposits at depth ($\sim$ >30 m) may be of both a Coromandel and Central Volcanic Region source.

Clay mineral assemblages in the upper Matua Subgroup also indicate an acid volcanic source, with halloysite originating from older air-fall tephra deposits and allophane and halloysite from the younger Hamilton Ash beds.

TABLE 6.11 Main Ignimbrite source rock contributing sediment to different broad areas within the Tauranga Basin (based on subaerial exposure)

Grid Reference	Area	Ignimbrite source rock				
		Te Ranga	Waimakariri	Te Puna	Wairoa	Waitearikl
U14/745865	Whakamarama Plateau					*
	Katikati				*	*
U14/700952	Aongatete				*	*
	Sharp Rd				*	
U14/785915	Omokoroa			*		
U14/755915	Pahoia			*		*
U14/815860	Te Puna	*	*	*		
U14/845820	Cambridge Rd	*	*		*	
U14/825760	Belk Road	*	*			
U14/850770	Pyes Pa Road	*	*			
U14/855740	Joyce Road		*			
U14/783730	McClaren Falls		*			*
U14/793759	Ruahihi Ivy Bridge		*			*
U14/845850	Bethlehem	*	*		*	
U14/855885	Matua	*	*			
U14/875798	Waimapu Rd		*			
U14/862810	Greerton	*	*			
U14/905825	Maungatapu Plateau		*			
U14/906820	Welcome Bay		*			(Papamoa lg.)
U14/893853	Tauranga City	*	*			

CHAPTER SEVEN

SEDIMENTARY STRUCTURES, HYDRODYNAMICS AND PALEOENVIRONMENTS OF FLUVIAL DEPOSITS OF THE MATUA SUBGROUP

7.1 INTRODUCTION

Fluvial sedimentary deposits in the Tauranga Basin are either gravel-, sand-, or mud-dominated. Gravels form either clast-supported deposits or, more commonly, poorly sorted matrix-supported deposits. The three major lithologies can be further subdivided into a number of lithofacies, principally on the basis of relationships between sedimentary structures, sorting and texture. Lithofacies may be interpreted as reflecting certain major sedimentary controls exerted within the fluvial environment (Miall, 1977; 1978). In particular, it is often possible to interpret the hydrodynamic conditions responsible for lithofacies formation within the Basin. Origins can be established by inferring relationships between sediment properties such as sedimentary structures and hydrodynamic factors (Allen, 1965; Harms and Fahnestock, 1965; Picard and High, 1973; Miall, 1977).

7.2 SEDIMENTARY STRUCTURES OF FLUVIAL DEPOSITS

A variety of different sedimentary structures occur at various scales in the Tauranga Basin deposits (Table 7.1). Field exposures suggest there is a preponderance of horizontally bedded and low-angle cross-bedded strata.

Contributions are also made by high angle cross-stratified deposits which range from large scale, where set thickness is $\geq$ 5 cm, to less significant small-scale sets with a thickness $\leq$ 5 cm (Allen, 1965; Sherwood, 1972).

Deformation structures and post-depositional structures are recorded at sites exposed in cliffs and banks adjacent to the estuary.

TABLE 7.1

Fluvial structures in the Tauranga Basin deposits

Syndepositional

1. Planar - Stratification

   Lenticular

   Horizontal Parallel

   Horizontal Discontinuous

   Graded

2. Cross - Stratification

   Low Angle -

   Avalanche Front - (Alpha -)

   Rho -

   Nu -

Post-depositional

1. Deformation Structures

   Injection

   Slump

   Synsedimentary deformation

   Compactional

The approach taken in this chapter in which the intention is to develop a fluvial paleoenvironmental model for Tauranga Basin deposits, is shown in Fig. 7.1.

7.2.1 Planar Stratification

Four dominant forms of planar stratification are recognised (following Picard and High, 1973 terminology): Lenticular, horizontal parallel, horizontal discontinuous and graded (Fig. 7.2). Criteria used to identify each type are given in Tables 7.2 and 7.3

(a) Lenticular Stratification

This structure (Fig. 7.3) occurs in poorly sorted gravelly sands to sands. Because of the abundance of gravel-sized material in the structure, notably rhyolite and pumice clasts (up to 3 cm diameter), stratification within sets is generally obscure. Individual sets are large scale, commonly with a thickness of 5 - 20 cm, and persist laterally for several metres before pinching out. Stratification thickness and type is variable, and horizontal and low-angle cross-lamination are dominant. These structures are associated with internal trough cross-bedding and avalanche front cross-stratification. Lenticular stratification usually overlies low-angle cross-bedded sands which are moderately to well sorted. The deposits are generally weathered and as a result contain a relatively high percentage of mud ($\sim$ 10%) compared to other units in the Matua and Te Puna sections.

(i) Hydrodynamic Interpretation

This type of structure is formed by shifting sedimentary regimes (Picard and High, 1973; Miall, 1978) resulting in a composite set of strata which does not share the internal consistency of a sedimentary unit.

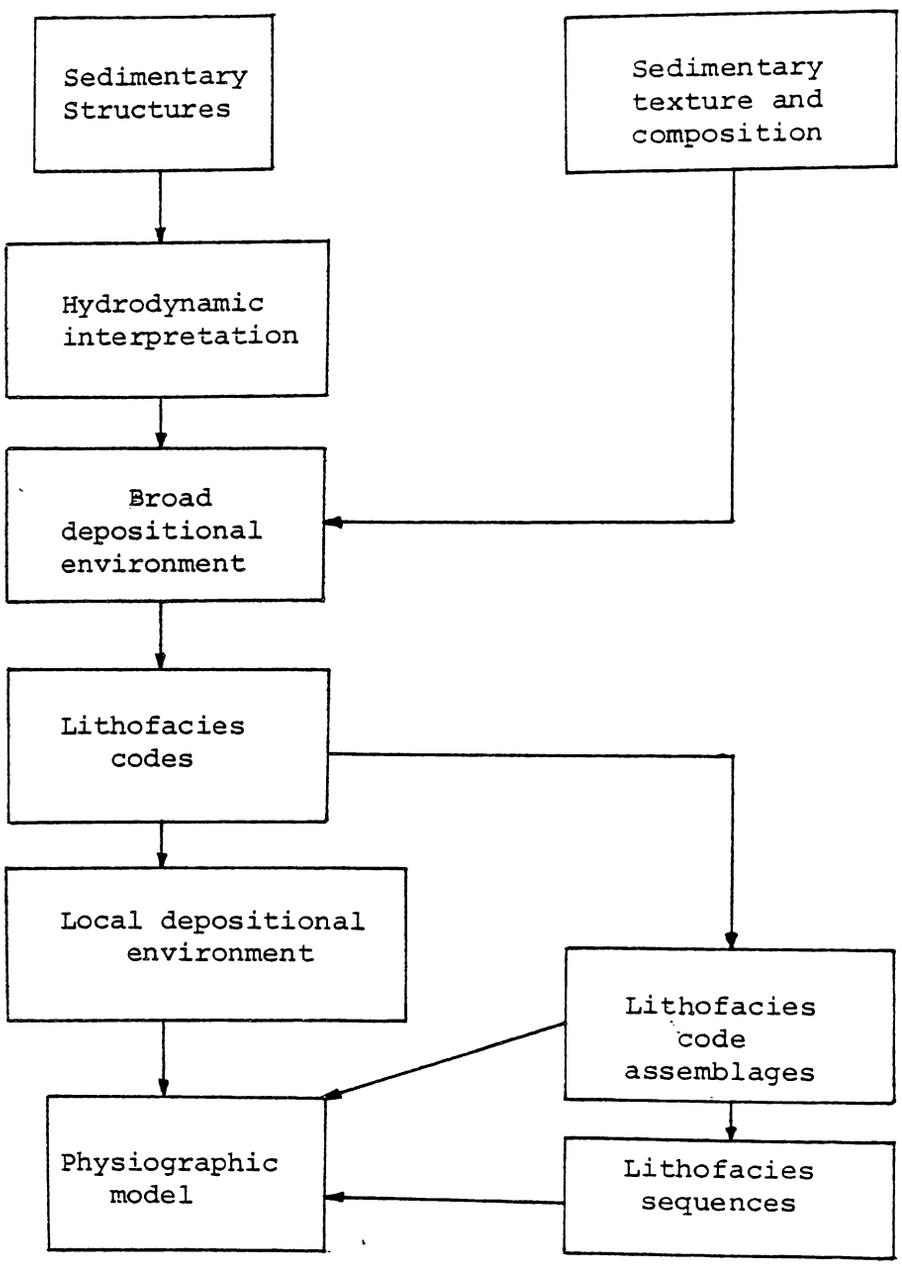


Fig. 7.1 Summary of the approach taken in this chapter to develop a paleoenvironmental model.

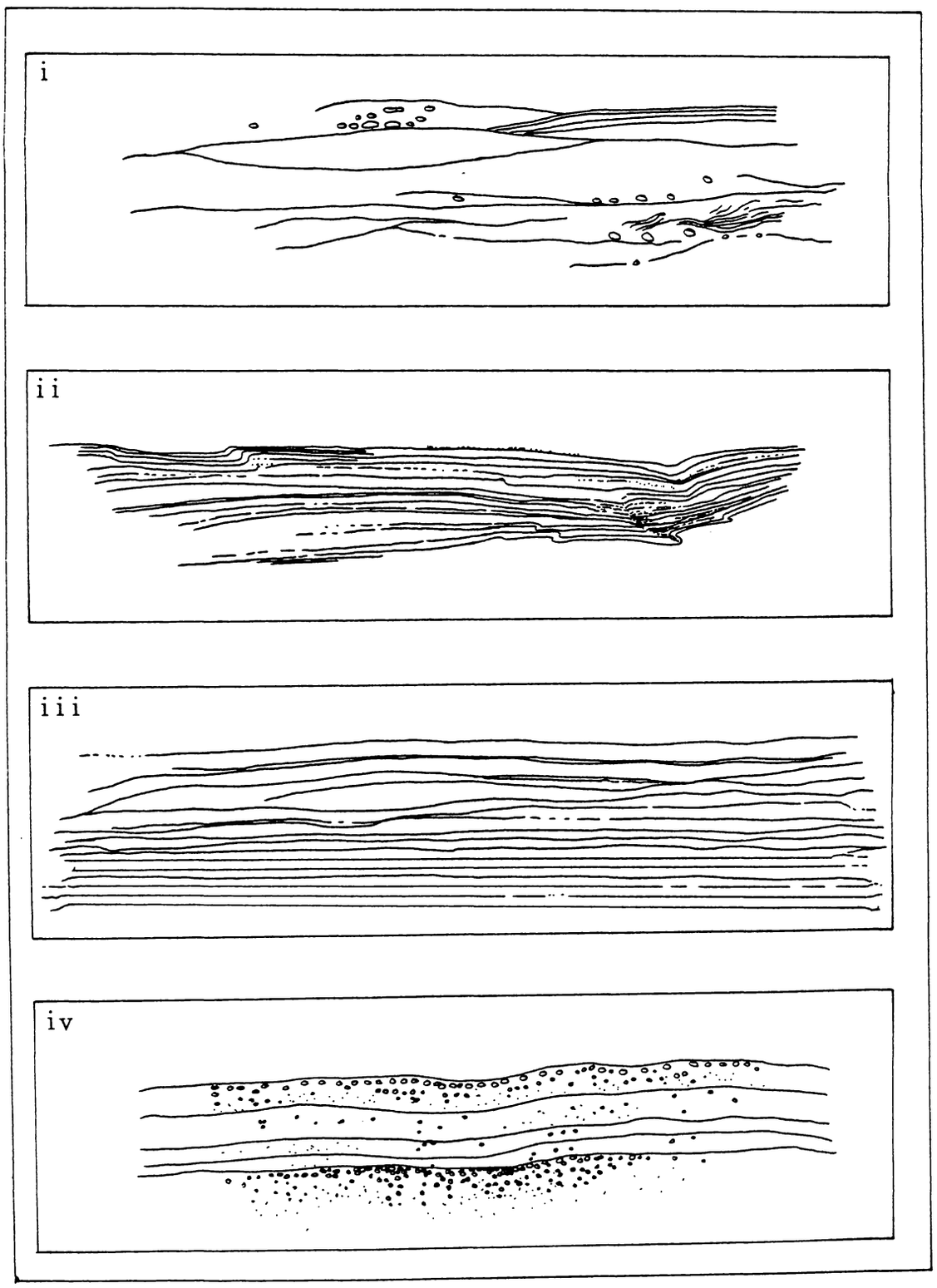


Fig. 7.2 Planar stratification types. (i) lenticular; (ii) horizontal parallel; (iii) horizontal discontinuous; (iv) graded; (from Picard and High, 1973).

TABLE 7.2 Planar stratification types in the Tauranga Basin

Criteria for recognition	Planar Stratification			
	lenticular	horizontal parallel	horizontal discontinuous	graded
Occurrence	Common	Common	Common	Common
Grading	normal	inverse and normal	inverse and normal	inverse and normal
Set thickness	>20 cm	>20 cm	>20 cm	>5 cm
Scale	large	large	large	large
Stratification	obscure	sharp	sharp	sharp and obscure
Shape of lower bounding surface	planar and low angle cross lamination	planar	planar and low angle cross lamination	planar
Angle of upper bounding surface	low <15°	low <10°	low <15°	low <5°
Texture	slightly gravelly to gravelly sands	sands to gravelly sands	sands to gravelly sands	sands to gravelly sands
Compositional character of upper part of set	(a) poorly sorted sands and gravelly sands (b) rhyolite clasts (c) pumiceous	(a) intermittent well sorted beds with poorly sorted beds (b) pumice - glass shard	(a) pumiceous bands of sand and gravelly sands (b) glass shards	(a) pumiceous bands of sand and gravelly sands (b) glass shards
Compositional character of lower part of set	(a) pumiceous - glass shards - rock fragments (b) heavy minerals	(a) pumiceous - glass shards - rock fragments	(a) pumiceous glass shards	(a) pumiceous glass shards

TABLE 7.3 Planar stratification types. Classification on the basis of types described by Picard and High (1973)

Type / Criteria	lenticular	horizontal parallel	horizontal discontinuous	graded
Magnitude	large scale	large scale	large scale	medium and large scale
Character of lower boundary surface	gradational	gradational and erosional	gradational	gradational and erosional
Shape of lower boundary surface	planar and low angle	planar	planar and low angle	planar
Relations of planar strata to lower boundary surface	concordant	discordant	discordant and concordant	discordant and concordant
Lithology	heterogeneous	heterogeneous	heterogeneous	heterogeneous and homogeneous
Grouping of sets	grouped	grouped	grouped	grouped and individual

Fig. 7.3 Lenticular stratification in pumice and rhyolite fragment rich, poorly sorted sandy gravels (Petrofacies D).

Fig. 7.4 Horizontal parallel stratification showing parting lineation in pumice clast and glass shard rich moderately sorted sands and slightly gravelly sands (Petrofacies A).





A steady and progressive change in conditions within a single regime therefore is not recorded and preservation may indicate several subenvironments. Lenses of material are developed under the fluctuating flow regimes (McKee *et al.*, 1967; Picard and High, 1973) with deposition of sediment being horizontally discontinuous. Horizontal beds with grains aligned parallel to the current are produced (Doeglas, 1962; Harms and Fahnestock, 1965; Picard and High, 1973) as upper flow regime conditions are reached and bedforms assume a more planar surface. This type of stratification may record a vertical sequence of bar-channel-bar.

(b) Horizontal Parallel Stratification

Horizontal parallel stratification (Fig. 7.4) is associated with parting lineation. The stratification is small scale and thin even strata are 0.2 - 2 cm thick in horizontal sets 10 - 20 cm thick. Texturally it occurs in moderately to well sorted sands, and slightly gravelly sands. Each stratum is very fine and parallel with others in the set, and individual strata are laterally continuous for distances exceeding 30 cm. Composition is mainly glass shard-pumice-rock fragment.

(i) Hydrodynamic Interpretation

This type of bedding is found underlying lenticularly stratified sets (Picard and High, 1973) and overlying cross-bedded sets. The sequence of bedding types seen particularly at Kings Avenue and at Te Puna indicates that it is associated with low velocity currents (McKee *et al.*; Picard and High, 1973) but the exact regime is uncertain. The beds possibly represent deposits of bars (as shown by modern examples e.g. studies in the United States by McKee *et al.*, 1967 and Picard and High, 1973) and the downstream segments of channels

(Picard and High, 1973) and therefore may be indicative of shallowing in a fluvial or marine environment. This could be due to elevation of the bar or channel bottom as a flood waned.

(c) Horizontal Discontinuous Stratification (Fig. 7.5)

(Doeglas, 1962; Harms and Fahnestock, 1965; McKee *et al.*, 1967; Picard and High, 1973).

Stratal thickness is up to 10 cm greater than in horizontal parallel stratification. Sets are large scale with a thickness from 30 - 80 cm. Texturally the deposits are moderately sorted to poorly sorted, slightly gravelly and gravelly sands. Individual strata are laterally discontinuous over several metres, but form planar bedding and are associated with streaming lineation. Microlensing (6 - 10 cm) is common. These deposits often underlie cross-stratified and microcross-stratified structures and overlie cross-stratified normally graded and inversely graded structures. Composition is mainly glass shard-pumice-feldspar-quartz-heavy mineral sands. Deposits may contain individual laminae usually alternating between (a) pumice-glass shard and (b) heavy mineral-glass shard-feldspar-quartz sand.

Characteristic features of these deposits are that sets are multiply repeated to give very thick sedimentation units and inverse grading is very common. Four main types of horizontal discontinuous stratification are recognised in the Tauranga Basin deposits:

1. Type 1 - This is recorded in inversely graded, 5 - 30 cm thick sets occurring in the Kings Avenue section. The base of each set is marked by glass shard-pumice-feldspar-quartz-heavy mineral sands which pass upwards through pumice sands to matrix-supported pumice clasts (2 - 8 mm size), but some sets may show a layer which is clast-supported. Upper boundaries of sets may contain a higher mud content,



Fig. 7.5 Horizonal discontinuous stratification in pumice clast and glass shard rich moderately to poorly sorted, slightly gravelly sands.



Fig. 7.6 Graded stratification showing inversely graded pumice rich, moderately sorted slightly gravelly sands (Petrofacies E). Lens cap is 5 cm diameter.

and weathering can pick out mud laminae. Upper and lower boundaries of sets can be erosional. Clasts at the top of sets vary in form from rounded to subangular to flattened, while at the base, pumice is fragmented and angular.

2. Type 2 - Sets are 5 - 20 cm thick, commonly inversely graded and consist of individual laminae alternating between pumice-glass shard-feldspar-quartz sands and glass shard-pumice-heavy mineral sands. An erosional contact at the upper boundary is formed with overlying cross-stratified sets at Kings Avenue.

3. Type 3 - Horizontal strata which show normal grading occur at Bethlehem and Matua. Composition and texture are similar to Type 1 deposits.

4. Type 4 - Horizontal stratification recorded in 2 - 20 cm thick sets, which are commonly stacked, show a greater range of grain sizes than in Type 2 deposits.

Individual strata pinch out over several metres in pumice-glass shard-heavy mineral moderately sorted sands and gravelly sands. These individual layers often form laminations which grade into low-angle cross-stratified laminae. Upper and lower boundaries are non-erosional, except where horizontal strata overlie trough cross-stratified sets. The Type 4 structure overlies trough cross-bedding and low-angle cross-stratification in several coastal exposures. Inverse grading is a characteristic feature in individual sets.

(i) Hydrodynmaic Interpretation

Horizontal discontinuous stratification (Doeglas, 1962; McKee *et al.*, 1967; Picard and High, 1973) is typically formed in the lower part of the upper flow regime (Allen, 1965; Harms and Fahnestock, 1965;

Picard and High, 1973) when high velocity currents are just over the threshold of the lower flow regime. Usually it is the lowest sequence in most channel deposits (McKee *et al.*, 1967; Picard and High, 1973) resting on an erosional surface.

This structure occurred beneath trough cross-stratified deposits and above low-angle cross-stratified deposits at several sites in the Tauranga Basin. Horizontal discontinuous stratification is interpreted as being present in most channel deposits because of its position in vertical sequences in the Tauranga Basin and as described from examples of McKee *et al.* (1967) and Picard and High (1973).

(d) Graded Stratification

Graded stratification (Fig. 7.6); (Picard and High, 1973; Miall, 1978) can be divided into two types:

(i) normal, where grain-size fines upwards

(ii) inverse, where grain-size coarsens upwards.

Most deposits in the Tauranga Basin show the latter with grain-sizes ranging from silts and fine sands to coarse sand and gravels at the top of a single stratum or set. This type of stratification may form cosets (> 20 cm thick) or individual sets 2 - 40 cm thick and usually occurs within horizontally stratified deposits. Sets are composed of pumice-glass shard sand and silt at the base grading upwards into pumiceous gravelly sands.

(i) Hydrodynamic Interpretation

These structures are often associated with horizontal stratification and trough cross-stratified sets which may underlie or overlie these sets. They occur in channel and bar sequences (McKee *et al.*, 1967; Picard and High, 1973; Miall, 1977, 1978) and may form either during decreasing velocities due to pumiceous clasts continually being

worked to the surface during development of individual beds (Fiske, 1969) or during backfilling as the velocity slackens (Picard and High, 1973).

7.2.2 Cross-Stratification

(a) Low-Angle Cross-Stratification

Distinctive and volumetrically important in the Tauranga Basin, these structures (Fig. 7.7) form thick sets (5 cm - 50 cm thick) having wavelengths of several metres. Boundaries are usually non-erosional except where these beds overlie trough cross-stratified sets where they develop a more planar surface. Sets are often repeated vertically but amplitudes are out of phase. Individual strata may be concave and often as they approach the lower boundary they either become concordant with underlying strata or they pinch out and intersect them at a very low ($\sim$ 1 - 3^{o}) angle. Maximum dips (maximum dips of only 7^{o} were recorded at Matua and Te Puna) in this type of strata are assumed to be downcurrent indicating the flow direction (Allen, 1965; Picard and High, 1973).

(i) Hydrodynamic Interpretation

Low-angle cross-stratification develops in moderately to well sorted sand-sized material and forms under low flow regime conditions which are appraoching an upper flow regime (McKee *et al.*, 1967; Picard and High, 1973). The lateral continuity of thin strata, low angles of inclination and predominant finer grain sizes compared to grain-sizes in other sedimentary structures indicate a down-current migration of point and longitudinal bars, creating their own depositional surface.

Deposition occurs during the receding period of a flood but while the bar is still flooded. The depth of water is indicated by the lack of ripple stratification. As the velocity decreases trough cross-

Fig. 7.7 Low angle cross-stratification underlying trough cross-stratification at Te Puna (U14/819888).

Fig. 7.8 Avalanche front cross-stratification in pumice clast and rhyolite rock fragment rich, well sorted, slightly gravelly sands to sandy gravels (Petrofacies D). Imbricated pebbles have been sorted and have avalanches down the foreset slope.





stratification, microcross-stratification and alpha cross-strata may be formed (Allen, 1965; McKee *et al.*, 1967; Picard and High, 1973; Miall, 1977, 1978). Often this type of structure grades laterally into horizontal discontinuous strata in channels and inclined strata may be found in the more energetic margins of flow.

(b) Avalanche Front Cross-Stratification (Alpha -)

Avalanche front cross-stratification (Fig. 7.8) (Allen, 1965; Picard and High, 1973) is commonly associated with lenticular stratification and this is the case in the Tauranga Basin. A typical suite may show development from the base of horizontally stratified sets: Avalanche front cross-stratification/ Rho and Nu cross-stratification/ horizontal stratification. Texturally the deposits are poorly to moderately sorted gravelly sands composed of rhyolitic and pumiceous gravels alternating with heavy mineral-glass shard sands and glass shard-pumice-quartz sands. Single thick tabular sets (5 - 15 cm thick) and strata (1 - 2 cm thick) are generally straight. These are inclined down current at angles between 35 - 45°. The lower surface is planar and coarsest grains (up to 1 cm in diameter) tend to be concentrated at the base. Grains may be imbricated at the top of sets (Fig. 7.8).

(i) Hydrodynamic Interpretation

Avalanche front cross stratification (Fig. 7.8) is associated with low-angle cross-stratification, lenticular stratification and small-scale trough cross-beds (i.e. ∿ 10 cm thick Rho-, and Nu-types). It formed by the downcurrent migration of avalanche faces (Figs. 7.9, 7.10) at the margins of bar surfaces. Imbricated pebbles and granules indicate that material was transported by traction across the surface of the bar in water at least 5 cm deep in upper flow

Fig. 7.9 Avalanche cross-stratification formed by migrating sand-waves (after Harms *et al.*, 1975).

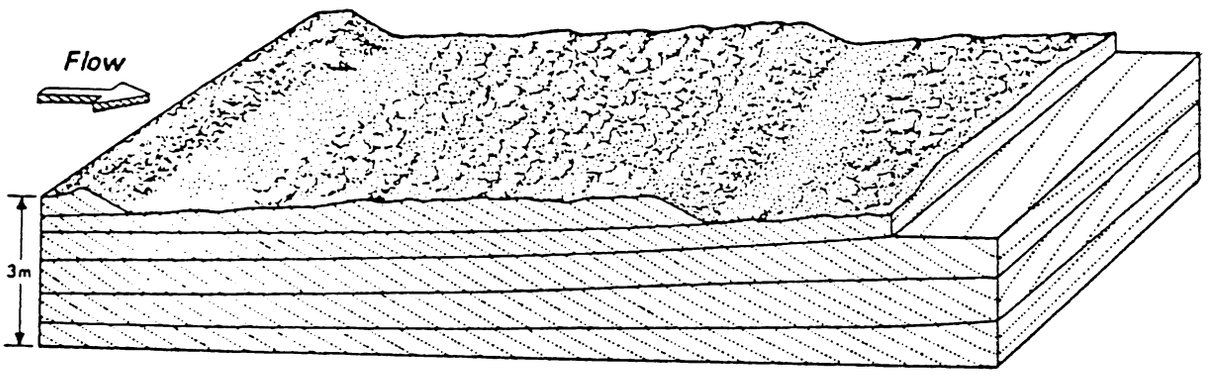
Fig. 7.10 Infill of a trough by aggradation to a profile of equilibrium under uniform conditions of flow and transport. The axis of the trough is taken to be at right-angles to the plane of the basal contact changes with variation in the depth-ratio. The sub-horizontal beds in the closing stages of infill are typical of a high depth-ratio (after Jopling, 1965).

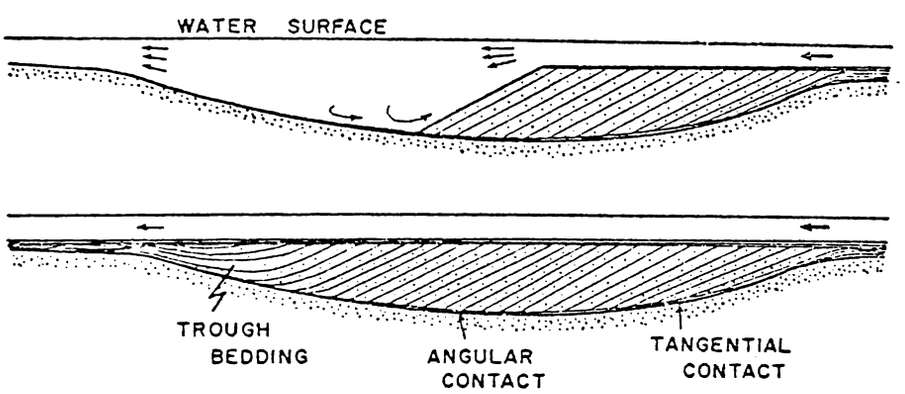
Fig. 7.11 Origin of coarse and fine foreset laminae by continuous avalanching.

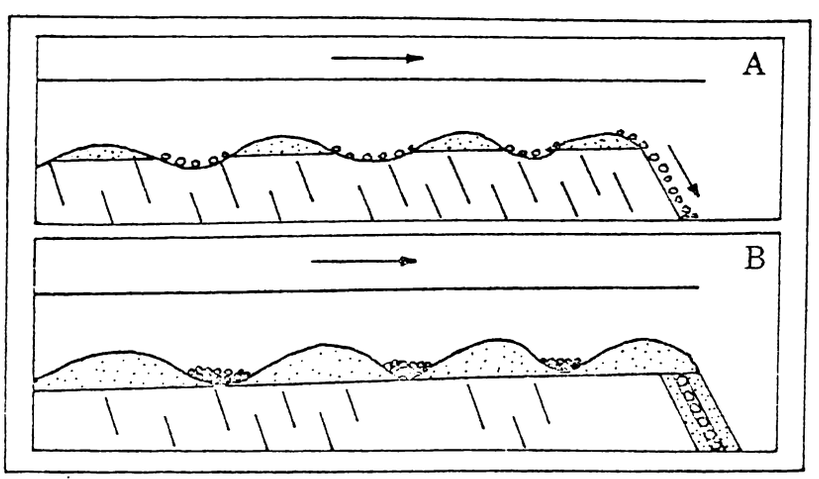
A - finer sediment composing the small scale asymmetrical bed form spills over the bar edge followed by B.

B - avalanching of heavy minerals and coarse clasts previously segregated into leeside scour pockets. Thickness of laminae depends on length of foreset and size of surface bedforms.

(From Smith, 1972)


Flow
3m


WATER SURFACE
TROUGH BEDDING
ANGULAR CONTACT
TANGENTIAL CONTACT


A
B

regime currents (Jopling, 1964; Allen, 1965; Picard and High, 1973). The finer matrix moved by saltation (Jopling 1964; Smith, 1970; Picard and High, 1973) and as flow velocities and the depth decreased over the bar a progression of bedforms was produced dominated by trough cross-stratification and planar cross- stratification. The sediment is crudely sorted and avalanche faces result from sediment slumping into quieter waters (Picard and High, 1973) on the lee face of the migrating bar, with coarser material being deposited over the slope break followed by the spilling over of finer grain sizes. Jopling (1964) found that if the load of suspended sediment is high, sorting of foreset laminae may result from differential settling velocities when this material is carried over the slip face (Fig. 7.11). This mechanism would be important during high flows because of the original poor sorting of sediment.

The function of depth is related to its ability to reduce current strengths in the lee side current shadows in water ≥60 cm deep (Picard and High, 1973). This condition is indicated by the high angle (30 - 40°) of repose and the resulting straight tabular sets, inclined down-current. The thickness of these sets is determined by the height of the foreset and the size of the parent bedform. As a flood wanes these fronts are deactivated suddenly and bedforms typical of decreasing current velocities result from scouring and degradation of the slip faces, producing angles less than the angle of repose, and the shallower depths cause incomplete separation of the currents around the bars (Smith, 1970; Picard and High, 1973). Jopling (1965) and Smith (1972) noted that this foreset angle decreases also when flow strength increases with increasing depth and this instability at the upper slip face is due to a zone of flow detachment.

(c) Rho-Cross-Stratification

Rho-cross-stratification (Fig. 7.7 and Figs 7.12 - 7.14) occurs in association with low angle cross-stratification and horizontally bedded deposits and shows discordant contacts with upper and lower bounding surfaces. Set contacts are scoop-shaped in sections perpendicular to the flow direction while coset contacts are more horizontal.

It is preserved mainly in gravelly and slightly gravelly sands but occurs occasionally in sands. Sets are usually large scale (5 - 50 cm thick), inversely graded and grouped, so that cosets range in thickness from 1 - 3 m. Occasionally cosets reach a thickness of 5 m, while set width and height ranged from 0.32 - 1.46 m and 0.24 - 0.90 m respectively. This type of structure (Fig. 7.13) may extend laterally for tens of metres in areas proximal to pyroclastic flow deposits, but is more confined in areas nearer the coast.

Contacts are marked by coarse material of the underlying set and finer material of the overlying set.

At a number of localities set contacts are enhanced by a mud film (2 - 5 mm thick) continuous for 40 - 60 cm (Fig. 7.16).

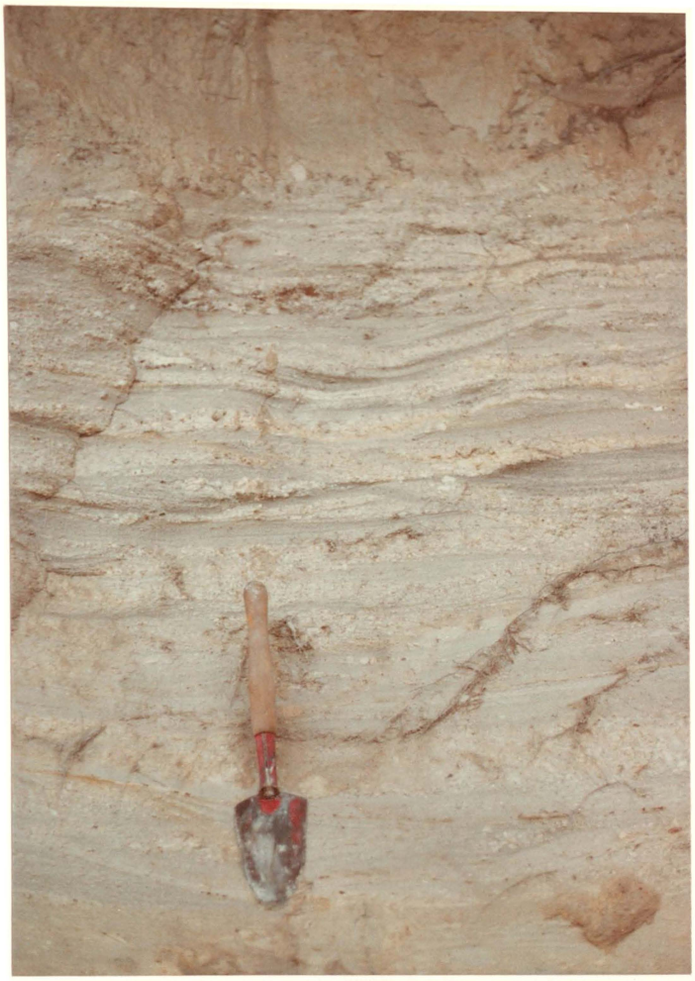
Four characteristic types of Rho cross-stratification are recognised in the Tauranga Basin (Table 7.4). All are composed of pumice-glass shard-feldspar-quartz-heavy minerals with variable amounts of rock fragments. Depending on location, rock fragment composition is dominantly rhyolite, fragmental obsidian and/or ignimbrite.

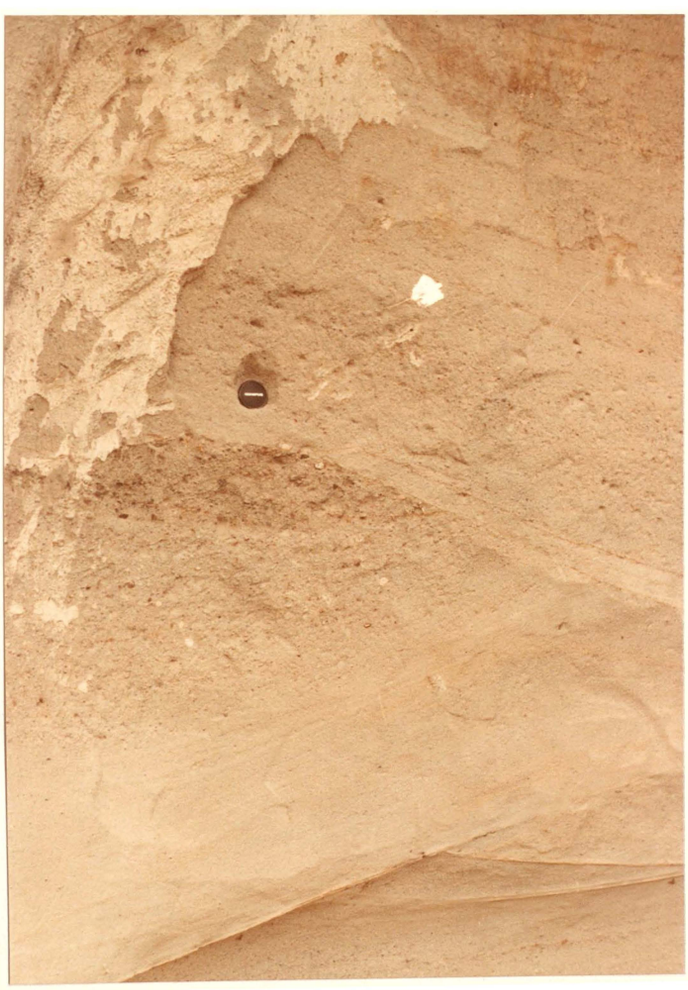
(d) Nu Cross-Stratification

Nu cross-stratification (Table 7.5 and 7.6) was only a minor structure in the map area, occurring in conjunction with Rho cross-

Fig. 7.12 Rho- cross-stratification in moderately sorted pumice rich sediments (Petrofacies E).

Fig. 7.13 Large scale trough cross-beds in pumice rich moderately sorted slightly gravelly sands, exposed at the Pyes Pa Road quarry (U14/845768). Lens cap is 5 cm diameter.





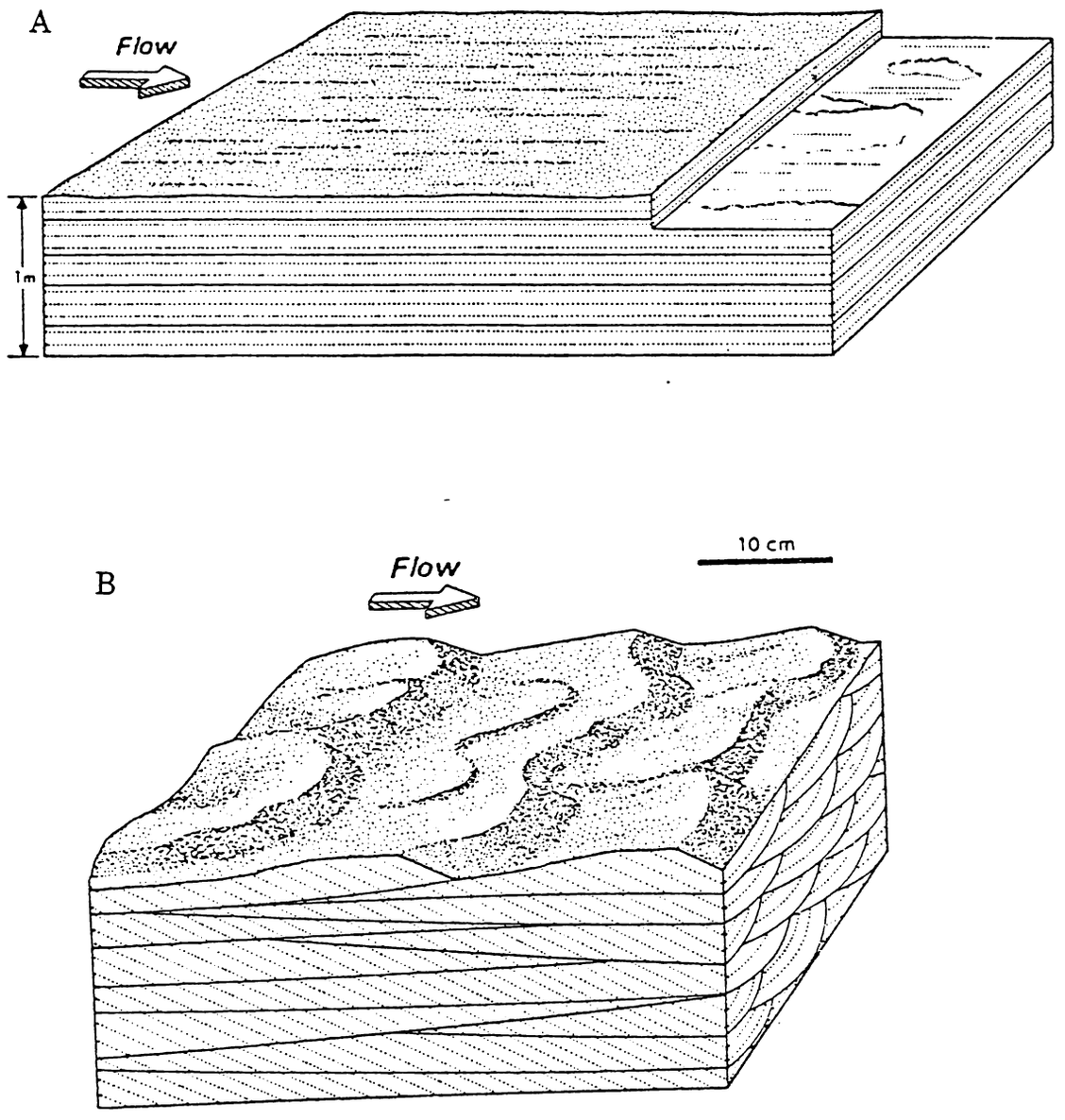


Fig. 7.14 Block diagrams of Planar and Rho-stratification types (from Harms *et al.*, 1975).

A - Horizontal stratification produced by upper flat bed (or plane bed) with current lineation. Internal surfaces show parting lineation.

B - Current ripples on sand, near equilibrium, forming trough cross-stratification, Rho - and/or Nu - types.

TABLE 7.4

Criteria for recognition	Rho Cross-Stratification Type			
	1	2	3	4
Occurrence	abundant	common	common	rare
Grading	inverse	inverse >> normal	normal	normal
Set thickness	(a) >20 cm (b) >10 cm	>20 cm	5 - 10 cm	5 - 10 cm
Scale	large	large - medium	large - small	large - small
Shape of lower bounding surface	scooped	scooped - inclined	scooped	scooped
Angle of upper bounding surface	high >15^{o}	5 - 15^{o}	>15^{o}	10 - 20^{o}
Texture	gravelly sands	gravelly sands	slightly gravelly sands - silts	gravelly sands - sands
Compositional character of upper part of set	(a) mud film may be present (b) clast-matrix supported (c) pumiceous	(a) clast-matrix supported (b) pumiceous or vice versa with lower part	(a) mod. sorted matrix (b) silt (c) glass shard - pumice sand	(a) gravelly sands - sands (b) diffuse (c) mod. sorted sands
Compositional character of lower part of set	pumiceous	pumiceous	pumiceous	heavy minerals
Character of lower bounding surface	erosional	erosional	erosional	erosional
Compositional grading within sets	Top - pumice - glass shard Vs pumice - glass shard - quartz - feldspar - heavy minerals Base - minor rock fragments	Top or Base - pumice pumice - glass shard pumice - glass shard - rock fragments - quartz - feldspar - heavy minerals	Top - pumice - glass shard Base - quartz - feldspar - heavy minerals - rock fragments	Base - well sorted heavy mineral layers 1 - 4 mm thick - diffuse upper surface - sharp lower surface Top - heavy minerals - glass shard - quartz - feldspar

TABLE 7.5 Criteria used to define Rho- and Nu- cross-stratification types on the basis of Allen's (1963) and Hume *et al.* (1975) descriptive criteria.

Type / Criteria	1	2
Classification	Rho	Nu
Magnitude	medium and large scale	small scale
Grouping of sets	grouped	grouped
Character of lower boundary surface	erosional	erosional
Shape of lower boundary surface	scoop-shaped	scoop-shaped
Relation of cross-strata to lower boundary surface	discordant	discordant
Lithology of cross-strata	heterogenous	heterogenous to homogeneous

TABLE 7.6 Two main types of Nu cross-stratification are recognised in the map area.

Type	1	2
Composition	Lag deposits (a) concentrations of heavy minerals (b) thin laminations (1 - 5 mm) (c) composition grades upward into pumice - rock fragment - glass shard sands (d) iron and manganese staining	Pumice rich (a) pumice-glass shard-rock fragments-quartz-feldspar-heavy minerals
Texture	(a) mud content 5-30% (b) laminations of gravel and coarse sand	(a) mud content indurates deposit 10-40% (b) gradational textural change over 1 - 2 cm in sands and slightly gravelly sands (c) cross-laminated

stratification and horizontal stratification. It is characteristically small scale and does not develop into cosets > 10 cm thick, although it may develop within units containing larger scale trough cross-stratification and the remains of ripple cross-laminated deposits. In transverse section sets are trough-shaped (with dips ranging from 8° - 30°) and strata within a set are concave upward and conform to a lower erosional surface. In longitudinal section sets become more wedged shaped and inclined downstream, whilst lower boundaries of cosets are terminated by planar surfaces (1 - 5° dip). The lower boundary of sets and cosets is commonly marked by concentrations of heavy minerals (1 - 4 mm thick) and individual strata are thin (1 - 5 mm). Commonly associated also with this boundary are gravel to coarse sand lag deposits, and iron and manganese staining. Usually the upper boundary of sets is more diffuse. Texturally the deposits range from moderately sorted gravelly sands to well sorted sands and where deposits are weathered, sizes grade down into muds.

(i) Hydrodynamic Interpretation of Rho- and Nu-types

Trough cross-stratification is produced by migrating trains of asymmetrical ripples and dunes (Harms and Fahnestock, 1965).

Cosets of cross-strata indicate unidirectional flow, and the thickness of trough shaped sets is affected by the minimum average flow depth (Allen, 1963, 1965). This minimum depth is usually twice that of the thickness of individual sets. Distinctive types of cross-bedding are usually a result of ripple size and geometry, current velocity and sediment supply (Allen, 1963). The cosets of cross-strata indicate that erosional and depositional processes have operated, the former accounting for the surfaces between sets and the latter for the growth of sets and shapes and attitudes of cross-strata (Allen, 1963; Hume *et al.*, 1975).

(i) Rho cross-stratification is formed by moderate velocity currents in the lower flow regime but flow conditions may range into the lower part of the upper regime (McGowen and Garner, 1970). It pertains to migrating lunate and possibly linguoid asymmetrical dune bedforms in which higher current velocities are more persistent than current velocities in which smaller-scale trough cross-stratification forms (Williams, 1968). Williams and Rust (1969) have also suggested formation by the downcurrent migration and interference of avalanche faces at the lobate margins of bars.

(ii) Nu cross-stratification develops in association with the migration of trains of linguoid small scale asymmetrical ripples in the lower part of the lower flow regime (Allen, 1963; Harms and Fahnestock, 1965).

7.2.3 Deformation Structures

The following types are recognised:

(D1) Injection structures

(D2) Slump features

(D3) Synsedimentary deformation

(D4) Compactional faulting

Type (D1)

(a) On Motuhoa Island, sand overlying a chalazoidite bed has moved downward into a mud layer to form ball and pillow sand intrusion. Injection has accompanied deformation of the surrounding strata (Fig. 7.15) and this is shown by severe deformation of chalazoidites causing discontinuity of their skins and flattening them into elliptical and thin tubular lense shapes at the base of the bed.



Fig. 7.15 Chalazoidite bed on Motuhoa Island intruded by sand. Accretionary lapilli in the bed are flattened and deformed near the base.



Fig. 7.16 Compactional faulting in Rho- cross-stratified slightly gravelly sands (Petrofacies A).

(b) Exposures adjacent to the estuary, near Omokoroa Point, Motuhoa Island, Bethlehem and Te Ranga, show examples of injection of coarse pumiceous sediment into finer grained fluvial sediment. This may result from small scale deformation within sets of strata of granule and sand size or may occur on a larger scale (metres) effectively concentrating coarse pumice clasts up to cobble size (e.g. sometimes cutting through sets of strata). It usually involves an upward or lateral injection of material into overlying deposits and may reactivate and rework previously laid sediments.

Type (D2)

Slump features are post-depositional disturbances. Often the attitude of the strata is altered while stratification is left intact. On Motuhoa Island the strata, though disturbed, are unbroken and convoluted into a recumbent isoclinal fold (Fig. 8.11). The amplitude of the fold is 10 - 15 cm.

Type (D3)

Synsedimentary deformation (Fig. 4.9) is contemporaneous with sediment deposition. On Motuhoa Island normal faults within fluvial strata have disrupted the sedimentary beds. The collapse and movement apart of the hanging wall has created spaces adjacent to the faults. These openings have been intruded downwards by coarse material (gravel and coarse sand) and sand during infilling of the overlying fluvial sediment.

Type (D4) Compactional faulting

Post-depositional structures occur in sediments derived from the Te Ranga Ignimbrite in the Pyes Pa Road area (Fig. 7.16). The faults (some continue vertically for ∿1 m and laterally for several

metres) cut vertically and obliquely through cross-trough stratified and planar-stratified beds and are enhanced by a mud vein resulting from post-depositional weathering. Several beds have been offset by up to ∿4cm.

7.3 BROAD DEPOSITIONAL ENVIRONMENT

Detailed evidence presented by Doeglas (1962), Allen (1965), McKee *et al.* (1967), Williams and Rust (1969), Picard and High (1973), Hume *et al.* (1975), and Miall (1977, 1978) would suggest that the upper Matua Subgroup exposed at Te Puna, Matua, Maungatapu, Greerton and Pyes Pa Road, depicts a dominantly braided river environment which exhibits sedimentary structures intimately associated with ephemeral conditions. Several criteria collectively serve to establish this braided origin : 1. predominance of gravelly and coarse sandy lithologies; 2. planar stratification; 3. poor sorting of sediments; 4. the presence of abundant medium - and large-scale trough cross-stratification; 5. sedimentary structures which indicate bar formation and shifting depositional centres; 6. many bedforms imply shallow water depths; 7. the description of sedimentary suites comparable with those from other modern braided river systems; 8. the absence of fining-upward cycles (e.g. in cross-strata); 9. variation in paleocurrent directions (Fig. 7.17); 10, the aerial distribution and thickness of the sediments; 11. the consistency of grain size statistic plots with those from modern braided river systems; 12. the mineralogically immature character of the deposits.

7.4 LITHOFACIES

Miall (1977, 1978) devised a letter code for facies nomenclature from braided river environments. It is these codes which are adapted

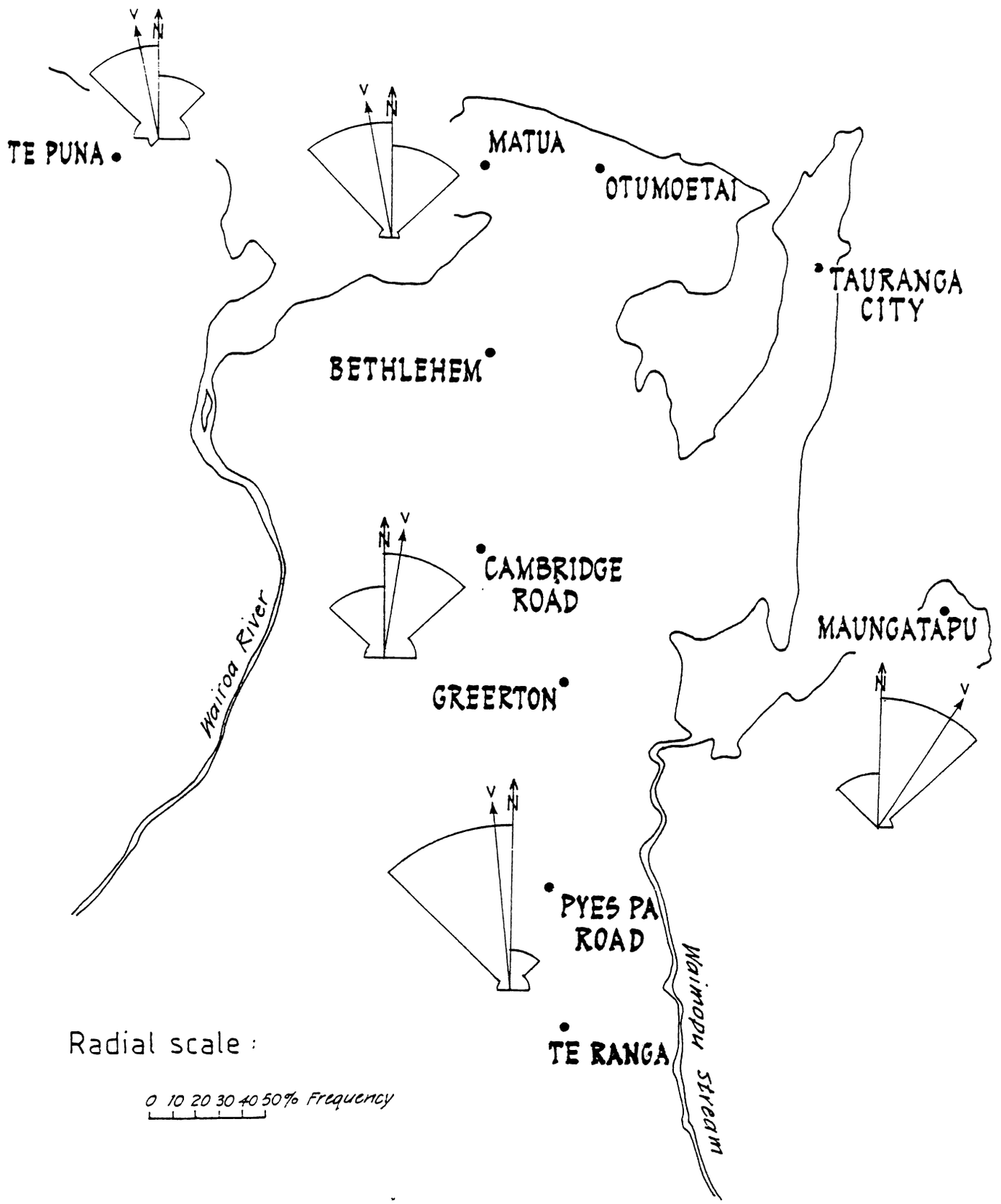


Fig. 7.17 Map showing paleocurrent data of the dip direction of cross-beds at 45° class intervals, at various localities studied in the southeastern part of the Tauranga Basin.

for use in interpreting lithofacies and developing a model for the upper Matua Subgroup fluvial sediments (Table 7.7).

The Sedimentary Structures discussed earlier are subdivided (e.g. St and Gt facies) or collectively grouped (e.g. Sh facies) into lithofacies which emphasize lithology and sedimentary characteristics that uniquely indicate the conditions of its deposition. A number of lithofacies are recorded in the upper Matua Subgroup. These lithofacies are typical of several subenvironments and can be defined in terms of local processes operating during deposition. The following processes act as a guide to interpretation of the local depositional environment as a whole:

(1) Bedform generation and migration (e.g. by asymmetrical ripples and dunes, etc.)

(2) Channel scour and fill.

(3) Low-water accretion and modification processes.

(4) Sedimentation in overbank areas.

1. Bedform generation and migration

(Facies Sh, Sp, St, Gt, Gp)

Documentation from modern rivers indicates that a wide variety of bedforms can be formed on non-cohesive sand beds, depending on grain size, flow depth and velocity, and rate of sediment supply (Miall, 1977).

During flood stage, active bedforms of a variety of scales can be superimposed on each other. Many of the sedimentary sequences in the upper Matua Subgroup result from continuous deposition involving successions of individual floods where one or more sets of strata are deposited continuously. Flow, however, may be episodic and under

TABLE 7.7 Lithofacies of the upper Matua Subgroup

Physiographic model facies code	Facies code after (Miall, 1978)	Lithofacies	Sedimentary structures	Interpretation
A2, A1	Gt	gravel, stratified	trough crossbeds	minor channel fills
B2	Gp	gravel, stratified	planar crossbeds	linguoid bars or deltaic growths from older bar remnants
B1	St	sand, medium to coarse may be pebbly	solitary (theta) or grouped (pi) trough crossbeds	dunes (lower flow regime)
B2	Sp	sand, medium to coarse may be pebbly	solitary (alpha) or grouped (omikron) planar or avalanche cross beds	linguoid, transverse bars, sand waves (lower flow regime)
B1	Sr	sand very fine to coarse	ripple marks of all types	ripples (lower flow regime)
C1, C2, C3, C4, C5, C6	Sh	sand, very fine to very coarse, often granulitic	horizontal lamination parting or streaming lineation	planar bed flow and regime
A3	Sl	sand, fine to very coarse often granulitic	low angle (<10°) cross beds	scour fills, crevasse splays, antidunes
C3, C4, C6, A3, D, B1, A1	Ss	sand, fine to coarse may be granulitic	broad, shallow scours including eta cross-stratification	scour fills
D	Fl	sand, silt mud	fine lamination, very small ripples	overbank or waning flood deposits
D	Fm	mud, silt	massive, desiccation cracks	overbank or drape deposits
E	C	lignite, carbonaceous mud, carbonaceous pumice silts	plants, mud films	swamp deposits
F *	Gm	crudely bedded gravel	planar stratification	channel lag deposits

* Description included with facies C1-C6.
For relative abundance of structures in the upper Matua Subgroup refer to Table (7.10).

these conditions each event would have a limited duration. Thick sequences along Pyes Pa Road, at Matua and at Te Puna, suggest continuously varying conditions.

(i) Sh

Because a plane bed is a specific response to combinations of grain size and flow velocity (e.g. upper flow regime conditions and the hydraulic behaviour of sand and vesicular grains) it can be regarded as a bedform when there is virtually continuous particle movement. These bedforms have been described from both in-channel and channel-bar sequences (Picard and High, 1973). Planar stratification can occur under two quite different conditions (i.e. usually under upper flow regime, Harms and Fahnestock, 1965) : in shallow water and during flood stage (Miall, 1977, 1978).

(ii) Gt and St

Lithofacies Gt and St represent cross-stratified deposits.

(iii) Gp and Sp

Alpha cross-stratification, avalanche cross-stratification and or planar cross-beds are formed by the down-current migration of avalanche faces at the margins of bar surfaces (Smith, 1972; Picard and High, 1973; Miall, 1977, 1978). Avalanche bedforms are associated with channel-bar and bar sequences (Picard and High, 1973; Miall, 1977, 1978).

2. Channel scour and fill

(Facies Gt, Ss, Sh, St)

Shallow channels filled with sand and/or gravel represent minor channels formed by avulsion or bar dissection during falling water. Scours occur at the lateral margins of unconsolidated distal

ignimbrites (e.g. Te Puna) which have formed thick lobes in the Basin. Small scours may be related to strong separation eddies in the lee of advancing dunes or sand waves, or to local vortices developed around obstructions (Miall, 1977). Minor channels are often infilled by Sh and St lithofacies.

3. Low-water accretion and modification processes

(Facies Sr, Sh, Fl, Fm)

Bedforms which are typically small scale develop during low water, particularly on the bar surfaces, or in a channel-bar sequence.

Several subfacies may be produced (Miall, 1977). During low-flow conditions, ripple migration can be maintained on the sand bed but the record for accretion on bar surfaces (Miall, 1977) is poor in the upper Matua Subgroup deposits. Lack of preservation results from higher flow velocities which have flattened bedforms, and erosion in major and minor channels.

Bar-front accretion during falling water stage is represented by sand wedges and avalanche slopes which develop straight foresets.

During low water stage, drape deposits are formed in abandoned channels and in pools of standing water on the bar surface. Mud settles out as a veneer over cross-bedded deposits.

4. Sedimentation in overbank areas

(Facies Fl, Fm)

Lithofacies Fl and Fm occur in areas where sedimentation has occurred from suspension. Flow velocities will be slow in such areas because of shallow depths in lower flow regime conditions, and because of obstructions (e.g. vegetation) which are uncovered during low water stage (Miall, 1977). The lithofacies represent abandoned channel and floodplain sub-environments.

7.5 FACIES ASSEMBLAGES

Having interpreted facies and internal bedding types in terms of local processes it is necessary to develop a depositional model consisting of representative facies assemblages typical of various sedimentary cycles in the upper Matua Subgroup. Many of these fluvial cycles interdigitate with episodes of pyroclastic deposition.

Several features are suggestive of episodic flow (e.g. horizontal discontinuous stratification, lenticular stratification, continuous bar sequences usually covering channel deposits, channel-bar and channel sequences) within this braided river environment. These cycles may be discontinuous or continuous. If the latter applies it infers that sedimentation resulted from a single episode which can be called a sedimentation unit (Picard and High, 1973). A sedimentation unit is "one or more sets of strata deposited continuously under uniform or continuously varying conditions" (Picard and High, 1973). Subenvironments therefore may be recognised on the basis of their characteristic sedimentary features, and by completely or incompletely preserved sedimentation units.

Miall (1977, 1978) reviewed and summarised the main lithofacies types and facies associations (Fig. 7.18) that have been recorded in modern and ancient braided stream deposits. A number of vertical profile models were erected which represent these lithofacies assemblages. An indication of the type of environment at the time of deposition is given when this procedure is followed.

When facies of the upper Matua Subgroup are stacked vertically, they closely match assemblages presented by McKee *et al.* (1967), Picard and High (1973), and Miall (1977, 1978) for braided river environments having ephemeral characteristics. The deposits in the Tauranga Basin appear to be coarser than those described in similar

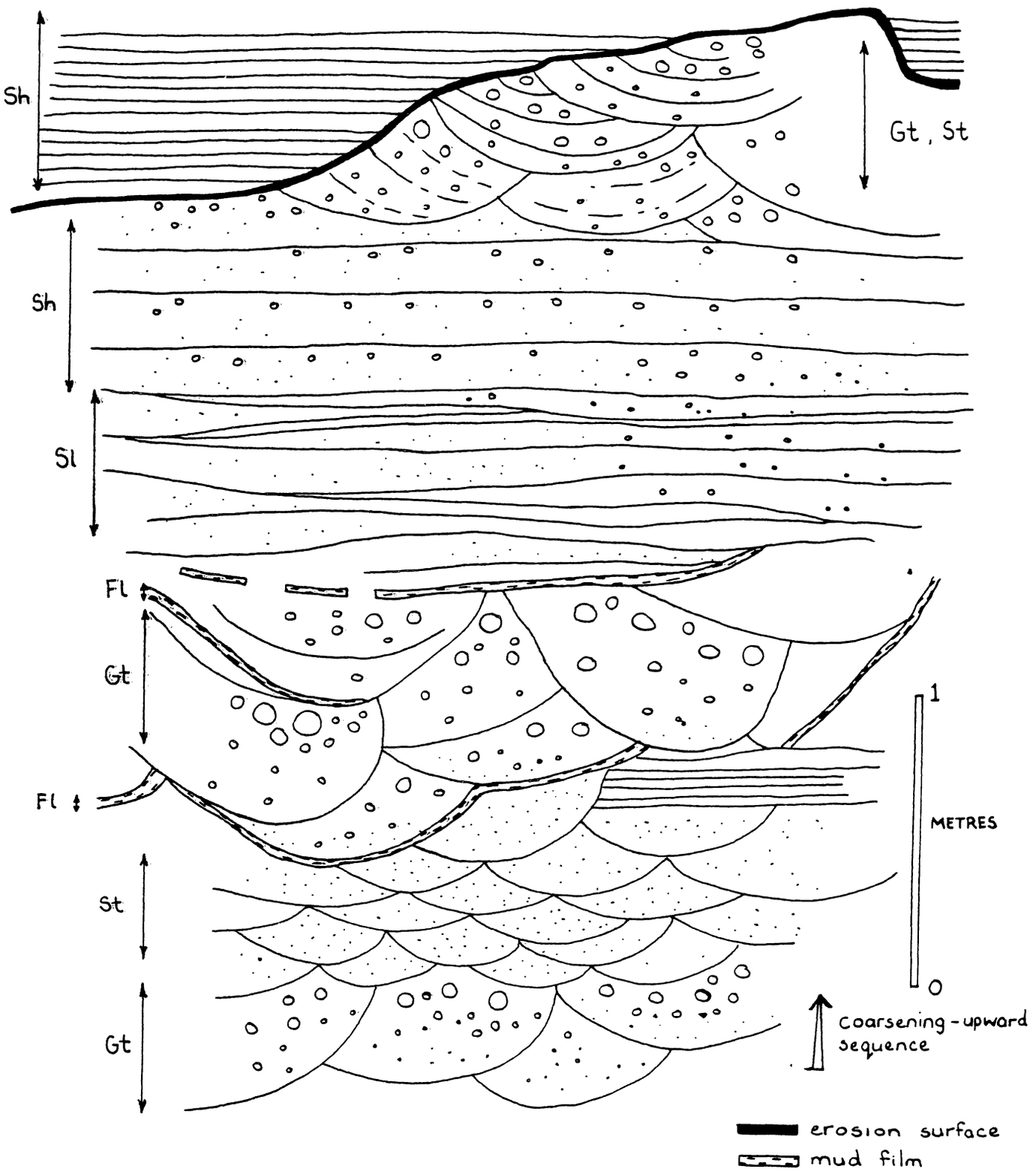


Fig. 7.18 Stratigraphic section of part of the Matua Subgroup at Pyes Pa Road.

models by Miall (1977, 1978) and this may be explained by the proximity of the fluvial sedimentary sequences to coarse pumice source deposits, rapid deposition, and a high sediment input from unconsolidated distal ignimbrites and airfall-tephra deposits. The following assemblages (Fig. 7.19) are described from the upper Matua Subgroup:

(a) Assemblage I : most closely matches facies assemblages recorded by McKee *et al.* (1967), Picard and High (1973) and the Bijou Creek type and Saskatchewan type models of Miall (1977, 1978). Some discrepancies arise, namely the abundance of gravel, coarsening upward cycles and the predominance of Sh, St and Gt lithofacies in the same assemblage.

The model consists of planar stratified (including low-angle cross-bedding) gravelly sands and sands, and sedimentation units may not be completely preserved. The assemblage includes trough and avalanche bedding. Sand bars, each of longitudinal, point and transverse kinds, are dominant depositional features (Fig. 7.20). The sand and gravel was in many instances transported under upper flow regime conditions.

Assemblage I represents a variety of vertical model types (i.e. usually associated with horizontally laminated sand) outlined by previous authors, dominated by petrofacies B, C, and E, and derived from the Late Ignimbrite Period sediments (Chapter 9).

(b) Assemblage II : represents assemblages further inland (2 - 4 km) from the coast, and at Te Puna. The assemblage is characterised by Gt and St facies and a predominance of gravel and sand lithotypes which are commonly inversely graded. Assemblage II shows a number of cyclic sequences which resemble parts of the Donjek and South Saskatchewan type models (Miall, 1977, 1978) and identifies

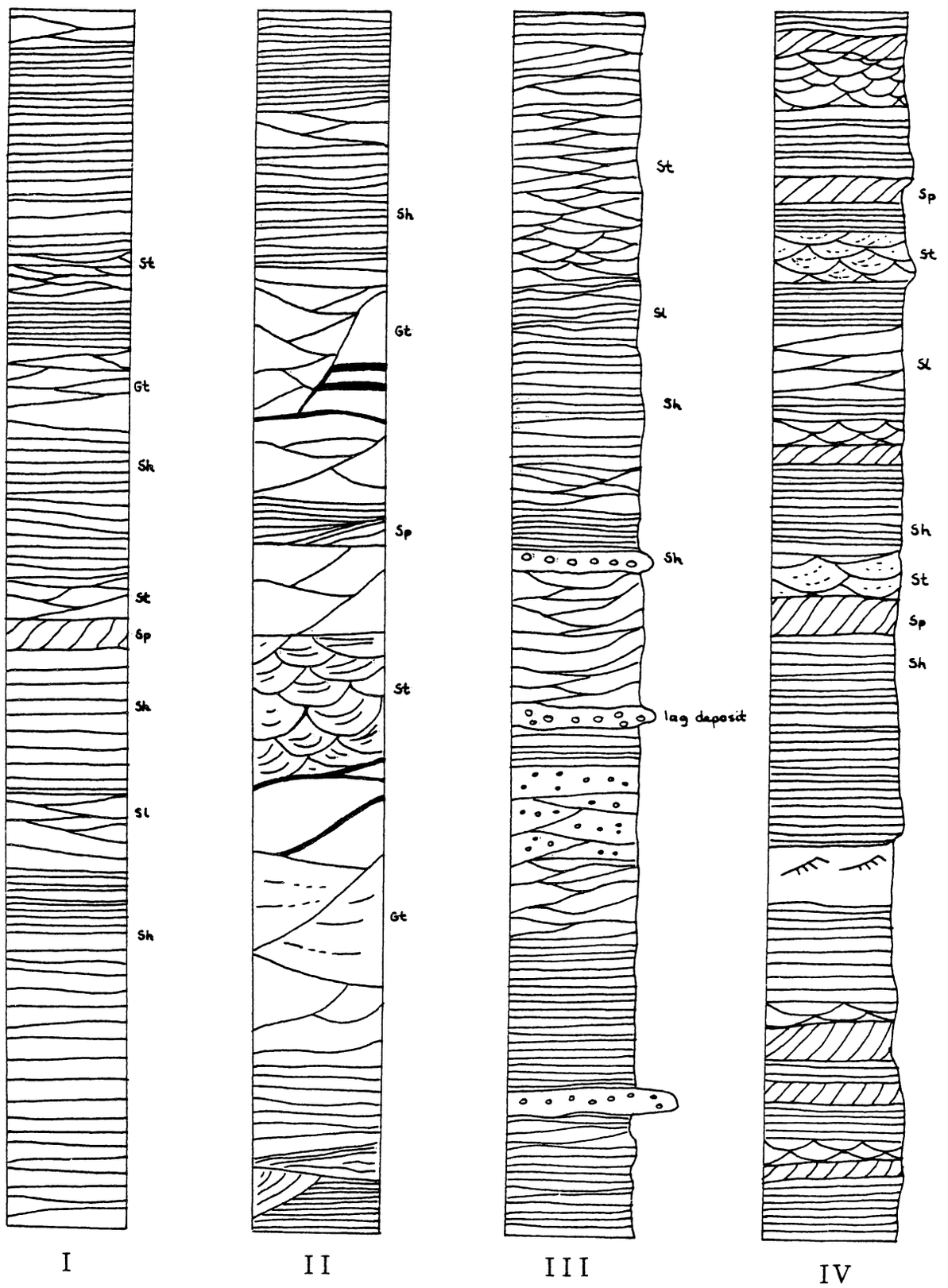


Fig. 7.19 Fluvial sediment assemblages recognised at the Pyes Pa Road, Cambridge Road, Matua and Te Puna sites.

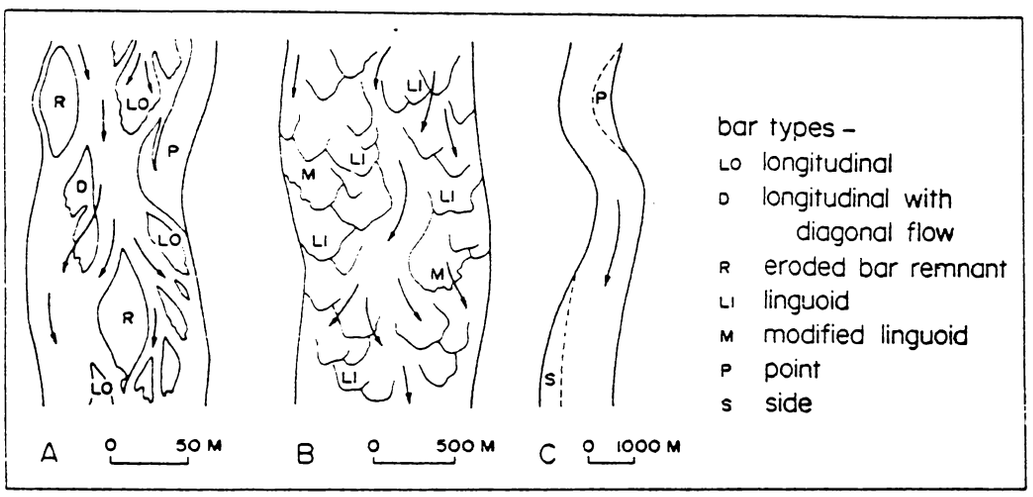


Fig. 7.20 Principal bar types (after Miall, 1977).

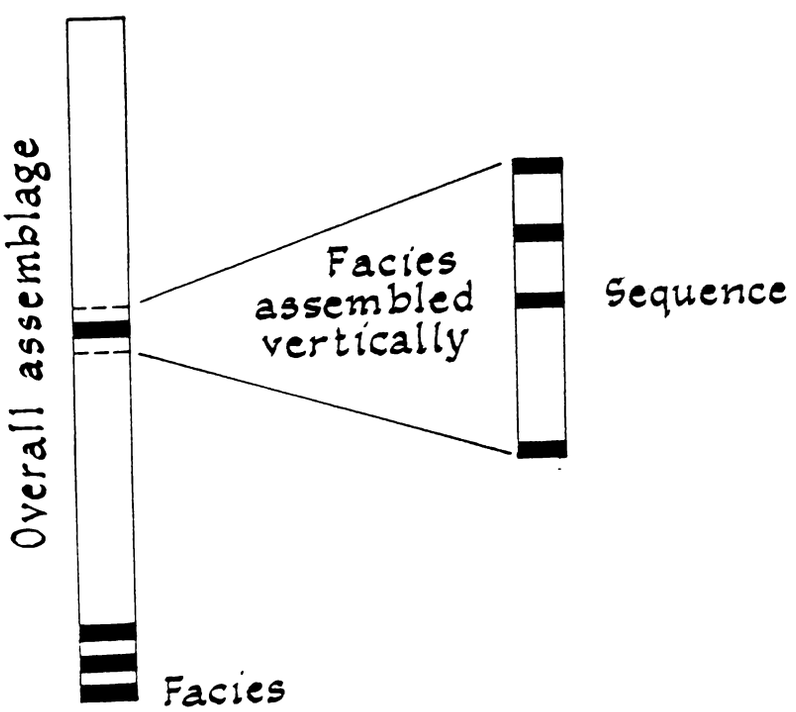


Fig. 7.21 Sequences as interpreted from the overall assemblage.

both major and minor channel systems. Another part of the Assemblage is interpreted as having been deposited during episodes of greater discharge and is dominated by Sh facies. The Assemblage is dominated by petrofacies A and B.

(c) Assemblage III : represents varied types of the Donjek, Saskatchewan and Bijou Creek models (Miall, 1977, 1978). It is dominated by petrofacies F derived from Early Ignimbrite Period sediments. The assemblage is characteristically represented by St, Sp, Sl, Sr and Sh facies of sand to gravel lithotypes and channel lag deposits.

(d) Assemblage Iv : dominated by petrofacies A and D. These fluvial sediments are derived from the erosion of the Te Ranga Ignimbrite and Minden Rhyolite with minor contributions from the Wairoa and Te Puna Ignimbrites. The assemblage represents alluvial wash and braided fluvial material, which has been reworked in some areas, especially at Te Puna. It is characteristically represented by Sh, St and Sp facies of slightly gravelly sand lithotypes.

7.5.1 Sequences

Within the facies assemblages which have been stacked vertically in a number of general models, certain sequences (Figs 7.21 and 7.22) can be extracted and interpreted from the overall assemblage (Tables 7.8 and 7.9, Figs 7.23 and 7.24). Many of the assemblages studied interdigitate with the next assemblage or with pyroclastic deposits, reflecting overlapping sedimentary and pyroclastic processes. Within the fluvial deposits or facies assemblages several flood cycles and channel re-occupation episodes are recorded. Flood cycles are recognised by superposition of lithofacies representing progressively

FACIES	INTERPRETATION
(a) Bar Sequence	
Fl	muds, laminated silts, massive silts deposited during low flow
Sr, St	low flow velocities
Gp, Sp	lower flow velocities (strata becomes inclined) over the bar
Sh	upper flow regime conditions
Sl	flow in channel still vigorous
(b) Channel - Bar Sequence	
St	diminishing current velocity
Gp, Sp	sediment carried to the front of the bar is deposited as avalanche strata
Sh	on top of the bar shallow water and high flood discharge result in high current velocities and upper flow regime conditions
Gp, Sp	record an advancing bar
(c) Channel - Fill Sequence	
Sh	renewed activity
St	diminishing current velocity
Gp, Sp, or Sh	flood waters high
Gm, Sh	lag deposit

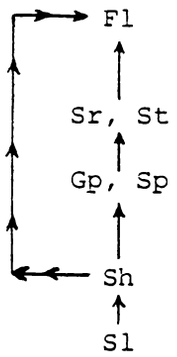


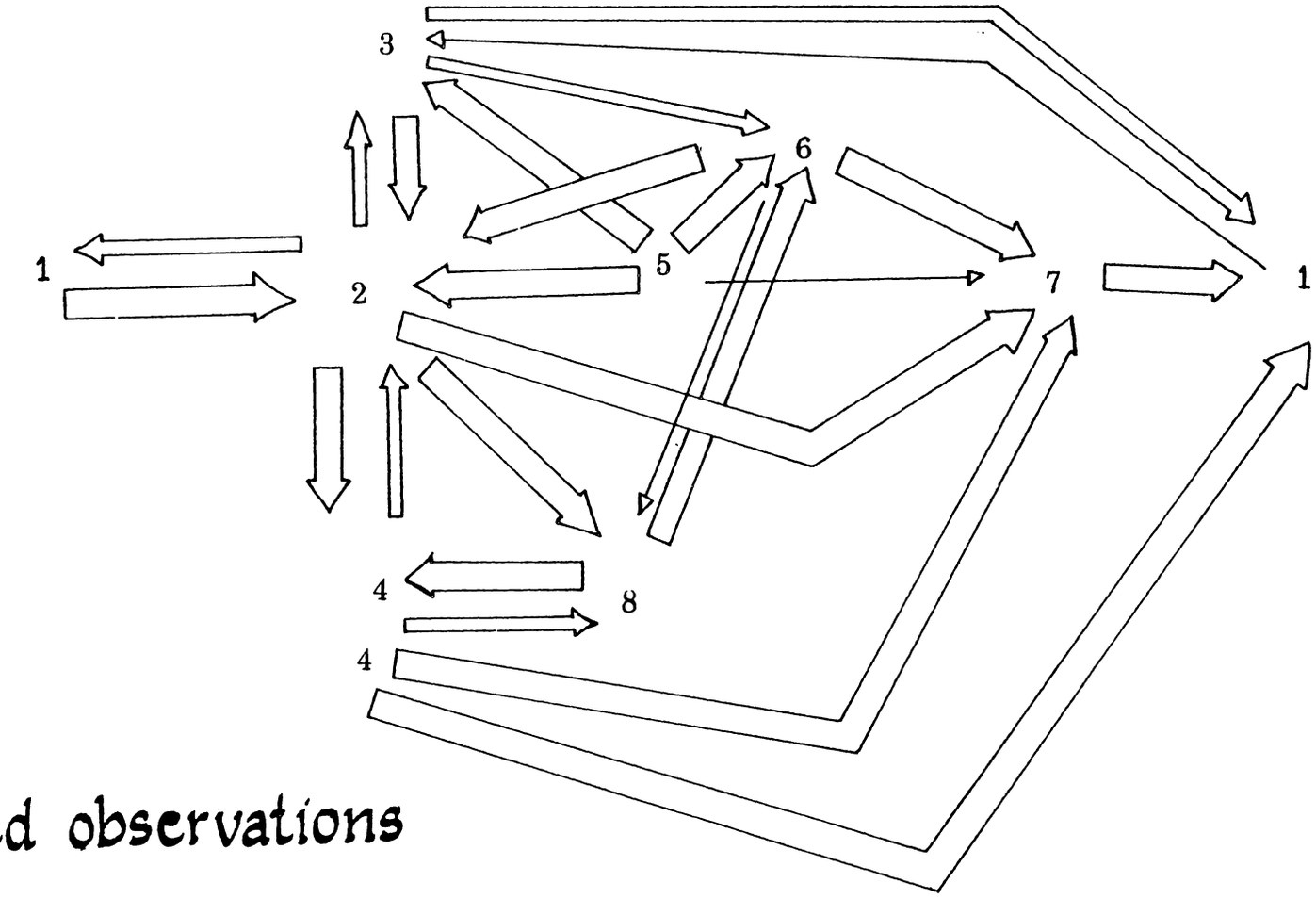
Fig. 7.22 Group assemblages recognised in sequences showing vertical stacking relationships and the interpretation for individual lithofacies. Group and lithofacies codes are defined in Table 7.7 and Figure 7.20 respectively.

TABLE 7.8 Some vertical sequences observed in the Matua Subgroup fluvial deposits (refer to Table 7.7)

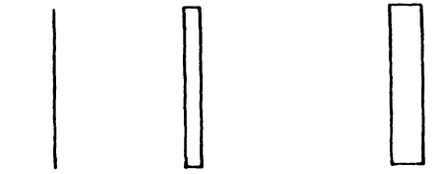
Sequence	Location	Grid Reference
Gn→Sh→Sl→St	Bethlehem, Cambridge Rd	U14/858836
Gt, St→Sh→Sl→Sh	Pyes Pa Road	U14/845768
Gt, St→Sh→Sl→Sh→Fl, Fm	Pyes Pa Road	U14/845768
Gt, St→Fm, Fl→Sl→Fl, Fm→Sl→Sh	Pyes Pa Road	U14/845768
Sh→Sl→Sh→Sp→Sr	Te Puna, Bethlehem	U14/821887 and U14/858836 respectively
Sh→Sp→Sh	Te Puna	U14/821887
St→Sp→Sh	Te Puna	U14/821887
St→Sh→Sl→Sp→St	Te Puna	U14/821887
Ss→Sh→St	Te Puna	U14/821887
Sh→Sl	Kings Avenue	U14/849875
Gt, St→Sl→Sh	Kings Ave, Te Puna	U14/849875 and U14/821887 respectively

Table 7.9 Observed facies relationship code, which relates to Figs. 7.23 and 7.24. See Table 7.10 for physiographic model code and Table 7.7 for braided river code.

Physiographic model code	Braided river code (after Miall, 1978)	Facies relationship code	Description
F	Gm	1	Channel scoured planar surface, lag material
C1 - C6	Sh	2	Planar stratification
A3	Sl	3	Low angle (<10°) cross strat.
A2 - A1	Gt	4	Trough cross-strat.
C3, C4, C6 A3, D, B1 A1	Ss	5	Channel scour
B1, C1 - C6	St, Sh	6	Trough cross-strat. + planar-strat sands
D	Fl, Fm	7	Mud draping and abandoned channel deposits
B2	Sp	8	Avalanche cross-strat. sands and gravels



Reported observations



≤2 2-6 >6

Fig. 7.23 Observed facies relationship in the Matua Subgroup (refer to Table 7.9 for description and code).

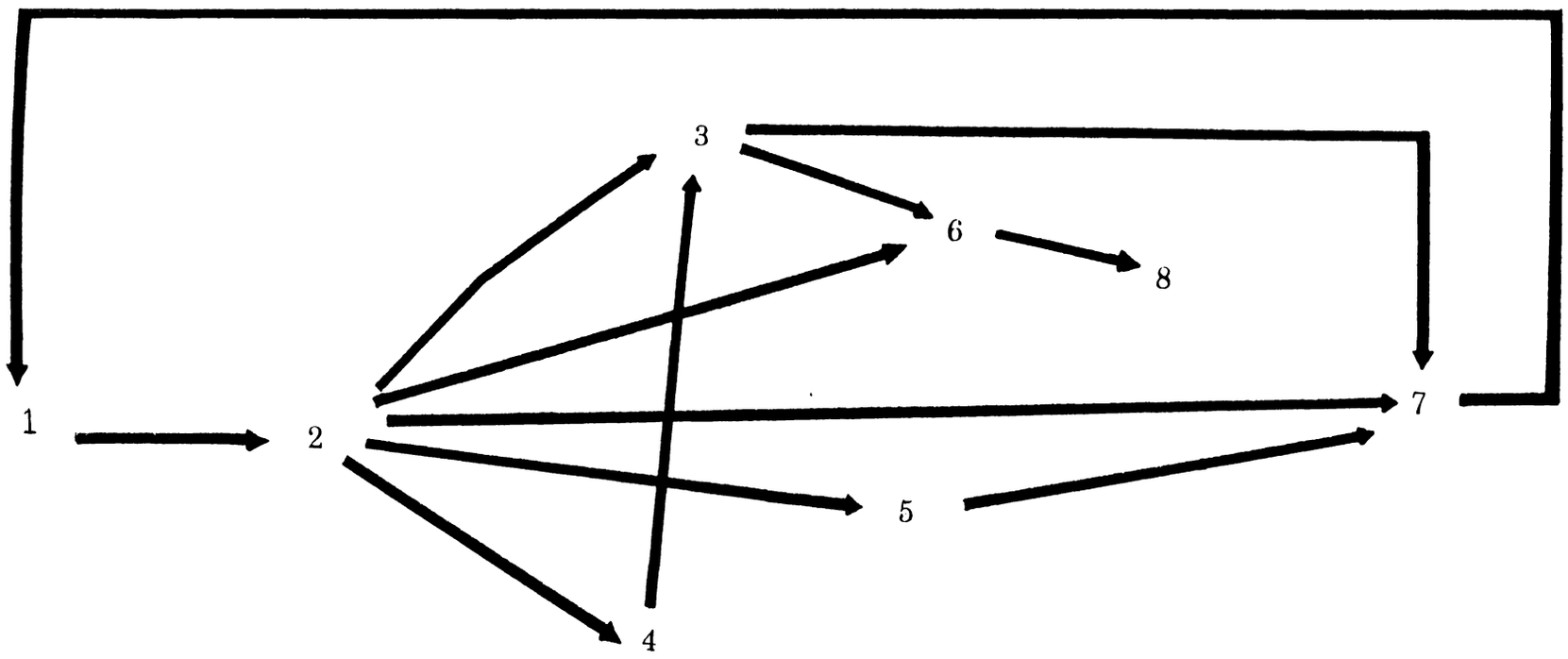


Fig. 7.24 Simplified facies relationship model constructed from lithofacies assemblages, sequences and the observed relationships model in Fig. 7.23.

decreasing energy levels. Three types of vertical sequences are identified (Fig. 7.22) :

(a) Bar sequence - the sequence is deposited during the waning stages of a flood and the bar is subjected to lower-flow regime conditions. If the bar remains awash while flow velocity in the channel continues to decrease, Sh facies may persist until conditions of decreased flow velocity enable silts to be deposited. During a transition phase, silts may accumulate in the bar sequence, as evidenced in the Matua and Te Puna coastal exposures. If the water level drops rapidly enough a ripple stage (uncommon in the upper Matua Subgroup) is by-passed and planar stratification can be followed by a mud veneer deposit.

Where the gravelly sand facies Gt and St persist, thin mud veneers are deposited during the falling water stage.

(b) Channel-bar sequence - longitudinal and transverse bars are deposited in channels. The sequence at any one point may be from foresets filling relatively deep and quiet water to horizontal discontinuous strata in shallow water. If the bar remains under water while the flood wanes, a series of bedforms indicative of diminishing current velocity are deposited. Deposition ceases when the bar is exposed by falling flood waters.

(c) Channel-fill sequence - the sequence develops during high water stage. Termination is through non-deposition or erosion.

7.6 LITHOFACIES OF UPPER MATUA SUBGROUP : PHYSIOGRAPHIC MODEL

Lithofacies (Table 7.7) are constructed from lithological, textural and sedimentary structural descriptions (Table 7.10). Twelve lithofacies, related to flow regime, have been erected for the upper

TABLE 7.10 Sedimentological characteristics and environmental interpretation of lithofacies of upper Matua Subgroup.

Lithofacies	Occurrence	Dominant Composition	Dominant Texture	Sedimentary Structures	Flow Regime	Bed Forms	Depositional Environment	Stratigraphic Position
A1	Common	pumice glass shards rhyolitic rock fragments	gravelly sand	Rho cross-stratification	Upper part of lower to lower part of upper	Dunes on longitudinal bars or longitudinal bar migration	Active braided channel	Channel
A2	Uncommon	pumice rhyolitic rock fragments	slightly gravelly sand	Rho cross-strat. and sigma cross-strat.	Upper part of lower to lower part of upper			
A3	Extremely Common	pumice glass shards	slightly gravelly	Low angle cross-strat.	Upper part of lower	Point and long. bar migration		
B1	Rare	pumice glass shards	sand	Nu cross-strat.	Lower part of lower	Ripples on bars		
B2	Uncommon	pumice rhyolitic granules and pebbles quartz feldspar	slightly gravelly	Avalanche cross-strat.	Lower part of lower	Avalanche faces of bars		
C1	Fairly Common	pumice glass shards	sand	Horizontal parallel strat.		Plane bed developed on bar		
C2	Common	pumice glass shards	slightly gravelly sand					
C3	Common	pumice glass shards	sand	Horizontal disc.	Upper	Deposition in Channel		
C4	Rare	pumice glass shards	sand					
C5	Uncommon	pumice glass shards	sand					
C6	Fairly common	pumice glass shards	gravelly sand	Lenticular stratification	Transitional	Shifting depositional centre		
D	Common	glass shards pumice	mud	Horizontal stratification or massive	Suspension deposits		Abandoned braided channel	Overbank

Matua Subgroup at Matua, Te Puna and Te Ranga (Pyes Pa Road) and form the basis for environmental interpretation. They are as follows:

A1. Rho cross-stratified, moderately- to poorly-sorted, rhyolitic and pumiceous gravelly and slightly gravelly glass shard rich/quartzo-feldspathic sands formed in the upper lower to lower upper flow regime. This lithofacies is predominant in sediments derived from the Te Ranga, Te Puna and Wairoa Ignimbrites.

A2. Large-scale Rho cross-stratification interrupted by some Sigma cross-stratification showing the same textures and lithologies as lithofacies A1, formed in the upper part of the lower flow regime, and the lower part of the upper flow regime.

A3. Low-angle cross-stratified, moderately to well sorted, slightly gravelly sands and sands formed in the upper part of the lower flow regime, but in conditions approaching the upper flow regime.

B1. Nu cross-stratified, moderately to well sorted, pumiceous sands, formed in the lower part of the lower flow regime.

B2. Avalanche cross-stratified, moderately to well sorted, gravelly sands and sands formed in the lower part of the lower flow regime and producing small-scale (i.e. $\leqslant$ 5 cm) and large-scale (i.e. $\geqslant$ 5 cm) features.

C1. Horizontal parallel stratification in moderately to well sorted, pumiceous sands formed in lower and upper parts of the upper flow regime.

C2. Type 1 Discontinuous horizontally stratified, poorly to well sorted, inversely graded pumiceous gravelly sands and sands formed in upper flow regime conditions.

C3. Type 2 Laminated, inversely graded, moderately to well sorted, slightly gravelly sands and sands formed in the upper flow regime.

C4. Type 3 Laminated, normally graded, moderately to well sorted, slightly gravelly sands and sands formed in the upper flow regime.

C5. Type 4 Inversely graded, gravelly sands to sands formed in the upper flow regime.

C6. Lenticularly stratified, poorly to moderately sorted, gravelly and slightly gravelly sands formed in fluctuating regimes in bar-channel-bar sequences.

D. Horizontally stratified and massive muds deposited from suspension in abandoned braided channels.

7.7 INTERPRETATION OF LITHOFACIES IN TERMS OF DEPOSITIONAL ENVIRONMENT: (Post-Te Ranga Ignimbrite emplacement)

Lithofacies A1 was deposited in rapidly shifting shallow braided streams during relatively high discharge by the migration of asymmetrical dunes (Williams, 1968) and/or by the downcurrent migration of avalanche faces associated with larger bedforms such as bars (Williams and Rust, 1969).

Lithofacies A2 was formed by the migration of larger dune bedforms than Lithofacies A1, as well as from washed out dunes in which beds developed a low angle of inclination transistional to plane bed deposition. Conditions are likely to have been in the lower part of the upper flow regime.

Lithofacies A3 compares with low amplitude bedforms (Miall, 1977) formed by shallow, high velocity flow in low relief scours. Picard and High (1973) have suggested point and longitudinal bar migration in the upper part of the lower flow regime, probably into the upper flow regime.

During periods of low discharge when only sand was transported, lithofacies B1 was developed from ripples migrating across the surface of newly formed low linear mid-channel mounds and transverse bars. These became exposed as flood waters receded and ripples also developed at the side of streams where tributaries of the main channel moved across slumping and incised bands (Doeglas, 1962).

Lithofacies B2 was formed during periods of high discharge when sorting occurred at the back of the bar, and gravels and sand moved down avalanche faces at the lee edge of transverse and longitudinal bars. The water was appreciably deeper in these areas and current velocities decreased progressively as the flood waned.

During high flood discharge, lithofacies C1 formed by plane bed movement on the surface of the longitudinal bars, upon which upper flow regime conditions were probably reached (Picard and High, 1973).

Lithofacies C2, C3, C4 and C5 all occupy channel-fill sequences indicative of forming during high velocity currents, just over the threshold of the upper flow regime (Harms and Fahnestock, 1965; Picard and High, 1973). As the flood discharge increases the channel bottom is scoured and little deposition occurs until the flood crest passes. Initially, currents are vigorous and capable of producing upper flow regime bedforms but as the flood waters fall, the current velocity decreases and a corresponding sequence of bedforms is produced (Picard and High, 1973; Miall, 1978). With fluctuating regimes, as from bar-channel-bar, a composite set of strata

comprising lithofacies C6 is developed from shifting depositional centres. In the different subenvironments within a braided stream, and because of the rapidly shifting regimes, lenses of sediment are deposited atop each other.

Lithofacies D represents overbank and abandoned channel deposits formed by suspension and very low current velocities following flooding. It may also represent silt deposition on the bar while the velocity decreases and water level drops.

7.8 DISCUSSION OF UPPER MATUA SUBGROUP MODEL

On the basis of information collated from the hydrodynamic origins of sedimentary structures, the vertical assemblage of facies, and the depositional environment, a general sedimentary model has been developed to account for post-Te Ranga Ignimbrite sedimentation (Fig. 7.25). This section discusses this sedimentary model by examining changing sedimentation patterns through time and within different areas in the Basin.

The bulk of sediment supplied to the upper Matua Subgroup was derived from unconsolidated pyroclastic deposits, namely the Wairoa, Te Puna, Te Ranga, and Waimakariri Ignimbrites, as well as rhyolitic air-fall tephra. As drainage systems developed, the topographic relief of the Te Ranga Ignimbrite was reduced substantially during erosion and supply of material. During successive floods, incised channels became blocked by channel aggradation and a braided river system developed (Fig. 7.25). Stable banks, vegetated islands and swamps developed during this early sedimentation period which included the upper parts of Assemblage III (i.e. $\sim$ 3 m) while burying the bulk of Assemblage III material (i.e. $\sim$ > 20 m). Assemblage III deposits are older (i.e. associated with the Wairoa Ignimbrite) and are interbedded with paleosols and air-fall tephra.

The Waimakariri Ignimbrite was emplaced over the Te Ranga Ignimbrite, Assemblage III, and over sediments derived from the Te Ranga during an earlier period. A number of flood cycles followed emplacement of the Waimakariri Ignimbrite and channels became incised once again, scouring, reworking and eroding out material from earlier sedimentation periods (e.g. Assemblage III and early Te Ranga-derived sediments). Assemblage I material (predominantly Sh facies) was deposited in the Matua and Otumoetai areas and covered Assemblage III material in the Cambridge Road area. Assemblage I was almost completely eroded out of the Cambridge Road area. Following a long fluvially inactive period interrupted by pyroclastic deposition (which is also represented by several unconformities and three paleosols at Matua) a reactivated fluvial sedimentation phase deposited Assemblage II material in the Pyes Pa Road and Te Puna areas. This was followed by Assemblage IV deposition, which conformably covered Assemblage II material. During deposition of Assemblage II the braided river environment gradually changed to a more anastomosing one in which wandering deeply incised channels were interconnected by a network of low gradient, sinuous gravelly sand channels. Separating the channels were floodplains consisting of vegetated islands, natural levees and swamps. Airfall tephra deposited over Assemblage I and II formed a thick ($\sim$ 4 m) cover, which has been preserved mainly in modern coastal exposures.

The vertical stacking of facies in the depositional environments was determined by the intensity of sediment input, as controlled by source area tectonics and erosion and the rate of basin subsidence and/or base level variations as related to sea level change (Chapter 4 and 9). Together these regulated the landward or basinward migration of facies and the lateral development of facies from the major channels.

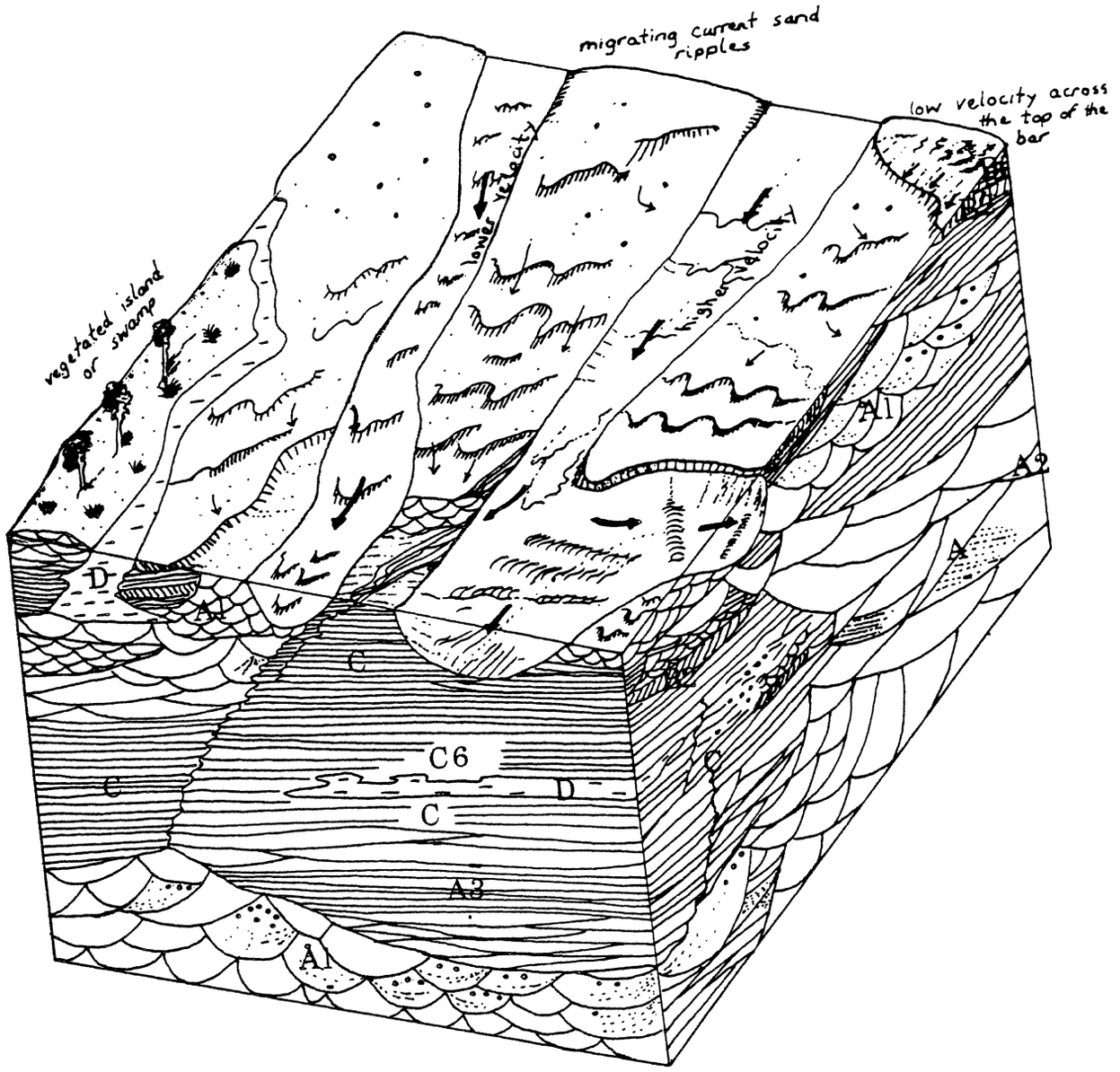


Fig. 7.25 Physiographic model showing schematic relationship of lithofacies in the Matua Subgroup. The code is defined in Tables 7.7 and 7.10. Figure 8.15 should also be consulted.

CHAPTER EIGHT

STRUCTURES AND EMPLACEMENT MECHANISMS OF PYROCLASTIC DEPOSITS OF THE MATUA SUBGROUP

8.1 TERMINOLOGY FOR PYROCLASTIC DEPOSITS AND FRAGMENTS

(i) Definitions

Because of the abundance of volcanic material in the Tauranga Basin, nomenclature for describing pyroclastic deposits and fragments is discussed below. The following terminology is based on Schmid (1981).

Pyroclasts : "individual crystals, crystal fragments, glass fragments and rock fragments generated by disruption as a direct result of volcanic action. The shapes assumed during disruption or subsequent transport from the primary deposit must not have been altered by later redeposition processes. If they were altered, the crystals or fragments would be called "reworked pyroclasts" or "epiclasts" (if their pyroclastic origin is uncertain)".

Pyroclastic deposits : "(= "pyroclastics") include both consolidated and unconsolidated assemblages of pyroclasts. They must contain more than 75% pyroclasts by volume".

Pyroclastic flow : "involves the lateral movement of pyroclasts as a gravity controlled, hot, high concentration gas/solid dispersion which may in some instances be partly fluidized" (Sparks, 1976; Wright *et al.*, 1980).

Tephra : a collective term for unconsolidated pyroclastic deposits, including all primary deposits of clastic, unwelded material of either pyroclastic flow or air-fall origin. (Howorth, 1975; Schmid, 1981).

Air-fall tephra : an unconsolidated, but usually weathered, pyroclastic fall deposit in which structural and testural descriptions can be recorded. Some beds show shower bedding and/or grading.

pyroclastic air-fall or fall deposits : unconsolidated and consolidate deposits which have an air-fall origin.

Tuff : consolidated (indurated or cemented) pyroclastic deposits.

Tuffite : rocks consisting of mixtures of pyroclasts and epiclasts (<75%, >25% epiclasts by volume).

Epiclast : "crystals, crystal fragments, glass fragments or rock fragments that have been liberated from any type of pre-existing rock (volcanic or non-volcanic) by weathering or erosion and transported from their place of origin by gravity air, water or ice".

Epiclastic deposit : consolidated or unconsolidated aggregate of epiclasts.

(ii) Granulometric Classification

Pyroclastic deposits are characterised by their size, which is generally taken as the average diameter of the pyroclasts (Tables 8.1 and 8.2).

Nomenclature for pyroclastic deposits:

Pyroclastic deposits have been separated into two subdivisions:

(1) Unimodal and well sorted.

(2) Polymodal, bimodal poorly sorted.

Because a large proportion of pyroclastic deposits in the Tauranga Basin are poorly sorted, the following terms adopting IUGS nomenclature have been used for deposits comprising more than one dominant size fraction.

Examples:

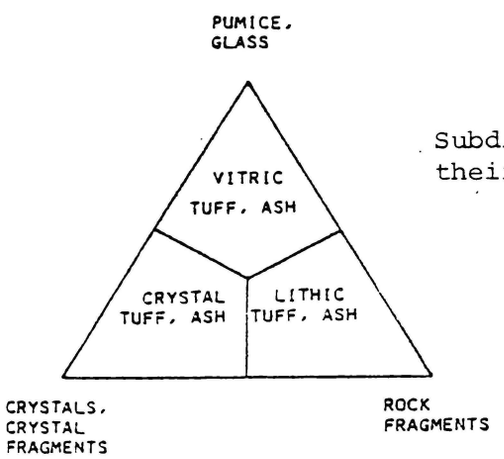
ash-lapilli tuff (lapilli > ash)

ash-lapilli tuff breccia

lapilli-ash tuff breccia (ash > lapilli)

Table 8.1 Granulometric classification of pyroclasts and of unimodal, well-sorted pyroclastic deposits (from Schmid, 1981).

Clast size (mm)	Pyroclast	Pyroclastic deposit	
		Mainly unconsolidated: tephra	Mainly consolidated: pyroclastic rock
64 mm	Bomb, block	Agglomerate, bed of blocks or bomb, block tephra	Agglomerate, pyroclastic breccia
2 mm	Lapillus	Layer, bed of lapilli or lapilli tephra	Lapilli tuff
1/16 mm	Coarse ash grain	Coarse ash	Coarse (ash) tuff
	Fine ash grain (dust grain)	Fine ash (dust)	Fine (ash) tuff (dust tuff)



Subdivision of tuffs and ashes according to their fragmental composition.

Table 8.2 Terms for mixed pyroclastic-epiclastic rocks (from Schmid, 1981).

Pyroclastic*		Tuffites (mixed pyroclastic-epiclastic)	Epiclastic (volcanic and/or nonvolcanic)	Avg clast size (mm)
Agglomerate, agglutinate pyroclastic breccia		Tuffaceous conglomerate, tuffaceous breccia	Conglomerate, breccia	64
Lapilli tuff				2
(Ash) tuff	coarse	Tuffaceous sandstone	Sandstone	1/16
	fine	Tuffaceous siltstone	Siltstone	1/256
		Tuffaceous mudstone, shale	Mudstone, shale	
100	75		25	0% by volume
← Pyroclasts				
→ Volcanic + nonvolcanic epiclasts (+ minor amounts of biogenic, chemical sedimentary and authigenic constituents)				

8.2 PYROCLASTIC FLOW DEPOSITS

8.2.1 Introduction

Many of the deposits exposed in the Tauranga Basin (Table 8.3) are interpreted as being the distal unwelded portions of ignimbrites, although the source of many of these deposits is speculative and is based on thickening of the deposits and lithic size. While many of these deposits are characterised by homogeneity, they also exhibit heterogeneity in the form of segregation structures, lithic and crystal enrichment layers, and grading.

(i) Emplacement Mechanisms

Pyroclastic flow deposits are topographically controlled, filling valleys and depressions. Each flow unit is the depositional product of a single pyroclastic flow (Sparks, 1976) but it is possible that as the flow advances it may split into several subsidiary flows (Smith, 1960; Wilson, 1980).

The nature of distal ignimbrites reflects the flow mechanism (Table 8.4) and the environments encountered (Sheridan, 1979; Wilson, 1980). A number of authors have suggested that ignimbrites show systematic variations within units (i.e. detract from homogeneity; Aramaki, 1969; Walker, 1971, 1972; Sparks, 1976; Sheridan, 1979; Wilson, 1980 (Fig. 8.1)). Evidence presented in this study indicates that most distal ignimbrites exposed in the Tauranga Basin show considerable variation in structure (Table 8.5).

(ii) The following section documents characteristics of the Tauranga Basin pyroclastic flow deposits. A number of structural models have been developed (Table 8.5) and are interpreted in the light of current literature and from structural interpretation in the field (Table 8.6). Lithofacies codes (Table 8.7) have been

Shows the various types of pyroclastic deposits recognised in the Tauranga Basin, as well as the syndepositional and post-depositional structures characteristic of these deposits. When mapping commenced in the Tauranga Basin pyroclastic flow deposits were simply given type names, as indicated. Further work indicated a correlation between these and certain formally named deposits, so that the latter terminology has generally been adopted.

PYROCLASTIC FLOW DEPOSITS							
Unit name		Page		Page			Page
Waimakariri	Type F1	244	Inter-pretation	247			
Te Ranga	Type F2	244			Type F2 SD structures*		249
					Type F2 PD structures*		252
Te Puna	Type F3						252
Wairoa	Type F4						255
Te Puna	Type F5	256	PD Struc-tures*	F5a	259	Interpretation	263
				F5b	260		
?	Type F6						264
?	Type F7						267
PYROCLASTIC FALL/AIRFALL TEPHRA DEPOSITS							
Type A1		268	Interpretation				268
Type A2		268					
Accretionary lapilli beds							270
* PD = Post-depositionally modified					SD = Syndepositional		

Table 8.4 Genetic classification of pyroclastic flow types based on fluidization behaviour (after Wilson, 1980).

Flow Type	Fluidization Behavior with Increasing Gas Flow Velocities	Description
1	Non-expanded	Ungraded flows; lack of expansion and high yield strength inhibits gravitational coarse-tail grading. If grading of larger clasts is present, it is due to some other mechanism.
2	Expanded	Expansion of flow allows gravitational coarse-tail grading of pumice and lithic clasts.
3	Segregating	High degree of fluidization results in extreme grading. Distinct concentration zones of pumice and lithics are found, and other segregation structures, including "fossil fumaroles" of the type described by Walker (1972a).

Type 1 flows are typical of denser-clast type pyroclastic flows (see Wright et al., 1980) and types 2 and 3 of pumice flows which form ignimbrites.

TABLE 8.5 Structural characteristics of pyroclastic flow deposits in the Tauranga Basin.

Deposit Code	Welded	Unwelded	Segregation Structures	Grading	Charcoal	Crystal rich (c >10%) total phenocrysts
Type F1	*	*	*		*	
Type F2		*	*		*	
Type F3		*				
Type F4		*				*
Type F5		*		*		
Type F6		*		*		
Type F7		*				

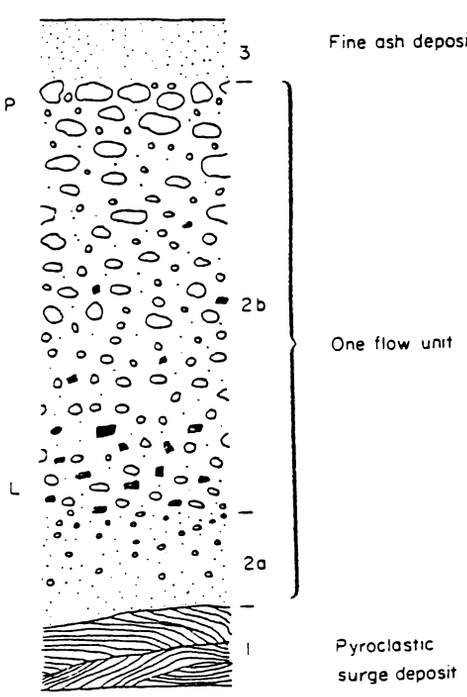


Fig. 8.1 Schematic section through the products of an ignimbrite eruption showing one flow unit with layers 2a and 2b, underlying pyroclastic surge deposit (layer 1), and fine ash deposit (layer 3);
P, pumice clasts;
L, lithic clasts
(After Sparks, Self and Walker, 1973).

TABLE 8.6 Criteria for distinguishing between pyroclastic flow and fall deposits in the Tauranga Basin (after Wright *et al.*, 1980)

Parameter	Pyroclastic flow	Pyroclastic fall
Relation to topography	Deposits are topographically controlled filling valleys and depressions	Deposits show mantle bedding, maintaining a uniform thickness over restricted areas while draping all but the steepest topography
Texture and bedding characteristics	Homogeneous - vitroclastic, and shows devitrification. However basal parts may show bedding and inverse grading occurs in <5 m thick deposits	Well bedded, normally graded bedding fines away from source.
Sorting	Poorly sorted $\sigma\phi \sim > 2.0$	Better sorted $\sigma\phi \sim < 2.0$
Extent and thickness	Extensive and thick	Extensive, but relatively thin
Mode of transport	Ground hugging - gas fluidized	Thrown into air
Direction	Follows pre-existing river valleys	All directions, but affected by wind
Other characteristics	Lithic and crystal enrichment towards the base. Segregation bodies and pipes often relatively enriched by lithics and/or crystals. Evidence of gas streaming, transporting relatively finer grains upwards. Welding, columnar jointing.	Crystal enrichment in some beds. Shower bedding. High vitric ash content. Sorting and grading which suggests gravitational sorting. Accretionary lapilli in some beds.

TABLE 8.7 Lithofacies of the upper Matua Subgroup

Physiographic model facies code	Facies code (adapted from Miall, 1978)	Lithofacies	Structures	Interpretation
PF_{pd}	Gms	massive matrix - supported gravels	laminations, horizontal stratification to massive	post-depositionally modified deposits
PF	Gms	massive matrix - supported gravels	inverse grading, pyroclastic flow emplacement type structures	distal ignimbrite
AF	SF_m	massive sands, silts	structureless to stratified (shower bedding)	air-fall tephra

used to record facies assemblage associations between fluvial and pyroclastic deposits (Fig. 8.15).

8.2.2 Types of pyroclastic flow deposits in the Tauranga Basin (Table 8.3)

Type F1 - (Ash - lapilli tuff breccia/lapilli - ash tuff breccia)

Texturally these deposits (Figs. 8.2A and 8.3) are poorly sorted, strongly cf. coarse-skewed, gravelly sands and sandy gravels. They are generally poorly welded to consolidated. Near the Wairoa River (U14/796 761) however, welded zones can be distinguished and divided into an upper moderately welded zone (∿ 30 m) showing columnar jointing (Fig. 3.6) and a lower poorly welded breccia zone (∿ 15 m). Large pumice clasts, commonly 5 to 10 cm diameter, are abundant and deposits generally contain ubiquitous glass globules (e.g. lining vesicle walls in pumice) and smaller glass fragments (i.e. acicular and flakes). Staining by iron oxides and sulphides is common, especially in and around clast and matrix-supported segregation structures which vary in form from cresentic to circular. Charcoal fragments are common, reaching 12 cm in diameter. The deposits are exposed at site localities along Belk Road, at Ruahihi and along the banks of the Wairoa River.

Type F2 deposits - (lapilli - ash tuff)

Texturally these deposits (Figs. 8.2B, 8.3 and 8.4) range from moderately sorted sands at the base (∿ 0.5 m) to poorly sorted slightly gravelly sands (upper zone 5-20 m). They occur stratigraphically below Type F1 deposits. Vertical variation is indicated by cross-bedding at the base grading upwards into a more homogenous deposit. Segregation structures are shown by elutriation in small vertical channels (∿ 0.5 - 5 cm wide and 20 cm long) at the base and

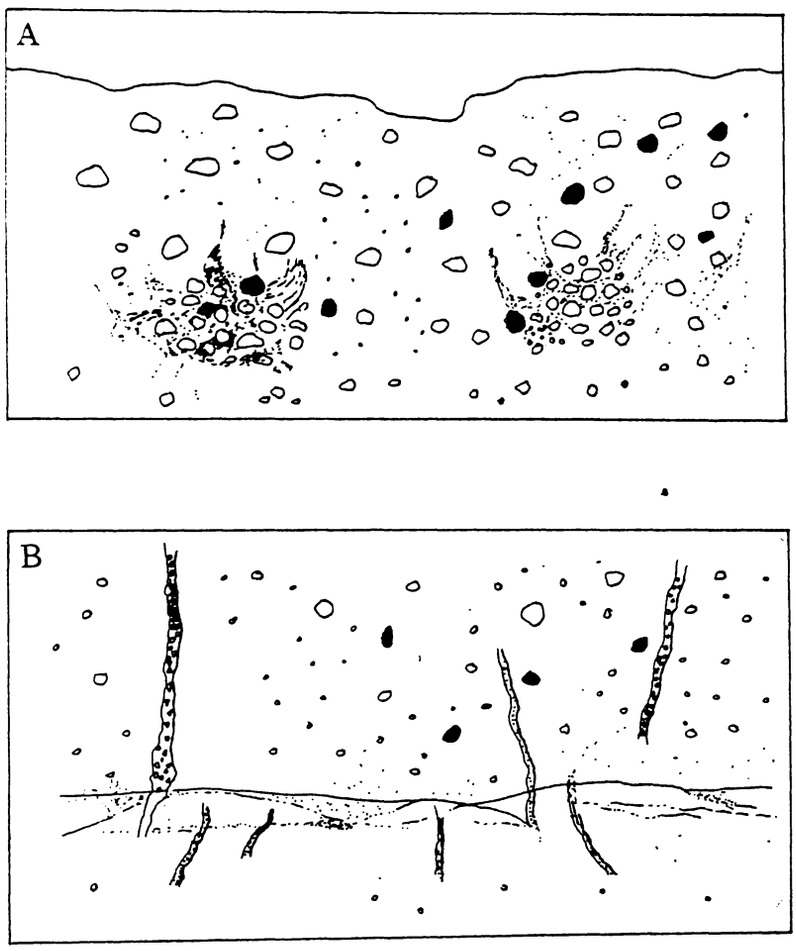


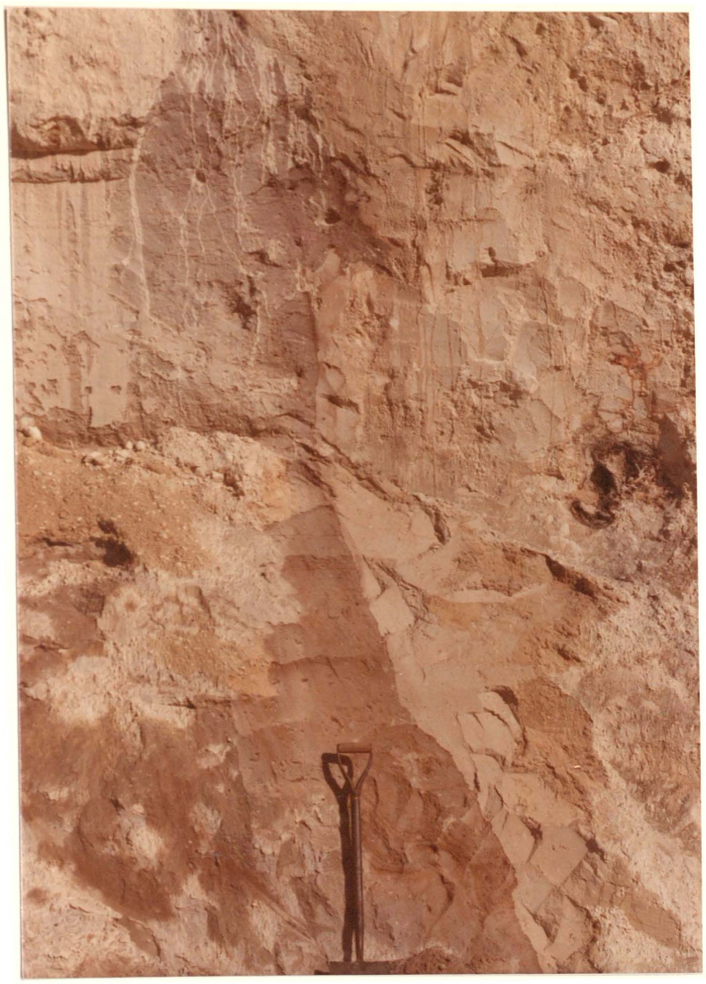
Fig. 8.2 Sketches showing the structure of the Type F1 and Type F2 deposits.

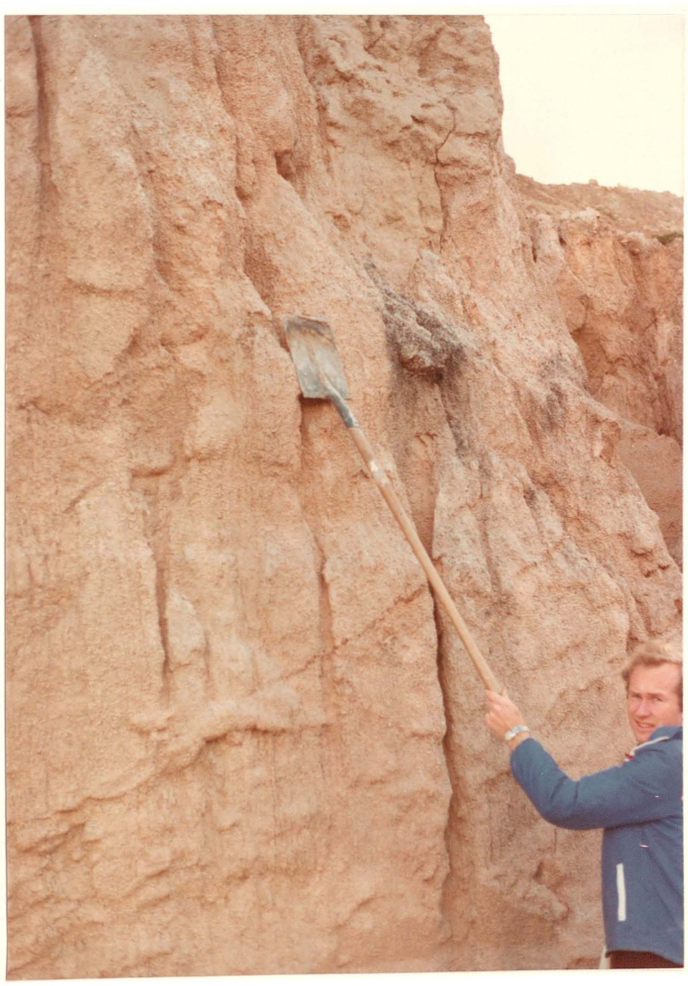
A - Type F1; ungraded, segregation structures, charcoal fragments.

B - Type F2; ungraded, segregation structures, charcoal fragments, basal cross-bedded structures.

Fig. 8.3 The Type F2 (Te Ranga Ignimbrite) deposit, scoured and separated by an erosional unconformity from the overlying Type F1 (Waimakariri Ignimbrite) deposit (at right) at Belk Road (U14/820770). Note the segregation structure and the charcoal fragments to the right. The Waimakariri Ignimbrite has infilled a valley at this site.

Fig. 8.4 The type F2 deposit (Te Ranga Ignimbrite) exposed at the Pyes Pa Road quarry (U14/845769).





larger structures which are more sinuous, lithic rich and reaching 2 m in length. Fluvial sedimentary structures are well developed on the surface and in the lateral extents of the deposits.

A high glass component throughout the whole of the deposits, consists of two types, vitreous fragments and abundant brown-black glass flakes. Obsidian rock fragments (1 - 5 mm) are also common. The high magnetite and obsidian content gives these deposits a distinctive grey/dark grey colour. Numerous charcoal fragments (0.5 to 10 cm) are also characteristic. Type F2 deposits are exposed at sites along Belk Road, at the Pyes Pa Road quarry and at the Melame Street quarry; well developed syndepositional structures are shown at the latter locality (Figs. 8.4 and 8.5).

Interpretation of Types F1 and F2 deposits

Both these deposits are thick, Type F1 ranging from ∿ 5 m to 40 m, and Type F2, from ∿ 2 m to 20 m. The internal structure and external morphology of these deposits may be explained by a fluidization type process (Sparks, 1978; Sheridan, 1979; Wilson, 1980). Fluidization is a state whereby a mixture of particles (solid or liquid) are suspended in a fluid phase (fluid or gas) such that the whole mass behaves as a fluid (Sheridan *et al.*, 1975). Segregation pipes, internal textural variations, such as those attributed to the selective removal of fine grains upwards from specific areas within the flow, and patterns of charcoal staining indicate that some type of vertical gas flow mechanism was operating at the time of emplacement (Sparks, 1978; Wilson, 1980). Wilson (1980) described segregation (e.g. "fossil fumorole"; Walker, 1972; Wilson, 1980) features as suggestive of flows with high internal gas flow rates and this would indicate an expanded and/or segregating flow type (Wilson, 1980). Fluidization gives the potential for this movement in which fluid

moving vertically through a particle aggregate exerts sufficient upward drag force on individual particles to be comparable with gravitational forces (Sparks, 1978). Distal flows are emplaced under laminar flow conditions (Wilson, 1980), their poor sorting (commonly $\sigma\ \phi$ >2.0) being attributed to high particle concentrations (Walker, 1971; Wilson, 1980) rather than turbulence.

Features characteristic and common to both the Type F1 and F2 deposits include:

- segregation structures
- charcoal staining and fragments
- homogeneity

Features characteristic of the Type F1 deposit include no visible grading and lateral (i.e. breccia lobes) and vertical (i.e. columnar jointing) zonation related to different degrees of welding. Type F2 deposits show textural variations, a thick ($\sim$ 10 m) ungraded layer above a thin ($\sim$ 0.5 m) well developed basal layer.

To explain these characteristics several processes may have supplied gas, and therefore aided the process of fluidization:

(1) Gas sources may have been provided internally by the gaseous diffusion and/or breakage and attrition of juvenile clasts, or externally by the entrapment of air at the flow front (Wilson, 1980). It is believed that the lowest part of a pyroclastic flow is least affected by gas flow processes from juvenile clasts but this systematically increases with the thickness of the flow (Sparks, 1978; Wilson, 1980). The fluidization process in which air is trapped at the flow head affects the whole flow thickness (Wilson, 1980; Wright, 1981);

(2) Charcoal fragments in both deposits, especially the Type F1 one(s), indicate that the incorporation and combustion of vegetation

was important (Wilson, 1980; Wright and Walker, 1981);

(3) Evidence presented in this study indicates that the Type F1, deposit flowed over an undulating topography and both Type F1 and F2 deposits probably flowed into pre-existing river valleys (Fig. 8.3).

(i) As the flow moved over or through a river channel, gaseous mechanisms were further enhanced by the heating of water (Wilson, 1980);

(ii) movement over rough topography also enhanced this gas supply (Wilson, 1980). The Type F1 deposit drapes topographic highs and fills depressions in the Ruahihi - Belk Road - Wairoa River area;

(4) on an appreciable slope, gas may induce secondary flows by slumping (e.g. subsidiary flows/Type F5 and Type F6).

Theoretical models (Sparks, 1978; Wilson, 1980) suggest that fluidization at the flow front may have resulted from a combination of the factors mentioned. The actual yield strength if low would have allowed internal structuring by a number of processes. Other factors such as shearing and frictional processes within the flow affect the flow profile and the degree of lateral mixing (Wilson, 1980). It is suggested by Wilson (1980) that any decrease in the velocity of a distal pyroclastic flow will reduce the amount of lateral mixing.

Syndepositional structures in Type F2 deposits

(i) Large-scale convoluted dish structures; (Fig. 3.5):

Well defined convoluted laminations occur in a zone at the top of Type F2 deposits (e.g. at the Melame Street quarry). These

convolutions may be several metres apart. Individual structures are 4 - 6 m from crest to crest, with amplitudes up to 6 m.

Laminations are continuous laterally for several metres and show only a very slight textural change from medium sand to very fine sand. Where the amplitude of the crest is highest, the curvature of the crest flattens out but the series of crests and troughs gives a general appearance of continuous undulation. Above these laminations are fluvial sediments

The laminations at the top of the Type F2 deposits indicate laminar grain flow. These flow lines could be caused by the flow movement in large waves (Davies *et al.*, 1978) or convoluted laminations may be derived from movement of the flow over topographic undulations or movement over rigid objects (Sheridan, 1979).

(ii) Cross bedding in pyroclastic flow deposits; (Fig. 8.5):

Near the base of the Type F2 deposits exposed at the Melame Street quarry is a well stratified, low angle cross-bedded layer (∿ 0.5 m thick) in which elutriation structures occur. The cross-strata have amplitudes between 3 and 10 cm and wavelengths approximately 15 cm. Sinuous segregation (i.e. elutriation structures) channels (0.3 - 1.5 cm wide and 10 - 15 cm long) occur perpendicular to the cross-strata and are filled with moderately well sorted coarse sand and slightly gravelly sands. Texturally the cross-bedded structures consist of moderately well sorted fine to medium sand sized grains, which pass abruptly upwards into more poorly sorted slightly gravelly sands.

The cross-bedding, elutriation structures and finer grain sizes in this layer possibly indicate the flow head deposits (Wilson, 1980) or the basal part of a pyroclastic flow unit (Sparks *et al.*, 1973;



Fig. 8.5 Cross-stratification at the base of the Type F2 deposit and vertical elutriation channels which intersect through these cross-beds.



Fig. 8.6 A post-depositionally modified Type F2 deposit showing a series of weathering bands. The deposit is exposed at the Pyes Pa Road quarry.

Sheridan, 1979; (Wilson, 1980). Sheridan (1979) has reported cross-stratification at the base of ash flow beds and laminations in the basal zone of ignimbrites. Sparks (1978) has also reported stratification as a result of pyroclastic flows interacting with water.

Post-depositional structures in Type F2 deposits

(i) Weathering bands : Differential weathering in the Type F2 deposit at the Pyes Pa Road quarry has produced many sinuous horizontal bands (Fig. 8.6) which often intersect, cross over and thin out. Bands are 4 - 8 cm thick and spaced 6 - 15 cm apart. They are consolidated and weathered and contain a greater clay and silt content (∿ 25%) than the adjacent gravelly sand deposit, so that they protrude slightly. Coarser grained vertical segregation channels pass up through these bands.

This type of structure develops in response to a fluctuating water table enhanced by the permeability of the deposit. Repeated cycles of wetting and drying have caused the water level to consistently shift, the effect being a series of indurated weathered bands. In the vicinity of the segregation channels and the bands, a marked decrease in grain size does not occur. This is possibly explained by the greater permeability in the coarser grained segregation channels, than that area outside the channels. These indurated bands may therefore be an equilibrium response to a number of factors, such as, permeability, hydraulic conductivity, grain size, and climate.

Type F3 - lapilli - ash tuff breccia)

Texturally these deposits (Figs. 8.7 and 8.8A) are poorly sorted gravelly sands with no vertical variation in properties. Pumice clasts, 1 - 6 cm across are matrix-supported through the entire deposit which may reach a thickness of 30 m. These deposits are exposed at



Fig. 8.7 The type F3 deposit showing pumice clasts set haphazardly in a glass shard-pumice-rock fragment matrix (petrofacies C).

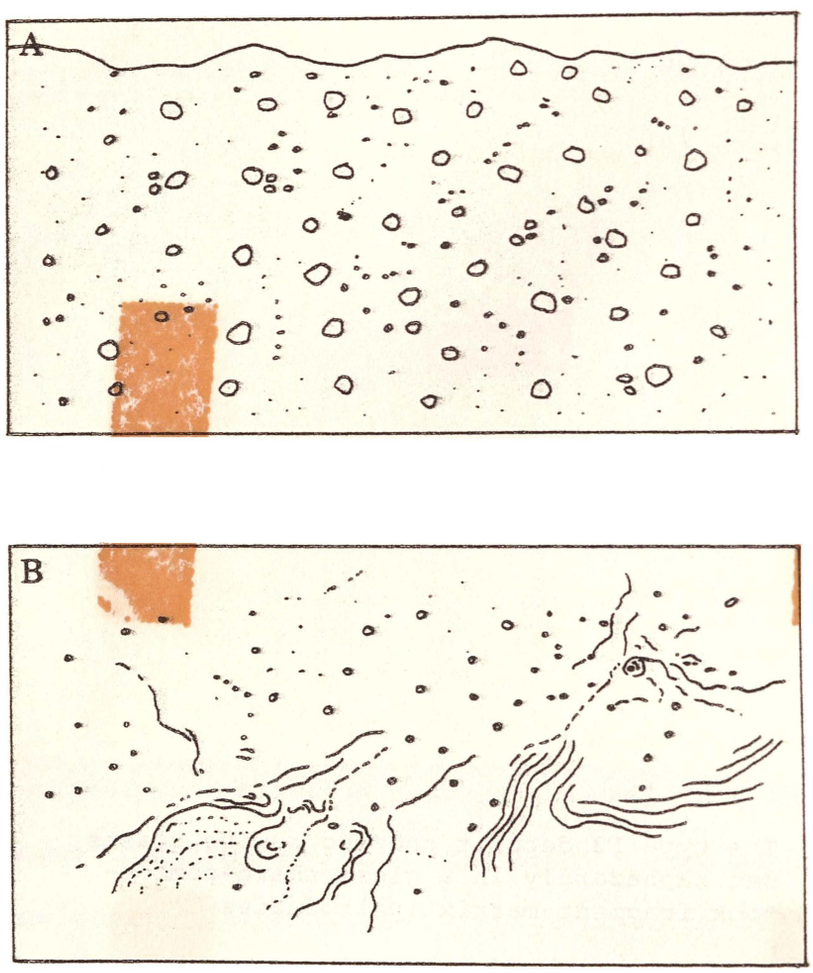


Fig. 8.8 Sketches showing the structure of the Type F3 and Type F4 deposits.

A - Type F3; ungraded, homogeneous with pumice clasts set haphazardly in fine matrix.

B - Type F4; ungraded, lithic and crystal rich, leisegang phenomenon.

several sites in the Te Puna area.

The Te Puna Type F3 deposit is ungraded, unwelded and shows homogenous characteristics. These deposits are interpreted as lobes of pyroclastic flow material. It is unlikely that these flows were substantially fluidized by exsolving gas and this could be due to a number of factors including cooling, lack of gas, high particle concentrations and matrix strength (i.e. high yield strength). Grain-dispersion force and buoyancy mechanisms may also be important in the transportation of pumice lapilli and blocks up to ∿10 cm (Sparks, 1978; Wilson 1980).

Type F4 - (ash - lapilli tuff)

Type F4 deposits (Figs. 3.3 and 8.8B) are structureless and contain abundant crystals and lithics as well as pumice and glass. They are poorly sorted, consisting of slightly gravelly sands, and are strongly weathered showing leisegang phenomena. These deposits are exposed in the Cambridge Road area.

The Type F4 deposit is interpreted as the basal part of a pyroclastic flow unit and is severely eroded, with fluvial sediments (∿ 5 m thick) overlying and derived from this deposit. The fluidization head model of Wilson (1980) is one possible explanation for this crystal and lithic enrichment. In a fluidized flow with a high degree of lateral mixing (e.g. caused by shearing) material will be transported to the flow front and agitated. During agitation, large amounts of fines are generated and lost in an overlying dilute cloud, while the coarse/dense fraction is deposited at the base of the flow by gravitational processes. A high vitric loss, greater internal mixing and systematic removal of fines (> 4 ϕ) could be expected (Sparks 1976, 1978; Wilson, 1980). This mechanism can be partly attributed to a "caterpillar track mechanism" (Wilson, 1980) and

to density differences within the matrix (Wilson, 1980).

Type F5 - (ash - lapilli tuff breccia/lapilli - ash tuff breccia)

The deposit, which is 5 m thick, comprises two units which unconformably overlie a lignite seam at Omokoroa (Figs. 8.10 and 8.12A). A large part of the upper unit (2 m thick) has been removed by erosion while the lower unit is intact. The lower unit is characterised by:

(i) Inverse grading (Fig. 8.9) - coarse skewed, poorly sorted gravelly sand at the base passes up through matrix - supported gravelly sand, to matrix-supported sandy gravel at the top of the unit. Pumice clasts averaging 4 cm and as large as 10 cm, and lithics up to 3 cm in diameter, are concentrated at the top of the unit. This pumice concentration layer is 20 cm thick and below this the deposit is more homogenous.

(ii) Compositional variation - the deposit is rich in pumice - glass shard - lithics - feldspar - quartz. The composition at the top of the deposit is pumice rich with abundant lithics and glass shards.

(iii) Internal structure (Fig. 8.10) - large spheroidal bodies, 20 - 80 cm in diameter, similar in appearance to rip-up-clasts but comprising matrix-supported coarse pumice fragments (average size 3 mm) are surrounded by a finer pumiceous matrix, in that part of the deposit which is largely homogenous (i.e. 2 - 5 m thick). Sand-blasting by wind and erosion by saltspray has removed finer grain sizes from around the spheroidal bodies and effectively sculptured the outside of these structures. The surface form has been further enhanced by iron oxide staining.

The most characteristic feature of the Omokoroa Type F5 deposit is the extreme inverse grading and distinct concentration zones of



Fig. 8.9 Inverse grading in the Type F5 deposit is a characteristic feature of pyroclastic flow deposits exposed in coastal cliff sections. Pumice clasts averaging 4 cm and lithics up to 3 cm are recorded at the top of each unit.

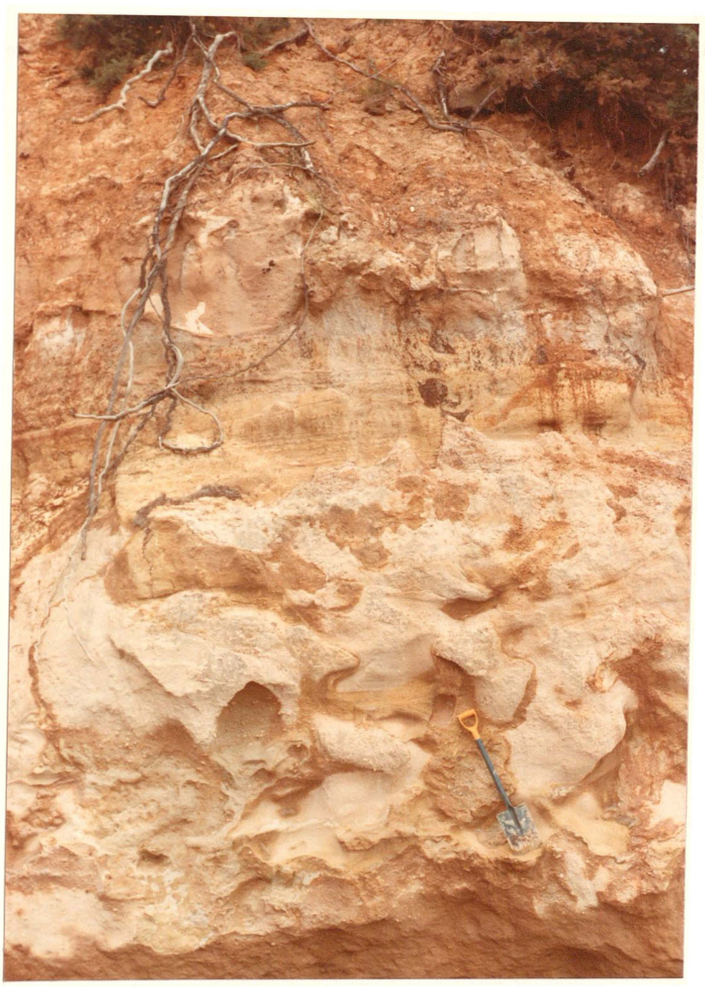


Fig. 8.10 The Type F5 deposit showing a chaotic assemblage of spherical structures possibly indicative of some type of turbulent emplacement.

pumice and lithics. The departure from homogeneity (e.g. grading) may be explained by gaseous flow mechanisms (Sparks *et al.*, 1980; Wilson, 1980). A unique feature of the deposit is the chaotic assemblage of spherical bodies throughout the entire deposit, enclosing coarse grains of pumice lapilli and ash compared to the matrix. The form of these bodies suggests turbulence.

The vesicular pumices (low specific gravity) have maintained their buoyancy in a fluid mass while lithics (high specific gravity) have been transported upwards, possibly by gas flow, shearing and grain-dispersion mechanisms. The lithic concentration zone and the range of lithic sizes at the top of the lower unit, and the random distribution of grain sizes throughout the unit below the upper concentration zone, however, cannot be directly attributed to gaseous flow. It is possible that the upward movement of lithics was in effect due to the upward transportation of pumice, and non-vesicular grains were subsequently depleted by gravitational and sieving-type processes in the upper part of the unit. Because of the pumice concentration at the top of the unit it is assumed that lithic grain sizes smaller than a specific size moved downward between pumice clasts.

The energy level of the transporting fluid can be indicated to some degree by C-M plots of grain size (Wright 1981; Wright and Walker, 1981). Because grain sizes of vesicular material reached 10 cm in diameter and non-vesicular grains of 3 cm are recorded it is assumed that the energy levels were comparable with pyroclastic flows deposited further inland in the Tauranga Basin (e.g. Type F1 and F2).

The emplacement mechanism appears to have involved some type of turbulence, possibly due to the interaction of the pyroclastic flow with vegetation and water. It is assumed, therefore, that the

Omokoroa deposit was enriched by gas as the flow moved over a swamp (i.e. the lignite facies underneath the deposit) incorporating gas by the heating of water (Wilson, 1980).

Other processes which may have aided the supply of gas to the Omokoroa pyroclastic flow are discussed later under the Type F6 deposit.

Post-depositional structures of the Type F5 deposit

Type F5a : Omokoroa deposit

This ∿4 m thick deposit is exposed at Omokoroa (Fig. 3.11). It is characterised by two zones:

(i) upper zone 1 - 3 m thick

(ii) lower zone 0.6 - 1.4 m thick

(i) The upper zone is largely massive, coarse-skewed, lithic-rich and poorly sorted. A gradual upwards increase in grain size occurs in two layers near the base of the zone, each ∿20 cm thick. Pumice clast size increases upwards from <0.2 cm to ∿0.5 cm. In these two layers gravelly sands at the base pass up into matrix-supported, gravelly sands and sandy gravels. Several fluvial intrusion structures appear at the top of the zone, and vague sedimentary laminations and massive lenses of sediment infill parts of the deposit.

(ii) The lower zone is normally to inversely graded, poorly to moderately sorted, lithic rich and stratified, with both horizontal bedding and low-angle cross-strata enhanced by iron oxide staining, iron pans and cementation. Lensing of coarse sediment occasionally occurs between these beds. In normally graded beds near the base, gravelly sands pass up through slightly gravelly sands to moderately

sorted sand. Inversely graded beds ∿5 cm thick show sands passing up into slightly gravelly sands. The upper part of the graded beds are often accentuated by an iron pan.

The Omokoroa deposit has fluvial characteristics which indicate its reworked nature. Sedimentary intrusions, lenses of coarse grains, low angle and planar stratification near the base overlain by massive, poorly sorted material are suggestive of a fluival/slump deposit.

This heterogenous deposit has been derived from lateral erosion of the Omokoroa pyroclastic flow deposit (i.e. Type F5). Inversely graded layers possibly indicate slumped pyroclastic flow material which has retained part of its original emplacement form.

Type F5b : Motuhoa Island deposit

The deposit (Fig. 8.11) is exposed in a cliff section on Motuhoa Island. It consists of two zones:

(i) upper zone 5 - 6 m thick

(ii) lower zone 2 m thick

(i) The upper zone is massive and consists of poorly sorted, coarsely-skewed, slightly gravelly sands. The zone is lithic-rich, consisting of rhyolite and weathered Te Puna ignimbrite fragments. Crude laminations spaced ∿1 cm apart are expressed by elongated and stretched pumices 2 - 3 cm long. Pumice clasts are aligned parallel to each other and dip along their horizontal long axis 8^{o} to the north. This pumice elongation and the incorporation of mud clasts (1 - 2 mm diameter) is significant in that it possibly indicates some type of earth deformation. Less common are spherical pumice clasts, 1 - 2 cm in size.



Fig. 8.11 The Type F5b deposit, interpreted as a debris flow deposit or post-depositionally modified Type F5 deposit contains stretched pumice clasts. An isoclinal fold (in line with the hammer) occurs at the base of the debris flow and the Type F5b deposit overlies fluvial sediment.

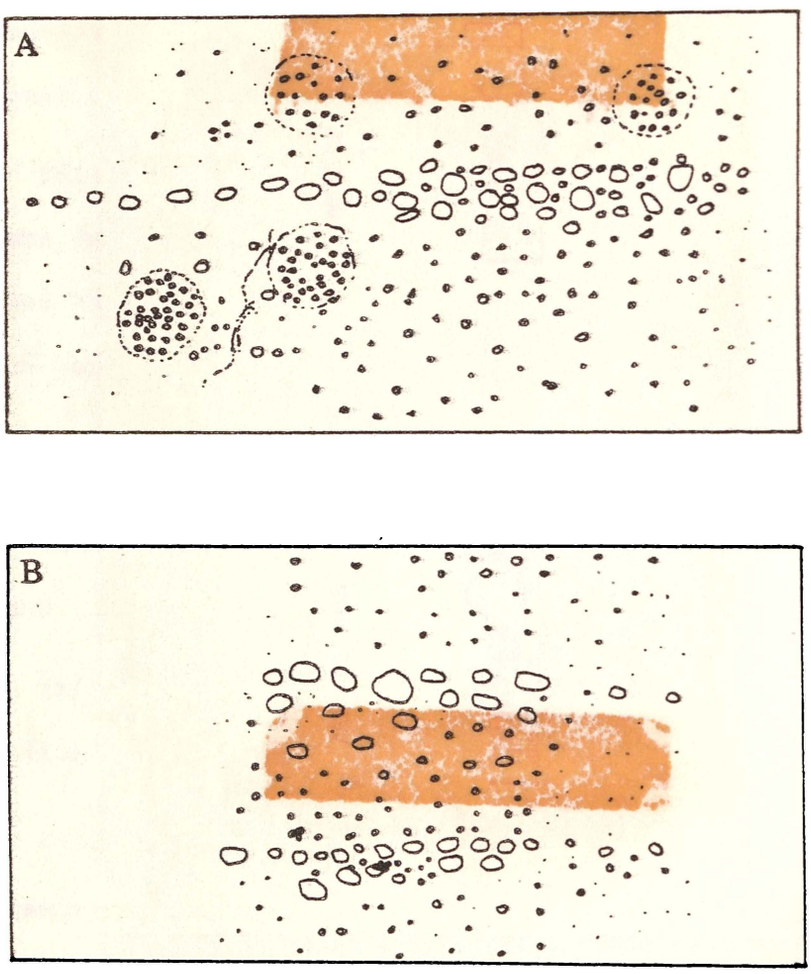


Fig. 8.12 Sketches showing the structure of the Type F5 and Type F6.

A - Type F5; inversely graded, lithic concentration zones, spheroidal structures set chaotically throughout deposit.

B - Type F6; inversely graded with pumice concentration zones. Normally graded lithics.

(ii) The lower zone consists of poorly to moderately sorted, slightly gravelly to silty sands which are both normally to inversely graded. The zone is characterised by horizontal bedding, low-angle cross-bedding and deformation structures similar to recumbent isoclinal folds. The middle section of the zone is faulted (see section 7.2.3 and Fig. 4.9). A massive, weathered silty sand layer (15 cm thick) occurs above both this faulted section and low angle cross-bedded sands.

The Motuhoa deposit, F5b, mineralogically and texturally similar to both Omokoroa deposits, F5 and F5a, shows many features suggesting it was emplaced as a debris flow/slump deposit. These include : laminar shear planes, often showing vague stratification along which pumice clast long axés have been aligned (Carter, 1975; Naylor, 1980); sedimentary fold structures, for example, recumbent and curled structures immediately below the zone containing stretched pumice clasts; and mud or weathered ignimbrite clasts incorporated in the deposit.

Interpretation of Type F5a and F5b deposits

A number of debris flow/slump deposits are identified in the Omokoroa and Te Puna areas. All have been derived from distal lobes of ignimbrites.

A debris flow can be defined as a slurry matrix incorporating a range of clast sizes (Carter, 1975). Many of the structures (e.g. inverse grading) in these deposits indicate the way in which the deposit came to rest or "froze" (Carter, 1975). Inverse grading can also be achieved by particle support mechanisms as the flow is in motion. Several interrelated processes are considered to induce material to slump or flow (Hampton, 1975; Carter, 1975; Naylor, 1980) and cohesive strength and buoyancy are considered to be primary

support mechanisms (Hampton, 1975).

Movement of material from the lateral margins and/or surface of ignimbrites in the Tauranga Basin may have been triggered by one, or a combination of the following:

earthquake jolts and localised small-scale faulting (e.g. Motuhoa Island); syntectonic deformation in underlying sediment (e.g. Motuhoa Island); failure along planes of weakness between consolidated and unconsolidated sheets of sediment (e.g. Omokoroa); loss of support as a result of erosion, for example undercutting by streams (e.g. Omokoroa).

It is assumed that once triggered, the homogenous matrix acts as the interstitial fluid medium, and grains can be thought of as being rafted in the fluid matrix. The movement of the debris probably occurs by laminar shear (e.g. Motuhoa Island), (Hampton, 1972).

Type F6 - (ash-lapilli tuff breccia/lapilli-ash tuff breccia)

The pyroclastic flow deposit (Figs. 8.12B and 8.13) which is exposed in a coastal cliff section at Matua reaches a thickness of 2.5 m and consists of three units. Each unit is recognised by variations in grading.

A representative unit is characterised by:

(i) Inverse grading - poorly sorted, matrix-supported, slightly gravelly sands at the base grade upwards through gravelly sands into matrix-supported pumice gravels. Pumice clasts at the top of the unit reach 4 cm across, while lithics (< 4 mm) show normal grading near the base and then a uniform grain size distribution towards the top of the unit.

(ii) Composition and Texture - large pumice clasts occur in a glass



Fig. 8.13 The Type F6 deposit exposed at Matua (U14/849878) consists of three inversely graded units. The pyroclastic flow deposit overlies low angle cross-stratified and planar stratified slightly gravelly sands.



Fig. 8.14 Chalazoidite bed underlying the Waimakariri Ignimbrite and fluvial sediments at Ruahihi (U14/795761). Accretionary lapilli average 20 mm diameter.

shard-lithic rich matrix. Matrix composition (glass shard - pumice - lithics - quartz - feldspar) is largely homogeneous throughout the deposit. At the top of each unit there is an increase in the mud content in the matrix, caused primarily by the weathering of pumice clasts which are very vesicular to fibrous in form.

The Type F6 deposit is interpreted as a pyroclastic flow deposit because of its structural (e.g. grading) and compositional characteristics. The deposit can be separated into three distinct units, each showing inverse grading of pumice, normal to homogeneous lithic grain size distribution and a distinct pumice concentration zone. The appearance of stratification in this deposit is due to the superposition of a number of flow units, and individual deposits generally lack internal stratification. Inverse grading indicates that internal sorting processes have occurred, which are possibly related to the fluidization behaviour (Sparks, 1978; Sheridan, 1978; Wilson, 1980) of the flow during emplacement. The deposit unconformably overlies fluvial cross-bedded gravelly sands. It is possible then, that the Matua pyroclastic flow deposit was enriched by gas as it moved over or through shallow water (e.g. in a river channel). Evidence presented by Sparks *et al.* (1980a; 1980b) indicates that pyroclastic flows may enter shallow water without an explosive interaction.

Two other processes may have aided the supply of gas to the Omokoroa and Matua pyroclastic flows:

(1) subsidiary flow detachment (i.e. thin pyroclastic lobes) and enrichment of gas supply from the upper part of the main pyroclastic body after detachment, results in the development of an overlapping series of thinner subflows (Aramaki, 1963; Wilson, 1980).

(2) A thin flow, after detachment, would be susceptible to incorporating air from the flow front (Sparks, 1978; Sheridan, 1979; Wilson, 1980).

A grading mechanism ultimately resulting from gas supply from several sources [including (1) and (2)] is discussed below:

Increasing gas flow velocities in a pyroclastic flow will result in a higher degree of fluidization which will allow the yield strength to decrease (Sparks, 1978; Wilson, 1980). This would enable a gas grading mechanism to operate, sorting out various grain sizes by gaseous flow. According to Wilson (1980) the fluidization behaviour with increasing gas flow velocities may lead to both expanded and segretating types of ignimbrites and this could explain the inverse grading and pumice concentration zones in the Type F5 Omokoroa and Type F6 Matua deposits. These mechanisms enable certain grain sizes to be detectably graded and finer grain sizes are often moved upward by gas flow processes while coarser dense grains may be sorted out by gravitational processes. The upward movement of low density pumice may be analogous to that process which acts on finer grain sizes (Wilson, 1980). However, grain-dispersion mechanisms and variations in shear stress acting on larger grain sizes in the flow cannot be discounted (Sparks, 1978; Wilson, 1980).

Type F7 deposit

A thin (< 1 m), massive deposit at Omokoroa interbedded with pyroclastic fall deposits shows features more characteristic of a pyroclastic flow deposit (Fig. 8.10). The deposit is indurated, poorly sorted and although highly weathered, pumice clasts up to 4 mm occur. The composition is mainly glass shard and pumice. Gradual thickening in depressions and thinning over ridges could possibly indicate a flow origin.

8.3 PYROCLASTIC AIR-FALL DEPOSITS

8.3.1 Pyroclastic air-fall deposits in the Tauranga Basin (Tables 8.3, 8.6, 8.7)

Type A1 - (Vitric ash tuff)

These deposits (Fig. 3.16) range from ∿5 to ∿60 cm thick, are principally rhyolitic and contain variable amounts of clay. They are consolidated, massive pumiceous sandy silts and silts, usually associated with paleosols. Massive beds are often intercalated with less weathered, moderately sorted, normally graded shower bedded units, commonly of coarser texture. The composition is usually glass shard - feldspar - quartz - clay minerals - heavy minerals. These deposits are exposed at coastal sites in the Omokoroa, Matua, Maungatapu and Welcome Bay areas.

Type A2 - (Vitric ash tuff/tephra and Vitric lapilli - ash tuff/tephra)

Deposits often exhibit stratification and normally graded horizontal laminations 0.2 - 1 cm thick. The deposits may be up to ∿50 cm thick, occassionally comprising of normally graded layers, up to ∿ 10 cm thick. The composition is glass shard - pumice, while texturally the deposits are moderately to poorly sorted pumice sands to slightly gravelly sands containing pumice lapilli. Laminations often alternate between more poorly sorted beds and well sorted beds giving an appearance of planar laminations with contrasting light and dark shaded bands.

Interpretation of Type A1 and Type A2 Deposits

Many pyroclastic deposits show features more characteristic of aerial deposition (Table 8.6), for example shower bedding and mantling of the topography, and are therefore interpreted as being emplaced by

pyroclastic fall mechanisms (Wright *et al.*, 1980). The particles are sorted due to their fall velocity and these deposits generally exhibit better sorting ($\sigma \phi$ <2.0), typically ranging from moderately to well sorted. The deposits in the Tauranga Basin conspicuously mantle the topography, and normally graded stratified beds enhance this characteristic particularly at the Matua coastal site. Air-fall tephra appears to drape the topographic irregularities of the underlying fluvial and pyroclastic flow deposits.

However many of the deposits in the Tauranga Basin are highly weathered and poorly sorted beds are common in massive air-fall tephra and tuffs (e.g. in exposures along the Omokoroa coast). The poor sorting may be attributed to a number of factors (Walker, 1971):

(1) fine-grained ash accumulating above coarser ash, with subsequent movement of fine material downward into the coarser resulting in poorer sorting.

(2) Several beds at Omokoroa show a mixing of grain-sizes in the upper parts of the bed. This may reflect some form of bioturbation which is attributed to rootlets or micro-organisms. Many deposits lack bedding, or have become structureless in specific areas of the deposit.

Compared to the pyroclastic flow deposits, the consolidated and least weathered air-fall deposits consist of finer grain-sizes. The average size is usually coarse silt to fine sand but the grain-size ranges from clay (.004 mm) to lapilli sized (up to 4 mm) pumice. Thin clay beds interbedded between ash deposits may be loess (e.g. Omokoroa Point) and possibly result from selective sorting by wind following deposition.

The geometry and size of pyroclastic fall deposits reflect the

height to which the grains attained in the eruption cloud, and the wind velocity and direction (Wright *et al.*, 1980). Sorting also reflects these factors (Walker, 1971). At several locations (e.g. at Matua and Omokoroa) tephra beds are of a uniform thickness and thick unweathered deposits (∿ 1 m) are built up of a sequence of thin (∿ 1 cm) beds. Pyroclastic fall deposits typically show well developed paleosols, which are likely to have formed over a 15 to 50 ky period (D.J. Lowe, 1983, pers. comm.). However the time needed for a paleosol to develop is highly speculative, as it depends on a number of variables such as climate and time.

Chalazoidite/Accretionary lapilli structures

Accretionary lapilli (Fig. 8.14), (i.e. chalazoidites, pellets, mudballs; ∿8 - ∿38 mm) are scattered randomly or concentrated in clusters throughout fine-grained ash material. Each ball consists of a homogeneous nucleus (4 - 12 mm) surrounded by several white-grey accretionary layers; individually these accretionary layers are thin (1 - 0.1 mm) and concentric. Outer layers may collectively reach thicknesses of 18 mm and show a foliated appearance. The set of concentric skins is usually continuous, although individual skins are sometimes discontinuous. Texturally the central nucleus is coarser (> 0.04 mm) while the outer layers become progressively fine (0.05 to 0.004 mm). These balls are texturally and physically dissimilar to the moderately to poorly sorted matrix (generally ranging in grain size from 0.09 to 0.008 mm) in which they are contained. These chalazoidite beds are found ∿ 50 cm beneath the Type F1 pyroclastic flow deposit (equates with the Waimakariri Ignimbrite) near the Wairoa River/Ruahihi area, above the Te Puna Ignimbrite on Motuhoa Island (Fig. 7.15), and are covered by ∿20 m of air-fall tephra and fluvial deposits at Omokoroa (see Chapter 3).

(i) Chalazoidite Formation Process (Table 8.8)

Mechanisms of formation of chalazoidites are not fully understood and four schools of thought exist as to their possible origin. These are:

(1) Accretion on the ground of fresh ash around a nucleus blown by the wind or rolled downslope (Moore *et al.* 1962; Kennedy, 1980);

(2) absorption of fresh ash by the water of a fallen/falling raindrop (Moore *et al.*, 1962);

(3) lapilli formed in water by gentle agitation of a nucleus in contact with unconsolidated ash (Moore *et al.*, 1962);

(4) accretion of moist ash in an eruptive cloud to form mud pellet rains. (Moore *et al.*, 1962; Barter, 1976; Self and Sparks, 1978; 1979).

Berry (1928), Moore *et al.* (1962), Barter (1976), and Self and Sparks (1978, 1979) gave evidence for an ash cloud origin and volcanic hail hypothesis.

The circumstances for formation may be by the explosive interaction of magma and water (Self and Sparks, 1978; 1979), by flushing out fine ash in the eruptive cloud (Self and Sparks 1978; 1979) or by formation of clumps of ash by flocculation in a steam-rich eruption column (Lowe, 1981). These clouds were thought to be of a high temperature (Berry, 1928; Moore *et al.*, 1962; Barter, 1976) in which ash particles grew by accretion as they descended through the cloud. A low temperature cloud was postulated by Battey (1942) whereby accretionary lapilli or "pisolites" formed by accretion in a water-laid environment in which the solid particle grew by rolling. This theory would explain discrete layers or bedded and ellipsoidal chalazoidites. However a rain/steam enriched-cloud theory is favoured because it explains differences in the texture and the physical appearance between accretionary lapilli and the matrix. It is also substantiated by field evidence (Moore *et al.*, 1962; Self and Sparks,

TABLE 8.8 Chalazoidites : Four phase development in an ash cloud

Phase	Mechanism	Characteristics of Chalazoidite
1. Rapid nucleus aggregation	Condensation $H_2O(g)$	Coarse grained Homogeneous No mineral orientation
2. Fall phase	low temp. high altitude ash high relative humidity ↓ high temp. low altitude ash low relative humidity	Selective accretion
3. Outer shell selective accretion (i) Aerial	(a) Accretion around nucleus in fall	(i) mud pellet rains, continuity of skins spherical chalazoidites
3. Outer shell selective accretion (i) Aerial	(b) Accretion around raindrops	(i) mud pellet rains, continuity of skins spherical chalazoidites
3. Outer shell selective accretion (ii) Terrestrial (e.g. waterlaid environment)	(c) Accretion by grain movement (e.g. rolling, agitation)	(ii) Discrete layering, ellipsoidal chalazoidites, discontinuous thickness of skins
4. Deposition in ash bed	(a) Layered	Preservation
4. Deposition in ash bed	(b) Random	Preservation

1978, 1979; evidence from Mt. St. Helens' eruptions).

(ii) Chalazoidite beds in the Tauranga Basin

Because of the continuity of the accretionary layers outside of the nucleus, the spherical nature of the chalazoidites and their ultimate preservation it is concluded that they formed before entering the matrix. The chalazoidites show no preferred orientation and do not reflect depositional layering. The accretionary layers have been sorted and particle sizes become progressively finer away from the nucleus.

Chalazoidite beds in the Tauranga Basin are likely to have been water saturated and soft when accretionary lapilli entered the deposit at random. This is indicated by load deformation and intrusion by sands which overlie the chalazoidite bed on Motuhoa Island, flattening the chalazoidites and disrupting their outer skins. It is probable that ash cloud conditions and intensity and duration of rainfall are important controls on chalazoidite formation.

8.4 CONCLUSIONS

Figure 8.15 presents some of the facies relationships recorded at various localities, between fluvial lithofacies defined in Tables 7.7 and 7.10 and the pyroclastic lithofacies defined in Table 8.7. Much structural variation is recorded in the pyroclastic flow deposits and this diversity is generalised upon by the lithofacies code. The facies variation in the pyroclastic flow deposits is the result of complex interactions between many processes and the deposits have anomalous textural and morphologic characteristics. Fluvial erosion has also affected the thickness of deposits at various localities. Due to this variation in both fluvial and pyroclastic deposits, several models are proposed (Fig. 8.15).

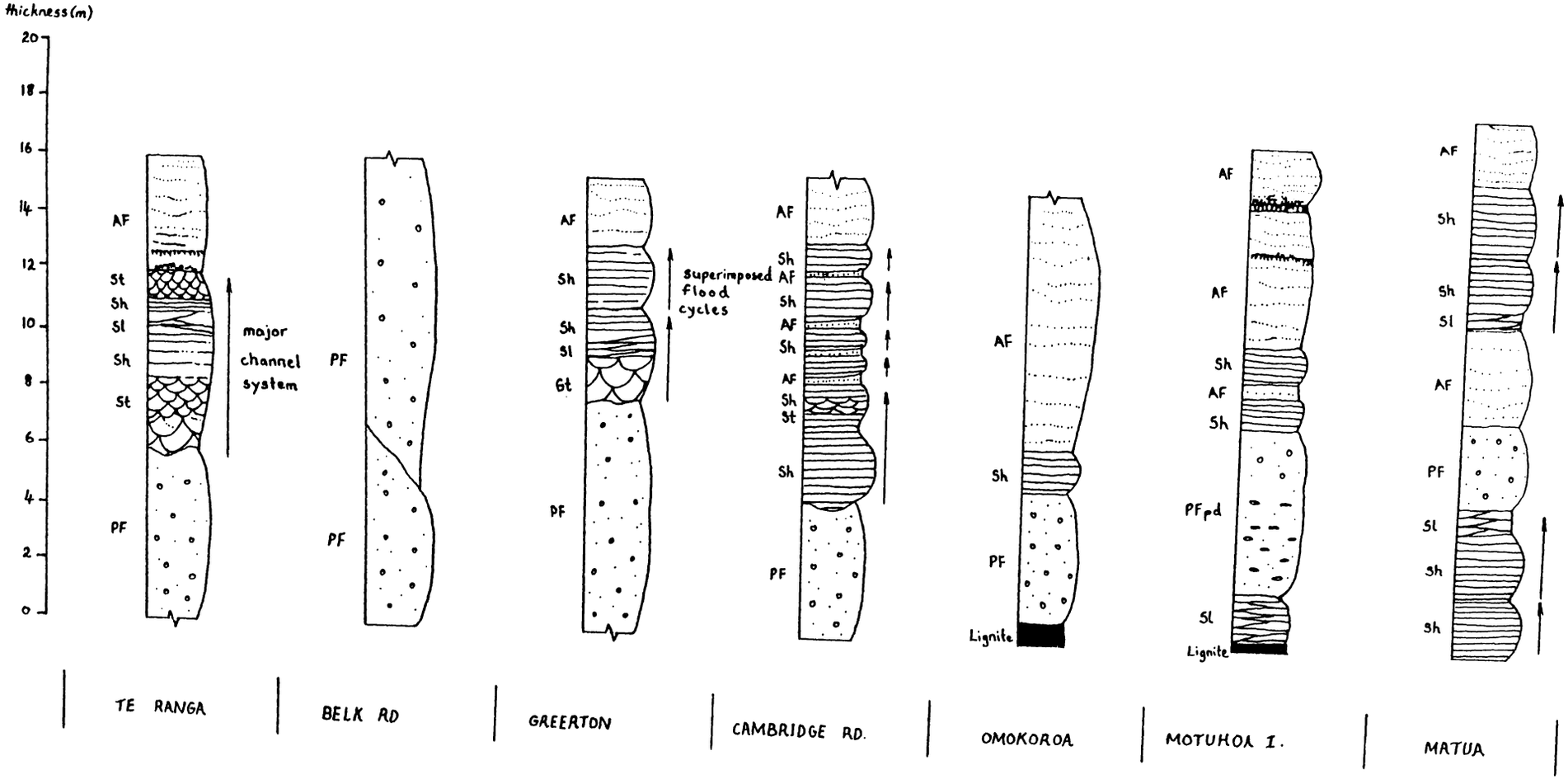


Fig. 8.15 Lithofacies diagram showing the relationships between pyroclastic and fluvial deposits at various localities in the southeastern part of the Tauranga Basin.

CHAPTER NINE

ENVIRONMENTAL SYNTHESIS

AND GEOLOGIC HISTORY

9.1 INTRODUCTION

During the Tertiary the landscape in the Coromandel-Tauranga region had been dominated by Beeson's Island Volcanics (16 - 17 m.y. B.P.) which covered greywackes and argillites of Jurassic age (Healy *et al.*, 1964; Adams *et al.*, 1975; Kear and Schofield, 1978). The age determinations on the andesites from Coromandel suggest volcanism began about 16 m.y. B.P. throughout the region, then ceased in the north, but continued in the south up to about 7 m.y. B.P. (Fig. 9.1); (Rutherford, 1978). About 6 m.y. B.P. extensive rhyolitic eruptions broke out, initiating a major change in the type of volcanism. Also at this time (5 - 6 m.y. B.P.; Cole, 1979) movement on the Indian and Pacific plate margins was compensated for by the creation of tensional graben structures in eastern Coromandel, perhaps forming the Tauranga Volcanic Zone some 2 - 3 m.y. B.P. (Fig. 9.2); (Cole, 1979). The rhyolitic eruptions may have been related to this tensional faulting episode. Minden Rhyolite overlies andesitic eruptives in the Tauranga region and the rhyolites exposed in the central parts of the Basin probably were active about 4.34 m.y. B.P. (Rutherford, 1978), an age based on fission track data on obsidians from Mt Maunganui. West of the Basin the Waitawheta dacite domes and flows have K-Ar ages ranging from 4. 0 - 3.75 m.y. B.P. (Stipp 1968; Richards *et al.*, 1966; Adams, 1975). Renewed andesitic and dacitic volcanism commenced in the Te Puke area to the south of the Tauranga Basin about 2.54 m.y. B.P. (K-Ar age, Stipp, 1968).

Since the beginning of the Quaternary the Tauranga Basin has been subjected to a complex sequence of events with overlapping periods of volcanic and sedimentary activity (Table 9.1). Three main periods are herein defined for convenience of discussion:

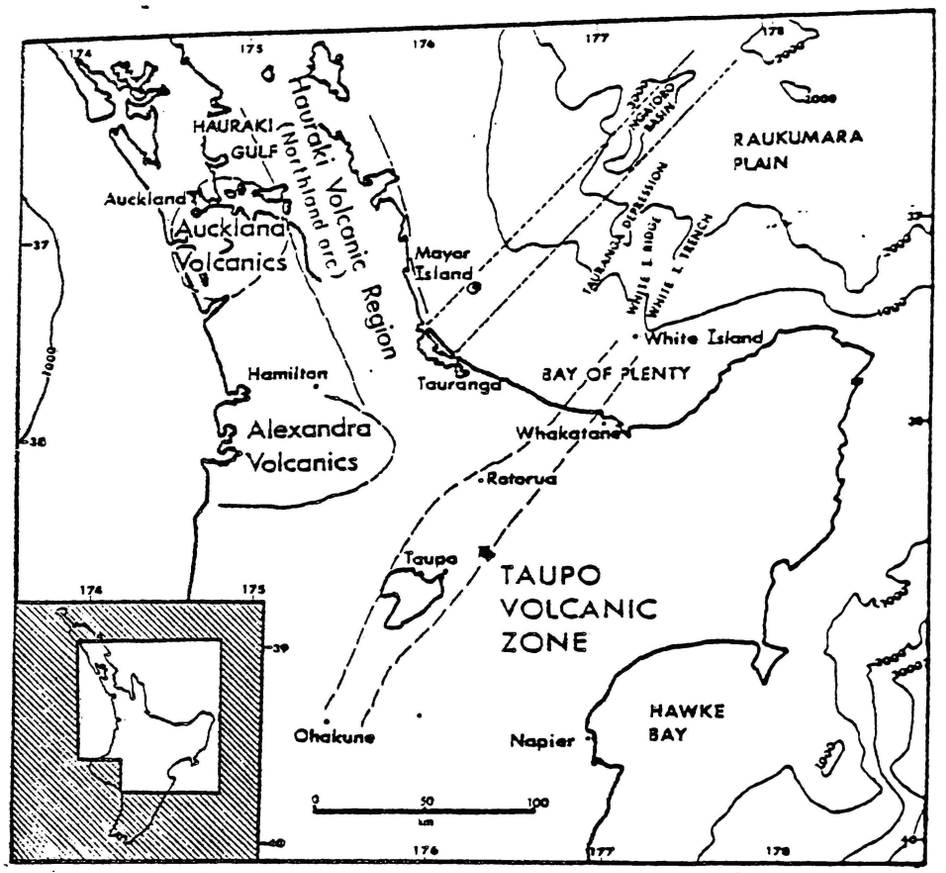


Fig. 9.1 Location of Taupo Volcanic Zone and its relationship to other volcanic regions of the North Island and offshore topography (Bathymetry shown in meters); (from Cole, 1979).

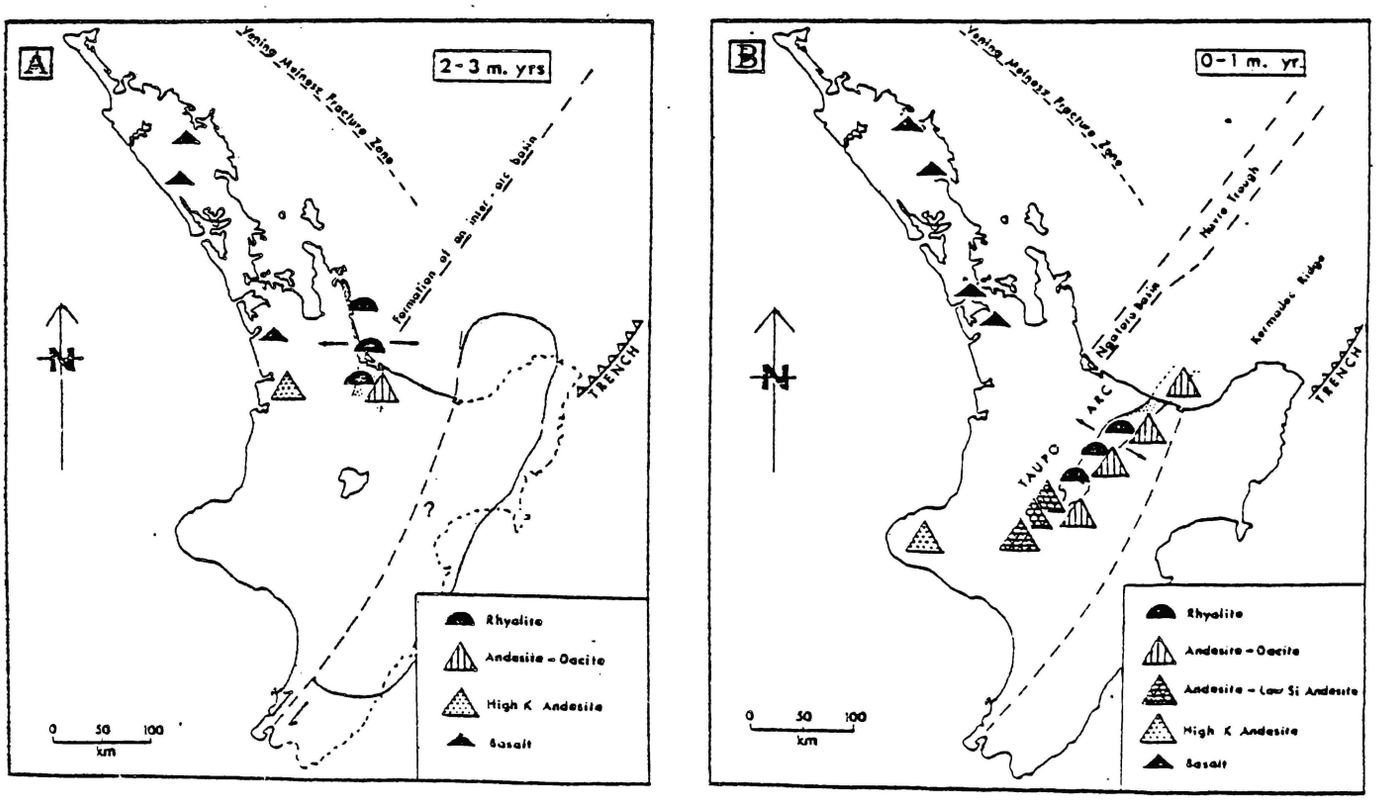


Fig. 9.2 Relationship of volcanism to the structural development in the North Island during the Late Cenozoic.

A - The Tauranga Volcanic Zone formed ∿2 - 3 m.y. ago.

B - The Taupo Volcanic Zone formed ∿1 m.y. ago.

TABLE 9.1 Summary table of events in the Tauranga Basin during the Quaternary

AGE (m.y. B.P.)	SERIES/EPOCH	VOLCANIC EVENT	VOLCANO-SEDIMENTARY EVENTS	AIR-FALL DEPOSIT	GROUP	SUBGROUP	TECTONIC EVENT
0.01	Holocene		(3)	Kaharoa Ash Taupo Lapilli			
0.02				Rotorua Ash			
0.03				Mangaone Lapilli			
0.04				Rotoehu Ash			
0.1		Mamaku Ignimbrite (0.14) Waimakariri Ignimbrite (0.18)		Hamilton Ash			
0.2			(2)		Tauranga	Matua	
0.3		Te Ranga Ignimbrite (∿0.3)		Pahoia tephars			
0.4		Te Puna Ignimbrite (∿0.4)					
0.5	Pleistocene						
0.6		Wairoa Ignimbrite (∿0.6)					
0.7							subsidence in the Tauranga area
0.8		Waitewariki Ignimbrite (0.84) Papamoa Ignimbrite (∿0.84)	(1)				
0.9							uplift of the Kaimai Range continues
1.0						Volcaniclastic sediments intercalated with Aongatete Ignimbrite	
1.1							
1.2		Aongatete Ignimbrite (1.26)					
1.3							
1.4							
1.5							
1.6							
1.7							
1.8							
1.9							
2.0							

(1) an early ignimbrite period;

(2) a late ignimbrite period;

(3) upper Matua Subgroup period.

Sedimentation was initiated in the Basin by the onset of volcanism in the early Pleistocene and high rates of sedimentation have continued since that time. Summary of events since the Middle Pleistocene is presented in Fig. 9.6 at the end of this chapter.

9.2 EARLY IGNIMBRITE PERIOD

The early ignimbrite period began with the eruption of the Aongatete Ignimbrite (1.26 m.y. B.P.; Healy, 1967). An apparent westward thickening of this ignimbrite away from the Tauranga Basin (e.g. Kaimai drillhole data) indicates a possible Coromandel source. It is assumed, therefore, that the ignimbrite flowed eastward into the Tauranga area and evidence from drillholes suggests that the ignimbrite is extensive in the Basin and was possibly emplaced to beyond Matakana Island. The surface form in the Basin must have been largely flat or sloping at a very low angle to the east, although Minden Rhyolite domes (4.3 m.y. B.P.) must have formed a higher relief than their present elevation, and presented major obstacles for early ignimbrites flowing into the Basin.

The Aongatete Ignimbrite initiated a renewed volcanic phase which lasted until approximately 0.86 m.y. B.P. A period of erosion followed the emplacement of the ignimbrite, removing parts of the weakly welded portions and depositing a large proportion of the derived sediment out onto the continental shelf and, to a lesser degree, into the Basin.

Eruption of the Waitearíki Ignimbrite (0.84 m.y. B.P., Kohn *et al.*, unpublished) probably coincided with the onset of volcanism in the Central Volcanic Region (Fig. 9.3); (Cuthbertson, 1981). The Waitearíki

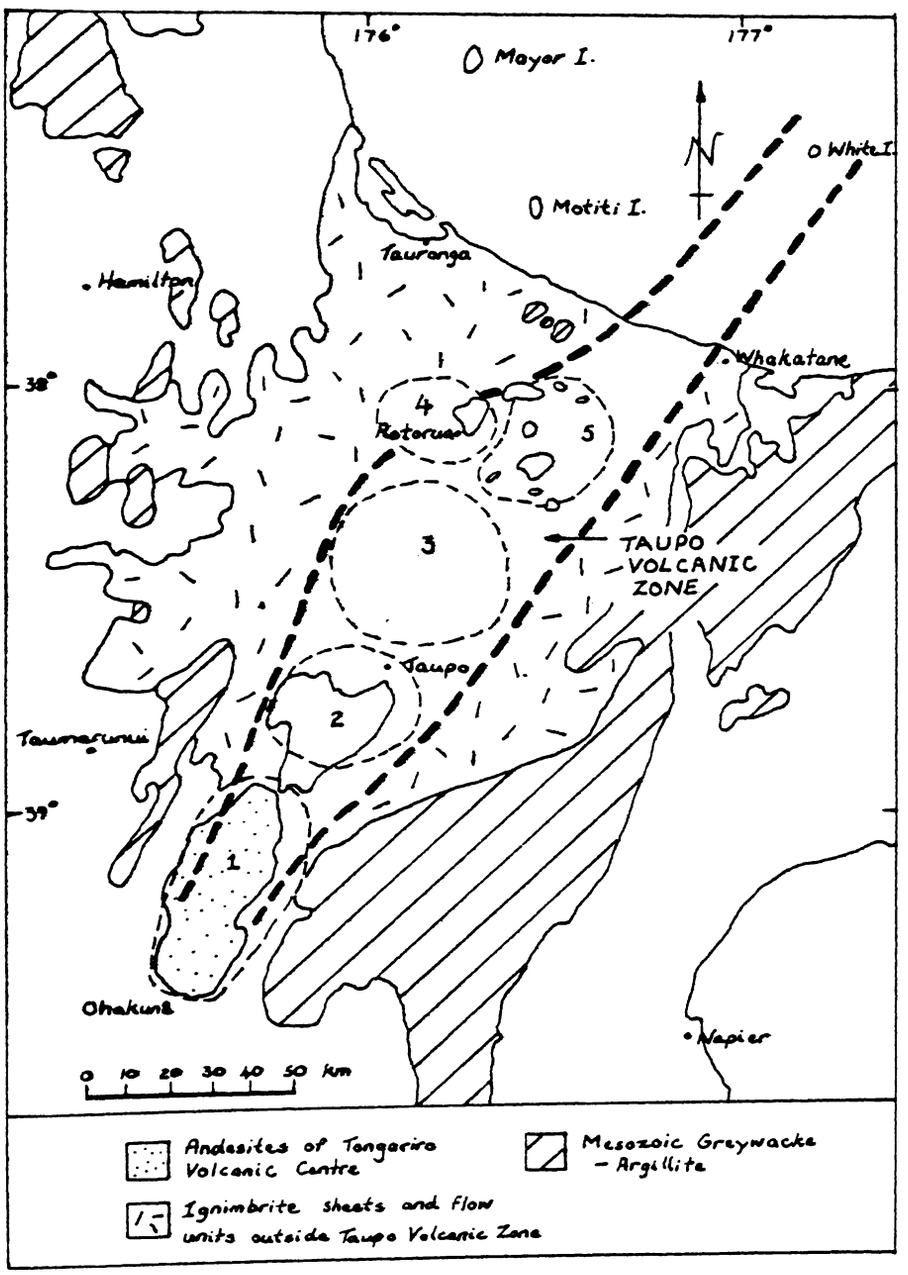


Fig. 9.3 Taupo Volcanic Zone and Volcanic Centres within this Zone.

1 - Tongariro Volcanic Centre;
2 - Taupo Volcanic Centre;
3 - Maroa Volcanic Centre;
4 - Rotorua Volcanic Centre;
5 - Okataina Volcanic Centre.

(Adapted from Cole, 1979).

Ignimbrite spread northwards into the Basin and covered an eroded surface relief of the Aongatete Ignimbrite, and then flowed eastwards in the Basin before terminating (suggested by present field investigations and from regional mapping by B.F. Houghton, pers. comm., 1982). Regional mapping suggests that the present Kaimai Range was elevated at this time in an area in line with the northern extremities of the Basin, which influenced the flow direction of the ignimbrite and caused it to thin over topographically higher ground. In an area south of Katikati, entry into the Basin was unrestricted and it is presumed that uplift of the Kaimai Range in the north preceded that to the south. After emplacement of the Waitearíki Ignimbrite the southern part of the Kaimai Range was uplifted by at least 450 m, indicated by a down-faulted block of the ignimbrite in the Hauraki Depression (Cuthbertson, 1981). The Waitearíki Ignimbrite crops out on the Kaimai Range but no displacement of the Waitearíki on the Tauranga Basin side of the Range is recorded, which suggests that the uplifted horst was simply tilted towards the Basin. The Waitearíki Ignimbrite effectively formed a local basement throughout the Tauranga Basin at this time, and possibly extended out onto the present continental shelf. By about 0.75 m.y. B.P. the Range had been uplifted sufficiently to represent a barrier to the Ongatiti Ignimbrite, which is well exposed in the Hauraki lowlands.

The Tauranga Basin has continued to subside since uplift and tilting of the Kaimai block ($\sim$ 0.84 m.y. B.P.), the influence of this tectonism being recorded in the Basin by rapid facies changes in the products of volcanism and by intercalated sedimentary deposits. The rate of sedimentation has undoubtedly been influenced by this subsidence. Ignimbrites entering the region from the Taupo Volcanic Zone appear to have been ponded within the Basin by a northern barrier (i.e. the present day Kaimai Range). This could be explained by uplift of the southern parts of the Kaimai Range during post-Waitearíki Ignimbrite emplacement time.

The Kaimai Range appears to gradually terminate in the south, in an area convergent with the Mamaku Plateau. It has been suggested that the throw on the faults in the Hauraki Rift die out southwards (Fransen, 1982) underneath the Mamaku Plateau, which may account for the decreasing surface relief.

The progressive uplift of the Kaimai Range caused the Waitearikí Ignimbrite to also become progressively tilted, thus increasing its susceptibility to widespread erosion. Several streams were diverted into the Basin from the Whakamarama Plateau, and in an area just south of Te Puna and extending to Welcome Bay, a major discharge centre developed in which large quantities of sediment were supplied into a major paleobasin. Other major contributions of sediment came from the Kaimai Ranges and the Minden Rhyolite domes proximal to the Basin.

The unwelded Wairoa Ignimbrite was deposited (0.84 m.y. B.P. > Wairoa Ig. > ∿ 0.5 m.y. B.P.) in the Basin as a thin deposit (σ.20 m) over a pile of Waitearikí Ignimbrite-derived sediments. The paucity of outcrops of Wairoa Ignimbrite in the Basin suggests that it was severely eroded, and was covered in turn by a sequence of fluvial sediments containing well developed paleosols, which are subaerially exposed to a thickness of 20 m near the Tauranga Dump. After emplacement of the Wairoa Ignimbrite successive air-fall tephra sequences became interbedded with alluvial sediments, and material subject to active erosional processes was reworked. Near the end of the early ignimbrite period large quantities of fluvial sandy and gravelly sediments were transported in braided/ephemeral channels towards the continental shelf. This sand was possibly shifted back towards the Basin during storm conditions and higher sealevels which inundated bifurcating channels proximal to the coastline. As coastal sand barriers became established, favourable conditions evolved for swamp development in

topographic depressions and low-lying flat areas. Stratigraphic evidence indicates that these areas were entrenched by tributaries flowing towards the main paleobasin near Te Puna and Matua, and that they were discharge sinks for streams which flowed across the Whakamarama Plateau.

The Kaimai Range had possibly reached an elevation close to that of today during the early ignimbrite period (0.84 - ∿ 0.5 m.y. B.P.). This is suggested from evidence of andesitic conglomerates (containing cobbles up to 15 cm diameter) derived from the Kaimai Range deposited in channels and interbedded with fluvial sediments derived from the erosion of the Wairoa and Waitekariki Ignimbrites, 2 km south of Katikati. Andesitic gravels occur at depth in several drillholes throughout the Tauranga Basin (Table 9.2). The elevation of the Range would have had to have been sufficient during the early ignimbrite period for andesite to be eroded from this area, transported and rounded in streams which flowed perhaps ∿ 3 km from source, and deposited as gravels and cobbles.

9.3 LATE IGNIMBRITE PERIOD

This is a loosely defined period but stratigraphic evidence suggests it began ∿ 0.5 m.y. B.P. During this period the unwelded Te Puna Ignimbrite (∿ 0.36 m.y. B.P., Kennedy, 1980) was emplaced, its age being based on correlation with a tephra-flow unit near Tirau having a fission-track age of ∿ 0.35 m.y. B.P. (Vucetich *et al.*, 1980). Stratigraphic relationships of the Te Puna Ignimbrite with air-fall tephra units in the Tauranga Basin indicate the ignimbrite is ∿ 0.4 - 0.5 m.y. old. This ignimbrite flowed northwards in the Basin, then divided into subsidiary flows, some of which spread northeastwards. Channel deposits, interpreted from drillhole data and topographic irregularities at the base of the ignimbrite, suggest that the environment before the

Table 9.2 Table showing recorded appearances of andesitic gravels in the stratigraphic record (adapted from unpublished borehole data, N.Z.G.S, Rotorua).

Grid Reference	Depth (m)	Area and Description
N57/406794	39.0 - 51.2	Katikati: andesitic river gravel.
U14/802876	103.6 - 109.7	Snodgrass Road, Te Puna: andesitic conglomerate with sandy matrix.
U14/871883	103 - 109.7	Otumoetai: a range of principally rounded rock fragments, white pumiceous rhyolite, conspicuous dark grey andesite, grey or pink lithic rhyolite, fluvial gravel.
U14/872883	96.0 - 115.8	Otumoetai: grey lithic rhyolitic and andesitic granules and pebbles at 96.0 - 115.8 m.
N57/406794	3.0 - 8.0	Sharp Road, Katikati: andesitic conglomerates (rounded) interbedded with fluvial sediments derived from the erosion of the Wairoa Ignimbrite.

ignimbrite was deposited was one of an anastomosing network of streams with local ponding in swamp areas. Swamp deposits immediately underlying and beneath the Te Puna Ignimbrite in the Te Puna and Omokoroa areas covered sedimentary deposits derived from the earlier ignimbrite period.

At Omokoroa two pyroclastic flow units are recorded which have been successively buried upwards by 15 m of air-fall tephra, interbedded weathered loess deposits, and possibly a further pyroclastic flow unit (< 15 cm thick; > 150 k.y.). The Omokoroa area has largely escaped fluvial erosion since the beginning of the late ignimbrite period (i.e. evidence from the preservation of ash deposits) except for fluvial reworking in air-fall tephra and pyroclastic flow deposits just after emplacement of the two pyroclastic flow units. These two pyroclastic flow deposits at Omokoroa are correlated with an ignimbrite cropping out in the Te Puna area (forming a constructional terrace adjacent to the present Wairoa River). The lateral parts ($\sim$ 1 - 3 m a.s.l.) of the Te Puna Ignimbrite exposed near the Wairoa River show fluvial scouring and channel infill deposits. Air-fall tephra deposits have been completely removed at this location.

The Tauranga Basin continued to subside during this period causing active erosion and accumulation of sediment in a major paleobasin near Te Puna and Otumoetai. A slump deposit post-dating small-scale normal faults (10 cm throw) at Motuhoa Island may testify to tectonic instability in the region after emplacement of the Te Puna Ignimbrite. Small scale slump deposits were common in the Basin, possibly being activated by earthquake jolts or by undercutting in streams causing material to be rafted.

A continuous core at Otumoetai indicates that there were repeated cycles of fluvial deposits with alternating tephric material throughout

this period, and the coarseness of deposits demonstrates both a high input of sediment and probably high energy floods. The dynamic depositional environment may have been related to alternating 'glacial' and 'interglacial' periods which ultimately affect the rate of erosion and sediment supply (Fig. 9.5), while contemporaneous and continued subsidence accommodated the bulk of material entering the system. Evidence that parts of the Basin were affected by glacially-induced changes in sea level at intervals during this period comes from estuarine sediments interbedded with swamp and fluvial deposits. These types of facies are recorded below the Te Puna Ignimbrite at Omokora, and in drill cuttings at two Te Puna locations. It appears that estuarine facies were more common at the beginning and towards the end of the late ignimbrite period, corresponding to 'interglacials'. Before emplacement of the Te Puna Ignimbrite and at the end of this period, swamp conditions existed in many localised parts of the Basin, particularly at Te Puna, where fibrous wood fragments and peat occur at several levels in the drillholes. The kinds of swamp vegetation can be indicative of the prevailing climate regime. Pollen analysis of the lignite underlying the Te Puna Ignimbrite at Omokoroa suggests the temperature in the Tauranga Basin was $3^{o}C$ lower than the present mean annual temperature of $14^{o}C$ (Hull, 1977), possibly indicating stadial conditions.

Emplacement of the unwelded Te Ranga Ignimbrite (older than Mamaku Ignimbrite which is dated at 0.14 m.y. B.P., Murphy and Seward, 1980) occurred near the end of this period. When this ignimbrite flowed northwestwards across the Basin it covered laterally extensive and thick accumulations of older sediments (mainly fluvial) derived from the Te Puna, Wairoa and Waitearikí Ignimbrites. It also came to abut against the dipping Waitearikí Ignimbrite forming the Whakamarama Plateau. The Te Ranga Ignimbrite probably formed an extensive sheet

($\sim$ 200 km^2) over the southwestern portions of the Basin (extending south under the Mamaku Ignimbrite). Progressive downcutting by braided streams removed large quantities of Te Ranga Ignimbrite in successive floods, until steep-sided valleys were incised into the landscape. These became established in vegetation in the southwestern areas of the Basin and indicate more stable features. This topographic form suggests a period of volcanic quiescence and decreasing sedimentary activity.

The Waimakariri Ignimbrite sheet (> 0.14 m.y. B.P.; Fransen, 1982) was emplaced over an eroded topography of the Te Ranga Ignimbrite, and also lapped onto the dipping Waiteriki Ignimbrite in the west. It obliterated vegetation cover and produced a barren landscape (Fig. 9.4). A chalazoidite bed underlying the Waimakariri Ignimbrite exposed near the Wairoa River at Ruahihi is possibly related to this eruption. A correlative chalazoidite bed is found above the Te Puna Ignimbrite at Te Puna and on Motuhoa Island. The Waimakariri Ignimbrite was possibly deposited during a cold climate (Fransen, 1982) and presumably formed a more extensive plateau ($\sim$ 300 km^2) than is indicated by present exposures in the southwest of the Basin. Presently, the Waimakariri Ignimbrite dips into the Basin at 3^{o} to the north. North-trending streams dissecting the Mamaku Plateau have exposed the Waimakariri Ignimbrite in cliffs at several locations. Outcrops throughout this southwestern section of the Basin are generally moderately to poorly welded, and vertical jointing occurs in a welded, 40 m thick outcrop at Ruahihi. Several localities at Ruahihi indicate that the ignimbrite was ponded in topographic depressions and became draped over topographic highs. At Belks Road the Waimakariri Ignimbrite forms a moderately welded, charcoal-enriched deposit (30 m thick) which has flowed into a valley cut into the Te Ranga Ignimbrite. At this location the ignimbrite has scoured the walls of the valley, and possibly a spur running down into the floor of the valley.

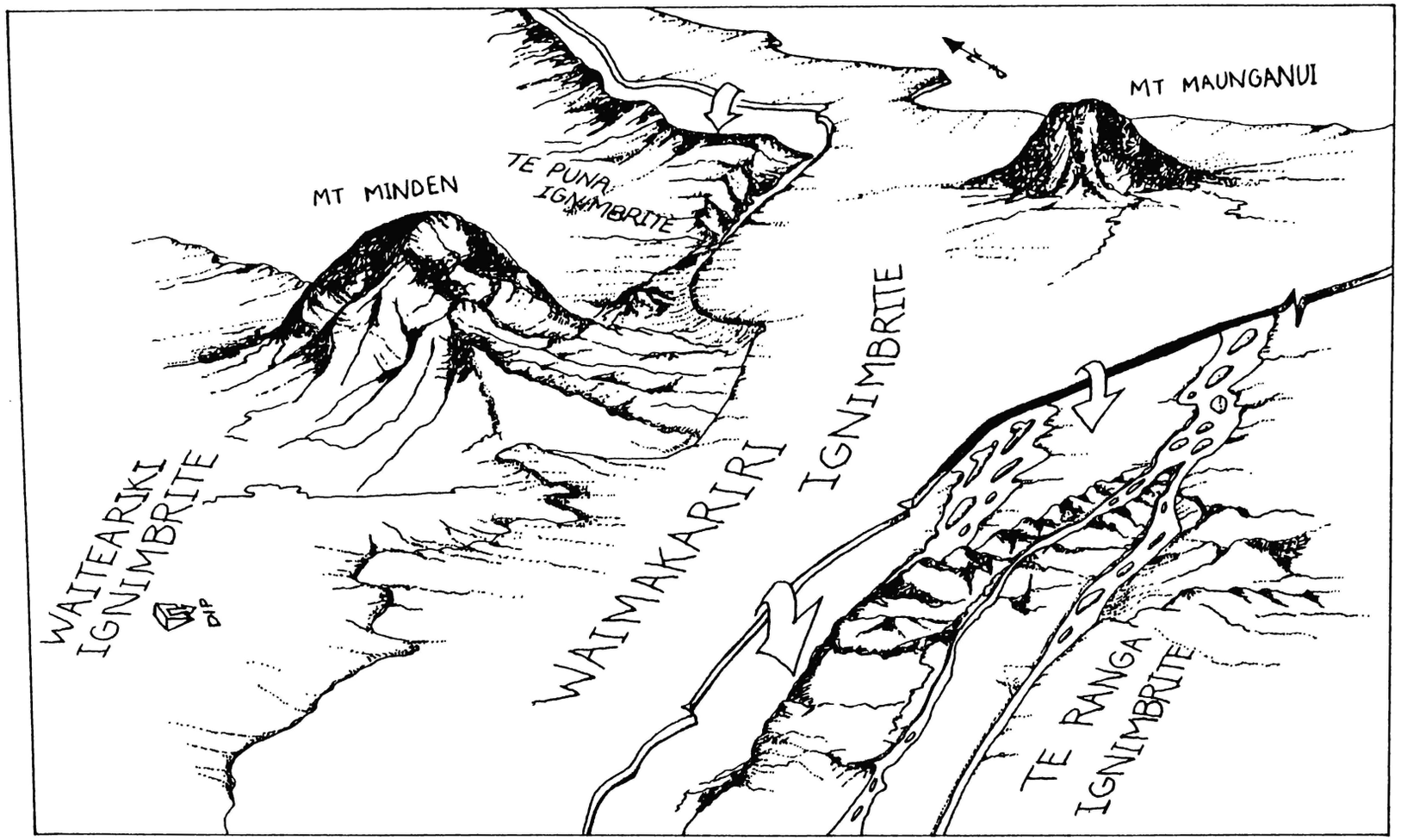


Fig. 9.4 A sketch showing the Waimakariri Ignimbrite (∿0.18 m.y. B.P.) immediately after emplacement over the Te Ranga Ignimbrite. Both these ignimbrites have been completely eroded out west of the Wairoa River, but once possibly onlapped onto the older Waitearíki Ignimbrite (∿0.84 m.y. B.P.). The arrows indicate the hypothetical lifting of the sheet to expose the underlying deposit.

The Mamaku Ignimbrite (0.14 m.y. B.P.; Murphy and Seward, 1980), which crops out in an area between McLaren Falls and Pyes Pa, presumable extended further into the Tauranga Basin shortly after (∿ 0.02 m.y.; Fransen, 1982) emplacement of the Waimakariri Ignimbrite. This is suggested because of its present thickness (∿ 40 m) in the Pyes Pa/ Oropi Gorge Road areas, just south of the map area. The only subaerial exposures of sediment eroded from a Mamaku Ignimbrite source occur above the Waimakariri Ignimbrite at Ruahihi and in road-cuts along Belks Road. It appears that the Mamaku Ignimbrite has been completely eroded from the lower parts of the Basin.

9.4 UPPER MATUA SUBGROUP PERIOD

An informal upper Matua Subgroup is defined as a thick (up to 40 m) sequence of sediments which are represented by subaerially exposed parts of the Matua Subgroup throughout the Tauranga Basin.

This period began after emplacement of the Waimakariri Ignimbrite (∿ 0.18 m.y. B.P.) which was subsequently severely eroded to re-expose the underlying Te Ranga Ignimbrite in the south of the Basin. Active fluvial erosion also re-exposed ignimbrites emplaced in earlier periods, producing interfingering lobes of sedimentary and ignimbrite material. There has been a continual degradation of pyroclastic and fluvial deposits and terrace structures since the beginning of this period up to the present. A number of rhyolitic tephras were deposited throughout the Basin during the late ignimbrite period and the upper Matua Subgroup period. These are the Pahoia tephras, which form thick (∿ 10 m) exposures, especially in the Omokoroa and Maungatapu areas. The Pahoia tephras are extensively covered by Hamilton Ash beds (commonly 1.0 m thick) in some parts of the Basin. Elsewhere, Hamilton Ash beds (< 1 m) rest directly on upper Matua Subgroup fluvial sediments

exposed in several coastal cliff sections (e.g. Te Puna, Matua). The removal and preservation of tephra sequences in different parts of the Basin reflects erosion by shifting streams and local base-level changes (e.g. due to subsidence and eustatism). Air-fall tephra deposits were removed or partially removed in some areas (e.g. topographic depressions) which being preserved in other parts of the Basin (e.g. swamp areas). Areas in which ash beds were preserved included those which largely escaped active erosion, as on exposed braided bars and terrace surfaces. Preservation of underlying material may have also been aided by the development of soils and subsequent deposition of fluvial sediment and/or air-fall tephras.

Valley incision from fluvial erosion throughout the upper Matua Subgroup period produced a variable topography (e.g. terraces) during degradation. The mantling of ash beds over several terrace heights, and subsequent fluvial erosion of some tephra sequences in valleys and low-lying areas, is suggested as the reason for the absence of specific tephras at various localities (Fig. 9.6).

Sedimentary characteristics of the upper Matua Subgroup indicate periods of episodic flooding and high discharge rates which necessitate intense rainfall. It is inferred that climatic seasonality and an environment largely devoid of vegetation are both very important controls on the high sediment input into the Basin and the braided nature of the environment (Picard and High, 1973).

At the beginning of the upper Matua Subgroup period ($\sim$ 0.16 m.y. B.P.) streams began to dissect the Waimakariri Ignimbrite surface. The Tauranga Basin was presumably affected by a glacial period (Fransen, 1982) which produced conditions favourable for intense weathering in the Central North Island (Fig. 9.5). Braided streams became quickly

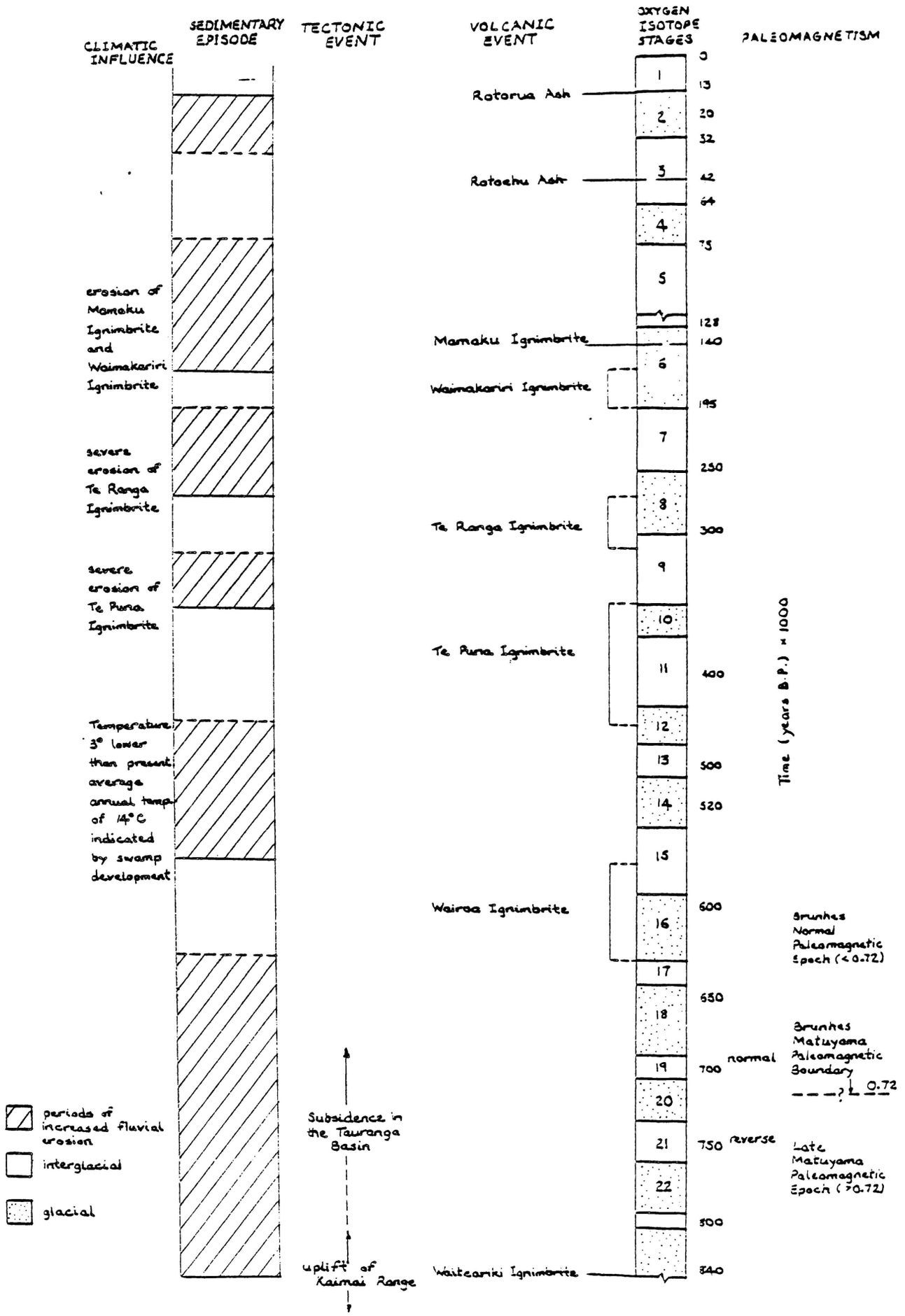


Fig. 9.5 . General timetable of events and effects in the Tauranga Basin.

entrenched in the ignimbrite sheet removing large quantities of detritus and depositing loads of material in the major paleobasin in the Matua and Otumoetai areas. A coastal cliff exposure at Matua indicates that after this period of intense erosion, sedimentation was interrupted by contemporaneous volcanic activity, evidenced by several rhyolitic tephra showers and a thin pyroclastic flow (2 m thick). The latter was presumably a subsidiary distal pyroclastic flow of an ignimbrite which flowed from the Taupo Volcanic Zone after emplacement of the Waimakariri Ignimbrite (or possibly correlated to the Waimakariri Ignimbrite).

The Te Ranga Ignimbrite then became re-exposed in another (possibly a glacial entering into an interglacial period) of erosion and valley incision which cut into both the Waimakariri Ignimbrite and the Te Ranga Ignimbrite (Fig. 9.5). Two major paleochannel systems were rejuvenated in the southwestern parts of the Basin in an area extending northwards from Pyes Pa Road and Belk Road. Initially paleochannel I deposited sediment eroded from the Te Ranga Ignimbrite in the Te Puna area, in which the Te Puna Ignimbrite also contributed sediment during initial development of the paleochannel. Then paleochannel II carried sediment into the Matua and Otumoetai areas. Several smaller tributaries flowed towards Welcome Bay. Sediments eroded from the Te Ranga Ignimbrite formed a thick ($\sim$ 30 m) sequence in the headwaters of the braided river, but have been pregressively eroded nearer the coast, and are presently only 5 m thick. A series of episodic floods followed, reworking the surface of underlying deposits (sediments eroded from the Te Ranga Ignimbrite) and carrying large volumes of reworked debris flow/alluvial fan material into the Te Puna, Matua and Welcome Bay areas. This material was transported in braided streams towards the coast during flood conditions from a source near the Mt Minden rhyolite dome. Stratigraphic sections at Te Puna, Matua, Bethlehem and Welcome Bay (Figs. 3.8 - 3.10) indicate that Hamilton Ash was still being deposited

in the Basin at the end of this period of sedimentary activity.

The upper Matua Subgroup was largely preserved during an interglacial period (0.12 - 0.75 m.y. B.P.; Shackleton and Opdyke, 1973; Fig. 9.5) by a cover of air-fall tephra beds (i.e. Pahoia tephras and Hamilton Ash beds) and by soil development on ash and sedimentary deposits. River channel deposits at 30 - 50 m depth in drillholes (Fig. 3.7) suggest that renewed erosion in the Basin possibly began during a glacial period about 75,000 yrs B.P. (Shackleton and Opdyke, 1973). This initiated a period of valley widening and incision by streams, responding to the lowering of base level, during which streams carried material beyond the present beach line at Matakana Island and dissected an exposed continental shelf. The interstadial which followed (64,000 - 32,000 yrs B.P.; Shackleton and Opdyke, 1973) produced high sea levels during a period between 50,000 - 35,000 yrs B.P. (Veeh and Chappell, 1970). Estuarine and beach sediments recorded in several drillholes at $\sim$ 30 m depth in the Basin were possibly deposited during these high sea levels. These sediments are covered by thick rhyolitic air-fall ash deposits which are interbedded with sediments at depths greater than 4 m in the central to southeastern parts of the Basin (e.g. Te Puna, Matua, Maungatapu). Several road cuttings (e.g. Joyce Road, Keenan Road) and coastal cliffs also record a series of eruptions from the Okataina Volcanic centre about 42,000 yrs B.P. (Howorth, 1975). These eruptions deposited the prominently shower bedded Rotoehu Ash above Hamilton Ash in the Basin. The Mangaoni Tephra (*c*. 32,000 yrs B.P.; Howorth, 1975) followed and was subsequently covered by several late Quaternary and Holocene tephras erupted from the Taupo Volcanic Zone. The present physiography of the Tauranga Basin can be attributed to the events of the last 100,000 yrs, dominated by intervals of fluvial and marine erosion. The last 40,000 yrs, however, has been particularly significant. Following the

last glacial period, a period of intense erosion occurred between 30,000 and 20,000 yrs B.P. (McCraw, 1973). This was followed by a very low sea level stand (20,000 to 15,000 yrs B.P.) some 100 m below present sea level (Carter, 1975) which would have greatly increased valley incision in the Basin. Further degradation of pyroclastic and sedimentary deposits occurred, these having previously aggraded to form higher surfaces. Many of these terraces are concordant tongues of pyroclastic material, while several less distinct terraces have been constructed by aggrading braided streams with levée deposits. There was a rapid rise in sea level from 15,000 to about 7,000 yrs B.P. (Cullen 1967; Veeh and Chappell 1970; Carter 1975) and then a slowing down before the present sea level was reached some 2,000 and 4,000 yrs ago. Most controversy concerns the sea level in the past 7,000 yrs. The most recent post-glacial marine transgression (Cullen, 1967; Norris, 1972; Carter, 1975) is represented throughout the Basin by several low terraces, 0.2 - 0.5 m (height includes ash cover) above present sea level, which fringe the coastline in the Tauranga Harbour (e.g. Otumoetai, Omokoroa). Deposits 30 - 50 cm below the surface of the terraces consist of a blue-grey muddy sand which is covered in places by pumice lapilli and sandy mud. In the Otumoetai core this deposit occurs between 0.2 - 3.0 m depth below the terrace surface. The Tauranga Basin became a ria complex but is now dominated by estuarine facies and enclosed by a barrier island. The Matakana Island barrier system probably developed between 4,000 and 7,000 yrs B.P. as the last glacio-eustatic sea level rise slowed. It was possibly due in part to drowning of the present harbour behind a series of ancient dune ridges.

Fig. 9.6 Summary sketches of events in the Tauranga Basin since the Middle Pleistocene.

(1) Prior to the early ignimbrite period.

(2) After emplacement of the Waitepariki Ignimbrite during the early ignimbrite period.

(3) During the early ignimbrite period the Wairoa Ignimbrite was deposited in the Basin and then severely eroded.

(4) A braided river system developed in the early ignimbrite period. Large quantities of material were eroded from the Waitepariki Ignimbrite.

(5) The late ignimbrite period was initiated by deposition of the Te Puna Ignimbrite.

(6) Down-cutting of the Te Puna Ignimbrite and renewed erosion of the Wairoa Ignimbrite.

(7) Re-exposure of older ignimbrites from early ignimbrite period, and active sedimentation in the Basin.

(8) Continued down-cutting of the Te Puna and Waitepariki Ignimbrites. Re-exposed Wairoa Ignimbrite.

(9) Emplacement of the Te Ranga Ignimbrite.

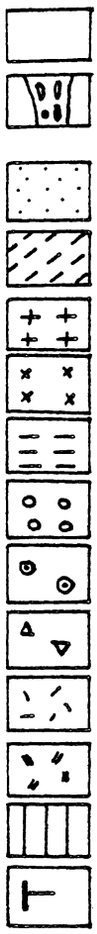
(10) Down-cutting of the Te Ranga Ignimbrite.

(11) Emplacement of the Waimakariri Ignimbrite.

(12) Gradual initiation of the upper Matua Subgroup period after emplacement of the Waimakariri Ignimbrite, re-exposing and eroding ignimbrites emplaced in earlier periods.

- Mamaku Ignimbrite was emplaced in the Basin during this period but has subsequently been completely eroded out of the Basin.

KEY



Sea

Braided river system

Matua Subgroup deposits (pyroclastic and fluvial, some unidentified)

Waimakariri Ignimbrite

Te Ranga Ignimbrite

Te Puna Ignimbrite

Wairoa Ignimbrite

Waitearíki Ignimbrite

Papamoa Ignimbrite

Aongatete Ignimbrite

Minden Rhyolite

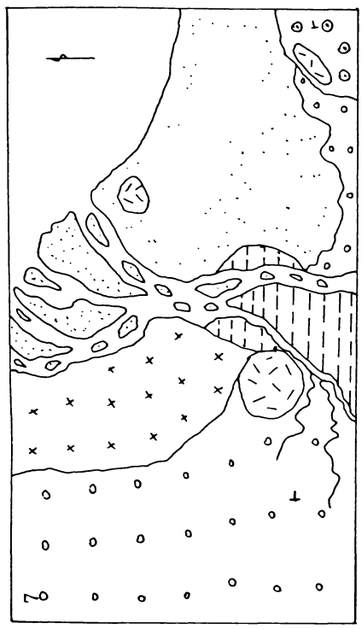
Miocene - Pliocene volcaniclastic sediments

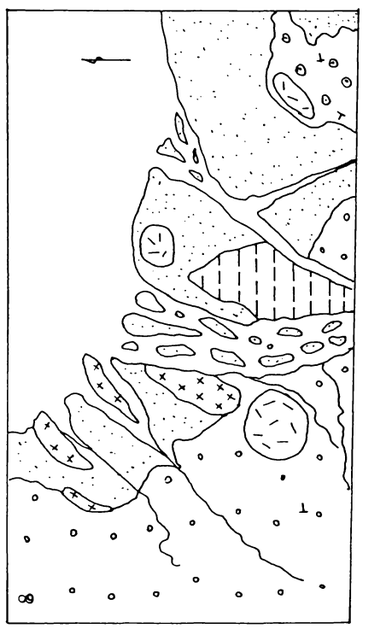
Andesite (Miocene to Pliocene)

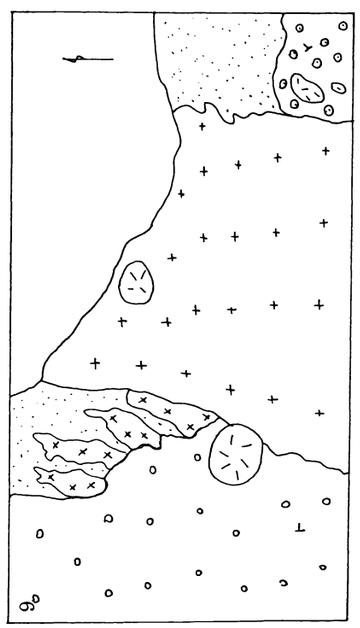
Dipping deposits

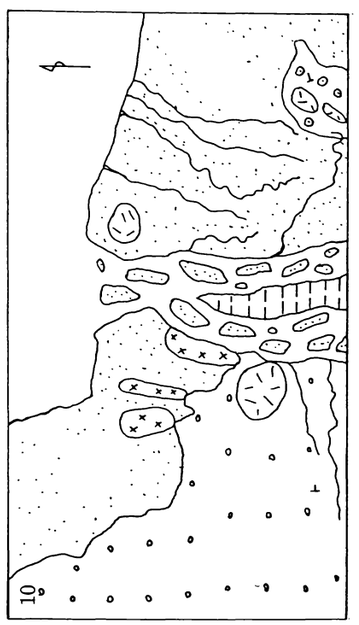
1 4 km

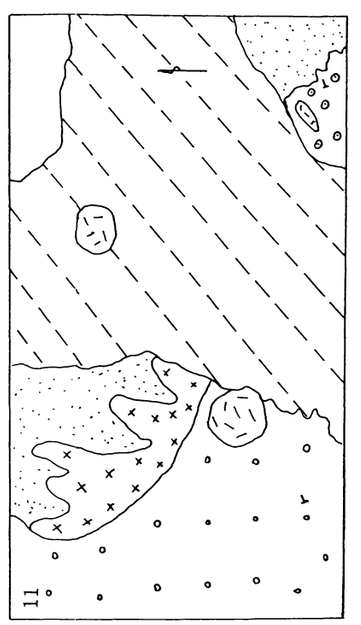
Approx. scale

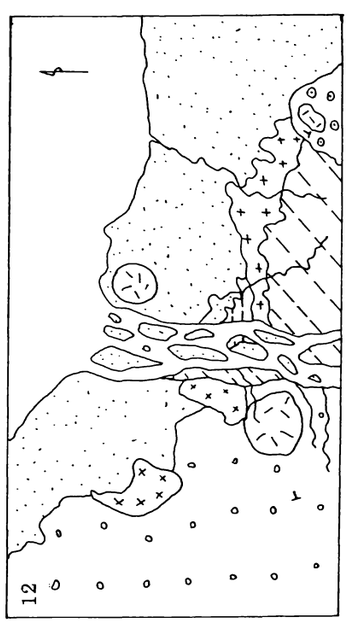

1
Q
T


2
T


3
T


4
T


5
T


6
T

7
T

8
T

9
T

10
T

11
T

12
T

CHAPTER TEN

CONCLUSIONS

INTRODUCTION

The major aims of this thesis as outlined in Chapter 1, are concerned with the age and structure of the Basin, determination of the stratigraphy of the Quaternary succession and the nature and pattern of its depositional paleoenvironments, and a synthesis of the geological history. The physiographic development of the Basin is also briefly discussed. Each of these aspects is now summarised.

STRUCTURE AND STRATIGRAPHY

The Tauranga Basin originates from the northeastward tilting of a fault block, the upturned western margin being the Kaimai Range. A middle Pleistocene succession up to 500 m thick has accumulated upon the eastern margin of this tilted block.

The Waiteariki Ignimbrite (0.84 m.y. B.P.) outcrops in the Whakamarama Plateau and also extends beneath the succession thereby forming an effective basement in the Basin. While most of the subsidence post-dates emplacement of the Waiteariki Ignimbrite there was probably some earlier subsidence as evidenced by underlying sediments within the Basin. The Waiteariki Ignimbrite is displaced 450 m between the Hauraki graben and the Kaimai Range. This further indicates that tilting of the Kaimai fault block, and hence subsidence of the Tauranga Basin occurred mainly after 0.84 My. The uplift pattern of the Kaimai Range was not a simple eastward tilting, but this was superimposed upon a regional trend for uplift to commence in the north and progress to the south along the range. The tilting was probably progressive as the Waiteariki Ignimbrite and older units dip at a greater angle than units within the Matua Subgroup which onlaps the Whakamarama Plateau.

Only very small scale fault displacements of up to 15 cm were noted in the field especially in coastal exposures, suggesting that the basement was tilted as a coherent block. The tilt block may have an eastern margin that corresponds with the present Continental Shelf.

Subsurface bore logs show that the Waitearíki Ignimbrite rests either upon the Aongatete Ignimbrite (∿1.26 - 0.84 m.y. B.P.), by way of an eroded contact, or upon fluvial volcaniclastic sediments derived from older units and perhaps mainly the Aongatete Ignimbrite. Elsewhere the Waitearíki Ignimbrite onlaps and overlaps Minden Rhyolite domes (4.3 m.y. B.P.) and Beesons Island Volcanics (16 - 7 m.y. B.P.). The Matua Subgroup (new name) lies immediately above the Waitearíki Ignimbrite. The subgroup comprises several newly identified subaerially exposed distal ignimbrites named from localities where they are best exposed. They include the Wairoa Ignimbrite (∿0.6 m.y. B.P.), the Te Puna Ignimbrite (∿0.4 m.y. B.P.), the Te Ranga Ignimbrite (∿0.3 m.y. B.P.), and the formerly named Waimakariri Ignimbrite (∿0.18 m.y. B.P.). Sediments derived mainly from the erosion of these ignimbrites are interstratified between them and are also included in the subgroup.

White to grey rhyolitic tephras named the Pahoia tephras (equivalent to Pahoia Tuffs of Pullar *et al.*, 1973) are part of the upper 40 m of the Matua Subgroup. These highly weathered tephras underlie the brown Hamilton Ash beds and are probably air-fall equivalents of the upper ignimbrites in more southern parts of the Basin. From field correlations, and in particular their occurrence stratigraphically above the Te Puna Ignimbrite, a maximum age of ∿0.4 m.y. B.P. is proposed for these tephras. The Mamaku Ignimbrite (0.14 m.y. B.P.) is not included as a stratigraphic unit within the Tauranga Basin, however, it crops out as a thick ∿40 m deposit ∿5 km south of the Basin

The post-depositional southeast tilting within the Basin has caused an outcrop pattern where successively older units of the early ignimbrite period outcrop in order towards the northwest especially between Matua and Katikati, and up the Wairoa River.

Thickening of the Waitearíki Ignimbrite (0.84 m.y. B.P.) and coarsening of lithics southwestwards away from the Tauranga Basin suggest that the ignimbrite flowed northwards into the Basin. Similar evidence suggests that this is also the case for all post-Waitearíki Ignimbrites. Thickening of the Aongatete Ignimbrite (1.26 - 0.86 m.y. B.P.) westwards towards the Kaimai Range suggests a source north of the Taupo Volcanic Zone, possibly the Coromandel Range. It is suggested in this study that volcanism, although moving southwards in the Coromandel Peninsula over the interval ∿16 - ∿2 m.y. B.P., was intermittently active nearer Tauranga during the interval ∿3 to 1 m.y. B.P. at about the time active volcanism started in the Taupo Volcanic Zone.

SEDIMENTS

A sedimentary model was presented in Chapter 7 to describe the fluvial environment of the Matua Subgroup between Pyes Pa Road and Matua. Seven major petrofacies were described to trace the changing sedimentation patterns in the Basin. Most of these sediments are considered to be derived from the erosion of the distal ignimbrite formations within the subgroup. Sediment derived from the Waitearíki Ignimbrite is not subaerially exposed within the mapped part of the Basin, but has been noted in the borelogs and outside the mapping area. Fluvial sediment derived from the erosion of the Mamaku Ignimbrite overlies the Waimakariri Ignimbrite in the Ruahihi area (U14/794750).

The textural characteristics and sedimentary structures of the Matua Subgroup indicate that they were deposited in a braided river environment of ephemeral nature.

Episodes of fluvial erosion and deposition in the Basin often followed the emplacement of pyroclastic flow and fall deposits. This indicates a strong volcanic control on sedimentation. There was probably also some influence upon sedimentation by the Quaternary glacio-eustatic sea level changes which acted to increase the extent of erosion of pyroclastic deposits during glacial ages.

The development of sedimentary systems in the Tauranga Basin has been referred to three main periods of geological activity informally named the early ignimbrite period (0.84 - 0.5 m.y. B.P.), the late ignimbrite period (0.5 - 0.14 m.y. B.P.), and the upper Matua Subgroup period (∿0.16 m.y. B.P. - Present). The early ignimbrite period includes the emplacement of the Waitetariki and Wairoa Ignimbrites, while the Te Puna, Te Ranga and Waimakariri Ignimbrites were emplaced during the late ignimbrite period.

PHYSIOGRAPHY

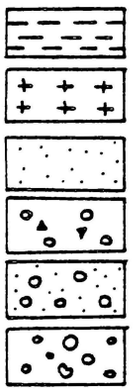
Within the Tauranga Basin there are many horizontal surfaces that could be described as terraces. Close attention has shown that most of them can not be mapped as extensive features. While some of the surfaces are clearly of constructional origin relating to the upper boundary of ignimbrite sheets, others result from variable degrees of mainly fluvial dissection and erosion. Some of the differences in elevation between terraces can be attributed to different thicknesses of Hamilton Ashes and Late Quaternary tephras. The different thicknesses of tephras is due mainly to variable erosion rather than differences in depositional thickness.

APPENDIX 1

Stratigraphic sections of the Tauranga Basin

Appendix 1.1: Key to the following Stratigraphic Sections

TEXTURE



Clay

Silt

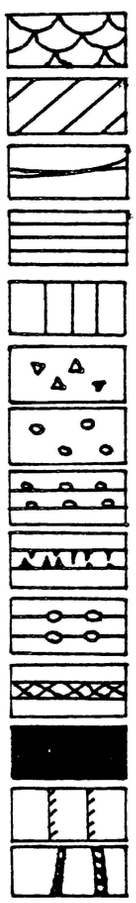
Sand

Slightly gravelly sand [(g) S]

Gravelly sand (g S)

Sandy gravel (s G)

STRUCTURE



Trough cross-stratification

Alpha cross-stratification

Low angle cross-stratification

Planar stratification

Massive

Pyroclastic flow deposit

Matrix supported mass emplaced deposit

Shower bedded air-fall tephra

Paleosol

Chalazoidite bed

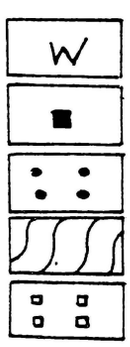
Post-depositional structures

Lignite

Columnar jointing

Segregation structures

OTHER ABBREVIATIONS USED



Highly weathered

Charcoal fragment

Manganese staining

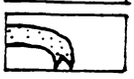
Leisegang phenomena

Iron staining

DEFORMATION



Injection



Slump



Infilling by sediment (syndepositional and post-depositional)

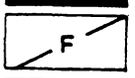


Compactional faulting

IN SITU



Lignite

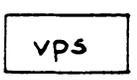


Fault

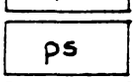


Iron Pan

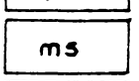
SORTING



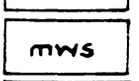
Very poorly sorted



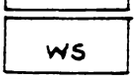
Poorly sorted



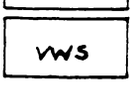
Moderately sorted



Moderately well sorted

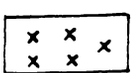


Well sorted

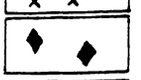


Very well sorted

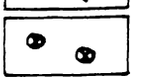
COMPOSITION



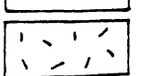
Glass shard-feldspar-quartz



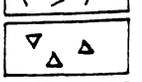
Heavy mineral



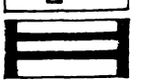
Ignimbrite fragments



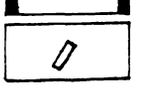
Pumice



Rock fragments



Carbonaceous

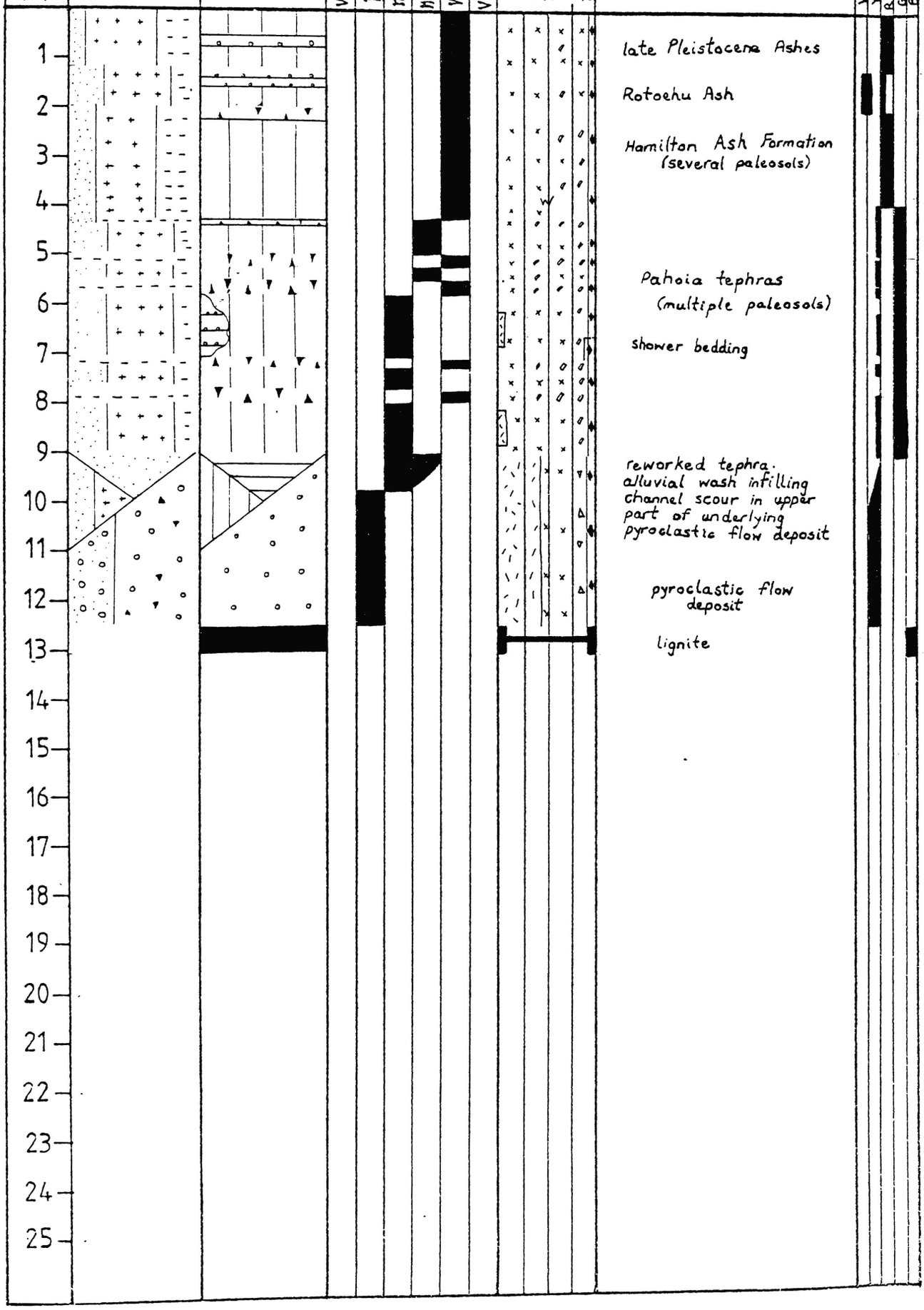


Clay minerals

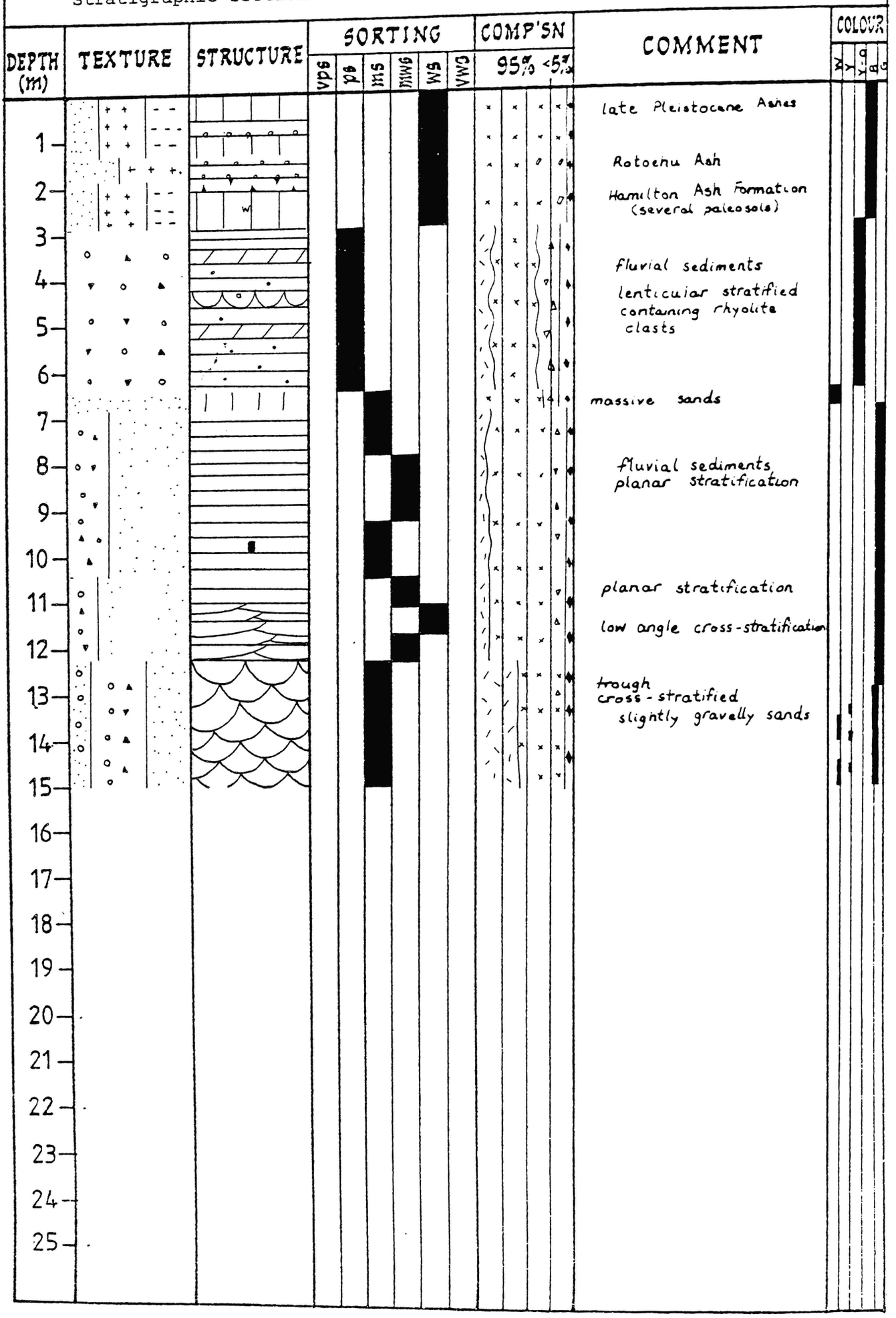
COLOUR

W-G	White to Grey
W	White
Y	Yellow
Y-O	Yellow to Orange
B	Brown
G	Grey
R-B	Red to Brown
Blk	Black

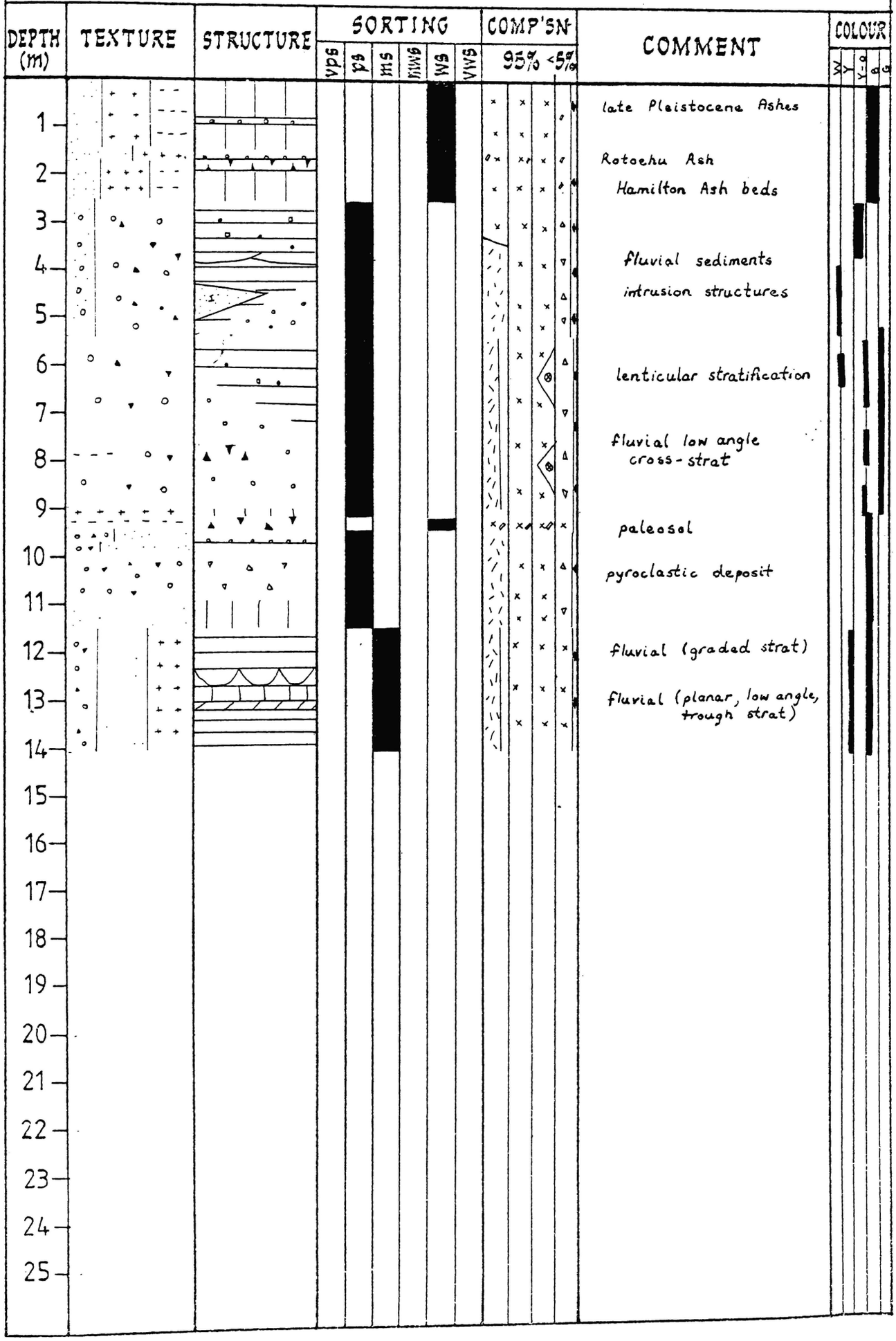
Stratigraphic section : 1 Omokoroa G.R.: U14/797927

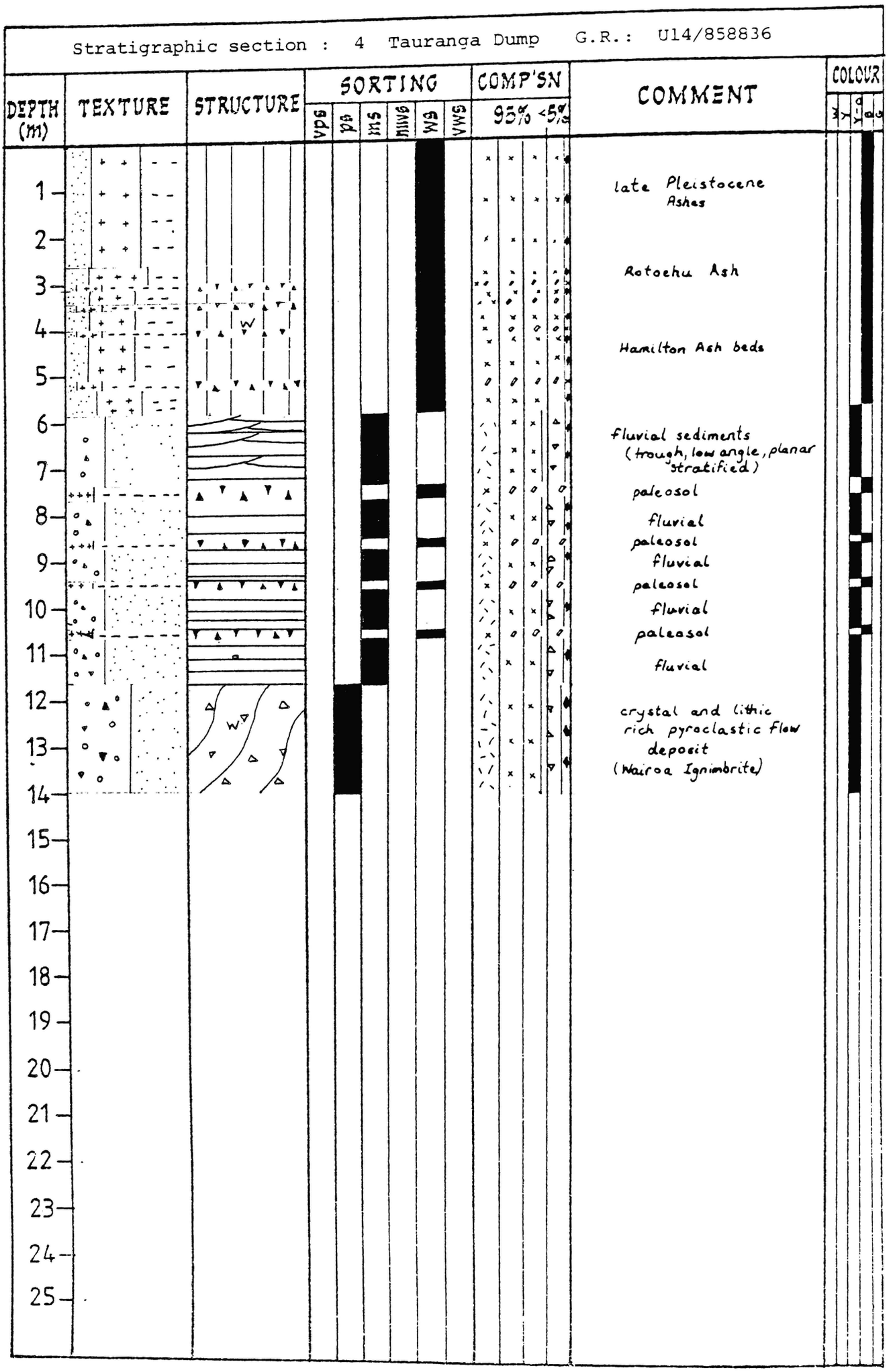


Stratigraphic section : 2 Te Puna G.R.: U14/819887

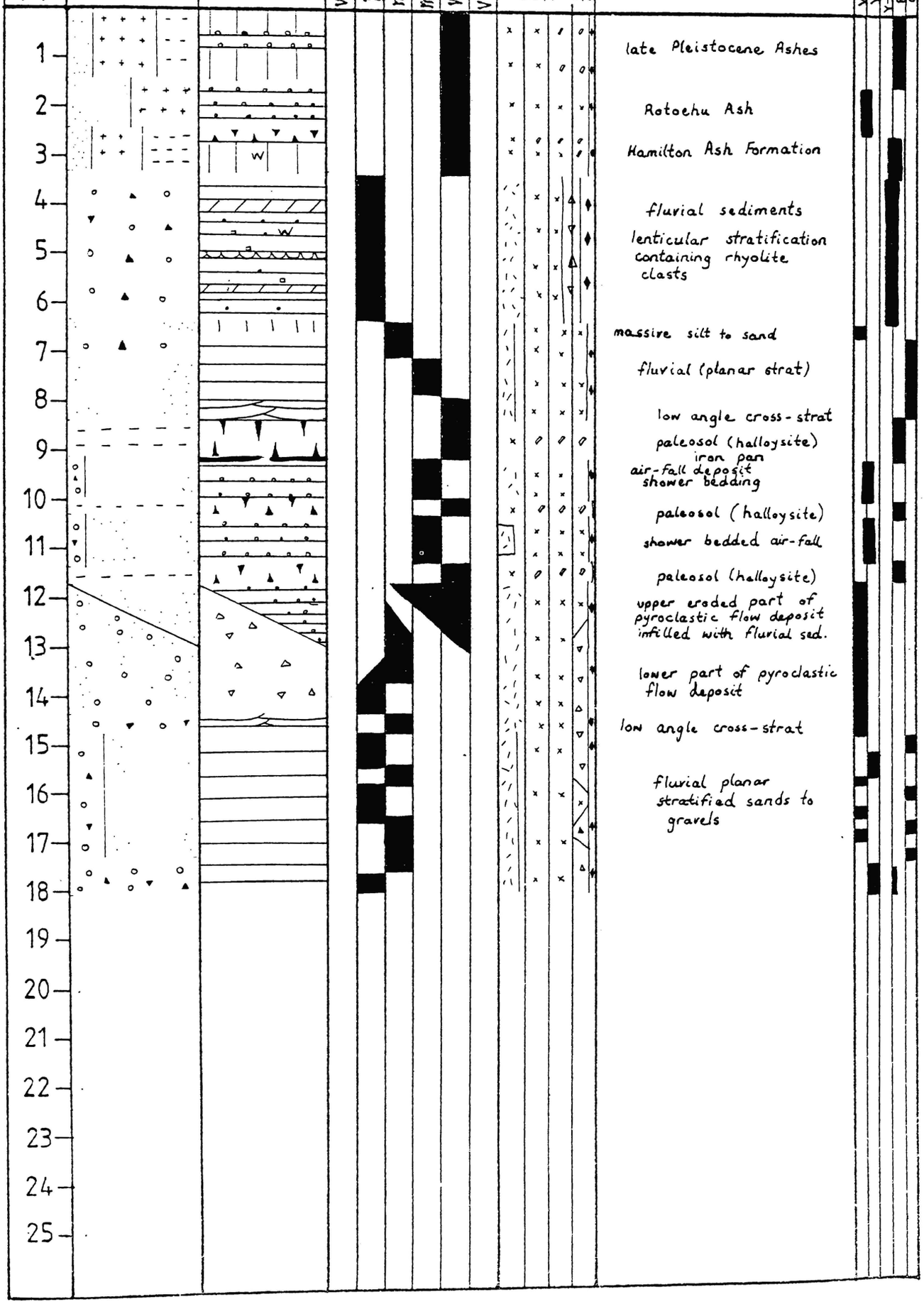


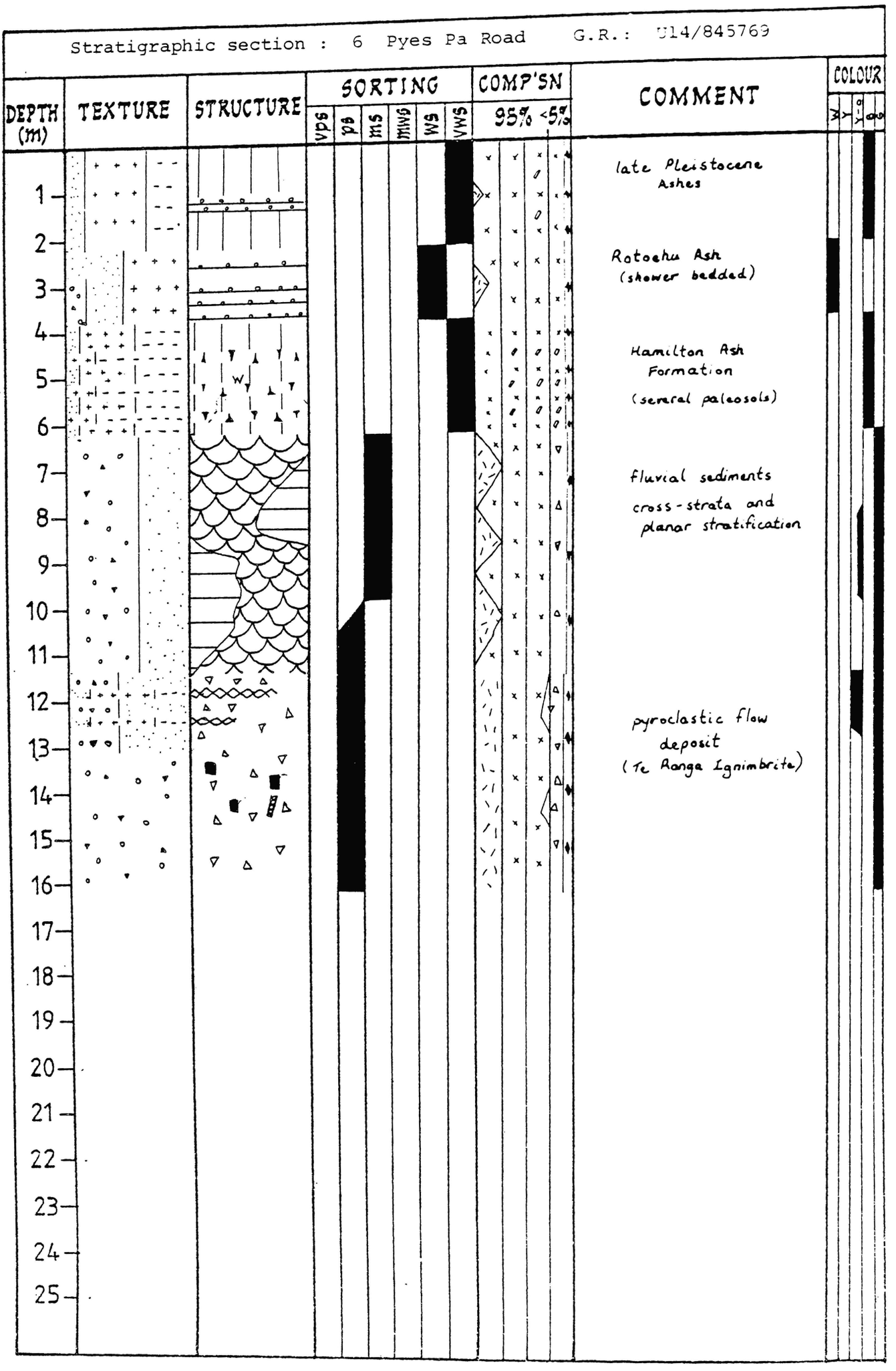
Stratigraphic section : 3 Bethlehem G.R.: U14/849867

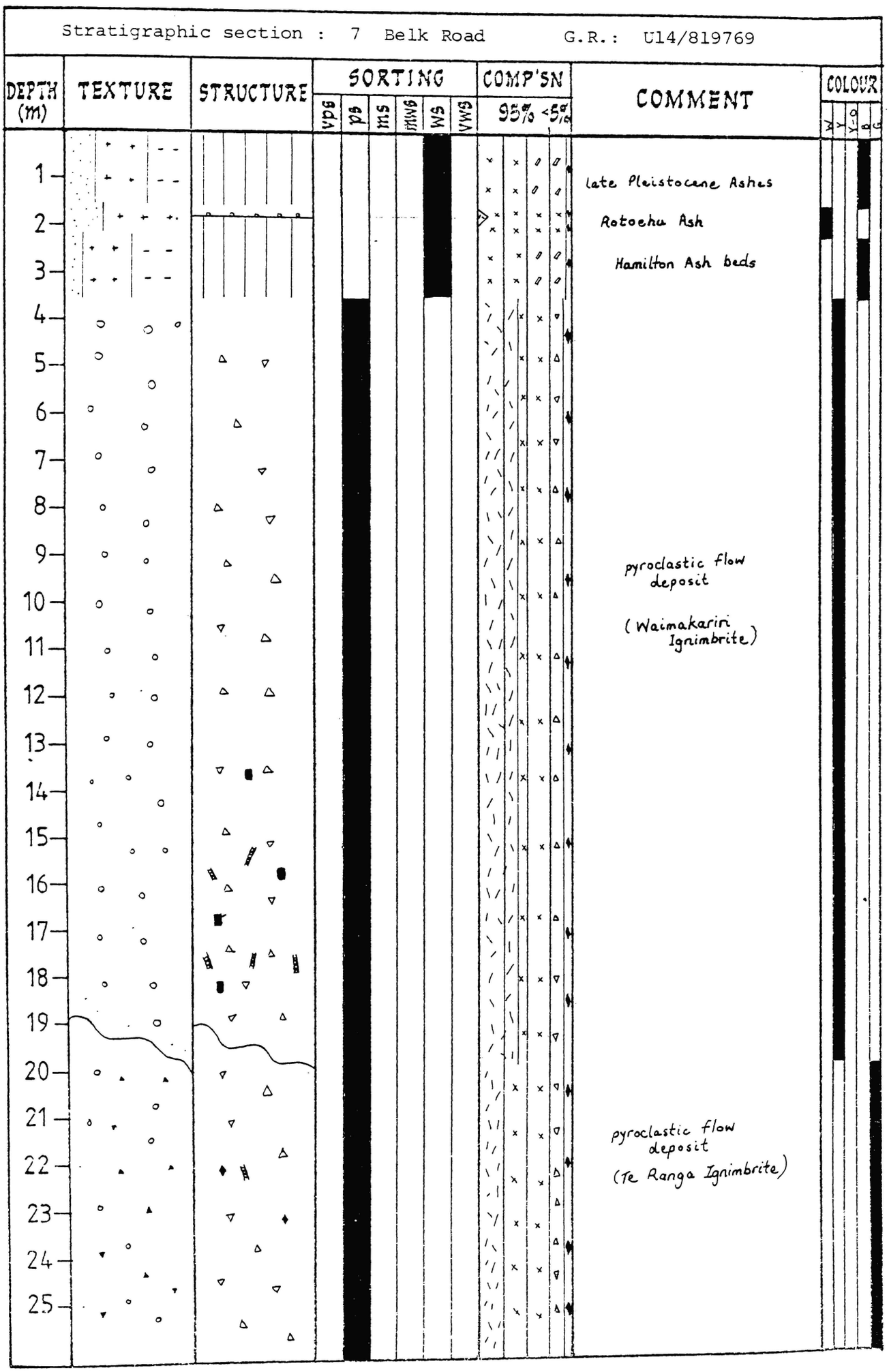



Stratigraphic section : 4 Tauranga Dump G.R.: U14/858836
DEPTH (m)
TEXTURE
STRUCTURE
SORTING
vps
ps
ms
mws
ws
vws
COMP'SN
95%
<5%
COMMENT
COLOUR
late Pleistocene Ashes
Rotoehu Ash
Hamilton Ash beds
fluvial sediments (trough, low angle, planar stratified)
paleosol
fluvial
paleosol
fluvial
paleosol
fluvial
paleosol
fluvial
crystal and lithic rich pyroclastic flow deposit (Wairoa Ignimbrite)

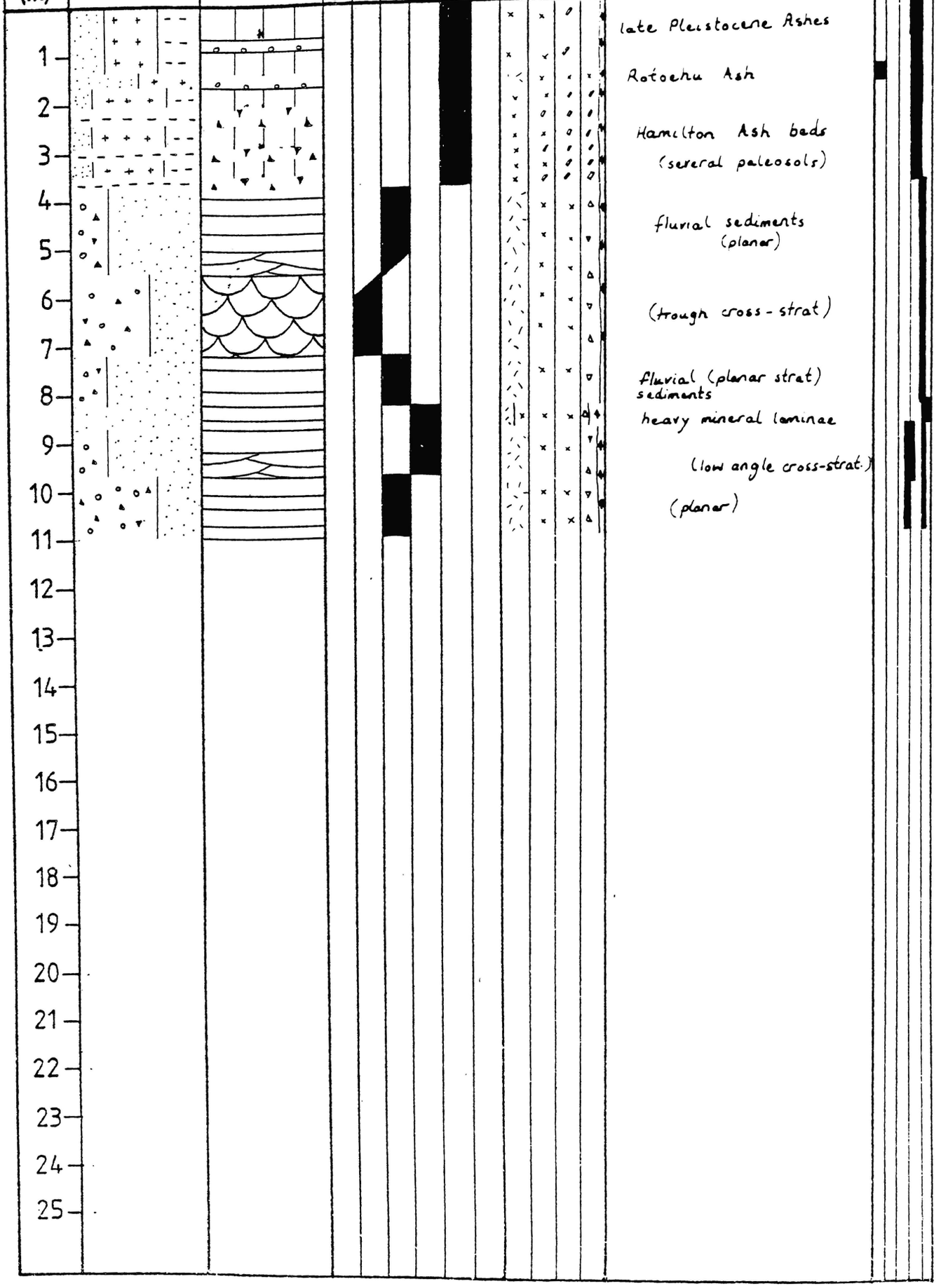
Stratigraphic section : 5 Matua G.R.: U14/849876



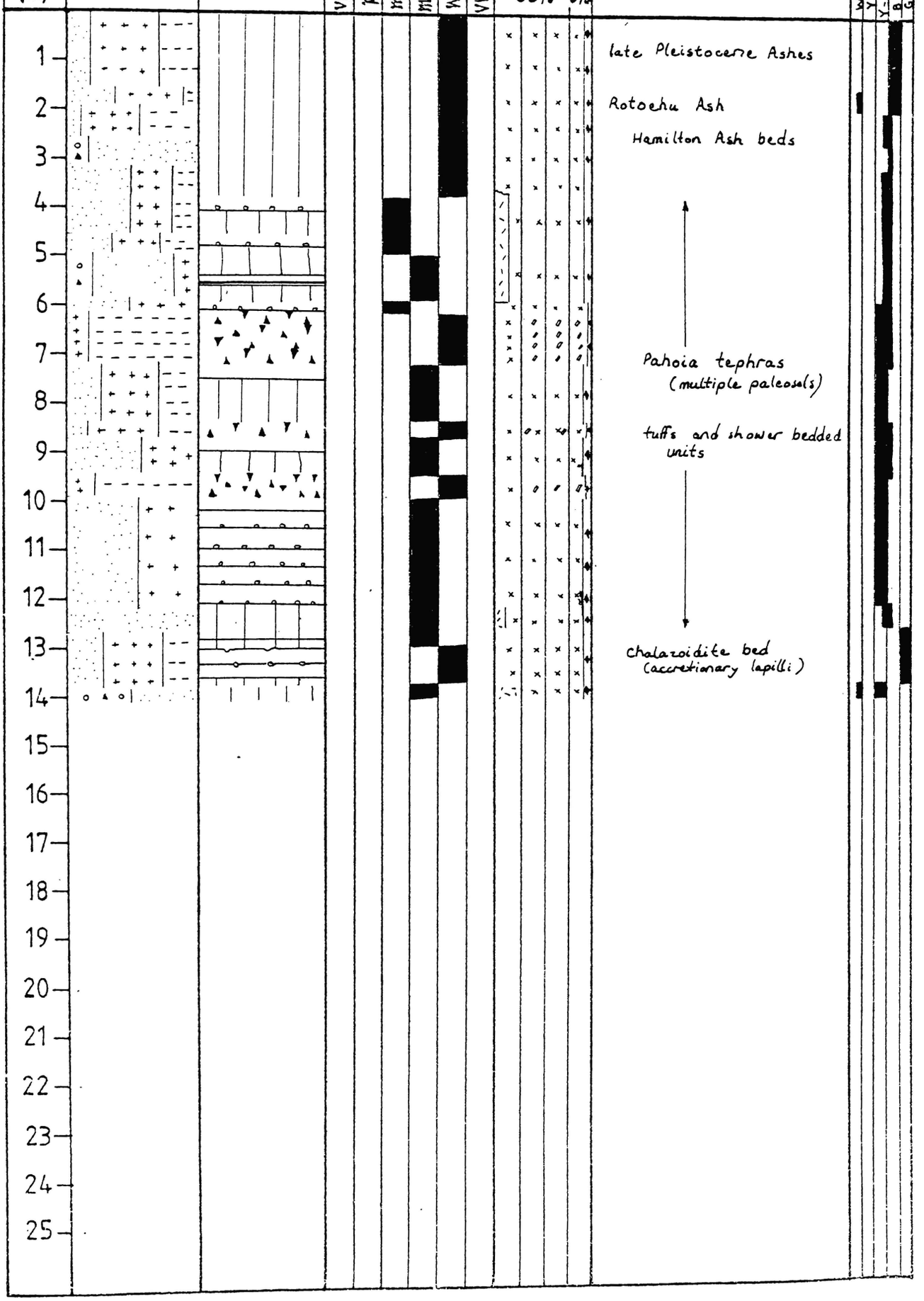

Stratigraphic section : 6 Pyes Pa Road G.R.: U14/845769
DEPTH (m)
TEXTURE
STRUCTURE
SORTING
VPS
PS
MS
MWS
WS
VWS
COMP'SN
95%
<5%
COMMENT
COLOUR
late Pleistocene Ashes
Rotoehu Ash (shower bedded)
Hamilton Ash Formation (several paleosols)
fluvial sediments cross-strata and planar stratification
pyroclastic flow deposit (Te Ranga Ignimbrite)
1
2
3
4
5
6
7
8
9
10
11
12
13
14
15
16
17
18
19
20
21
22
23
24
25


Stratigraphic section : 7 Belk Road G.R.: U14/819769
DEPTH (m)
TEXTURE
STRUCTURE
SORTING
vpg
pg
ms
mwg
ws
vws
COMP'SN
95%
<5%
COMMENT
COLOUR
late Pleistocene Ashes
Rotoehu Ash
Hamilton Ash beds
pyroclastic flow deposit
(Waimakariri Ignimbrite)
pyroclastic flow deposit
(Te Ranga Ignimbrite)

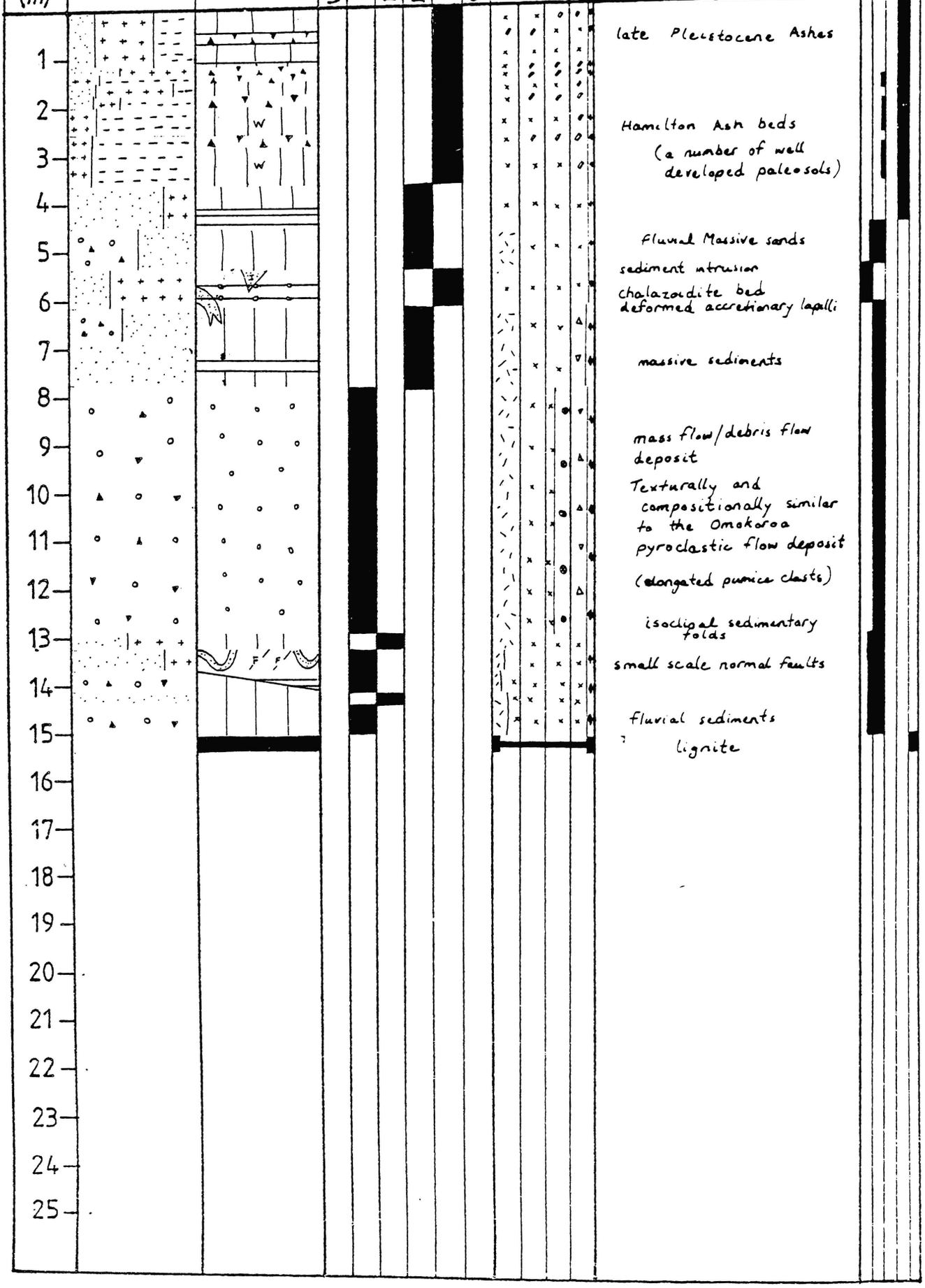
Stratigraphic section : 8 Greerton G.R.: U14/855805



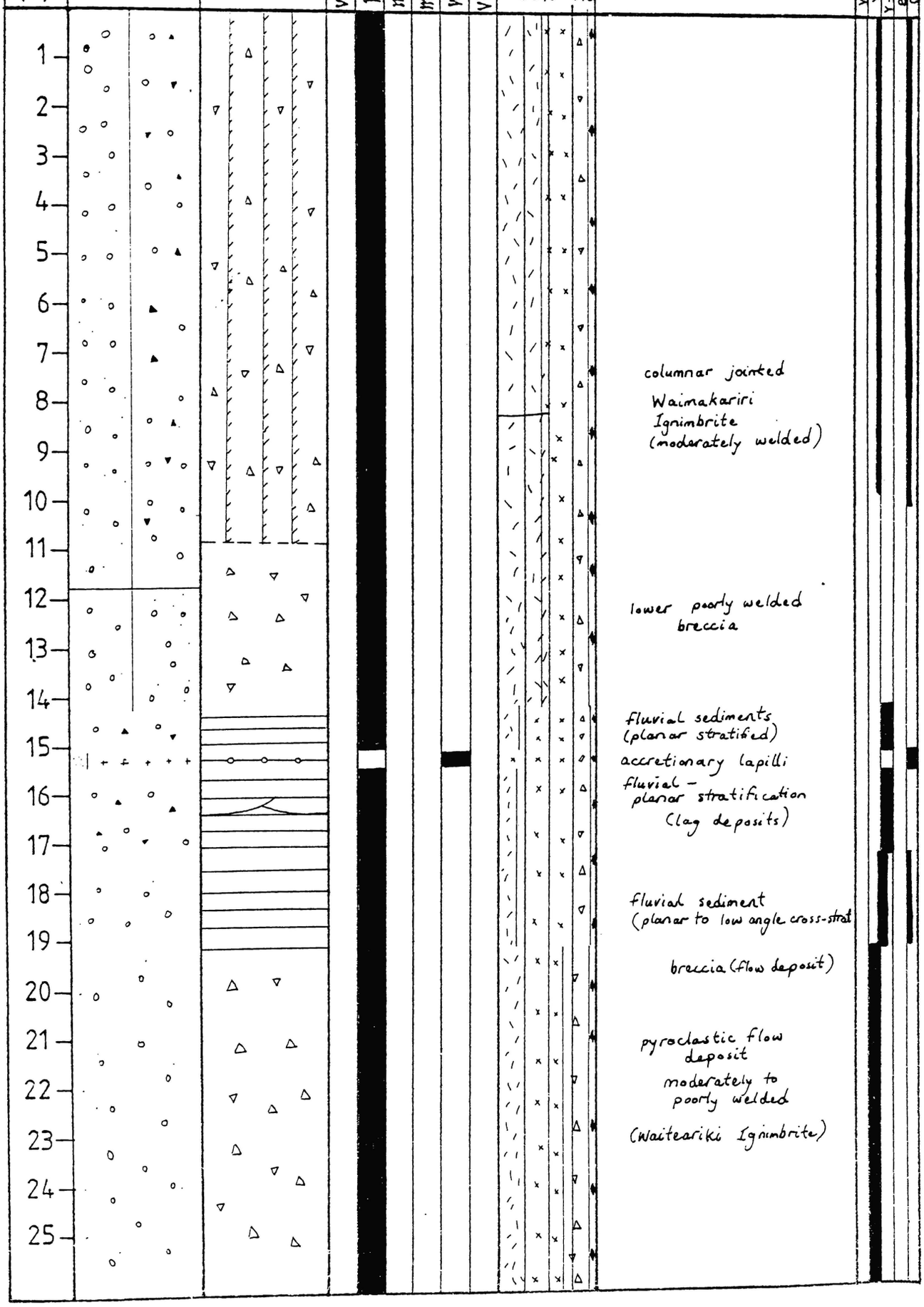
Stratigraphic section : 9 Omokoroa East G.R.: U14/790898



Stratigraphic section : 10 Motuhoa Island G.R.: U14/805910



Stratigraphic section : 11 Wairoa River G.R.: U14/796761



Appendix 1.2

Number key for following stratigraphic sections (from borehole data, N.Z.G.S., Rotorua)

Section	Location	Grid Reference
1	Otumoetai	U14/859886
2	Greerton	U14/862809
3	Welcome Bay	U14/942826
4	Te Puna	U14/802876
5	Otumoetai	U14/859868
6	Otumoetai	U14/883881
7	Matua	U14/856885
8	Te Puna	U14/798888
9	Bethlehem	U14/849844
10	Te Puna	U14/805878
11	Maungatapu	U14/897816
12	Otumoetai	U14/858866
13	Te Puna	U14/816865
14	Kennedys Road	U14/843784
15	Otumoetai	U14/872882
16	Otumoetai	U14/871883
17	Otumoetai	U14/888875
18	Tauranga City	U14/892827
19	Cameron Road	U14/894858
20	Tauranga City	U14/896866

Key to the following Stratigraphic Sections

The following descriptions are from N.Z.G.S, Rotorua, drillhole reports.

VOLCANIC DEPOSITS



Waitearikí Ignimbrite



Aongatete Ignimbrite



Minden Rhyolite


Undifferentiated ignimbrite



Base of ignimbrite sheet


Unwelded ignimbrite


Welded ignimbrite


Pumice lava flow or ignimbrite


Indurated pyroclastic flow deposit


Ignimbrite with interbedded lava or andesite inclusions


Pumice tuff breccia (pyroclastic flow deposit)


Pumice tuff


Tuff


Lava


Rhyolite lava


Rhyolitic pyroclastic flow or lava


Rhyolitic air-fall ash


Rhyolitic tephra


White pumice rhyolite



Pumice tephra



Weathered ash


Ash


Air-fall tephra



Vitric ash

SEDIMENTARY DEPOSITS


Fluvial



Weathered fluvial


Fluvial sand with interbedded tuff


River channel (gravels and sand)


High energy fluvial


Interbedded ash and fluvial sand


Beach sand

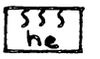

Muddy sand


Reworked ash

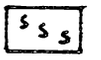

Reworked tephra


Reworked tuff


Estuarine silt



High energy estuarine


Estuarine



Low energy estuarine or marginal facies sediments


Fossiliferous silt

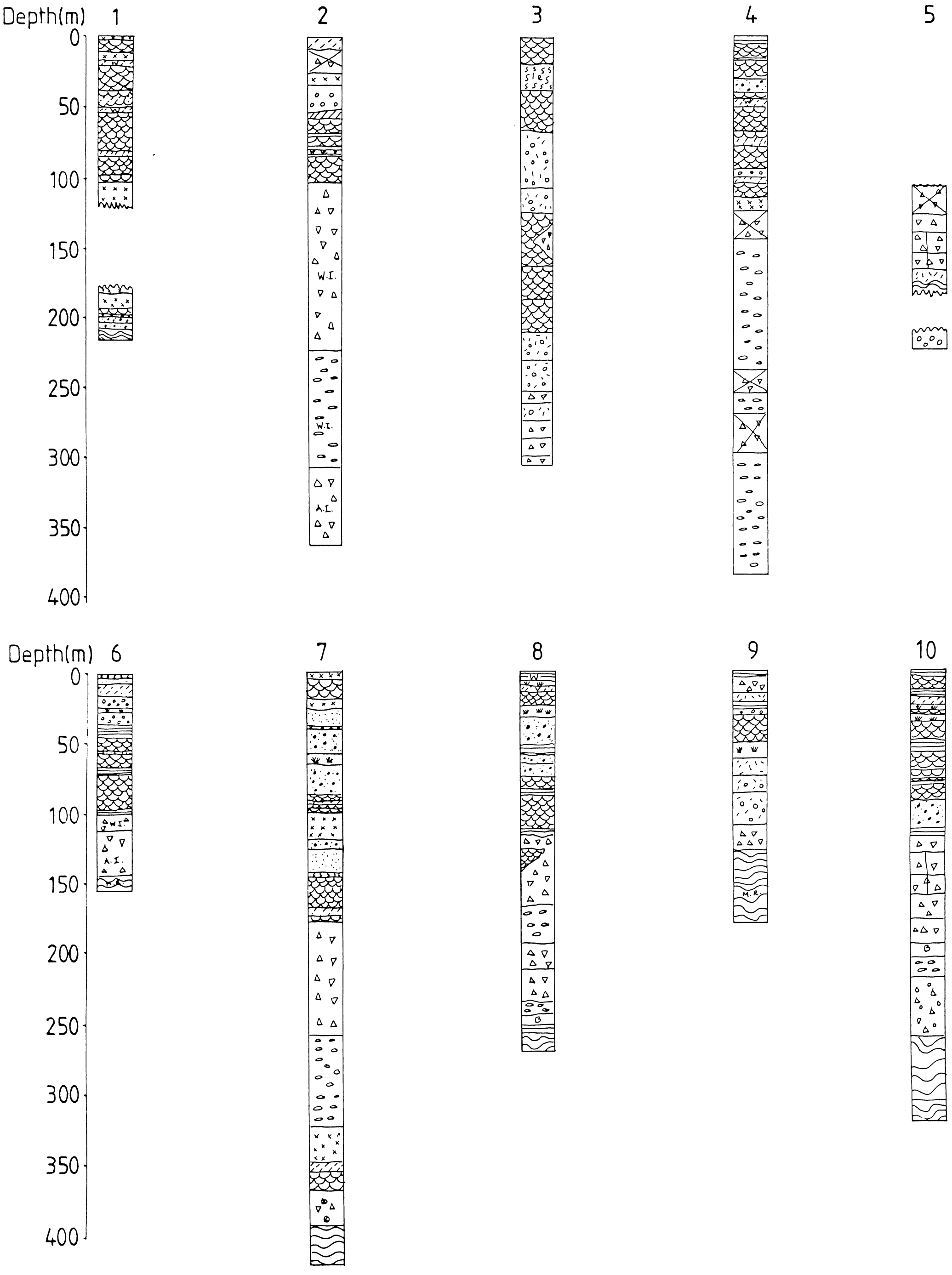

Clay

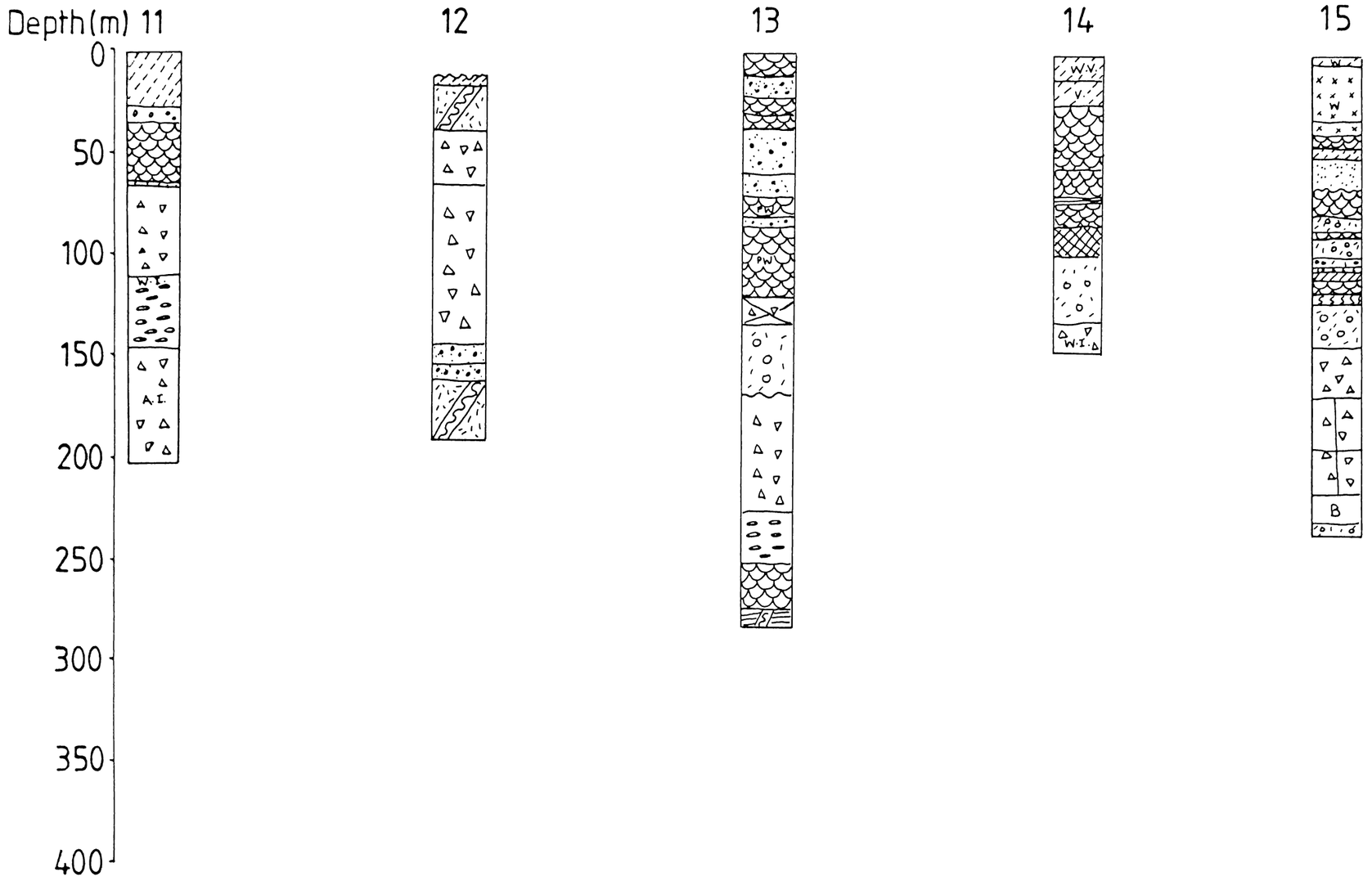

Siltstone

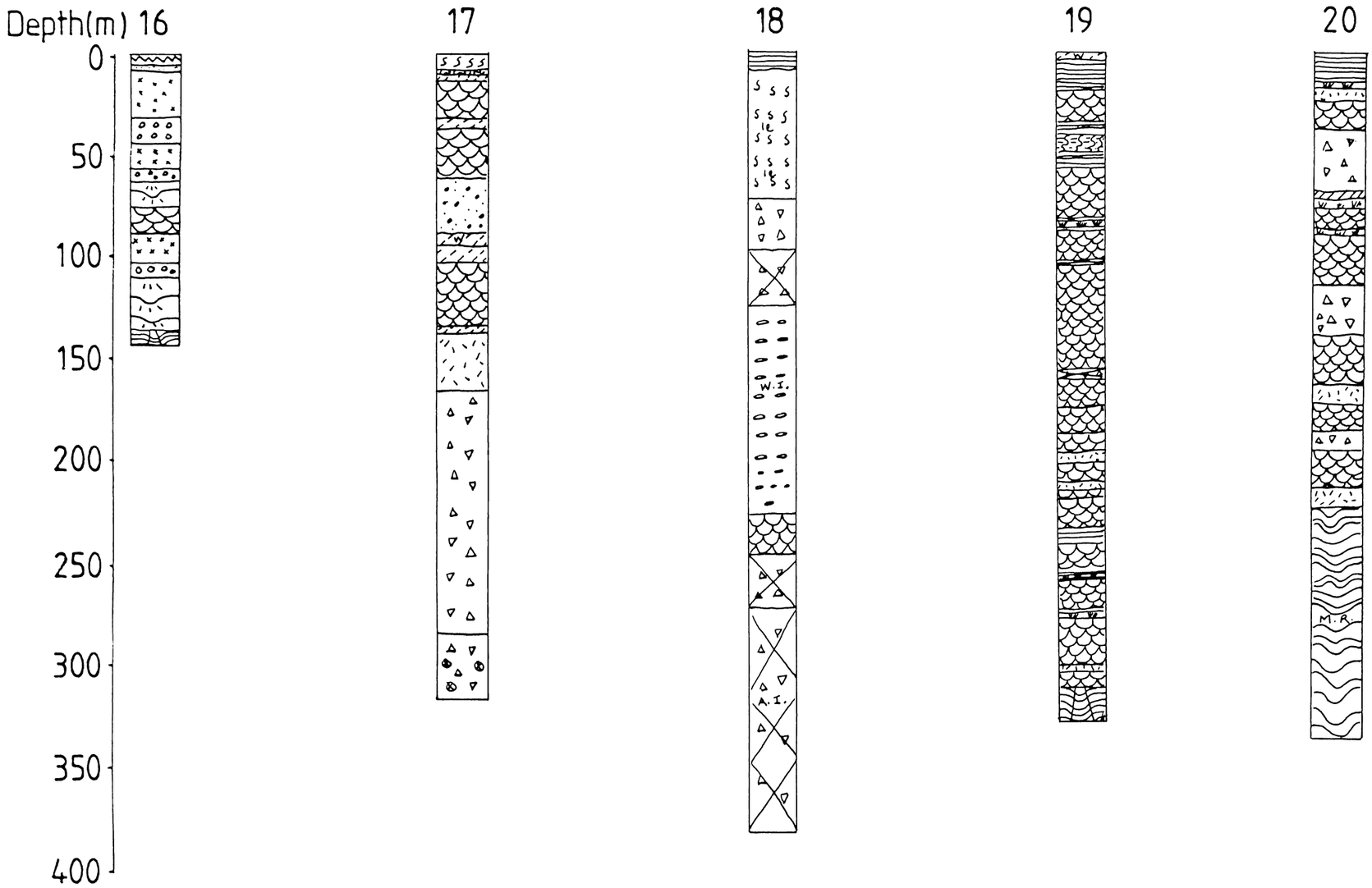

Carbonaceous


Swamp (peat)

Idealised Stratigraphy of Drillholes in the Tauranga Basin




Depth(m)
11
12
13
14
15
0
50
100
150
200
250
300
350
400
A.I.
P.W.
W.I.
W.
B


Depth(m)
16
17
18
19
20
0
50
100
150
200
250
300
350
400
W.I.
A.I.
M.R.

APPENDIX 2

Textural and Mineralogical data

Appendix 2.1: Sample reference and type

Appendix 2.2: Textural data of representative samples taken from the Tauranga Basin. Textural type and Statistical Parameter Symbols are defined in Figs. 2.3 and 5.1.

Appendix 2.3: Mineralogic analysis results.

2.31: Heavy mineral results.

Appendix 2.1

SAMPLE NO.	W.T. NO.	LOCATION	DESCRIPTION f = fluvial; p = pyroclastic flow deposit; pf = pyroclastic air-fall deposit
101	18401	U14/795927	p
103	18402	U14/795927	p
104	18404	U14/795927	pf
105	18405	U14/795927	pf
106	18406	U14/795927	f
107	18407	U14/795927	pf
108	18409	U14/795927	pf
109	18410	U14/795927	pf
110	18411	U14/795927	pf
1101	18412	U14/795927	pf
1051	18413	U14/795927	pf
1061	18414	U14/795927	pf
1071	18415	U14/795927	pf
1081	18416	U14/795927	pf
501	18417	U14/849875	f
502	18418	U14/849875	f
503	18419	U14/849875	f
504	18420	U14/849875	p
505	18421	U14/849875	p
507	18422	U14/849875	pf
509	18423	U14/849875	f
510	18424	U14/849875	pf
515	18425	U14/849875	pf
506	18426	U14/849875	pf
508	18427	U14/849875	pf
5151	18428	U14/849875	pf
511	18429	U14/849875	f
512	18430	U14/849875	pf
520	18431	U14/849875	f
522	18432	U14/849875	f
523	18433	U14/849875	f
605	18439	U14/862805	p
301	18451	U14/829859	p
302	18452	U14/829859	p
603	18441	U14/845768	p
6005	18448	U14/845768	f
401	18449	U14/858836	p
409	18450	U14/853834	f
6701	18446	U14/820769	p
7011	18438	U14/820769	p
701	18445	U14/820769	p
606	18460	U14/845768	f
801	18457	U14/907820	f
201	18465	U14/821887	f
203	18466	U14/821887	f
205	18467	U14/821887	f
2061	18468	U14/821887	f
2062	18469	U14/821887	f
207	18470	U14/821887	f
802	18453	U14/855805	f
803	18454	U14/855805	f
804	18455	U14/855805	f
805	18456	U14/855805	f

Sample No.	Mean Grain Size	Median Grain Size	C Statistic	Phi Values of Modes	Sorting	Skewness	Kurtosis
101	-0.62	-0.125	-4.52	-2.0, 0.0, 0.5	ps	scs	mk
103	0.95	1.0	-4.73	-2.0, 0.5, 1.5	ps	cs	mk
104	1.11	1.25	-2.47	-2.0, 1.5, 2.5	ps	ns	mk
105	3.96	3.97	-0.66	1.5, 3.0	ps	ns	mk
106	3.26	3.40	-0.65	1.5, 1.5	ps	ns	pk
107	3.36	3.70	-1.50	1.0, 1.5, 2.0	vps	cs	mk
108	2.66	2.80	-1.75	1.0, 1.5, 2.0	ps	cs	pk
109	5.14	4.82	-1.22	2.0, 3.0, 4.0	ps	fs	lk
110	5.45	5.45	2.06	2.0, 3.0, 3.5	ps	ns	mk
1101	5.08	5.20	1.81	3.0, 3.5, 4.0	ps	ns	mk
1051	2.61	2.80	-0.66	1.5, 2.0	ps	cs	pk
1061	1.83	1.80	-0.65	1.5, 2.0	ps	ns	pk
1071	1.08	1.12	-1.50	1.5, 2.0	ms	ns	pk
1081	0.61	0.75	-1.75	2.0	ps	cs	mk
501	0.38	1.00	-3.14	-2.0, 2.0	ps	cs	mk
502	1.88	1.95	-0.82	1.5, 2.5	ms	cs	lk
503	1.17	1.65	-3.17	-2.0, 1.5, 2.5	ps	scs	lk
504	0.93	0.95	-2.60	-0.5, 1.5, 2.5	ps	ns	pk
505	1.51	1.55	-1.25	0.5, 1.5, 2.5	ps	cs	pk
507	1.48	1.55	-3.92	1.5, 2.5	ps	cs	vlk
509	1.78	1.75	-2.46	1.0, 2.5	ms	ns	mk
510	1.17	1.12	-0.90	0.5, 2.5	ms	fs	mk
515	0.71	0.75	-1.92	0.5	ms	cs	mk
506	4.71	4.52	2.11	1.5, 4.0	ms	fs	vpk
508	4.90	4.71	0.19	1.5, 4.0	ps	fs	pk
5151	2.40	2.40	-0.68	0.5, 1.0	ps	ns	pk
511	1.83	1.85	-0.84	1.0, 2.5	ms	cs	pk
512	0.96	1.25	-3.12	1.5, 2.5	ps	cs	pk
520	1.85	1.80	-1.20	1.5	ps	ns	pk
522	0.53	0.75	-3.76	-2.5, 0.5, 2.0	ps	cs	pk
523	0.78	0.95	-3.80	-2.5, 0.5, 2.5	ps	cs	lk
605	1.50	1.50	-3.04	-2.5, 1.5, 3.0	ps	cs	lk
301	1.31	1.78	-4.34	-2.0, 1.5	ps	scs	pk
302	0.91	1.48	-4.45	-2.0, 1.0	vps	scs	vpk
603	1.78	2.00	-2.06	1.5, 0.5, 2.0	ps	scs	pk
6005	1.53	1.65	-1.52	-2.0, 0.5	ms	cs	lk
401	1.03	0.80	-2.68	-0.5, 2.5	ps	fs	mk
6701	1.62	1.86	-2.38	-0.5, 2.5	ps	cs	mk
7011	1.26	1.67	-4.56	-2.5, 2.0, 3.0	ps	scs	pk
701	-0.27	-0.58	-5.67	-2.0, 2.5	ps	scs	pk
606	2.23	1.95	-1.18	-2.0, 0.5	ps	fs	pk
801	0.26	0.25	-3.27	-2.0, 0.5	ps	sfs	vlk
201	1.09	1.40	-4.12	-2.5, 0.5, 1.5	ps	cs	pk
203	-0.08	0.25	-4.47	-2.0, 0.5, 1.5	ps	cs	vpk
205	0.11	0.50	-3.23	-2.5, 0.5, 2.5	ps	cs	vpk
2061	1.01	1.12	-2.17	0.5, 1.5	ms	cs	mk
2062	1.93	1.85	0.03	0.5, 1.5	ms	ns	pk
207	0.95	1.00	-2.34	1.0	ps	cs	lk

TEXTURAL DATA

SAMPLE NO.	WEIGHT % gravel (G)	sand(S)	mud (M)	TEXTURAL TYPE
101	27.36	70.84	1.80	gS
103	13.53	85.01	1.46	gS
104	10.98	87.02	2.00	gS
105	0.04	32.81	67.15	sZ
106	0.28	51.69	48.03	(g)mS
107	1.10	43.25	55.64	sZ
108	6.35	43.34	49.39	gM → sZ
109	1.29	6.28	92.43	Z
110	0.00	4.96	95.04	Z
1101	0.00	4.57	95.43	Z
501	27.45	71.73	0.82	gS
502	1.70	98.02	0.28	(g)S
503	16.42	83.58	0.00	gS
504	9.55	90.45	0.00	gS
505	2.05	97.85	0.10	(g)S
507	8.59	89.54	1.87	gS
509	2.31	95.13	2.56	(g)S
510	0.86	94.90	4.24	(g)S
515	7.02	91.82	1.16	gS
5151	3.9	95.28	0.82	(g)S
506	0.00	4.24	95.76	Z
508	0.00	4.59	95.51	Z
511	0.63	97.30	2.07	(g)S
512	15.40	82.97	1.63	gS
520	1.16	98.84	0.00	(g)S
522	20.64	70.05	9.31	gmS
523	16.32	77.66	6.02	gS
521	0.00	85.9	14.17	zS
801	1.8	97.97	0.23	(g)S
201	18.25	75.38	6.37	gS
203	31.28	67.51	1.21	sG
205	28.99	63.79	7.22	gmS
2061	4.56	94.51	0.93	(g)S
2062	0.00	94.47	5.53	S
207	6.00	93.02	0.98	gS
605	7.72	87.76	4.52	gS
603	4.38	91.35	4.27	(g)S
606	1.19	69.24	29.54	(g)mS
301	14.82	79.06	6.12	gS
302	21.17	73.54	5.29	gS
401	8.12	89.18	2.70	gS
6701	5.69	87.05	7.26	gS
701	28.93	65.25	5.82	gS → sG

SAMPLE NO.	σ_I	SK_I	K_G
101	1.19	-0.47	0.92
103	1.57	-0.13	1.07
104	1.52	-0.08	0.93
105	1.56	-0.01	1.09
106	1.84	-0.08	0.88
107	2.29	-0.13	0.98
108	2.34	-0.10	0.87
109	1.63	0.16	1.23
110	1.48	0.07	0.90
1101	1.03	-0.03	1.01
1051	1.40	-0.28	0.85
1061	1.08	0.02	0.83
1071	1.00	-0.00	0.70
1081	1.20	- .10	1.11
501	1.73	-0.19	1.05
502	0.87	-0.20	1.17
503	2.01	-0.31	1.13
504	1.44	-0.03	0.75
505	1.17	-0.12	0.80
507	1.43	-0.27	1.91
509	0.92	-0.04	0.92
510	0.82	0.13	1.01
515	0.89	-0.16	1.07
506	0.89	0.25	0.66
508	1.05	0.27	0.75
5151	1.10	-0.05	0.81
511	0.89	-0.16	0.67
512	1.70	-0.28	0.87
520	1.04	0.00	0.79
522	1.87	-0.16	0.83
523	1.73	-0.19	1.17
605	1.50	-0.14	1.38
301	1.79	-0.41	0.79
302	2.02	-0.35	0.62
603	1.28	-0.31	0.88
6005	0.85	-0.14	1.20
401	1.41	0.16	1.04
6701	1.81	-0.22	0.98
7011	1.76	-0.40	0.73
701	1.94	-0.49	0.85
606	1.48	0.28	0.87
801	1.10	0.40	1.60
201	1.86	-0.27	0.85
203	1.70	-0.10	0.66
205	1.79	-0.27	0.58
2061	0.93	-0.21	0.95
2062	0.92	0.07	0.83
207	1.01	-0.14	1.19

Appendix 2.3 Mineralogic Analysis Results SAND FRACTION MINERALOGY (weight %)

Sample	WR = whole rock P = phenocrysts	% Matrix (pumice + glass shard)	Rock Fragments	Total Phenocrysts	Plagioclase	Quartz	Pyroxene	Opaques	Hornblende	Biotite	Zircon
6005	WR	67.17	11.43	21.4	3.26	0.91	2.40	14.00	0.19		tr
	P				15.2	4.2	11.2	65.4	0.9		
803	WR	92.89	1.06	6.05	2.87	0.68	0.88	1.38	0.21		tr
	P				47.4	11.2	14.5	22.8	3.4		
804	WR	95.32	1.32	3.36	2.52	0.54	0.10	0.16	0.02		tr
	P				75.0	16.0	2.9	4.8	0.6		
805	WR	95.89	0.90	3.21	2.49	0.42	0.10	0.14	0.04		tr
	P				77.5	13.0	3.1	4.4	1.2		
801	WR	96.07	2.45	1.48	1.06	0.32	0.04	0.06	tr		
	P				71.6	21.6	2.7	4.0			
205	WR	77.67	16.48	5.85	2.15	1.00	0.09	2.43	0.12		0.04
	P				36.7	17.1	1.5	41.5	2.0		
207	WR	94.35	2.19	3.46	2.41	0.75	0.03	0.24	0.02		tr
	P				69.6	21.7	0.9	7.0	0.6		
203	WR	96.04	1.85	2.11	1.60	0.31	0.02	0.16	0.01		
	P				75.8	14.6	0.9	7.6	0.4		
201	WR	96.45	1.82	1.73	1.29	0.24	0.07	0.11	0.02	tr	tr
	P				74.6	13.8	4.0	6.3	1.0		
206	WR	93.72	2.90	3.38	2.39	0.69	0.04	0.22	tr		tr
	P				70.71	20.4	1.1	6.5			
501	WR	92.64	5.62	1.74	1.44	0.20	0.04	0.05	tr		tr
	P				82.7	11.4	2.3	2.8			
502	WR	94.85	3.17	1.98	1.25	0.63	0.03	0.05	tr		tr
	P				63.1	31.8	1.51	2.5			
503	WR	95.62	2.11	2.27	1.87	0.30	0.03	0.05	tr		tr
	P				82.3	13.2	1.3	2.2			
510	WR	94.02	0.06	5.92	4.43	1.04	0.02	0.40	0.04		tr
	P				74.8	17.6	0.3	6.7	0.7		
512	WR	95.21	0.01	4.78	3.61	0.87	0.06	0.22	0.01		tr
	P				75.5	18.2	1.2	4.6	0.2		
511	WR	95.29	0.04	4.67	3.27	1.40	0.09	0.38	0.02		tr
	P				70.0	29.9	1.9	8.1	0.4		
515	WR	94.12	0.01	5.87	3.68	1.39	0.04	0.36	tr		tr
	P				62.7	23.7	0.7	6.1			
509	WR	94.77	1.73	3.50	2.36	0.91	0.02	0.18	0.17		tr
	P				67.4	26.0	0.6	5.1	4.8		
521	WR	93.04	3.20	3.76	2.90	0.86	0.02	0.24	0.01		0.01
	P				77.1	22.9	0.5	6.3	0.3		
522	WR	91.90	4.70	3.32	1.74	0.49	0.06	1.0	0.04		0.03
	P				52.4	14.7	1.8	30.1	1.2		
523	WR	70.04	24.62	5.34	2.06	0.87	0.14	2.08	0.10		0.07
	P				38.5	16.3	2.6	38.9	1.8		1.3
7011	WR	92.92	1.12	5.96	4.21	0.74	0.36	0.53	0.12	tr	tr
	P				70.6	13.2	6.0	8.9	2.0		
6701	WR	86.24	3.43	10.33	7.61	1.74	0.18	0.74	.05		tr
	P				73.7	16.8	1.7	7.2	0.5		
603	WR	87.40	3.28	9.32	6.21	2.08	0.30	0.63	0.07	0.03	tr
	P				66.6	22.3	3.2	6.7	0.7	0.3	
605	WR	86.88	3.16	9.96	6.93	2.12	0.30	0.51	0.08	0.02	tr
	P				69.5	21.2	3.0	5.1	0.8	0.2	
504	WR	86.64	4.76	8.60	6.17	1.83	0.16	0.36	0.08		tr
	P				71.7	21.3	1.8	4.1	0.9		

Sample	WR = whole rock P = phenocrysts	% Matrix (pumice + glass shards	Rock Fragments	Total Phenocrysts	Plagioclase	Quartz	Pyroxene	Opaques	Hornblende	Biotite	Zircon
301	WR	90.30	2.56	7.14	5.13	0.98	0.20	0.35	0.30	0.07	tr
	P				71.8	13.7	2.8	4.8	5.7	1.1	
302	WR	89.98	2.71	7.43	5.41	1.11	0.20	0.35	0.30	0.07	tr
	P				72.8	14.9	2.6	4.7	4.0	0.9	
401	WR	79.93	5.85	14.22	7.80	4.98	0.20	0.70	0.50	0.04	tr
	P				54.8	35.0	1.4	4.9	3.5	0.28	
409	WR	77.77	6.68	15.55	8.10	6.46	0.1	0.56	0.33	tr	tr
	P				52.0	41.5	0.6	3.6	2.1		
4010	WR	73.87	7.92	18.20	9.85	6.38	0.36	0.93	0.67	0.06	tr
	P				54.1	35.0	2.0	5.1	3.7		
101	WR	84.72	4.79	10.49	7.16	2.31	0.10	0.58	0.34	tr	tr
	P				68.2	22.0	0.9	5.5	3.2		
103	WR	85.27	5.20	9.53	7.22	1.37	0.10	0.51	0.32	tr	tr
	P				75.8	14.4	1.0	5.3	3.3		

Appendix 2.3.1

HEAVY MINERAL PERCENTAGES (WEIGHT %)

SAMPLE NO.	% in 2 - 4ϕ	% in WR*
101	4.26	1.02
103	3.32	0.94
105	0.80	0.38
106	17.49	6.80
108	0.32	0.12
109	0.34	0.15
110	0.25	1.09
801	0.26	0.10
205	9.45	2.70
207	2.19	0.30
203	0.25	0.20
201	0.19	0.20
206	0.41	0.30
501	0.27	0.10
502	0.32	0.10
503	0.30	0.10
504	0.73	0.60
508	0.64	0.22
509	0.66	0.23
510	2.82	0.45
511	1.28	0.50
515	0.74	0.42
512	1.12	0.30
521	0.85	0.30
522	5.48	1.09
523	9.38	2.41
301	2.95	1.04
302	2.86	0.92
401	3.94	1.44
605	01.66	0.91
603	01.55	1.03
409	2.7	0.99
6005	74.11	17.2
805	0.74	0.30
803	5.55	2.50
804	0.86	0.30
7011	2.45	1.01
6701	1.16	0.98

* WR = Whole Rock

REFERENCES

Adams, C.J.D., 1975: New Zealand potassium-argon age list - 2. *New Zealand Journal of Geology and Geophysics 18(3)*:

Allen, J.R.L., 1963: The classification of cross-stratified units, with notes on their origin. *Sedimentology 2*: 93-114.

Allen, J.R.L., 1965: A review of the origin and characteristics of Recent alluvial sediments. *Sedimentology 5(2)*: 89-191.

Allen, J.R.L., 1970: A quantitative model of grain-size and sedimentary structures in lateral deposits. *Journal of Geology 7*: 129-146.

Allen, J.R.L., 1977: The possible mechanics of convolute lamination in graded sand beds. *Journal of the Geological Society of London 134*: 19-31.

Ballance, P.F., 1976: Evolution of the Upper Cenozoic Magmatic Arc and Plate Boundary in Northern New Zealand. *Earth and Planetary Sciences Letters 28*: 356-370.

Bird, G.A., 1981: *The nature and causes of coastal landsliding on the Maungatapu Peninsula, Tauranga, New Zealand.* M.Sc. Thesis, University of Waikato.

Birrell, K.S.; Pullar, W.A.; Searle, P.L., 1977: Weathering of Rotoehu Ash in the Bay of Plenty District. *New Zealand Journal of Science 20*: 303-310.

Bond, A.; Sparks, R.S.J., 1976: The Minoan eruption of Santorini, Greece. *Journal of the Geological Society of London 132, Part 1*: 1-16.

Bowen, D.Q., 1978: *Quaternary Geology.* Oxford-Pergamon. 221p.

Briggs, N.D., 1973: *Investigations of New Zealand pyroclastic-flow deposits.* Ph.D. Thesis, Victoria University, New Zealand.

Capaldi, G. *et al.*, 1978: Stromboli and its 1975 eruption. *Bulletin Volcanologique 41, No 3*: 259-285.

Carter, L., 1975: Sedimentation on the continental terrace around New Zealand, A Review. *Marine Geology 19*: 209-237.

Carter, L., 1976: *Cuvier Bathymetry "N.Z. Oceanographic Institute Chart, Coastal Series 1:200,000"*. N.Z. Department of Scientific and Industrial Research, Wellington.

Carter, R.M., 1975: A discussion and classification of Subaqueous Mass Transport with particular application to grain-flow, slurry-flow, and fluxoturbidites. *Earth Science Reviews, 11*: 145-177.

Carver, R.E., (Ed.), 1971: *Procedures in Sedimentary Petrology*. Wiley-Interscience, 635p.

Chappell, J., 1975: Upper Quaternary warping and uplift rates in the Bay of Plenty and west coast, North Island, New Zealand. *New Zealand Journal of Geology and Geophysics 18(1)*: 129-155.

Cole, J.W., 1978: Tectonic Setting of Mayor Island Volcano. *New Zealand Journal of Geology and Geophysics 21, No. 5*: 645-7.

Cole, J.W., 1979: Structures, Petrology, and Genesis of Cenozoic Volcanism, Taupo Volcanic Zone, New Zealand - a review. *New Zealand Journal of Geology and Geophysics 22(6)*: 631-657.

Colgate, S.A. and Sigurgeirsson, T., 1973: Dynamic mixing of water and lava. *Nature 244*: 552-555.

Collinson, J.D., 1978: Alluvial Sediments. *In*: Reading, H.G., *Sedimentary Environments and Facies*. Blackwell, Oxford. 557p.

Cullen, D.J., 1967: Submarine evidence from New Zealand of a rapid rise in sea level about 11,000 yrs B.P. *Paleogeography, Paleoclimatology, Paleoecology 3*: 289-298.

Cuthbertson, A.S., 1981: *The Hinuera Formation in the Southern Hauraki Lowland, Central North Island*. M.Sc. Thesis, University of Waikato, New Zealand.

Davies, D.K.; Vessell, R.K.; Miles, R.C.; Foley, M.G.; Bonis, S.B., 1978: Fluvial transport and downstream sediment modifications in an active volcanic region. *In*: Miall, A.D., 1978: *Fluvial Sedimentology*. Canada Society of Petroleum Geolgists, Memoir 5, Calgary, Alberta, Canada: 61-84.

Doeglas, D.J., 1962: The structure of sedimentary deposits of braided rivers. *Sedimentology 1*: 167-190.

Enos, P., 1977: Flow regimes in debris flows. *Sedimentology 24*: 133-142.

Ewart, A., 1966: Review of the mineralogy and chemistry of the acidic volcanic rocks of the Taupo Volcanic Zone. *Bulletin Volcanologique 29:* 147-172.

Fisher, R.V., 1961: Proposed classification of volcaniclastic sediments and rocks. *Bulletin of the Geologic Society of America 72*: 1409-1414.

Fiske, R.S., 1969: Recognition and Significancè of pumice in marine Pyroclastic rocks. *Bulletin of the Geological Society of America 80*: 1-8.

Fleming, C.A., 1975: The Quaternary Record of New Zealand and Australia. *In*: R.P. Suggate and M.M. Cresswell (Eds.) *Quaternary Studies, Royal Society of New Zealand, Wellington*: 1-20.

Folk, R.L., 1968: *Petrology of Sedimentary Rocks*. Hemphill's Austin, Texas: 170p.

Folk, R.L., Andrews, P.B., Lewis, D.W., 1970: Detrital sedimentary rock classification and nomenclature for use in New Zealand. *New Zealand Journal of Geology and Geophysics 13(4)*: 937-968.

Fransen, P.J.B., 1982: *Geology of the Western Mamaku Plateau and variations in the Mamaku Ignimbrite*. M.Sc. Thesis, University of Waikato.

Gibbs, H.S. and Pullar, W.A., 1961: Soils of the Bay of Plenty. *Proceedings of the New Zealand Grasslands Association Conference 23*: 1-12.

Gibbs, H.S., Cowie, J.D., Pullar, W.A., 1968: *In*: *Soils of the North Island, Part 1, New Zealand Soil Bureau Bulletin 26(1)*: 47-88.

Gibson, ., 1974: A review of the geology, petrology and geochemistry of the Volcano, Fantale. *Bulletin Volcanologique 38(3)*: 791-802.

Gulf Research and Development Company, 1972: *Gulfrex Marine Science Survey, N.Z. Geological Survey Open File*; Petroleum File 614 (unpublished).

Hampton, M.A., 1975: Competence of fine-grained debris flow. *Journal of Sedimentary Petrology 45*: 834-844.

Hampton, M.A., 1979: Buoyancy in debris flows. *Journal of Sedimentary Petrology 49*: 753-758.

Harms, J.C., Fahnestock, R.K., 1965: Stratification, bed forms and flow phenomena (with an example from the Rio Grande), *In*: Middleton, G.V., 1977: *Sedimentary Processes: Hydraulic interpretation of primary sedimentary structures. Society of Economic Paleontologists and Mineralogists. Reprint Series, Number 31*: 95-127.

Harms, J.C., Southard, J.B., Spearing, D.R., Walkers, R.G., 1975: *Depositional environments as interpreted from primary sedimentary strucutes and stratification sequences.* Society of Economic Paleontologists and Mineralogists, Short Course 2, Dallas: 161p.

Hawkins, J.W., 1974: Geology of the Lau Basin, a marginal sea behind the Tonga Arc. Pp. 505-20 in Burk, C., Drake, C.L. (Eds.): *"Geology of Continental Margins"* Springer-Verlag, Berlin.

Healy, J., 1946: Geology of the Karapiro District, Cambridge. *New Zealand Journal of Science and Technology 27 (Sec. B), 3*: 199-217.

Healy, J., 1967: Geology of the Kaimai Tunnel section (abs.), Geological Society of New Zealand Conference, 1967. (Unpublished).

Healy, J., 1969: Geological report on proposed tunnel line: Kaimai railway deviation. Department of Scientific and Industrial Research. (Unpublished).

Healy, J., Schofield, J.C., Thompson, B.N., 1964: Sheet 5, Rotorua (First Edition). "Geological Map of New Zealand 1:250,000. "Department of Scientific and Industrial Research, Wellington.

Henderson, J., Bartrum, J.A., 1913: The geology the the Aroha Sub-division, Hauraki, Auckland. *New Zealand Geological Survey Bulletin, New Series 16*: 127p.

Hochstein, M.P., Nixon, I.M., 1979: Geophysical study of the Hauraki Depression, North Island, New Zealand. *New Zealand Journal of Geology and Geophysics 22*: 1-19.

Hochstein, M.P., Tearney, K.W., 1981: Revised geophysical geological model of the Hauraki Rift. *In: Programme and Abstracts, Geological Society of New Zealand, Hamilton Conference, 23-26th November, 1981*: p.49.

Hogg, A.G., 1974: *A pedological study of the Hamilton Ash Formation at Te Uku.* M.Sc. Thesis, University of Waikato.

Hogg, A.G., 1979: *Identification and correlation of thinly bedded late Quaternary tephras of Coromandel Peninsula, New Zealand.* Ph.D. Thesis, University of Waikato, New Zealand.

Hogg, A.G., 1980: Late Quaternary Tephras on the Coromandel Peninsula, North Island, New Zealand: The Whangamata Ash (Abstract). *In: Howorth, R., et al., 1981: Proceedings of Tephra Workshop, June 30th - July 1st, 1980, Victoria University, No. 20.*

Howorth, R., 1975: New Formation of Late Pleistocene Tephras from the Okataina Volcanic Centre, New Zealand. *New Zealand Journal of Geology and Geophysics 18(5)*: 683-712.

Houghton, B.F., 1982: *Unpublished borelog reports.* N.Z.G.S., Rotorua.

Hull, A.G., 1977: *Lignite and its relation to the stratigraphy of the eastern Tauranga Basin.* Dissertation for B.Sc.(Hons.), Victoria University, New Zealand.

Hume, T.M., 1972: *The petrology of the Hinuera Formation.* M.Sc. Thesis, University of Waikato, New Zealand.

Hume, T.M., Sherwood, A.M., Nelson, C.S., 1975: Alluvial Sedimentology of the Upper Pleistocene Hinuera Formation, Hamilton Basin, New Zealand. *Journal of the Royal Society of New Zealand 5*: 421-462.

Hume, T.M. and Nelson, C.S., 1982: *X-ray diffraction analytical Procedures and some Mineralogical Characteristics for South Auckland Region Sediments and Sedimentary Rocks, with special reference to their Clay Fraction.* Occasional report, No. 10, University of Waikato, New Zealand.

Jopling, A.V., 1964: Laboratory study of sorting processes related to flow separation. *Journal of Geophysical Research 69*: 3404-3418.

Jopling, A.V., 1965: Hydraulic factors controlling the shape of laminae in laboratory deltas. *In*: Middleton, G.V., 1977: *Sedimentary processes: Hydraulic interpretation of primary sedimentary structures.* Society of Economic Paleontologists and Mineralogists, Reprint Series No. 3: 49-63.

Jopling, A.V., Walker, R.G., 1968: Morphology and origin of ripple-drift cross-lamination, with examples from the Pleistocene of Massachusetts; *In*: Middleton, G.V., 1977: *Sedimentary Processes: Hydraulic Interpretation of primary sedimentary structures.* Society of Economic Paleontologists and Mineralogists, Reprint Series No. 3: 74-87.

Kamp, P.J.J., 1978: *Stratigraphy and sedimentology of Conglomerates in the Pleistocene Kidnappers Group, Hawkes Bay*. M.Sc. Thesis, University of Waikato, New Zealand.

Karig, D., 1970: Ridges and basin of the Tonga-Kermadec island arc system. *Journal of Geophysical Research 75(2):* 239-254.

Kear, D., Waterhouse, B.C., 1961: Quaternary surfaces and sediments at Waihi Beach. *New Zealand Journal of Geology and Geophysics 4(4)*: 434-445.

Kear, D., Schofield, J.C., 1978: Geology of the Ngaruawahia Subdivision. *New Zealand Geological Survey, Bulletin 88*: 168p.

Kennedy, N.M., 1980: Use of tephra as marker beds in the Rotorua and Bay of Plenty Districts. *In*: Howorth, R., *et al.*, 1981: *Proceedings of tephra workshop, June 30th - July 1st 1980, Victoria University No. 20.*

Kirkman, J.H., Pullar, W.A., 1978: Halloysite in Late Pleistocene Rhyolitic Tephra beds near Opotiki, Coastal Bay of Plenty, North Island, New Zealand. *Australian Journal of Soil Research, 16*: 1-8.

Kohn, B.P., 1973: *Some Studies of New Zealand, Quaternary Pyroclastic rocks*. Ph.D. Thesis, Victoria University.

Leopold, L.B., Wolman, M.G., 1957: River channel patterns: braided, meandering and straight. *United States Geological Survey Professional Paper - 282 B*: 39-85.

Lewis, D.W., 1981: Practical Sedimentology, University of Canterbury; Apteryx Books.

Lowe, D.R., 1975: Water escape structures in coarse-grained sediments. *Sedimentology, 22*: 157-204.

Lowe, D.R., 1976(a): Subaqueous liquified and fluidized sediment flows and their deposits. *Sedimentology 23*: 285-308.

Lowe, D.R., 1976(b): Grain-flow and grain-flow deposits. *Journal of Sedimentary Petrology 46*: 188-199.

Lowe, D.R., Lo Piccolo, R.D., 1974: The characteristics and origins of dish and pillar structures. *Journal of Sedimentary Petrology 44*: 484-501.

McCraw, J.D., 1975: Quaternary air-fall deposits of New Zealand. *In*: Suggate, R.P., Cresswell, M.M., (Eds.). *Quaternary Studies; Royal Society of New Zealand. Bulletin 13*: 35-44.

McGlone, M.S.; Topping, W.S., 1977: Aranuian (post-glacial) pollen diagrams from the Tongariro Region. *New Zealand Journal of Botany 15*: 749-760.

McGowen, J.H., Garner, L.E., 1970: Physiographic features and stratification types of coarse-grained point bars: modern and ancient examples. *Sedimentology 14*: 77-111.

McKee, E.D., Crosby, E.J., Berryhill, H.L., 1967: Flood deposits, Bijou Creek, Colorado June, 1965. *Journal of Sedimentary Petrology 37(3)*: 829-851.

McKnight, D.G., 1968: Recent and relict molluscan faunas from off Cape Farewell, New Zealand. *Journal of Marine and Freshwater Research 2*: 708-711.

Miall, A.D., 1977: A review of the braided river depositional environment. *Earth Science Reviews 13*: 1-62.

Miall, A.D., 1978: Lithofacies types and vertical profile models in braided river deposits: A summary. *In*: Miall, A.D. (Ed.): *Fluvial Sedimentology*. Canadian Society of Petroleum Geologists. Memoir 5: 597-604.

Moore, J.G., Peck, D.L., 1962: Accretionary lapilli in volcanic rocks of the Western Continental United States. *Journal of Geology 70*: 182-193.

Müller, G., 1967: Sedimentary Petrology, Part 1. *Methods in Sedimentary Petrology*. Hafner, New York/London.

Nairn, I.A., 1972: Rotoehu Ash and the Rotoiti Breccia Formation, Taupo Volcanic Zone, New Zealand. *New Zealand Journal of Geology and Geophysics 15*: 251-261.

Naylor, M.A., 1980: The Origin of Inverse Grading in muddy debris flow deposits - A review. *Journal of Sedimentary Petrology 50(4)*: 1111-1116.

Nelson, C.S., Cochrane, R.H.A., 1970: A rapid X-ray method for the quantitative determination of selected minerals in fine grained altered rocks. *Tane 16*: 151-162.

Norris, R.M., 1972: Shell and gravel layers on the western continental shelf, New Zealand. *New Zealand Journal of Geology and Geophysics 15*: 572-589.

Passega, R., 1957: Texture as characteristic of clastic deposition. *American Association of Petroleum Geologists, Bulletin 41*: 1952-1984.

Picard, M.D., High, L.R., 1973: *Sedimentary Structures of ephemeral streams*. Developments in Sedimentology 17. Elsevier.

Pierson, T.C., 1981: Dominant particle support mechanisms in debris flows at Mt. Thomas, New Zealand and implications for flow mobility. *Sedimentology 28(1)*: 49-60.

Pullar, W.A., Heine, J.C., 1971: *Ages inferred from 14C dates of some tephra and other deposits from Rotorua, Taupo, Bay of Plenty Gisborne and Hawkes Bay Districts*. Radiocarbon Users Conference, Wellington: 117-138.

Pullar, W.A., Birrell, K.S., 1973: *Age and Distribution of late Quaternary pyroclastic and associated cover deposits of the Rotorua and Taupo area, North Island, New Zealand*. New Zealand Soil Survey Reports 1 and 2.

Pullar, W.A., Birrell, K.S., Heine, J.C., 1973: Named tephras and tephra formations occurring in the central North Island, with notes on derived soils and buried paleosols. *New Zealand Journal of Geology and Geophysics 16*: 497-518.

Reading, J.G. (Ed.), 1978: *Sedimentary environments and facies*. Blackwell Scientific Publications; Oxford: 557p.

Reineck, H.E., Singh, I.B., 1975: *Depositional sedimentary environments*. Springer-Verlag, New York: 439p.

Richards, J.R., Cooper, R.A., Black, P.M., 1966: Potassium-argon age of plutonic intrusives on Cape Colville and Cuvier Island. *Nature 211*: 725-6.

Roobol, M.J., Smith, A.L., 1976: Mt Pelée, Martinique, a pattern of alternating eruptive styles. *Geology 4*: 521-524.

Rust, B.R., 1978: Depositional models for braided alluvium. *In*: Miall, A.D. (Ed.), 1978: *Fluvial sedimentology*. Canadian Society of Petroleum Geologists; Memoir 5: Calgary Alberta, Canada: 605-625.

Rutherford, N.F., 1978: Fission-track age and trace element geochemistry of some Minden Rhyolite obsidians. *New Zealand Journal of Geology and Geophysics 21*: 443-448.

Scheidegger, A.E., Potter, P.E., 1968: Textural studies of graded bedding. *Sedimentology 11*: 163-170.

Schmid, R., 1981: Descriptive nomenclature and classification of pyroclastic deposits and fragments; Recommendations of the I.U.G.S. Subcommission on the systematics of Igneous rocks. *Geology 9*: 41-43.

Schofield, J.C., 1965: The Hinuera Formation and associated Quaternary events. *New Zealand Journal of Geology and Geophysics 8*: 772-791.

Schofield, J.C., 1968(a): Regional aspects of Cainozoic Volcanology in the North Island of New Zealand - Crustal fusion produces intermediate magma. *New Zealand Journal of Geology and Geophysics 11(2).*

Schofield, J.C., 1968(b): Dating of recent low sea level and Maori rock carvings, Ongari Point. *Earth Science Journal 2(2)*: 167-175.

Selby, M.J., Pullar, W.A., McCraw, J.D., 1971: The age of Quaternary surfaces at Waihi Beach. *Earth Science Journal 5(2)*: 106-114.

Self, S.; Sparks, R.S.J., 1978: Characteristics of widespread pyroclastic deposits formed by the interaction of Silicic Magma and water. *Bulletin Volcanologique 41(3)*: 196-213.

Seward, D., 1974: Age of New Zealand Pleistocene substages by fission-track dating of glass shards from tephra horizons. *Earth and Planetary Science Letters 24*: 242-248.

Shackleton, N.J., Opdyke, N.D., 1973: Oxygen Isotope and Paleomagnetic stratigraphy of Equatorial Pacific Core V28-238: Oxygen Isotope Temperatures and Ice Volumes on a 10^5 year and 10^6 year scale. *Quaternary Research 3(1)*: 39-55.

Sheridan, M.F., 1971: Particle size characteristics of pyroclastic tuffs. *Journal of Geophysical Research*: 5627-5634

Sheridan, M.F., 1979: Emplacement of pyroclastic flows: A review. *Geological Society of America; Special Paper 180.*

Sherwood, A.M., 1972: *Sedimentary structures, textures and paleoenvironment of the Hinuera Formation.* B.Phil. Thesis, University of Waikato.

Skinner, D.N.B., 1976: *Sheet 40. Northern Coromandel "Geological map of New Zealand 1 : 63,630".* New Zealand Department of Scientific and Industrial Research, Wellington.

Smith, N.D., 1971: Transverse bars and braiding in the Lower Platte River, Nebraska. *Geological Society of America Bulletin 82*: 3407-3420.

Smith, N.D., 1972: Some sedimentological aspects of planar cross-stratification in a sandy braided river. *Journal of Sedimentary Petrology 42*: 624-634.

Smith, N.D., 1974: Sedimentology and bar formation in the upper Kicking Horse River a braided outwash stream. *Journal of Geology 82*: 205-223.

Smith, R.L., 1960: Ash flows. *Geological Society of America Bulletin 71*: 795-842.

Smith, N.D., 1970: The braided stream depositional environment. Comparison of the Platte River with some Silurian clastic rocks north-central Appalachians. *Geological Society of America Bulletin 81*: 2993-3014.

Sparks, R.S.J., Self, S., Walker, G.P.L., 1973: Products of Ignimbrite Eruptions. *Geology 1*: 115-118.

Sparks, R.S.J., 1976: Grain-size variations in ignimbrites and implications for the transport of pyroclastic flows. *Sedimentology 23*: 147-188.

Sparks, R.S.J., Walker, G.P.L., 1977: The significance of vitric-enriched air-fall ashes associated with crystal-enriched ignimbrites. *Journal of Volcanology and Geothermal Research 2*: 329-341.

Sparks, R.S.J., 1978: Gas release rates from pyroclastic flows. An assessment of the role of fluidization in their emplacement. *Bulletin of Volcanology 41*: 1-9.

Sparks, R.S.J., Sigurdson, H., Carey, S.N., 1980a: The entrance of pyroclastic flows into the sea, I. Oceanographic and geologic evidence from Dominica, Lesser Antilles. *Journal of Volcanology and Geothermal Research 7 (1/2)*: 87-96.

Sparks, R.S.J., Sigurdson, H., Carey, S.N., 1980b: The entrance of pyroclastic flows into the sea, II. Theoretical considerations on subaqueous emplacement and welding. *Journal of Volcanology and Geothermal Research 7(1/2)*: 97-106.

Suggate, R.P., Stevens, G.R., Te Punga, M.T. (Eds.), 1978: *The Geology of New Zealand. Vol. 11.* Government Printer, Wellington: 820p.

Taylor, N.H., 1953: The soil pattern. *In*: Baylis, G.T.S. (Chairman). *"The ecological significance of the Central North Island ash showers".* Report of second annual meeting on N.Z. Ecological Society: 11-12.

Taylor, N.H., 1954: *General Survey of the Soils of North Island, New Zealand. A reconnaissance by the Staff of the Soil Bureau, New Zealand Department of Scientific and Industrial Research, and Department of Agriculture. Bulletin 5.* 286p.

Thornbury, W.D., 1964: *Principles of Geomorphology.* John Wiley and Sons, Inc.

Veeh, H.H. and Chappell, J., 1970: Astronomical theory of climatic change: support from New Guinea. *Science, 169*: 862-65.

Villari, L., 1974: The island of Pantellaria. *Bulletin Volcanologique 38(3)*: 680-724.

Visher, G.S., 1969: Grain-size distributions and depositional processes. *Journal of Sedimentary Petrology 39*: 1074-1106

Vucetich, C.G., Pullar, W.A., 1964: Stratigraphy and chronology of Late Quaternary volcanic ash in Taupo, Rotorua and Gisborne Districts, N.Z. *Geological Survey Bulletin 73; Part 2*: 43-88.

Vucetich, C.G., Pullar, W.A., 1969: Stratigraphy and chronology of Late Pleistocene volcanic ash beds in Central North Island, New Zealand. *New Zealand Journal of Geology and Geophysics 12*: 784-837.

Vucetich, C.G., Birrell, K.S., Pullar, W.A., 1978: Ohinewai Tephra Formation; a c.150,000-year-old tephra marker in New Zealand. *New Zealand Journal of Geology and Geophysics 21(1)*: 71-3.

Vucetich, C.G., Kohn, B.P., Pullar, W.A., 1980: Correlation of Aratora Tephra, Ahuroa cover bed type section, Te Kuiti. *In*: Howorth, R., *et al.*, 1981: *Proceedings of tephra workshop, June 30th - July 1st 1980, Victoria University; No. 20.*

Walker, G.P.L., 1971: Grain-size characteristics of pyroclastic deposits. *Journal of Geology 79(6)*: 696-714.

Walker, R.G., 1979: Facies Models. *Geoscience Canada*, Reprint Series 1.

Ward, W.T., 1967: Volcanic Ash beds of the Lower Waikato Basin, North Island, New Zealand. *New Zealand Journal of Geology and Geophysics 10(4)*: 1109-1136.

Ward, W.T., 1972: Pleistocene Ash in the Waikato Basin. Ages implied by changes in sea level (note). *New Zealand Journal of Geology and Geophysics 15(4)*: 678-685.

White, J.R., Williams, E.G., 1967: The nature of a fluvial process as defined by settling velocities of heavy and light minerals. *In*: Middleton, G.V., 1977. *Sedimentary processes: Hydraulic Interpretation of primary sedimentary structures.* Society of Economic Paleontologists and Mineralogists. Reprint series number 3: 64-74.

Williams, G.E., 1968: Formation of large scale trough cross-stratification in a fluvial environment. *Journal of Sedimentary Petrology 38*: 136-140.

Williams, P.F., Rust, B.R., 1969: The sedimentology of a braided river. *Journal of Sedimentary Petrology 39*: 649-679.

Wilson, C.J.N., 1980: The role of fluidization in the Emplacement of Pyroclastic flows: An Experimental approach. *Journal of Volcanology and Geothermal Research 8*: 231-249.

Wright, J.V., Smith, A.L., Self, S., 1980: A working terminology of pyroclastic deposits. *Journal of Volcanology and Geothermal Research 8*: 315-336.

Wright, J.V., 1981: The Rio Caliente Ignimbrite : Analysis of a compound Intraplinian Ignimbrite from a major Late Quaternary Mexican eruption. *Bulletin of Volcanology 44(2)*: 189-212.

Wright, J.V., Walker, G.P.L., 1981: Eruption, transport and deposition of an Ignimbrite : A case study from Mexico. *Journal of Volcanology and Geothermal Research 9*: 111-131.

Yamazaki, T., Kato, I., Muroi, I., Abe, M., 1973: Textural analysis and Flow mechanism of the Donzurubo Subaqueous Pyroclastic flow deposit. *Bulletin Volcanologique 37(2)*: p.231.